Thesis for Doctor of Philosophy

in Petrology and Volcanology research group,

Division of Earth and Planetary Science,

Department of Natural History Sciences,

Graduate School of Science, Hokkaido University

Geochemical studies of volcanic rocks from the northern part of Kuril-Kamchatka arc: Tectonic and structural constraints on the origin and evolution of arc magma

（クリル・カムチャッカ弧北部の火山岩に関する地球化学的研究：
深部構造が島弧マグマの起源および進化に与える影響について）

Bergal-Kuvikas Olga

Hokkaido University

August 2015

Acknowledgement

I am wishing to thank Japanese government for the chance to study at Japan. Scholarship for research students (Monbukagakusho: MEXT) was spent at Hokkaido University under guided by Prof. Mitsuhiro Nakagawa since October 2010 to September 2015.

Especially thanks for all members of Petrology and Volcanology research group at Hokkaido University. I am grateful to Dr. Mizuho Amma-Miyasaka, Dr. Akiko Matsumoto, Ms. Ayumi Kosugi, Prof. Takeshi Kuritani for assistance and support in analytical experiences. Thanks for Mr. K. Nakamura for helpful recommendation in making thin sections.

My dissertation is a part of Japanese-Russian project of study Klyuchevskoy volcano. I grateful to geologists and volcanologists of this project. For many years cooperation, I gratitude to Dr. Ya. Muravev, Ms. N. Malik, Mr. A. Ovsyannikov, Dr. Y. Ishizuka, Dr. T. Hasegawa, Dr. S. Uesawa. Geological team of project wish thanks to Mr. S. Chirkov, Mr. Y. Demyanschuk, Mr. S. Serovetnikov, Ms. E. Klimenko, Mr. Shimada, Mr. I. Kosuke, Ms. E. Nikonova, Ms. O. Muravyeva and geophysical team of project for support in field works on Kamchatka.

I am indebted to my first teacher Prof. Gennady Avdeiko for many years assistance. Thanks to him I made first steps in petrology and geodynamic. Prof. G. Avdeiko is a main source for me of knowledge about geodynamic, tectonic setting of Kamchatka. I was a glad to work together with Prof. G. Avdeiko as a highly professional specialist truly dedicated to passion.

Colleagues from Russian Academy of science, especially Prof. V. Ponomareva, Dr. M. Portnyagin, Dr. T. Churikova. Dr. N. Gorbach are thanked for their constructive discussion and critical comments of my research.

Sincere appreciation to my parents, Kuvikas Luidmila and Valery, for belief me and development of my personality. Thanks for my brother Maxim Kuvikas for encouragement.

My graduation will be impossible without moral support and everyday aid from my husband Bergal Valdemar. I wish to thank my lovely sons Valdis and Algis for everyday happiness and smiles. For me they are main sources of forces for study and work.

Contents

General introduction

Magmatism is global Earth process and indicator of inner activity of our planet. Many types of volcanoes exist and located on different plate boundaries (Fig. 1). Convergent type of the tectonic plate is also known as a destructive plate boundary (or subduction zone). In subduction zone, lithospheric plate has moved to the other plate and subducted material circulated in the global Earth`s cycle. Subduction zone produces new continental crust and island arcs. As a result of pressure, friction, and plate material melting in the mantle, earthquakes and volcanoes are common near convergent boundaries. Because the strongest eruptions with high volcanic magnitude are dominant in subduction zone, the study of arc volcano is very important.

Process of magma genesis and evolution is very complicated and includes many events. In the root zones, primary magma with specific geochemical features is generated by partial melting. During ascending of magma diapir in the crust, numerous processes of magma evolution exist, e.g. magma mixing, fractional crystallization, assimilation, degassing and etc. After eruptions, petrologists analyze pyroclastic material of volcano in order to recognize deep Earth process of magma formation and evolution. On the basis of the comparison with the volcanoes from different geodynamic settings, researcher can understand special process of magma genesis.

Circum Pacific “Ring of Fire” is the largest convergent boundary on the Earth. Single massive oceanic plate which called Pacific plate forms 75% of active volcano on the Earth (Schmincke, 2005). The Pacific Plate contains an interior hot spot forming the Hawaiian Islands, toward to moving plate hot spot formed Hawaii Emperor Seamounts chain (Fig. 2). On the NE part of Pacific “Ring of Fire” rates of moving tectonic plate is 8~9 cm/year (Minster

and Jordon, 1978). This is one of the faster rate for moving tectonic plate in convergent boundaries.

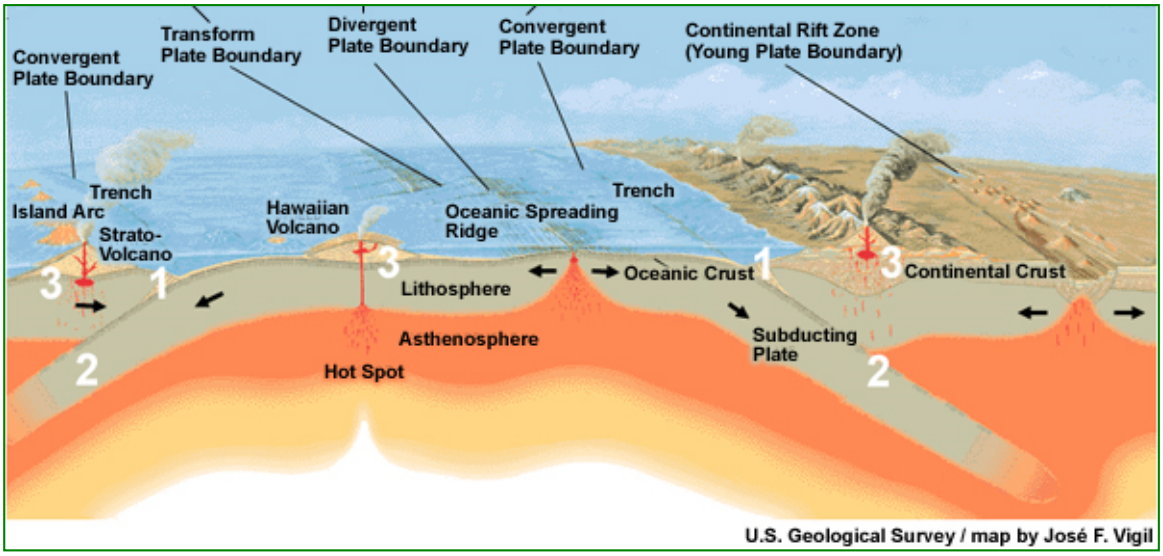

Fig. 1. Different types of tectonic boundaries and generated sources of magmatism.

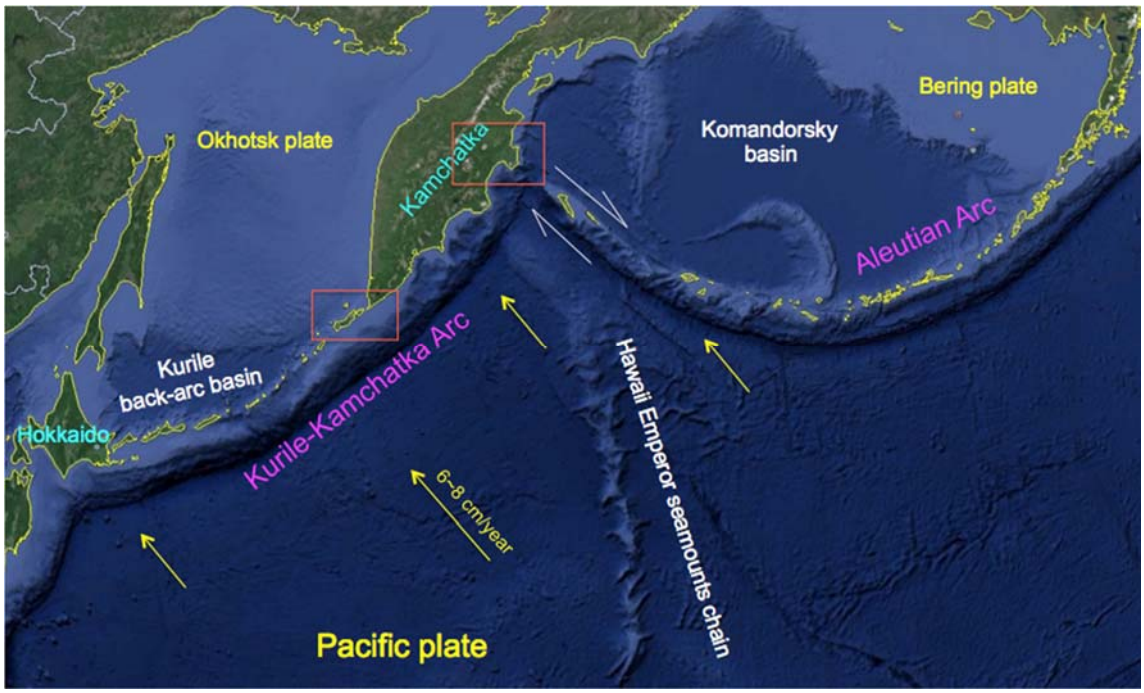

Fig. 2. Geodynamic setting of North, North-Eastern part of circum Pacific "Ring of Fire". Red squares show areas for detailed studies. (Google Earth)

The Aleutian arc reflects subduction of the Pacific plate beneath the North American plate. It extends 3,000 km from the Kamchatka Peninsula in the west to the Gulf of Alaska in the east. Oblique type of the subduction produce rocks with adakite signature (Yogodzinski et al., 2001; Yogodzinski et al., 2015). Western boundary of Aleutian Arc connected to Kamchatka by transform faults and formed arc-arc junction (Fig. 1).

The Kamchatka peninsula is located at the NE convergent boundary of the Eurasian and Pacific plates (Fig. 2). Volcanic activity on Kamchatka dates back to the Cretaceous. The current plate-tectonic configuration, however, formed only in the Late Miocene to Early Pliocene (Churikova et al. 2001). Plateau basalts, partly with intra-plate characteristics, were erupted from only in the Late Miocene to Early Pliocene. The northern termination of volcanic activity at Shiveluch volcano is related to the Aleutian-Kamchatka triple junction (Yogodzinski et al., 2001). Here the plate boundary changes from convergent in the south (Pacific-Eurasia) to strike-slip motion in the north (Pacific-North America). Quaternary arc volcanism on Kamchatka recognize from east to west three parallel to the trench: 1. The Eastern Volcanic Front (EVF): 2. The Central Kamchatka Depression (CKD) with Klyuchevskaya Group: 3. The Western Volcanic zone of the Sredinny Ridge (Fig. 3).

The Kurile volcanic archipelago stretches for 1150 km a width from 100 to 200 km from Kamchatka (Russia) to Hokkaido (Japan). The system develops at the convergent plate boundary between the overriding Okhotsk lithospheric block and the subducting northwestward Pacific plate. The Kurile island arc is a classical Mariana type subduction system (Stern, 2002), which consists the Kurile–Kamchatka trench, the Greater Kurile volcanic islands, and the Kurile Basin. The Greater Kurile island arc and Southern Kamchatka started to develop in the Early Miocene or Oligocene (Avdeiko et al., 2007). By Baranov et al. (2002) back-arc spreading of Kurile Basin was predominant in the Miocene. However since Late Miocene

compression of the basin started and continues currently. The Kurile Arc is divided into northern, central and southern segments (Fig. 4). Obtained segments are different by thickness of crust, distance to crust, angle of plate and geochemical features (Kimura, 1986; Zlobin et al., 1987; Avdeiko et al., 1992; Syracuse et al., 2006). Across arc variations identified by enriched incompatible elements, LILE and LREE and depleted of the HFSE, HREE from front to back arc zone (Bindeman, Bailey, 1999; Ishikawa, Terra, 1997; Martynov et al., 2010). Additionally along arc variations was observed with increasing K and another incompatible elements (Fedorchenko et al., 1989; Antonov, 2006; Dril et al., 2005; Martynov et al., 2010).

Kuril-Kamchatka Arc formed by single massive subducted Pacific plate. However, generated geodynamic settings for all volcanoes are different. Consequently, in order to study process of magma genesis and evolution we should concentrate on the most complicated area, where geodynamic conditions for produce magma change significantly. Representative dissertation includes two objects of investigation. One is Klyuchevskoy volcano. This is the voluminous arc`s volcano in the Earth, with basic magma composition. In case of arc-arc junction Klyuchevskoy volcano is the best candidate for study deep process for magma formation and evolution. Another object of study is northern Kurile volcanoes, which located on the transition zone between continental Kamchatka arc and island arc of Kurile Island arc.

Main aim of this dissertation is study process of magma genesis and evolution in complicated geodynamic settings on the example of Kurile-Kamchatka arc. Main purposes are follow: (1). using modern high-precious analytical methods to get data of contents major, trace elements and isotopic compositions, (2) to recognize process which are formed different types of primary magmas, study process of magma evolution, (3) to investigate spatial variations of different types of magma in space and time. Investigation of magma genesis in complicated

geodynamic settings are very important for recognize inner activities of the Earth and for protect people from natural disasters.

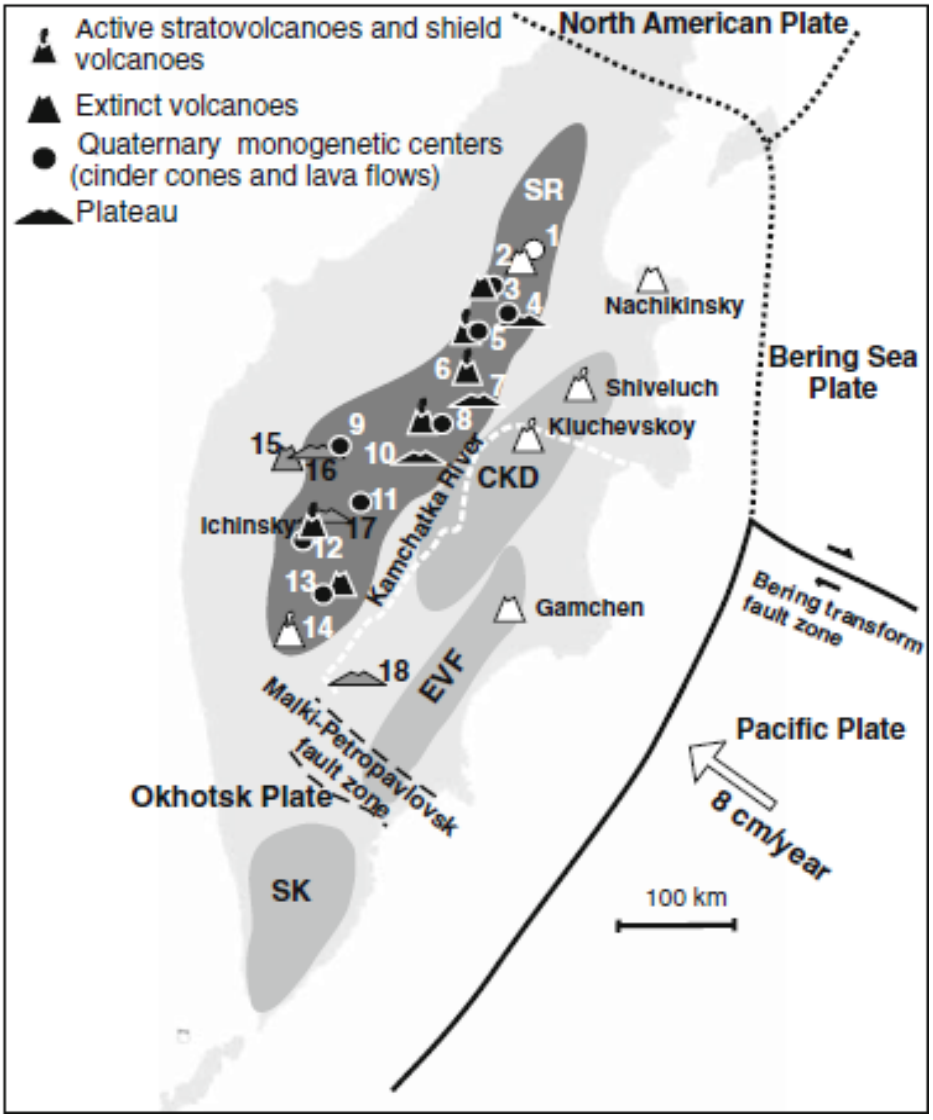

Fig. 3. Tectonic setting of Kamchatka. Red point shows locations of Klyuchevskoy volcanic group. (Churikova et al., 2001)

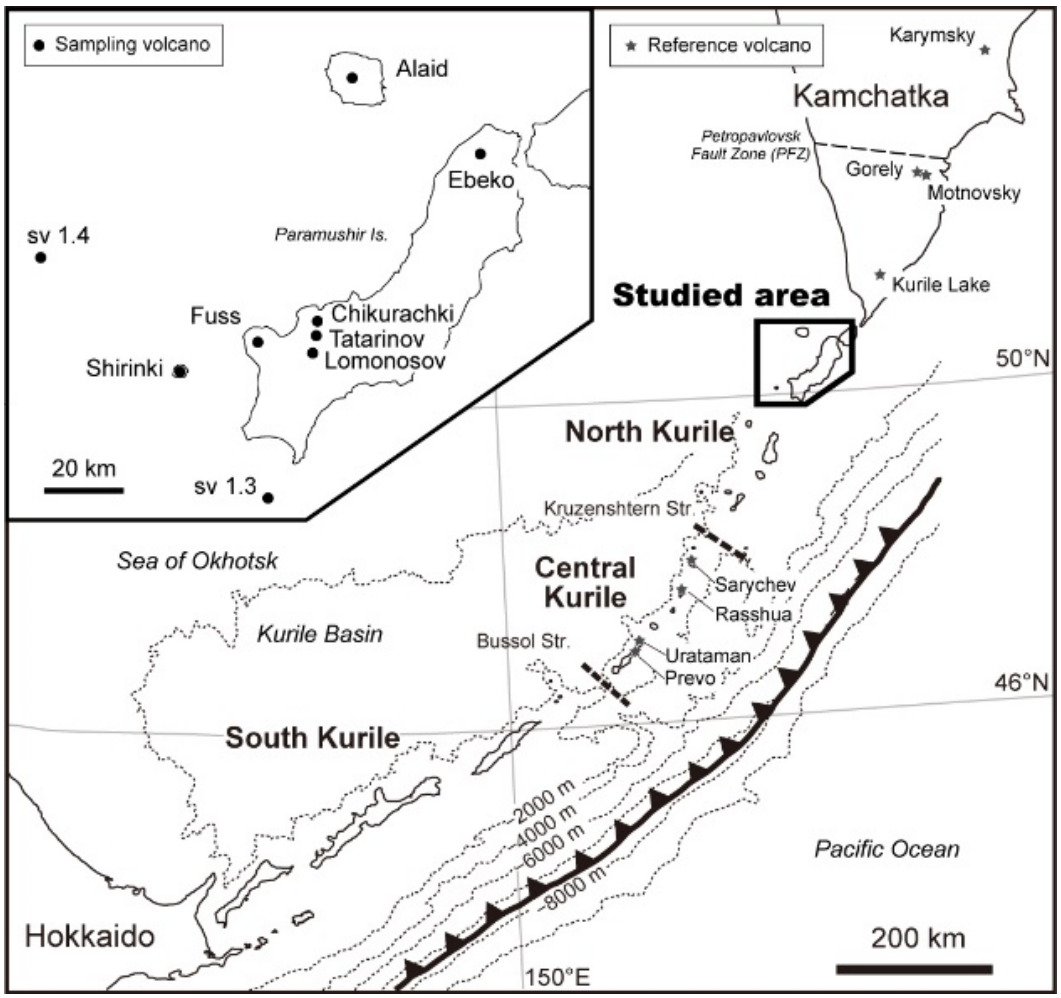

Fig. 4. Tectonic setting of Kurile Island Arc. Square shows studied area.

Part I

Geochemical studies on time-series samples from the Klyuchevskoy volcano, Kamchatka arc

Part I. Geochemical studies on time-series samples from the Klyuchevskoy volcano, Kamchatka arc

Abstract

The generation and evolution of mafic magmas were investigated for the Klyuchevskoy volcano in the Kamchatka arc, which is one of the most active arc volcanoes on the Earth. The eruptive products show significant variations in their whole-rock compositions (51.5–55.6 wt.% SiO_2), and they can be divided into low-K and high-K groups on the basis of the K/Zr ratios. The high-K samples are characterized by relatively higher SiO_2 and Ba and lower Al_2O_3 contents than the low-K samples, and the high-K magmas cannot be derivative from the low-K magmas through crustal processes. In most of the evolution of the volcano, the low-K magmas were dominated, and the high-K magmatism was mostly limited to 1932-1966 AD. In the individual groups, Mg-rich samples (>9 wt.%) are present, and their petrological features suggest that they represent primary or near primary magmas. The low-K and high-K primary magmas are estimated to have been generated though ~13.6% and ~11.8% melting of the depleted MORB-source mantle, respectively, by influx of slab-derived materials into the melting region. Considering the constraints of multi-component thermodynamics, the low-K primary magma is estimated to have been generated in the source mantle with 0.7 wt.% H_2O at ~1265°C and ~1.6 GPa, although the generations conditions for the high-K magma cannot be estimated. The slab-derived materials had high Ba/La ratios, as well as high Th/Yb ratios; they are considered to have been supercritical liquids. The slab-derived materials for the high-K magmas are suggested to have been more enriched in melt component than those for the low-K magmas, and they are likely to have been released from the subducting slab at deeper levels than those for the low-K magma. Therefore, the initiation of the high-K magmatism at ~1932

AD suggests that it was triggered by the influx of a new batch of slab-derived materials transported from the subducting slab. After the generation of the magmas, the low- and high-K magmas are suggested to have evolved through assimilation and fractional crystallization in the middle ~ lower crust.

Chapter 1. Introduction

The Kamchatka arc is located at the NE convergent boundary of the Eurasian and Pacific plates, below which the Pacific plate subducted at the rate of~9 cm/year (Geist and Scholl, 1994). Volcanic activity of Kamchatka dates back to the Cretaceous, however, the current plate-tectonic configuration formed only in the Late Miocene to Early Pliocene (Churikova et al., 2001). The plate boundary changes from convergent in the south (Pacific-Eurasia) to strike-slip motion in the north (Pacific-North America). The present volcanisms are concentrated in three zones parallel to the trench: the Eastern Volcanic Front (EVF), the Central Kamchatka Depression (CKD), and the Sredinny range (SR), from east to west (Fig. 1-1). The depth to the subducting slab is 90-110 km (EVF), 180-200 km (CKD) and 300-400 km (SR) (Gorbatov et al., 1997). Chemical composition show systematic variations from the volcanic arc front at Komarovsky volcano to the back-arc at Ichinsky volcano, and indicate the involvement of distinct sources (Churikova et al., 2001). Several parameters have mainly affected to the across-arc geochemical zonation; variably depleted and enriched mantle sources, the fluid flux from the slab to the mantle wedge and variable degrees of melting (Fig. 1-2).

In this study, we investigate the origin of temporal geochemical variations of erupted materials from the Klyuchevskoy volcano, located in the Central Kamchatka Depression. This volcano is well known to be one of the most active arc volcanoes in the world, and has erupted frequently even in the last 10 years; 2005, 2007, 2008-2009, 2009-2010, 2011, 2012-2013, 2013, and 2015 AD. The Klyuchevskoy volcano is also characterized by the underlying subduction of the Hawaiian-Emperor seamount chain. Therefore, as the cause of the exceptional magma productivity, a high flux of slab-derived fluids from the thickened oceanic

crust has been proposed (Dorendorf et al., 2000), while Portnyagin et al. (2007) also suggested an additional role of mantle upwelling associated with detachment of the subducted slab fragment (Fig. 1-3). Because of the interest in the remarkable magma production of the volcano, many petrological and geochemical studies have been carried out (e.g., Khabynaya et al., 1993; Kersting and Arculus, 1994; Dorendorf et al., 2000; Ozerov, 2000; Churikova et al., 2001; Auer et al., 2009; Mironov and Portnyagin, 2011; Kayzar et al., 2014). Most of these studies have divided the eruption products into high-MgO basalts and high-Al_2O_3 basalts (Fig. 1-4), and the genetic relationship between the two types of magmas has been discussed. Although some researchers have contended that the high-Al_2O_3 magma can be derivative from the high-MgO magma (e.g., Kersting and Arculus, 1995; Ariskin et al., 1995; Khubunaya and Sobolev, 1998; Ozerov, 2000; Mironov et al., 2001), others attributed the difference in the geochemical features of the two magmas to the source mantle processes (e.g., Dosseto et al., 2003; Auer et al., 2009).

To understand the origin of the evolutional history of the Klyuchevskoy volcano, it is essential to elucidate the genetic relationship among different magma types with distinct geochemical features. Therefore, we obtained high-quality geochemical data of time-series samples (from ~3500 BP to 2014 AD). Our data, along with literature data (from ~7000 BP to ~3500 BP; Auer et al., 2009), were then classified into two groups by a different category from that of the previous studies. We show that there must have been at least two different types of primary magmas with distinct K_2O content, and on this basis, the origin of the temporal variation in magma compositions is discussed.

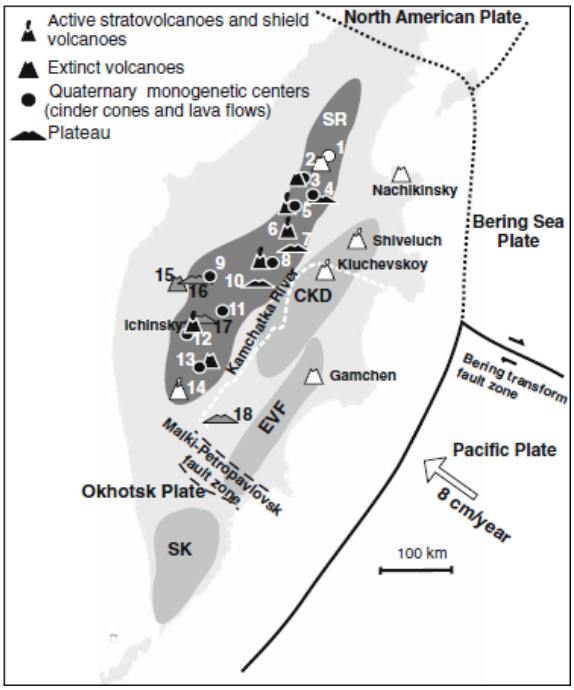

Fig. 1-1. General plate tectonic position of the Kamchatka (Churikova et al., 2001).

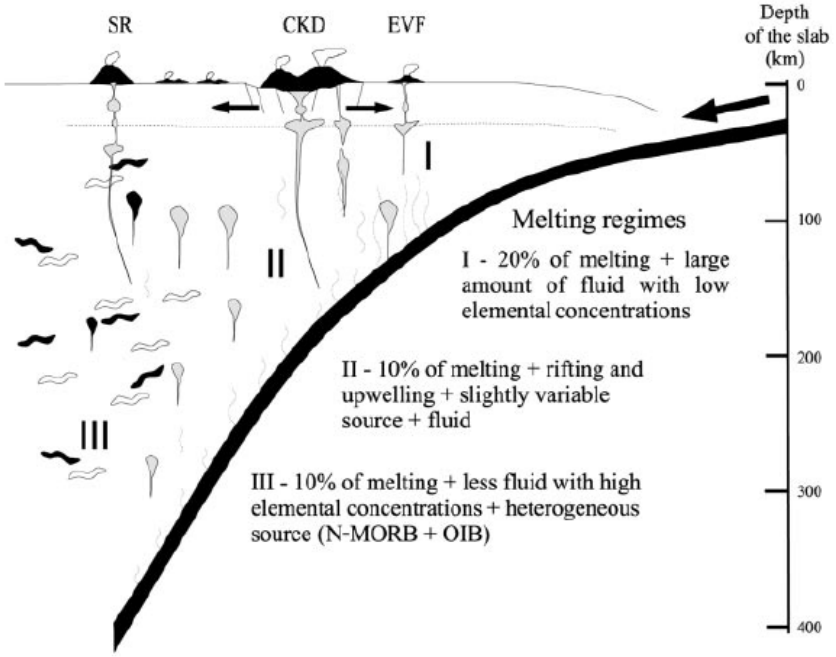

Fig. 1-2. Schematic model showing features of magma genesis under Kamchatka (Churikova et al., 2001).

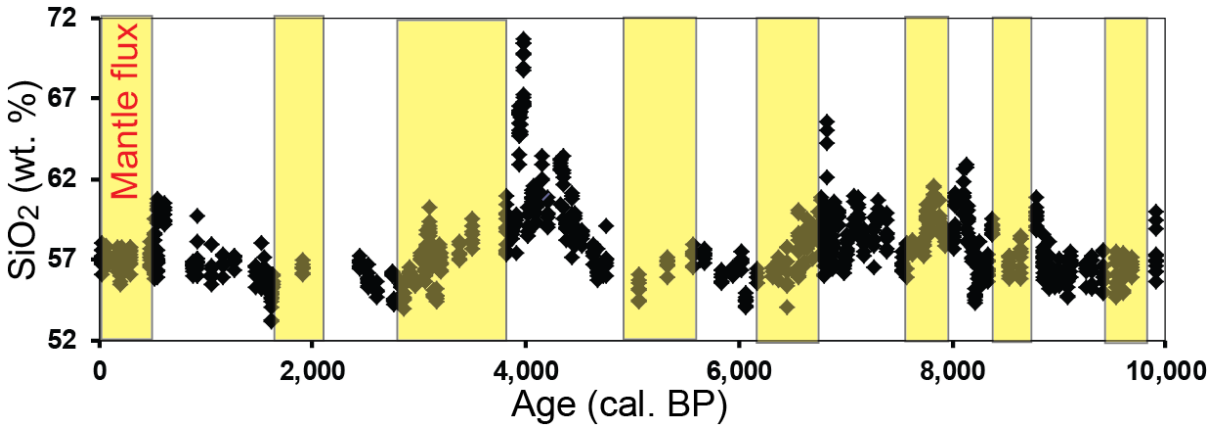

Fig. 1-3. SiO_2 variations of Klyuchevskoy magmas through time. Modified after Portnyagin et al. (2009). Yellow field indicate intensive mantle flux.

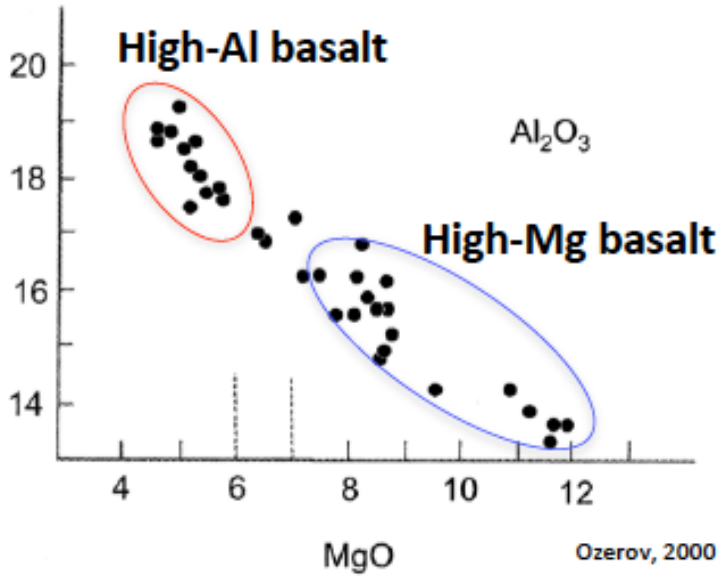

Fig. 1-4. MgO vs. Al_2O_3. Classification lones of Klyuchevskoy rocks (Ozerov et al., 2000).

Chapter 2. Tectonic setting and general geology of Klyuchevskoy volcano

2.1. Tectonic setting of Central Kamchatka Depression

The Central Kamchatka Depression (CKD) is a ca. 100km-wide valley between two volcanic belts, the Sredinny Ridge (SR) and the Eastern Volcanic Front (EVF) in the middle of the Kamchatka Peninsula. According to Churikova et al. (201X), the CKD is situated directly at a triple junction area (Fig. 1-5) where the Pacific, Bering and Okhotsk plates come together and convergence changes from a southwest-northeast direction to the northwest-southeast trending Aleutian-Bering-Alfa transform fault zone. Several different tectonic processes have been proposed for this area (Fig. 1-6): (1) slab window opening (Yogodzinski et al., 2001), (2) detachment of fragments from the Pacific plate (Levin et al., 2002), (3) slab edge heating in the mantle wedge due to decreasing thickness of the Pacific plate to the north of the Emperor Faults (Davaille and Lees, 2004; Portnyagin et al., 2007 a), and (4) a large input from slab melting (Portnyagin et al., 2007 b). Churikova et al. (201X) suggests that all of these processes could result in or contribute to the observed massive and voluminous mafic volcanism at CKD, which makes it one of the most volcanically active places on Earth.

Portnyagin et al. (2007a) suggest that the Pacific plate would bend toward the Kamchatka-Aleutian junction, and depths to the subducting slab beneath the CKD should be variable (80–180 km) in this area. Since the crustal thickness beneath the CKD is relatively constant (30–35 km) (Balesta et al., 1981), the mantle wedge thickness (i.e., “mantle column” beneath a volcano) decreases substantially towards the slab edge. The length of the mantle column, which can be potentially involved in magma generation, decreases from ~ 65 km beneath Tolbachik to ~55 km beneath Shiveluch volcano.

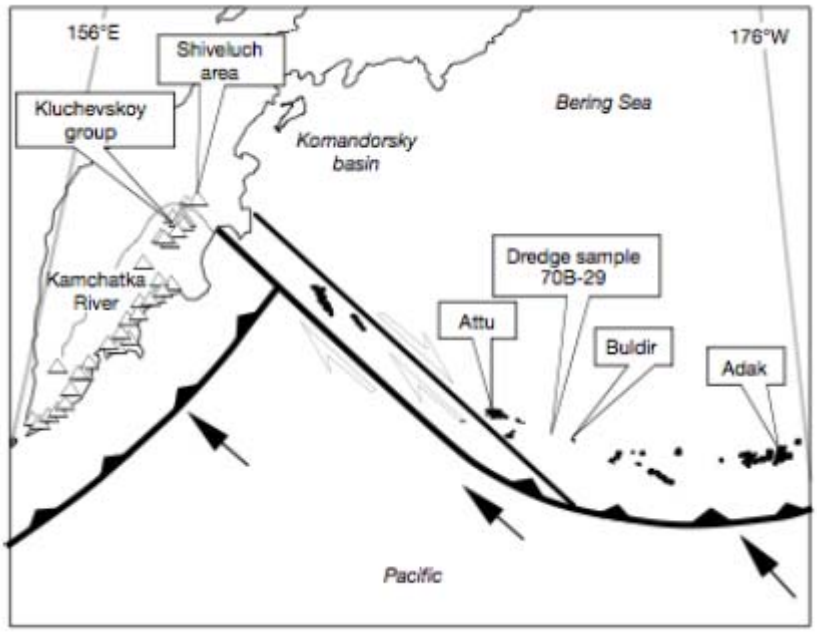

Fig. 1-5. Tectonic setting of Aleutian-Kamchatka Arc junction (Yogodzinski et al., 2001).

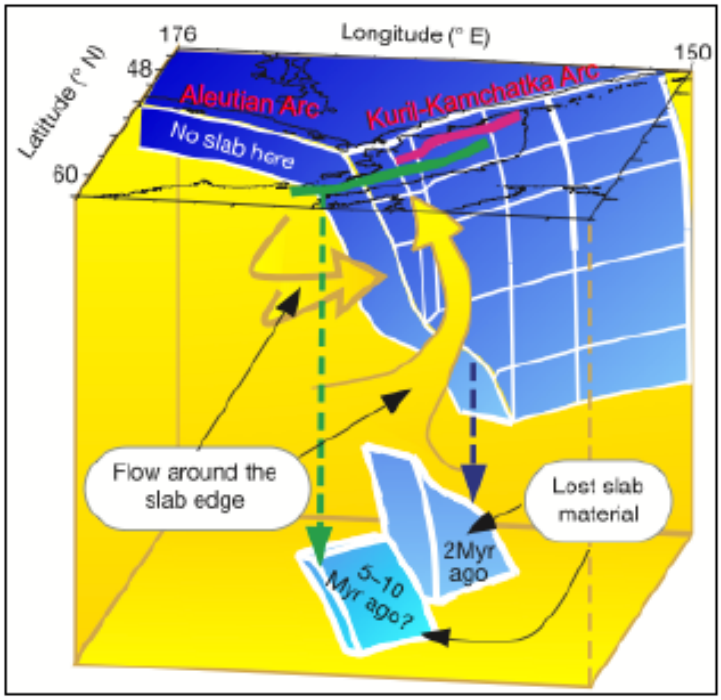

Fig. 1-6. Geodynamic model of Aleutian-Kamchatka junction and deep mantle flow (Levin et al., 2001).

2.2. Volcanoes of Central Kamchatka Depression and their temporal evolution

The Central Kamchatka Depression (CKD) is divided into northern (2000 km^2) and southern (6500 km^2) parts by Kamchatka River (Fig. 1-7). Northern CKD includes active Shiveluch volcano and extinct Kharchinsky, Zarechny volcanoes. Southern CKD include four active volcanoes: Klyuchevskoy, Bezymianny, Plosky Tolbachik, and Plosky Dalny (Fedotov and Masurenkov, 1991). The other 10 are extinct, including Kamen, Plosky Blizhny, Sredny, Ostry Tolbachik, Ovalnaya Zimina, Ostraya Zimina, Bolshaya Udina, Malaya Udina, Gorny Zub and Nikolka (Churikova et al., 201X). Klyuchevskoy, Kamen and Bezymianny volcanoes and the Ploskie Sopky massif are located on a large plateau of basalt-basaltic andesite composition with an elevation about 1500 m.

By Churikova et al., (201X) the sequence of activity that is repeated as several CKD volcanoes includes initial formation of volcanic plateaus, followed by constraction of stratovolcanoes and then monogenetic fissure systems (Fig. 1-8). The most plateau lavas were erupted ~262-274 ka. Recent geochronologic studies show that the basement to Tolbachik formed at 86 ka (Churikova et al., 2014) and at Shiveluch volcano about 82 ka. The youngest KGV volcanoes, Klyuchevskoy and Bezymianny, started to grow only at 7 ka (Braitseva et al., 1995) and 5.5 ka (Braitseva et al., 1991), respectively and are still highly active.

Fig. 1-7. Volcanoes of CKD.

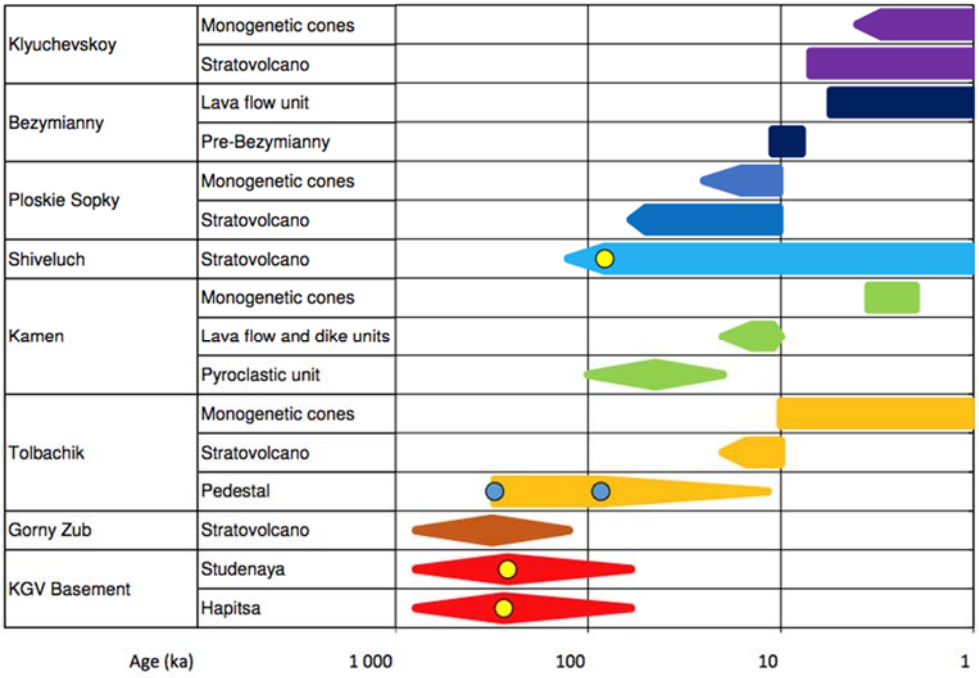

Fig. 1-8. Age-distribution diagram for CKD volcanoes. Data from Churikova et al., 201X.

2.3. Geology of Klyuchevskoy volcano and characteristics of activities

2.3.1. General geology

The Klyuchevskoy volcano (4750 m) is mainly composed of basaltic and andesitic lava flows and pyroclastic deposits (Fig. 1-9).

Basement of the volcano consists of volcanic and sedimentary deposits with layers of sands, ashes, breccias, volcanic conglomerate, bombs (Paleogene~Neogene), ashes and plateau basalts of late-Neogene~Pleistocene, and Pl-phyric basaltic and andesitic lavas (Vlodavets and Piip. 1957; Zavaritsky, 1935).

The volcano has been developed on the extinct Kamen and Ploskie Sopky volcanoes in the last 7000 years to form a main stratovolcano. It repeated explosive and effusive eruption on the summit and the flank, and there formed numerous amount of cinder cones and lava flows (Fig. 1-10). Diameter of central crater is approximately 700 m. Shape of crater vary frequently by eruptive activities and erosion process.

Fig. 1-9. Photograph of Klyuchevskoy volcano.

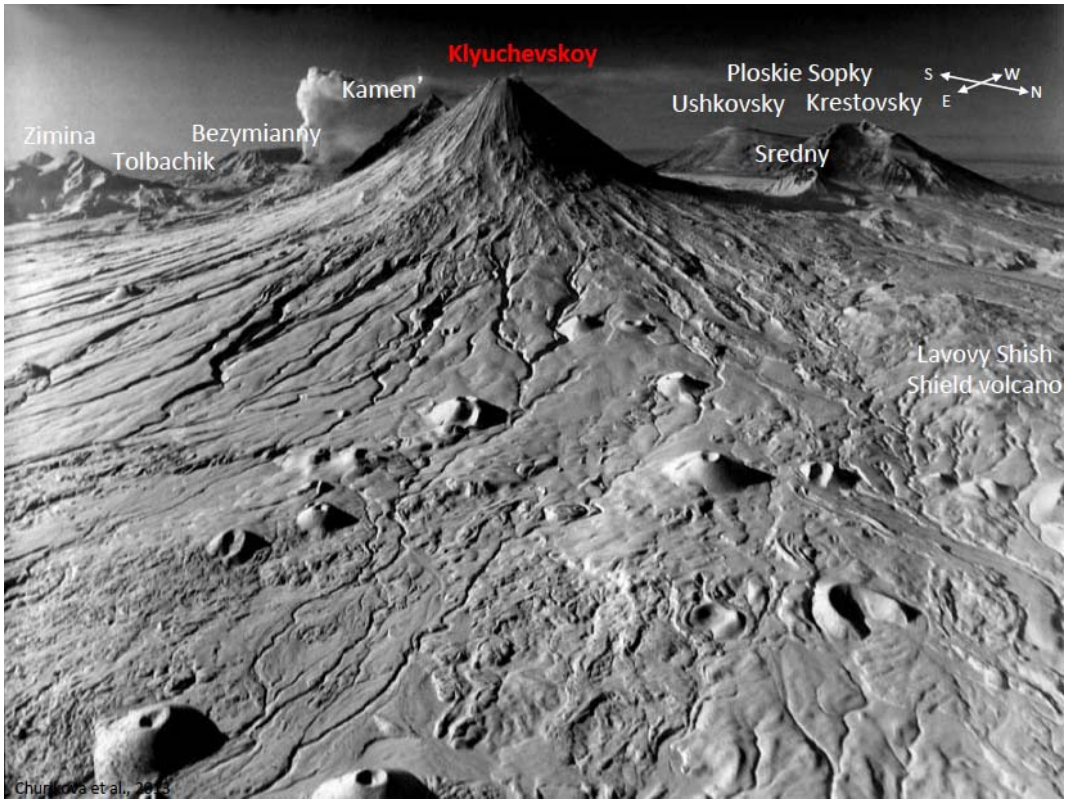

Fig. 1-10. Klyuchevskoy volcano with numerous cinder cones.

2.3.2. Prehistorical activities

The Klyuchevskoy volcano repeated flank eruptions since at least 3500 BP (Braitseva et al., 1995). In present time, number of cinder cones are more than 80. Most of the cinder cones concentrated on eastern slopes with the altitude of 500-3600 m (Fig. 1-11). According to the Atlas of Kamchatka (1974), CKD was formed by extension forces and main regional faults extended in NE direction. The cinder cones of Klyuchevskoy volcano located nearly on these faults (Melekestsev et al., 1974).

Some of the cones are partly destroyed (Fig. 1-12), and old lava flows has been covered by younger ones (Fig. 1-13). However, most of the cones keep good-shapes and we can easily detect them on the slopes.

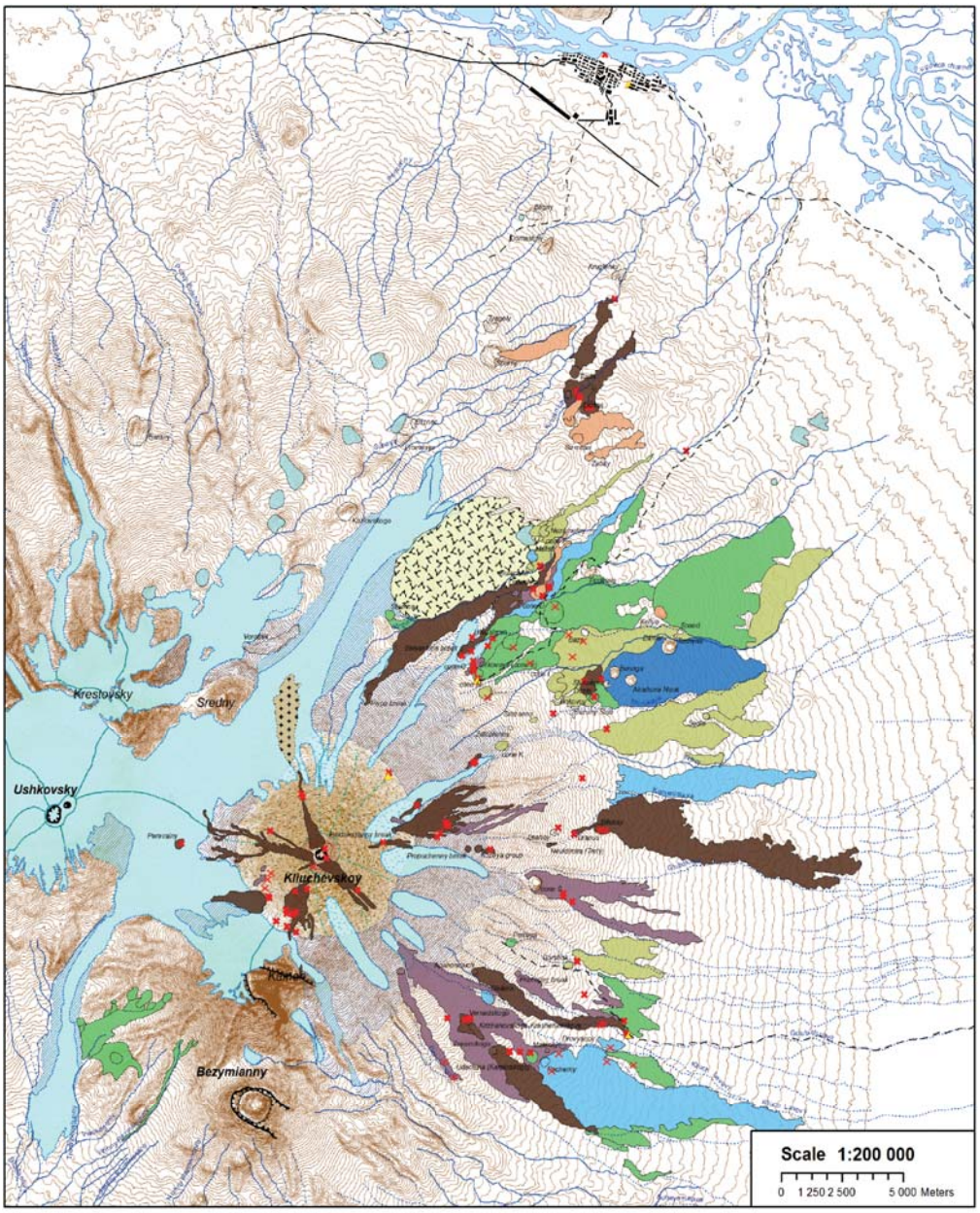

AGE OF LAVA FLOWS AND CINDERY CONES

observed eruptions (80-20 y.a.)
1500-1350 y.a.
2750 - 2100 y.a.
600 - 400 y.a.
1700-1650 y.a.
2950 - 2800 y.a.
4000 - 3000 y.a.
shield volcano Lavovy Shish
Tiltmeter stations
Sampling points

Fig. 1-11. Gelogical map of Klyuchevskoy volcano. Made by E. Klimenko.

Fig. 1-12. Cinder cone of prehistorical eruption (2750-2100 BP).

Fig. 1-13. Cinder cones named Ochki which are formed 600-400 BP.

2.3.3. Historical activities

Historical activities started since 1697 AD. Before 1932 AD, eruptions of Klyuchevskoy volcano were concentrated on the top of volcano. However, eruption style of the volcano had changed since 1932 AD (Fig. 1-14, 1-15). After a strong earthquake, a new flank eruption occurred and flowed down lava flows (Fig. 1-16, 1-17, Kulakov, 1934). The summit eruptions usually coexisted with the flank eruption after the eruption (Appendix, Table 1). The volcano repeated voluminous eruptions during 1932-1945 AD, and eruption rate is high compared with other stages, The altitude of flank eruption continuously goes up to the summit until 1989 AD. After strong, paroxysmal eruption of Klyuchevskoy volcano in October 1994 AD, volcanic activities concentrated on the top of volcano.

New effusive eruptions formed scoria cone in the central crater on the top of the volcano in 2003-2005 AD. Voluminous lava flows and explosive eruption has changed the shape of the central crater. Altitude of volcano has also changed to 4850 m.

Stronger eruptions started on 15th August 2013 AD (Fig. 1-18). Seismic tremor increased and light was observed on the top. Since 26th September, new lava flows streamed to east-southern slopes. Ash falls were observated in October. Colomn of ash clouds ascended to 7-8 km. According to Girina et al. (2014), new flank eruption began in October 2013 AD.

Late in 2014 AD, KVERT reported that both the abundance and the magnitude of shallow volcanic earthquakes began to increase during 19-20th December 2014 AD and again on 31st December 2014 AD; tremor became constant. The volcano was cloaked in clouds during 31st December 2014 AD to 1st January 2015 AD, but KVERT judged that a strombolian eruption probably began on 1st January 2015 AD, which is consistent with a satellite thermal anomaly. On 2nd January 2015 AD, the Aviation Color Code rose from Green

(normal) to Yellow (which is a sign of elevated unrest). During the course of January 2015 AD the volcano resumed frequent eruptive activity and that month KVERT issued ~15 VONAs for Klyuchevskoy. The eruption stopped on 24th March 2015 AD and any later events after 6th April 2015 AD extend beyond the current reporting period (www.kscnet.ru, www.volcano.si.edu).

Average productivety of Klyuchevskoy volcano is 60 million tons/year and is believed to be the most productive arc volcano on Earth (Fig. 1-14).

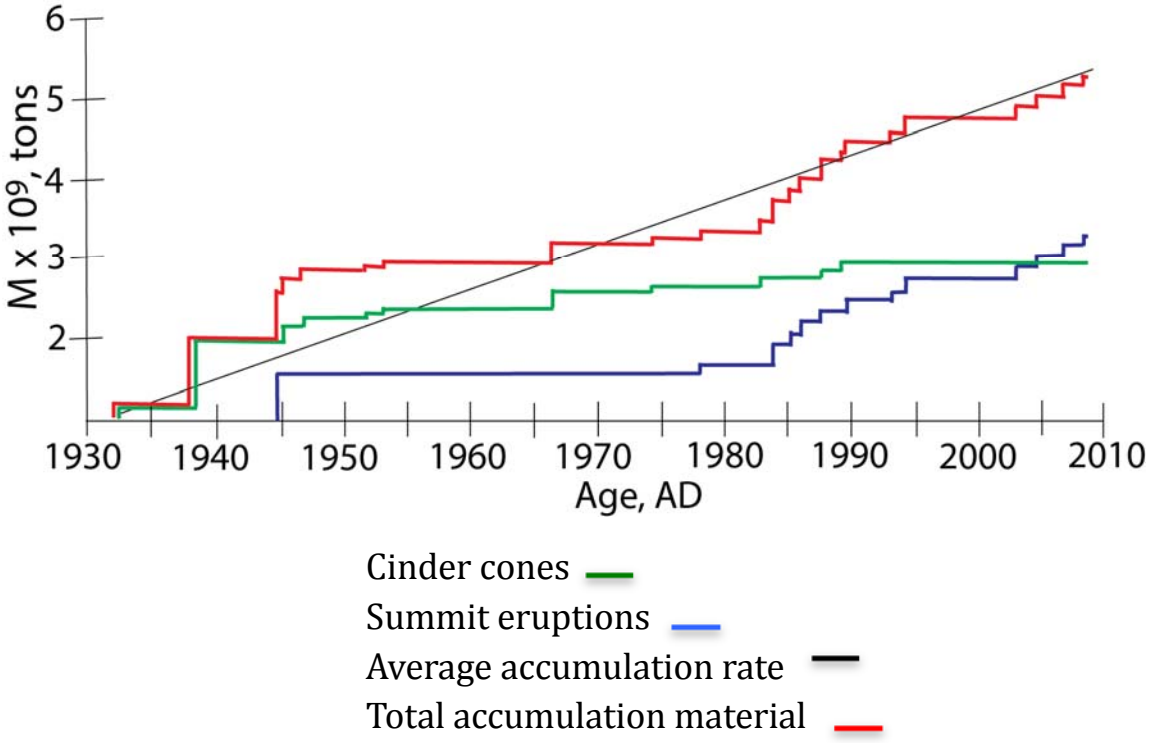

Fig. 1-14. Productivity of Klyuchevskoy volcano in historical time by Fedotov et al., 2005.

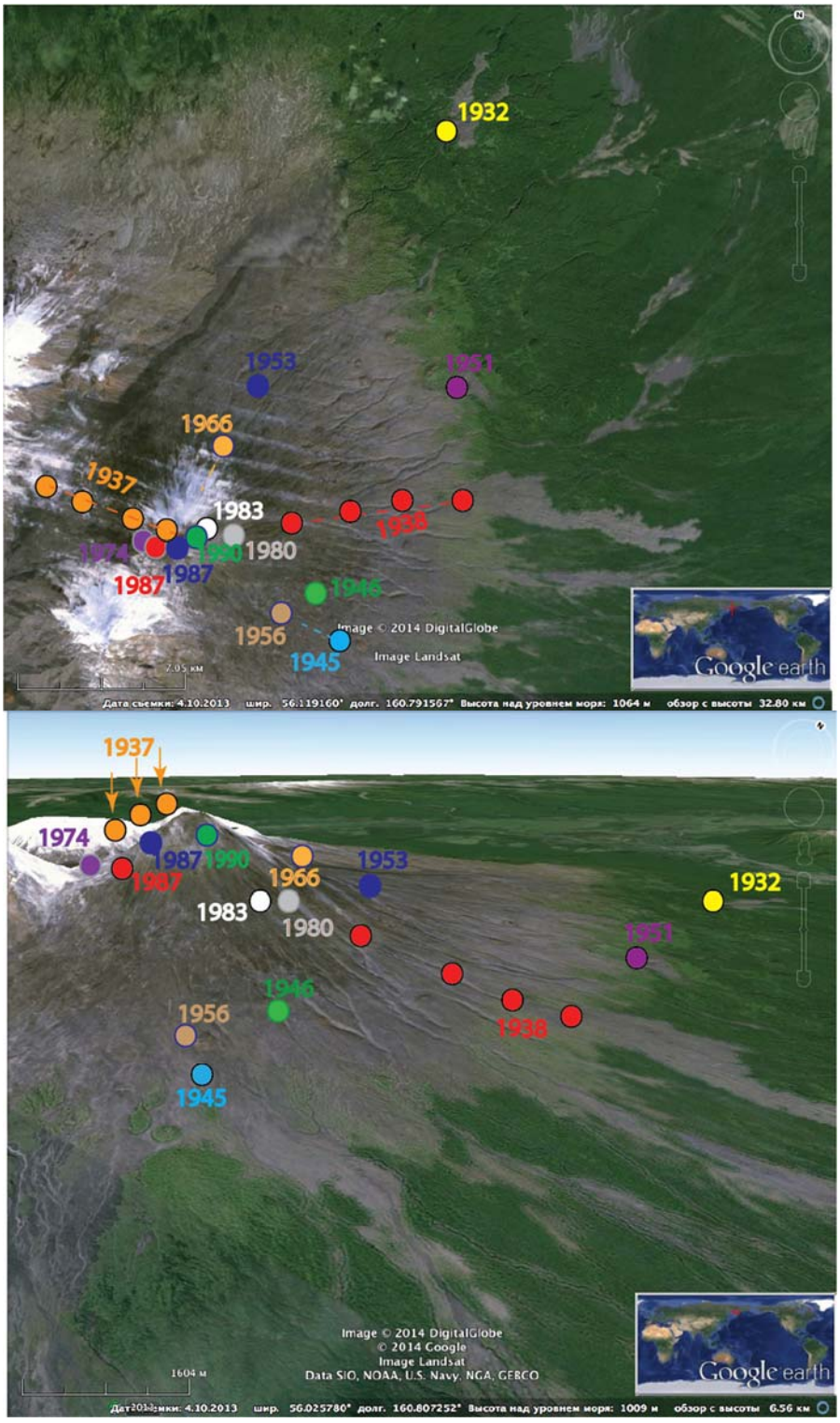

Fig. 1-15. Scheme of location historical cinder cones. Map wsd used from Google Map.

Fig. 1-16. Lava flows of Tuila flank eruption in 1932-1933.

Fig. 1-17. Lava flows of Bilyukai flank eruption in 1938.

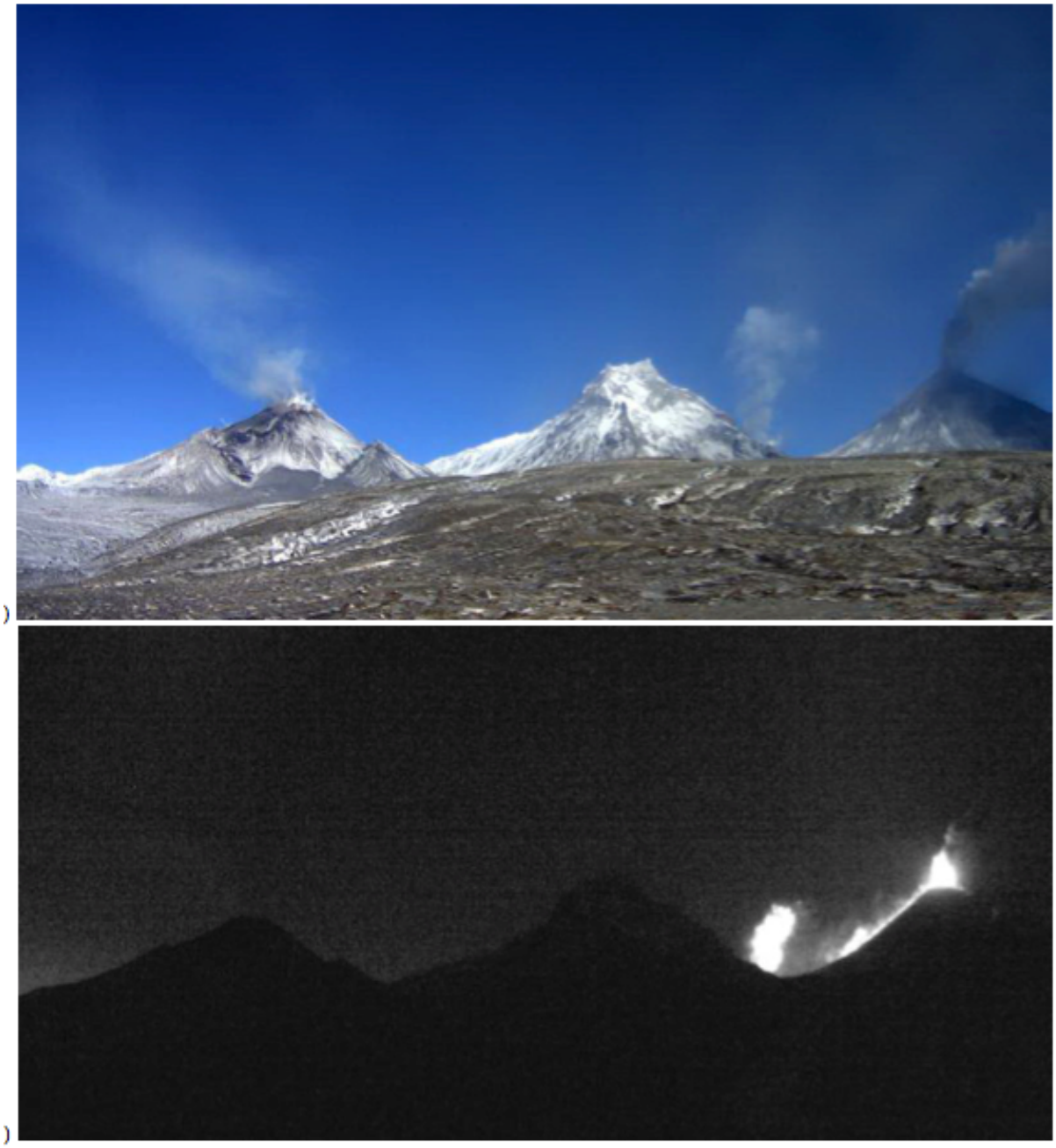

Fig. 1-18. Activity of Klyuchevkoy volcano in day and night. 12th October, 2013. (Girina et al., 2014).

Chapter 3. Samples and analytical procedures

In this study, we have collected ~250 samples that span from ~4000 BP to 2014 AD in eruption ages. The sampling localities are shown in Fig. 1-11. The whole-rock compositions were determined for all these samples using X-ray fluorescence (XRF) spectrometry (Fig. 1-19). We have also determined the trace element concentrations by an inductively coupled plasma mass spectrometer (ICP–MS), and Sr, Nd, and Pb isotopic compositions by a multiple collector (MC)–ICP–MS and a thermal ionization mass spectrometer for selected samples.

Whole-rock major and trace element compositions were determined by XRF spectrometry, using a Spectoris MagiX PRO at the Graduate School of Science, Hokkaido University. Rock specimens were crushed to coarse chips 3–5 mm in diameter. The chips were rinsed with deionized water in an ultrasonic bath, and then dried at 110°C for more than 12 h. The washed chips were ground using an alumina puck mill. The compositions were determined on glass beads prepared by fusion with anhydrous lithium tetraborate (10:1 sample dilution).

Concentrations of additional trace elements were measured for selected samples using an ICP–MS, Thermo Electron X-series. Both the analytical reproducibility and the precision of natural samples are commonly better than 5% for most elements. The analytical procedures for chemical separation followed the methods of Pin et al. (1994) and Noguchi et al. (2011) for Sr, Pin et al. (1994) and Pin and Zalduegui (1997) for Nd, and Kuritani and Nakamura (2002) for Pb. Sr and Nd isotopic ratios were determined with a TIMS, Finnigan MAT262, and a MC–ICP–MS, Neptune plus, Thermo-Finnigan, at the Graduate School of Science, Hokkaido University. Mass fractionation factors for Sr and Nd were internally corrected using $^{86}Sr/^{88}Sr$ = 0.1194 and $^{146}Nd/^{144}Nd$ = 0.7219, respectively. Pb isotopic ratios were measured using the same MC–ICP–MS. Mass fractionation for Pb isotopes was corrected using Tl as an external

standard. Additional corrections were performed by applying a standard bracketing method using NIST987, JNdi-1, and NIST981 for Sr, Nd, and Pb isotopic analysis, respectively, and the data were finally normalized to $^{87}Sr/^{86}Sr = 0.710214$ for NIST 987, $^{143}Nd/^{144}Nd = 0.512117$ for JNdi-1, and $^{206}Pb/^{204}Pb = 16.9424$, $^{207}Pb/^{204}Pb = 15.5003$, and $^{208}Pb/^{204}Pb = 36.7266$ for NIST981 (Kuritani and Nakamura, 2003). The isotopic ratios of the GSJ standard JB-3, measured in the course of this study, were $^{87}Sr/^{86}Sr = 0.703375 \pm 10$ (n = 7), $^{143}Nd/^{144}Nd = 0.513065 \pm 1$ (n = 3), and $^{206}Pb/^{204}Pb = 18.2962 \pm 5$, $^{207}Pb/^{204}Pb = 15.5393 \pm 7$, and $^{208}Pb/^{204}Pb = 38.2545 \pm 14$ (n =5).

Analytical methods	Number of samples
XRF	254
ICP-MS	81
TIMS	40
MC-ICP-MS	30
Description (microscopy)	82

Fig.1-19. Analytical methods and numer of samples.

Chapter 4. Petrography

Lavas and scoria from the Klyuchevskoy volcano are mainly basalts and basaltic andesites with plagioclase, olivine, clinopyroxene, orthopyroxene, and Fe-Ti oxides phenocrysts (defined as >0.1 mm in diameter). The phenocryst contents of pre-historic eruptions are variable at 35–70 vol.%; however those of recent eruptions are 55-65 vol.% (Figs. 1-20~22). In addition, prehistoric rocks generally contain large amounts of clinopyroxene phenocrysts (Fig. 1-20). The modal composition of plagioclase phenocrysts is 15-60 vol.%, with the maximum size of 3.8 mm. Phenocryst contents of olivine, which are up to 2.0 mm in diameter, are 2-10 vol.%. The clinopyroxene (2–12 vol.%) and orthopyroxene (<5 vol.%) phenocrysts are very large, which are up to 7.5 mm in length.

For historical eruptions, we found some difference due to eruption age (Fig. 1-21 and 1-22). In 1932 and 1938, Ol-bearing Opx, Cpx basaltic andesite erupted. Some of the rocks contain xenoliths with Ol, Opx, Cpx (Fig. 1-21, Group 1). Mineral assemblages are characterized by smaller amount of Pl and larger amount of Cpx, Ol. Crystals are typically anhedral. Honeycomb textures of Ol, Cpx and sponge sellular of Ol are observed. Phenocryst assemblages of Ol and Cpx usually exist. In 1945 to 1966, Opx-Cpx bearing Ol basaltic andesites are dominant (Pl-rich compared to other eruptions). Microcrystals of Pl, Ol, Cpx can be seen in groudmass (Fig. 1-21, Group 2A). Some rocks have mantle xenoliths. Some Pl crystals are anhedral, dusty and homey comb. Amount of mafic minerals are increasing in rocks of 1974-1988. Groundmass consists of small crystals of Ol and Cpx (Fig. 1-21, Group 2B). Mantle xenoliths with assemblage of Ol, Cpx, Opx are observed. Hopper, dusty zone and

honeycomb structure of Pl also exist. Comparing with previous eruptions, Pl crystals are dominant in 1993 and 1994 eruptions (Fig. 1-21, Group 3).

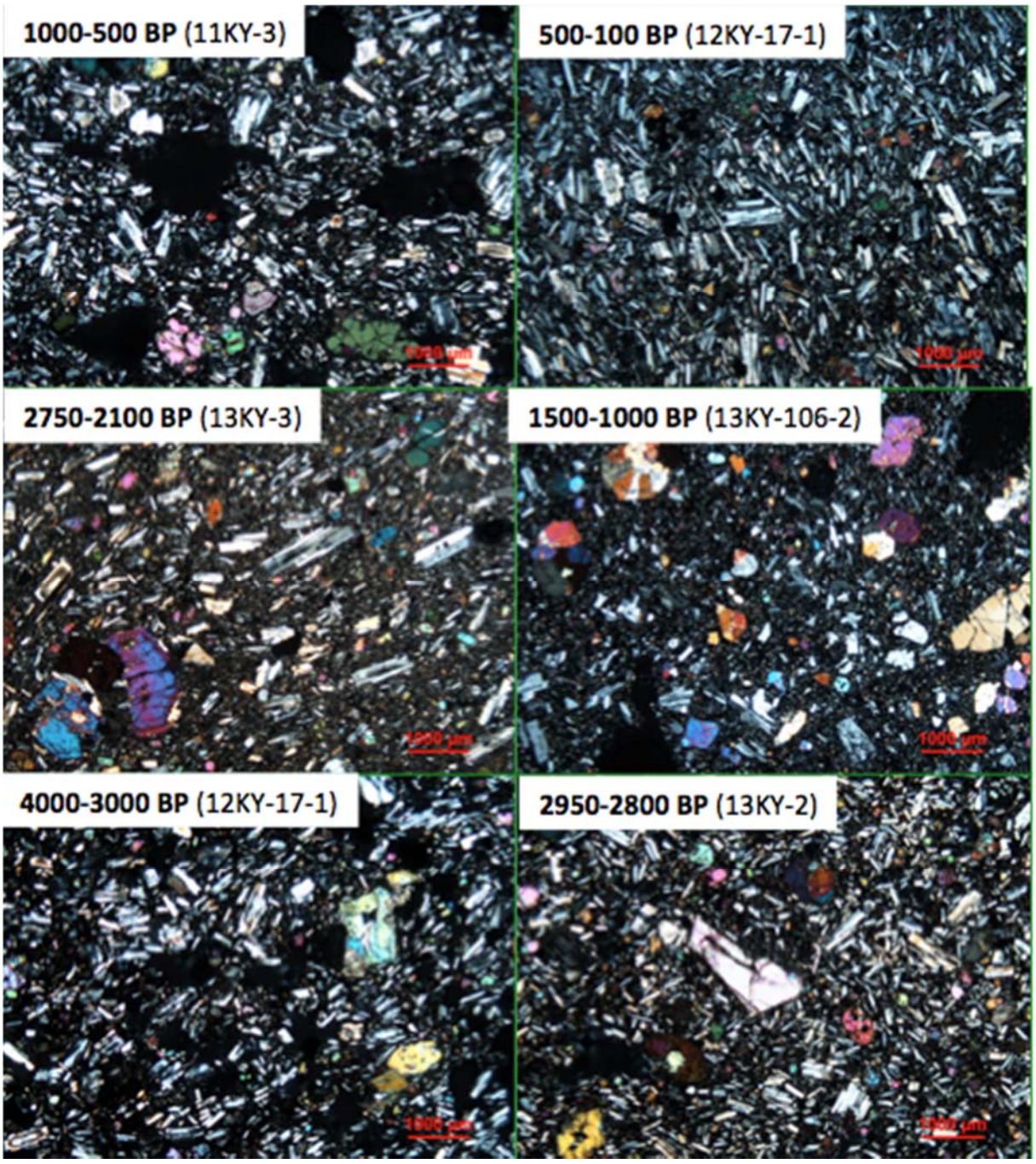

Fig. 1-20. Representative photos of prehistorical eruptions. Photos from Shimada san.

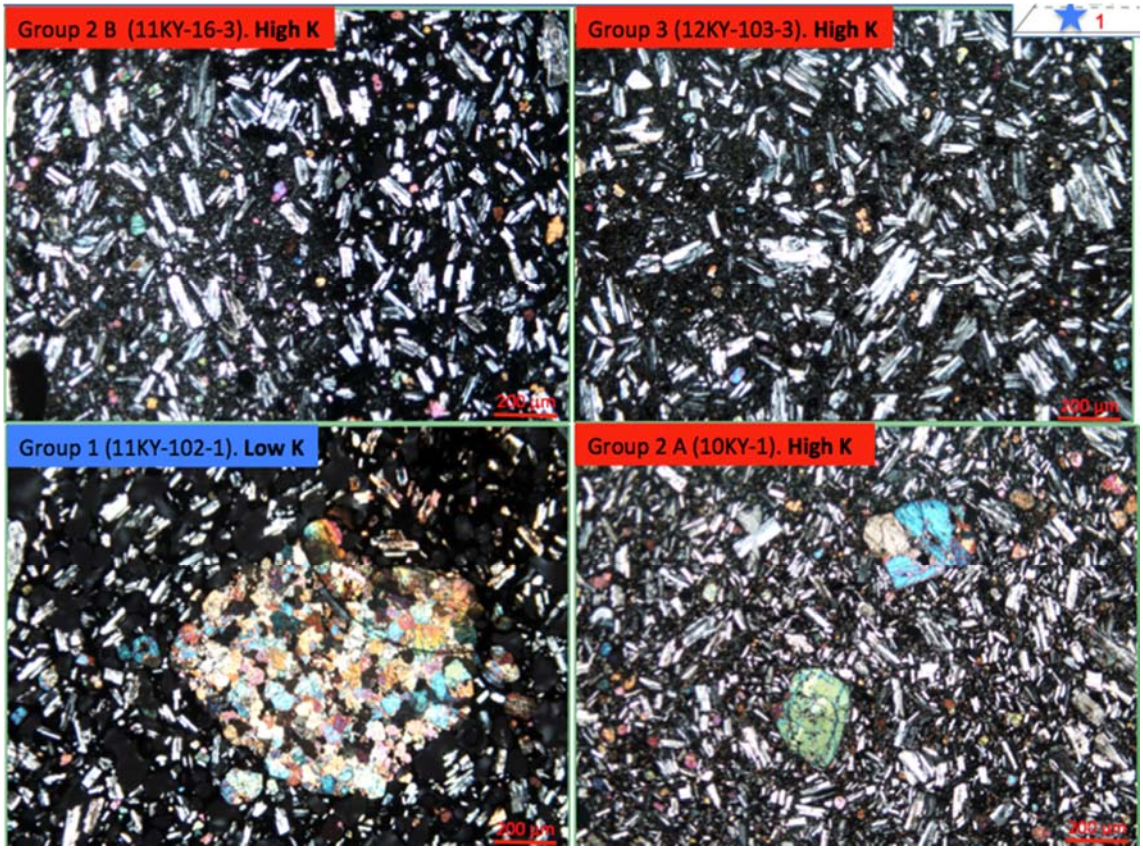

Fig. 1-21. Representative photos of historical eruptions.

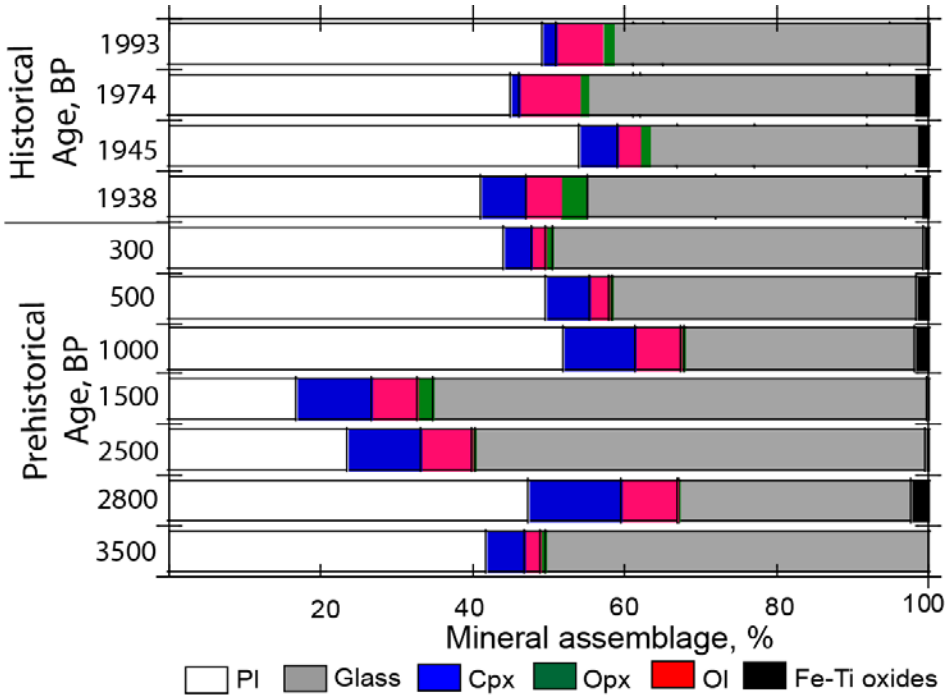

Fig. 1-22. Mineral assemblage of main stages of Klyuchevskoy volcano. Shimada san provided data for prehistorical eruptions.

Chapter 5. Geochemistry

5.1. Major and trace element compositions

Whole-rock major and trace element compositions of the samples, determined by XRF, are listed in Supplementary. The SiO_2 variation diagrams for TiO_2, Al_2O_3, MgO, CaO, and K_2O are displayed in Fig. 1-23, and those for Ni, Y, Zr, and Ba are shown in Fig. 1-24. In the figures, the data of Auer et al. (2009) for older products (>3500 BP) are also shown. The samples show large variation in SiO_2 content (51.3–55.6 wt.%). As has been reported in the previous studies (e.g., Kersting and Arculus, 1995; Ozerov, 2000), the products range in composition from high MgO–low Al_2O_3 to low MgO–high Al_2O_3; on this basis the compositions have been divided into "high-MgO basalts" and "high-Al_2O_3 basalts". The MgO-rich samples are also characterized by high CaO and Ni and low SiO_2, TiO_2, Na_2O, K_2O, and P_2O_5, Rb, Y, Zr, and Ba contents. The compositions of the eruption products also show some temporal variations. The samples of 2950-2800 BP products have relatively high MgO and low K_2O contents, and those of younger samples (≥1937 AD) have low MgO and high K_2O content. It is notable that the samples of the 1932 AD eruption have relatively high K_2O and MgO contents. These samples are also characterized by high CaO, Rb, and Ba and low Al_2O_3 and Y and Zr at a given SiO_2 content.

The primitive mantle and chondrite normalized multi-element diagram for the samples is shown in Fig. 1-25 and Fig. 1-26. The patterns for the Klyuchevskoy samples are characterized by negative anomalies of Nb and Ta, and positive spikes in Sr, which are characteristics of subduction-zone magmas. The trace element concentrations of the Mg-rich

samples are lower than those of the Mg-poor (SiO_2- and Al_2O_3-rich) samples. Prehistorical magma, especially for oldest rocks (2800~2950 BP), typically has lower contents of LREE (e.g. La, Ce, Nd, Sm). Toward to recent historical activities, magma became more enriched in LREE and HREE (e.g. Lu, Yb, Tm) (Fig. 1-26).

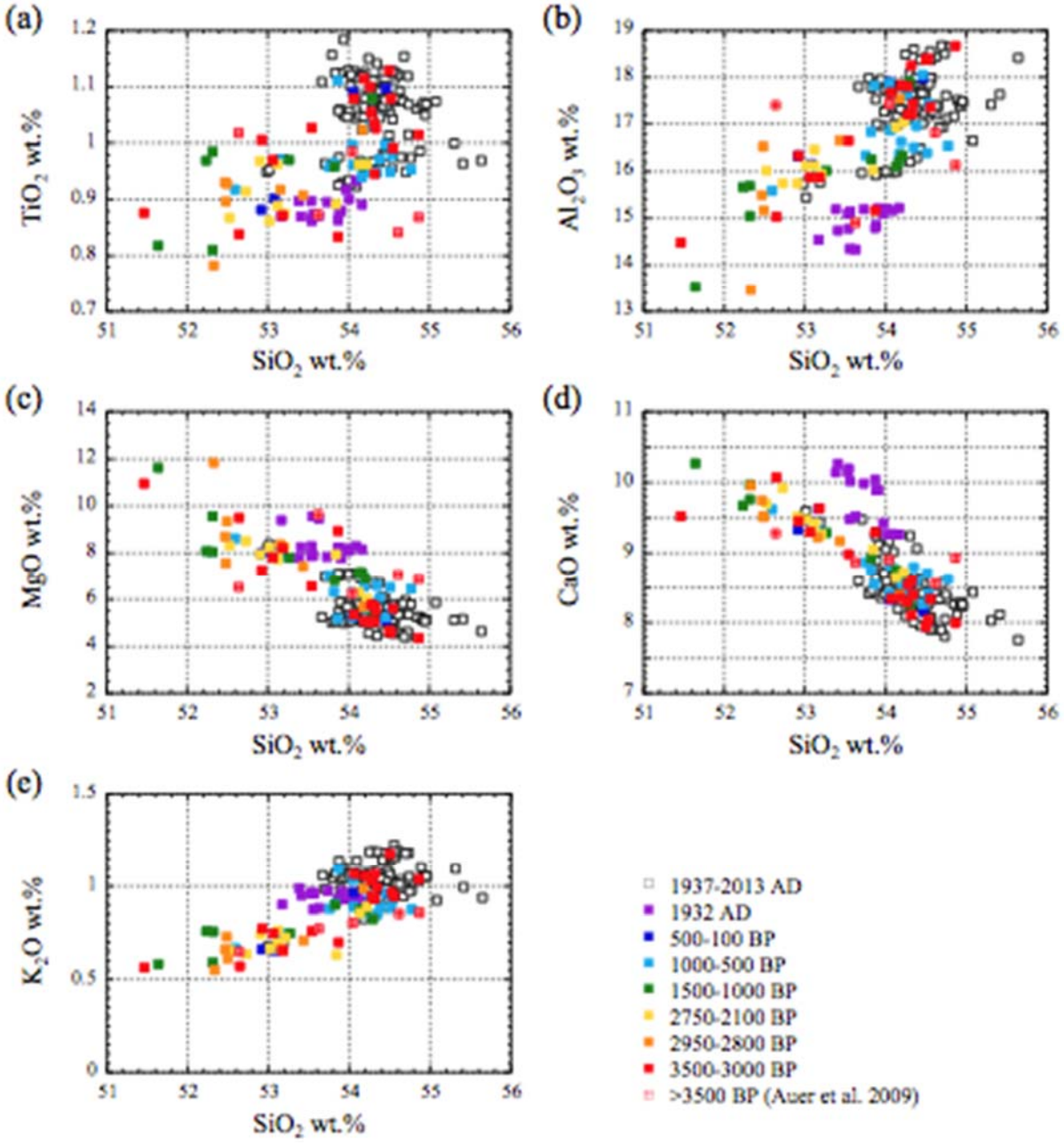

Fig. 1-23. The SiO_2 variation diagram for TiO_2, Al_2O_3, MgO, CaO, and K_2O of samples from Klyuchevskoy volcano. The data for >3500 BP are taken from Auer et al. (2009).

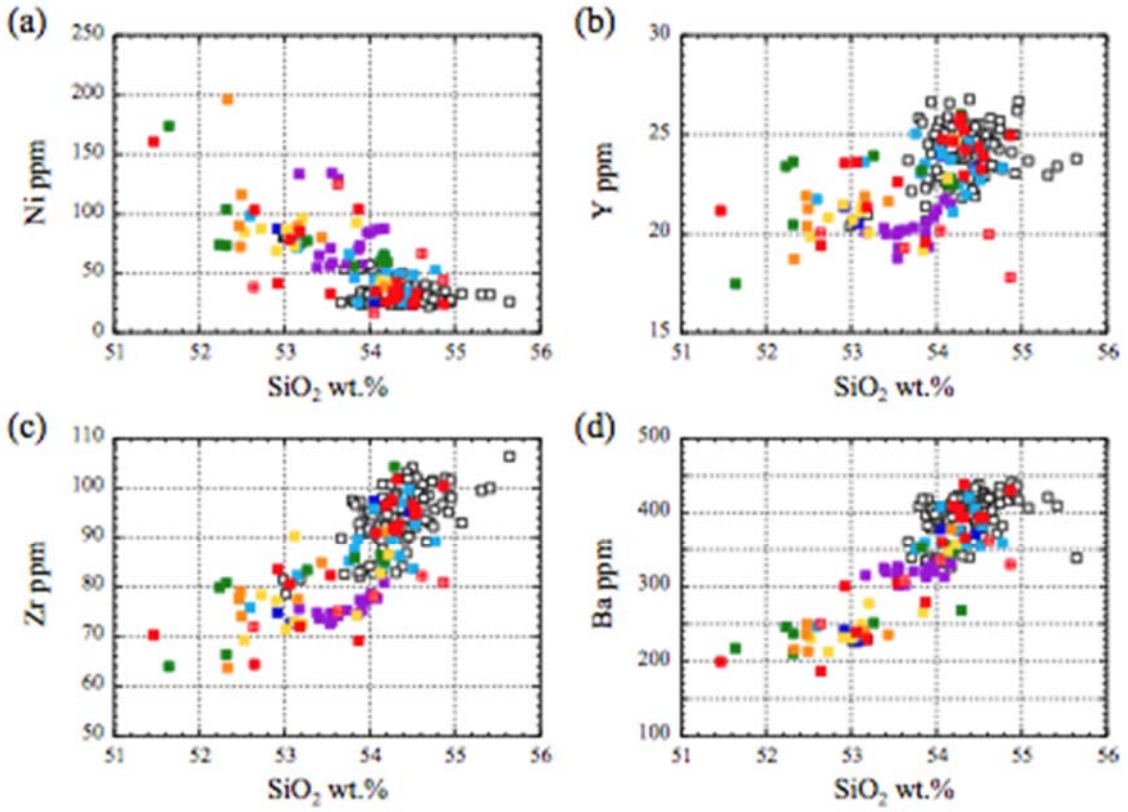

Fig. 1-24. The SiO_2 variation diagram for Ni, Y, Zr, and Ba of samples from Klyuchevskoy volcano. The legend is the same as Fig. 5-1-1.

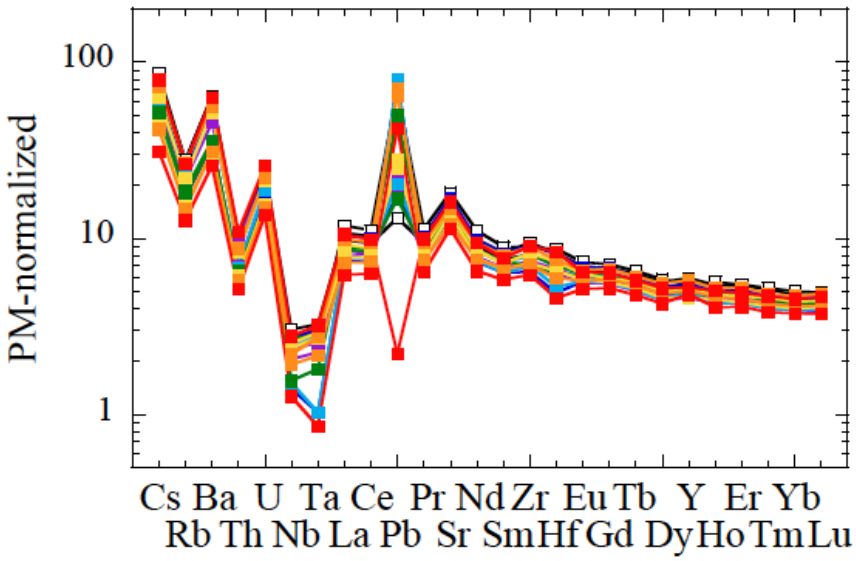

Fig. 1-25. Primitive mantle normalized multi-element concentration diagram for representative

samples of the Klyuchevskoy volcano. Trace element concentrations of primitive mantle are taken from Sun and McDonough (1989).

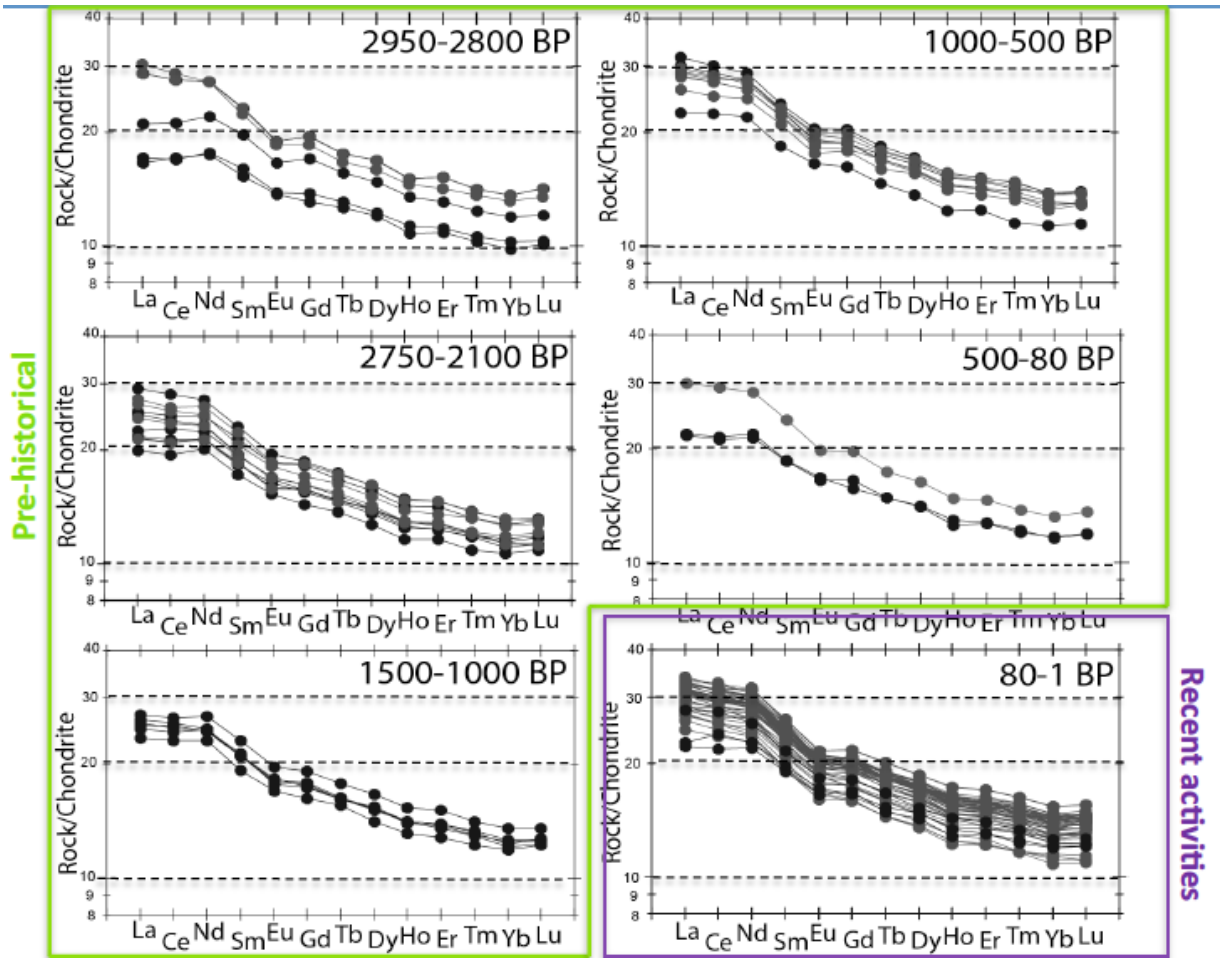

Fig. 1-26. REE patterns for klyuchevskoy volcanic group.

5.2. Radiogenic isotopes

Variations in Sr, Nd, and Pb isotopic compositions with SiO_2 content are shown in Figs. 1-27 a-c. The MgO-rich (SiO_2-poor) samples have relatively lower $^{87}Sr/^{86}Sr$ and $^{206}Pb/^{204}Pb$ ratios than those of the MgO-poor samples, while $^{143}Nd/^{144}Nd$ ratios of the MgO-rich samples are similar to those of the MgO-poor samples, with some exceptional samples. Figs. 1-27 d-f also shows $^{143}Nd/^{144}Nd$-$^{87}Sr/^{86}Sr$, $^{207}Pb/^{204}Pb$-$^{206}Pb/^{204}Pb$, and $^{208}Pb/^{204}Pb$-$^{206}Pb/^{204}Pb$ diagrams. In the $^{207}Pb/^{204}Pb$-$^{206}Pb/^{204}Pb$ and $^{208}Pb/^{204}Pb$-$^{206}Pb/^{204}Pb$ diagrams, the data essentially show linear trend, and the MgO-poor samples have relatively radiogenic Pb isotopic compositions.

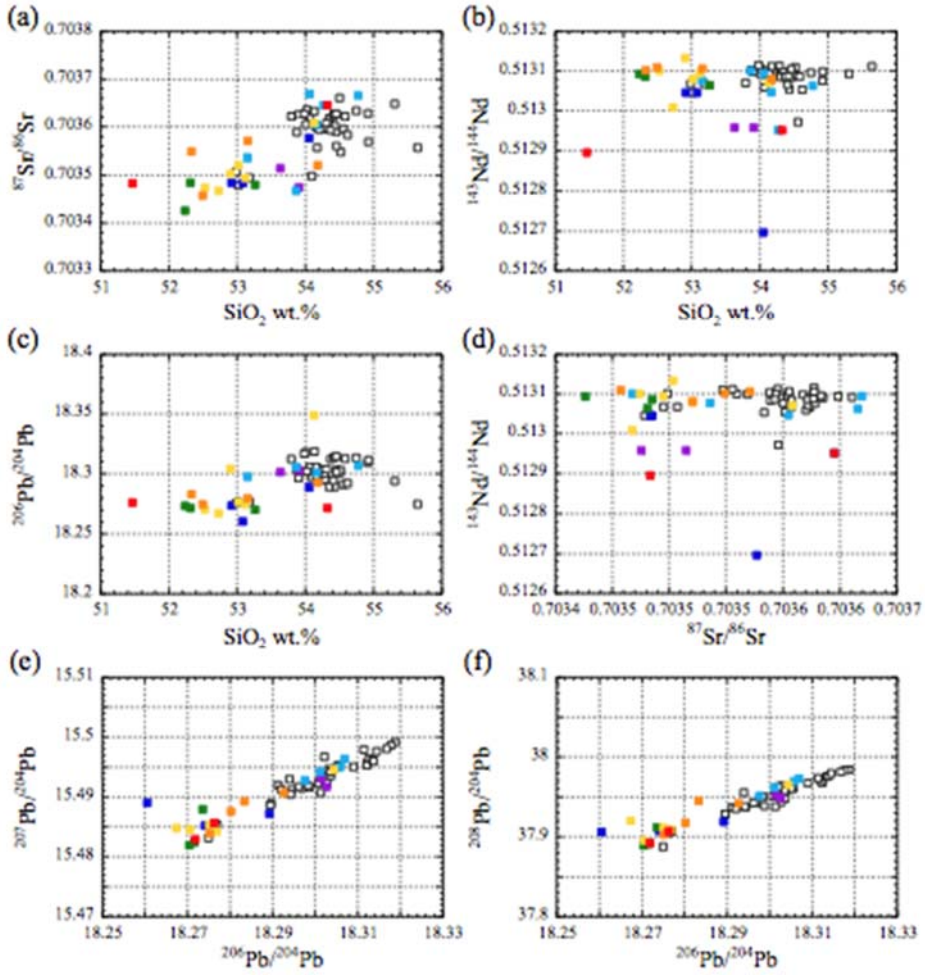

Fig. 1-27. The Sr, Nd, and Pb isotopic compositions for samples of the Klyuchevskoy volcano.

5.3. Comparison of Klyuchevkoy volcano with other volcanoes in Central Kamchatka Depression

Geochemical and isotopic comparisons were studied for volcanoes of CKD. This is important, because comparing volcanoes we can identify specific features of Klyuchevskoy volcano and temporal variations. Harker diagrams suggest that Klyuchevskoy and Tolbachik volcanoes characterized by more mafic and basic composition in comparing with another volcanoes of CKD (higher MgO contents, lower SiO_2) (Fig. 1-28). Harker diagrams suggest that Klyuchevskoy and Tolbachik volcanoes characterized by more mafic and basic composition in comparing with another volcanoes of CKD. However, Klyuchevskoy volcano has lower contents of incompatible elements (e.g. K2O, Zr, Rb, Ba) and higher HFS (Nb, Ta). Sr-Nd isotopic variations of Klyuchevskoy volcano are nearly same with another volcanoes of CKD. In most similarities are observed with Tolbachik and Bezymianny volcanoes. However, some of the Klyuchevskoy rocks have lower Nd isotopic ratios (Fig. 1-29).

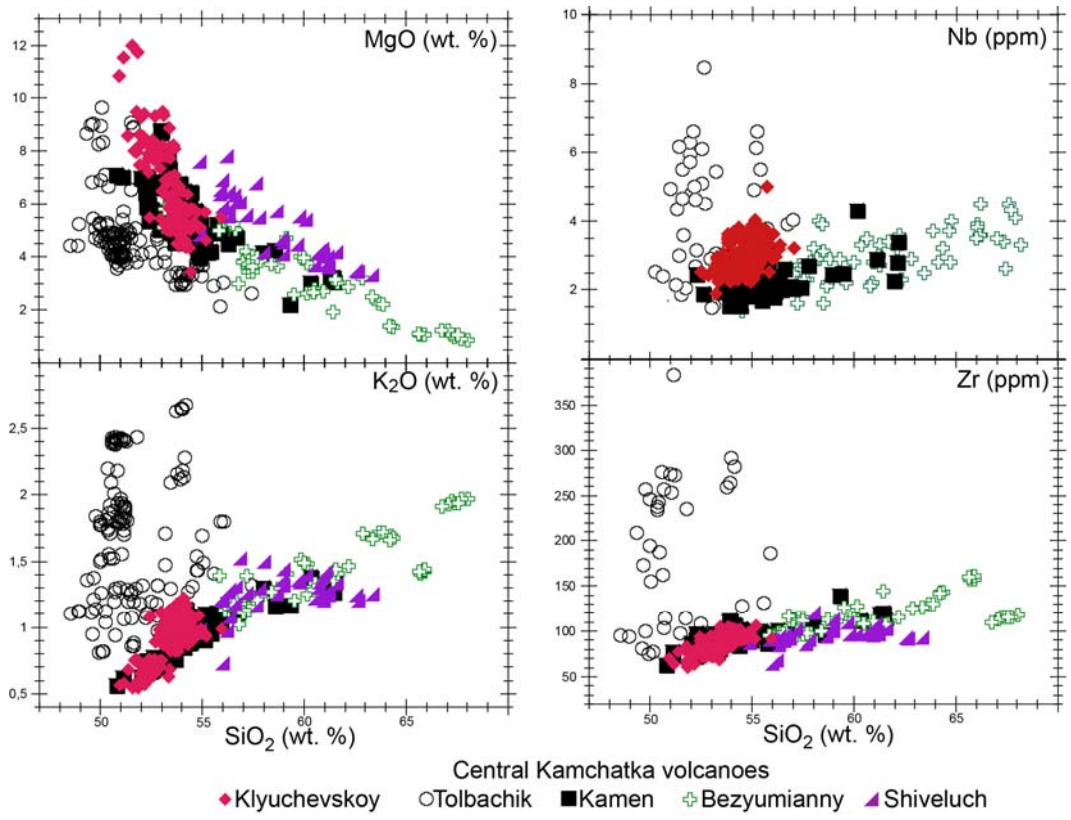

Fig. 1-28. Harker diagrams for Central Kamchatka Depression. With Using data Churikova et al., 2001; Churikova et al., 2013; Churikova et al., 201X; Almeetev et al., 2013, Gorbach et al., 2013.

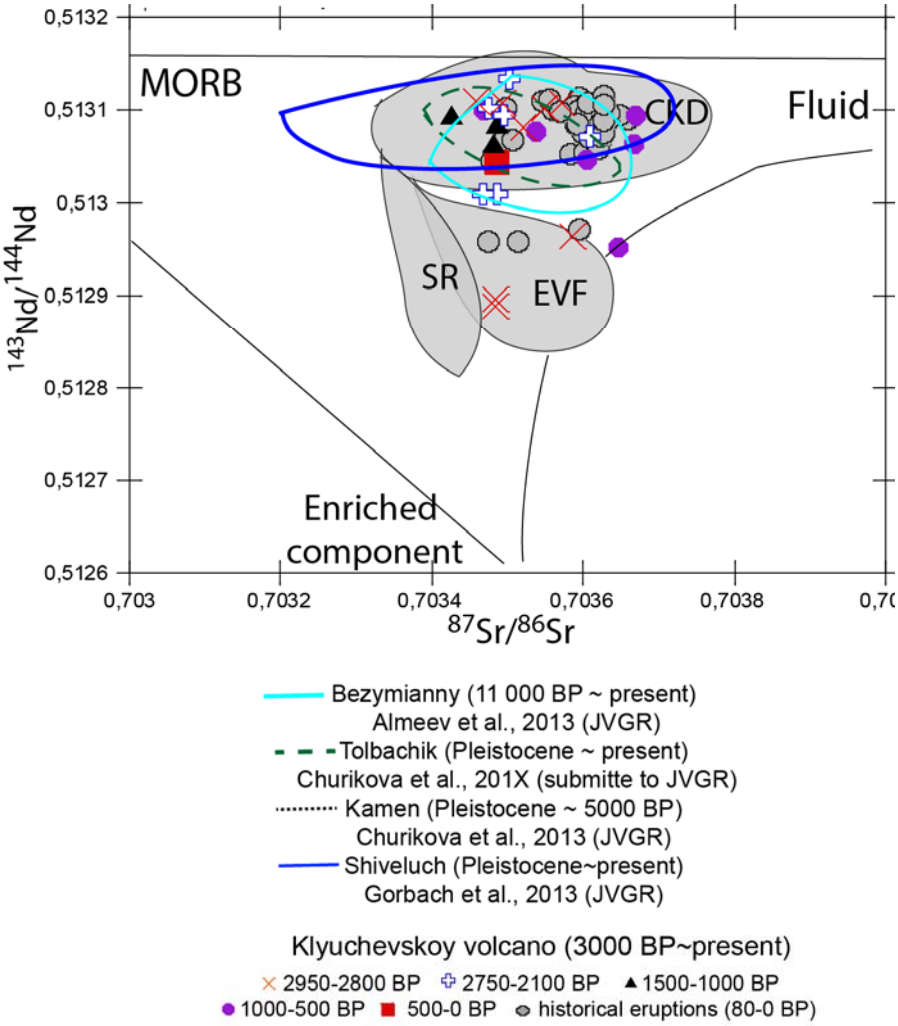

Fig. 1-29. Sr-Nd isotopic ratio of Central Kamchatka volcanoes.

Note: MORB- Mid-ocean ridge basalt. SR – Sredinny Ridge (Churikova et al., 2001). EVF – East volcanic front (Churikova et al., 2001). CKD – Central Kamchatka Depression (Churikova et al., 2001).

Chapter 6. Spatial and geochemical variations of cinder cones

6.1. Spatial variations of cinder cones

The location of cinder cones and geochemical characteristics can provide important information about spatial variation of magma in crust. Analysis of the location cinder cones suggests that flank eruptions mostly are located in North-East (NE) and South-East (SE) sectors (Fig. 1-30). By Atlas of Kamchatka (1974) CKD was formed by extension forces. Main regional fault extended in NE direction. Debris avalanches of another CKD volcanoes have direction of deposits valley in NE sector. This is one of the additional argument to important role of regional fault.

Analysis of the location historical cinder cones suggests that flank eruptions had gone up to the summit from 450 m to 4500 m since 1932 until 1989 (Fig. 1-31). Consequently, distance from central crater degrease with time. Clear dependence volume of volcanic material and years of eruptions are not observed. However, most effusive eruptions existed in the beginning of the cycle.

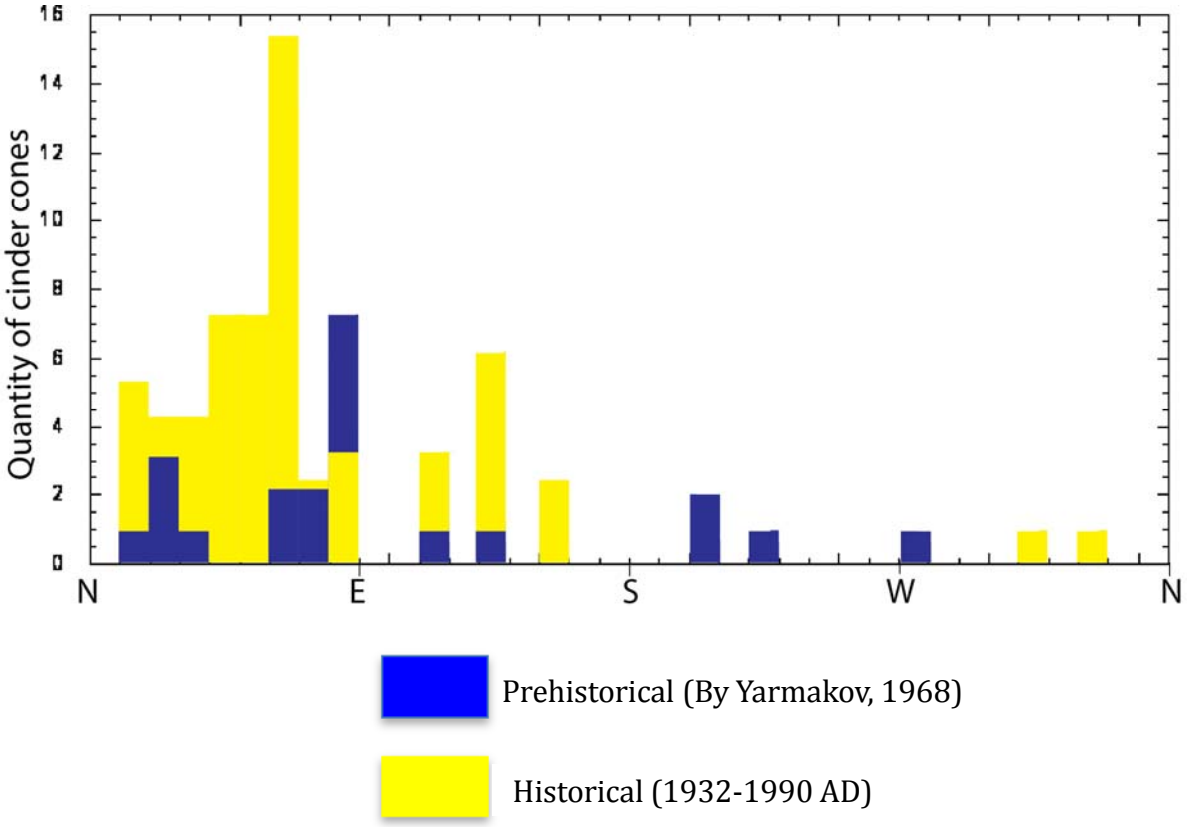

Fig. 1-30. Location of prehistorical and historical cinder cones.

Note: N - North, E – East, S – South, W-west.

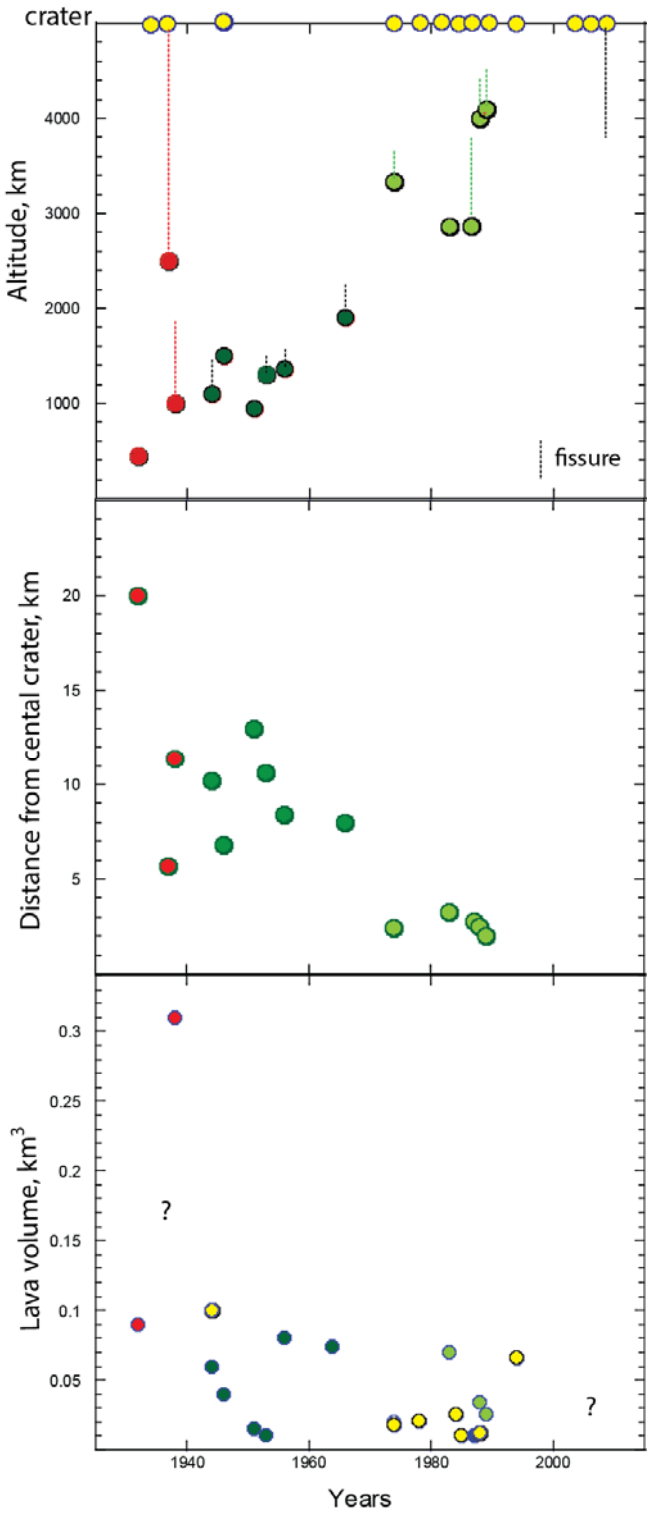

Fig. 1-31. Spatial variations of historical cinder cones. Different colors indicate following magmatic groups: red color is group1, dark green coloris group 2A, light green color is group 2B, yellow color is group 3.

6.2. Geochemical variations of historical magma

Location of cinder cones, geochemical composition and isotopic ratios can allow us determined several groups in historical eruptions. These groups have various year of cinder cones formation and specific petrographical features (Figs. 1-31~36).

Group 1. Eruptions on the flank formed cinder cones on North-North-East, East and West slopes of volcano in 1932-1938. These are the most productivity eruptions in historical time. Fissures were formed from 200 m to 1000 m of altitude. For this group are typically highest Mg, Ca. Lowest Sr, Ba, Rb, Y, K_2O, TiO_2,Na_2O. Lowest Ta-Nb min on the spaiderdiagram, lowest contents of HREES.

Group 2 A include flank eruption since 1945 to 1966. Most of the cinder cones concentrated on East-East-North and East-Southern slopes. Altitude of cinder cones changed since 800-2000 m. For group 2 A and 2 B are typically Highest Zr, Cs, Rb, Ba. Higher contents Ta-Nb on spaider diagrams, Higher contnets of HREES. However, difference in the highest Sr, P_2O_5, Al_2O_3, the highest K_2O allow us clearly determinate group 2 A and group 2 B.

Eruptions in 1974 to 1990 are classificated as a group 2 B. cinder cones of this group erupted on South-Western slopes of volcano. On the altitude 3400-4400 m. Specific geochemistry features shows that composition of group 2 B have Intermediate positions between 2A and 3 groups on Sr, P_2O_5, TiO_2.

Group 3 include only eruptions on the summit since 1993-2013. For this group typically the highest MnO, Fe_2O_3, Y. Intermediate positions between 2B and 1 groups on Zr, K_2O, MgO, Na_2O.

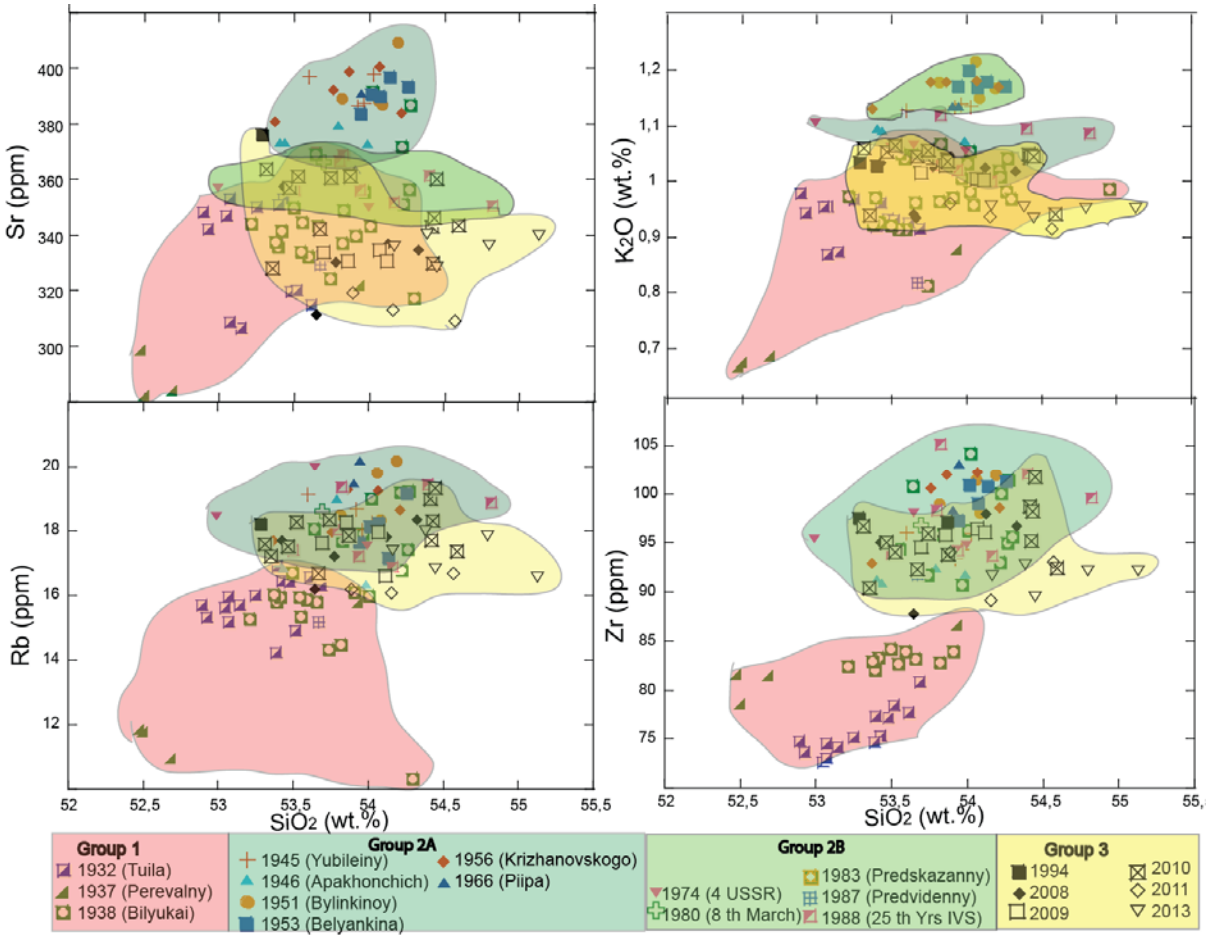

Fig. 1-32. Harker diagrams of historical eruptions.

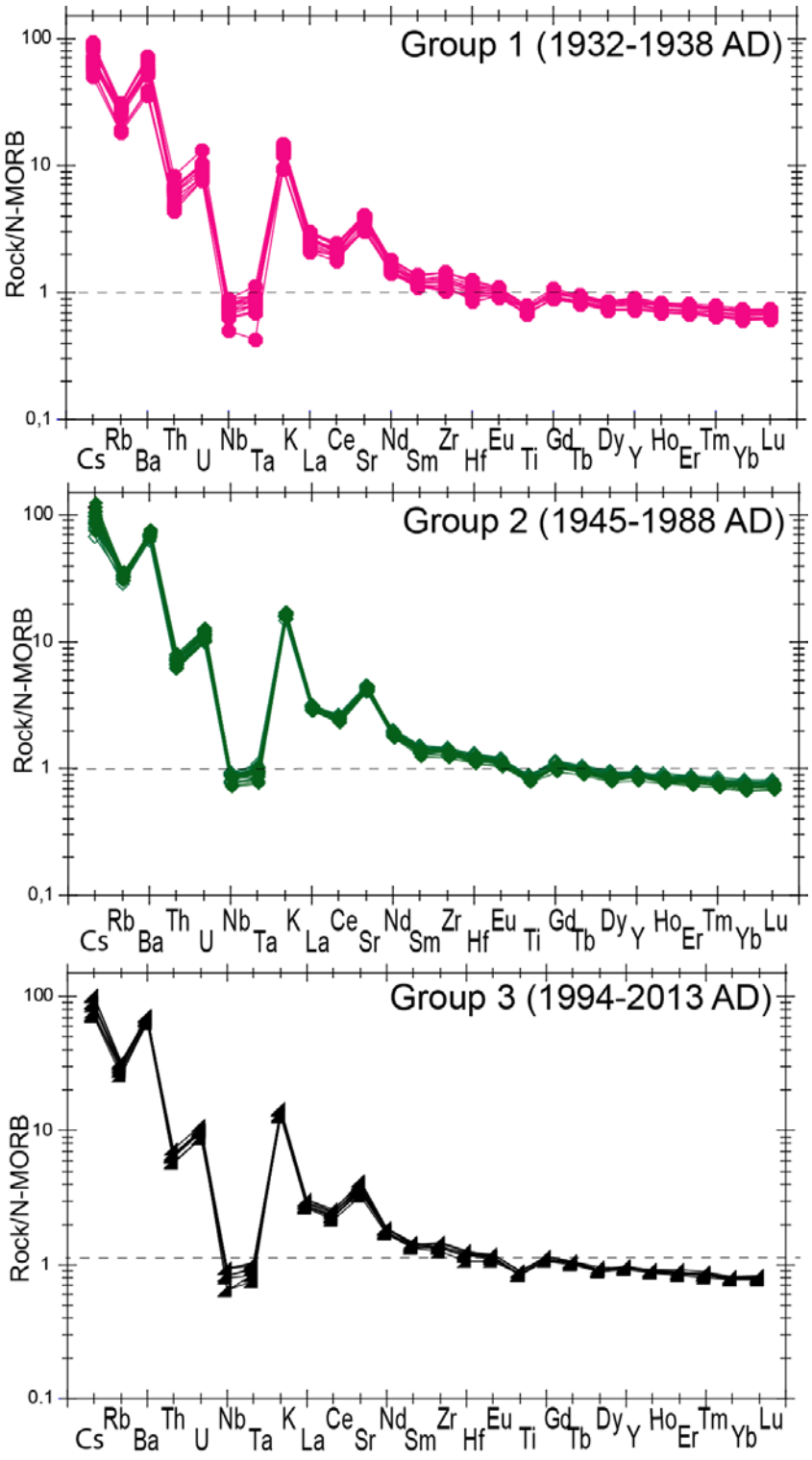

Fig. 1-33. N-MORB-normalized trace element patterns for Klyuchevskoy historical eruptions.

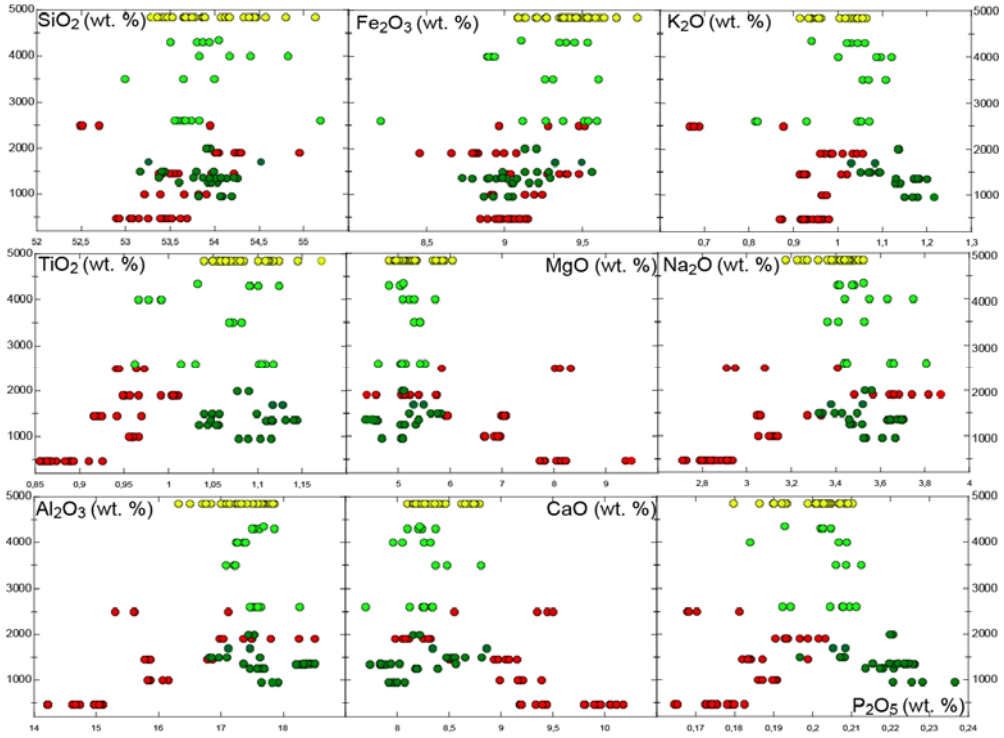

Fig. 1-34. Dependence compoaitions of magma from altitude of eruptions. Different color indicate volcanic group. Detailes on Fig. 1-32.

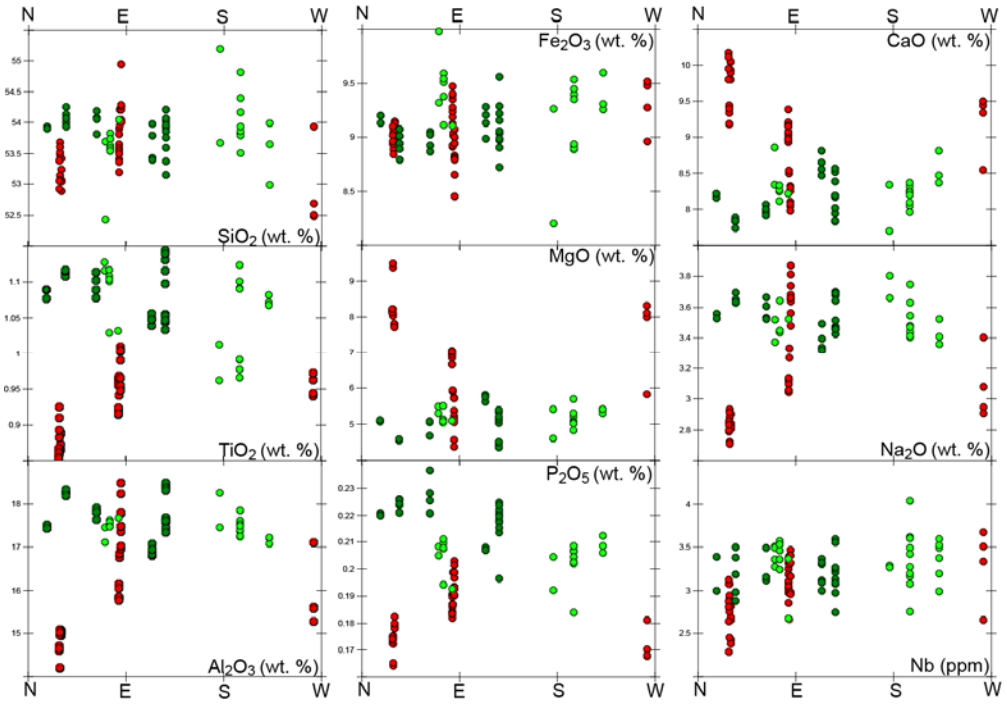

Fig. 1-35. Dependence compoaitions of magma from location cinder cones. Different color sindicate volcanic group. Detailes on Fig. 1-32.

Specific features	**Group 1**	**Group 2A**	**Group 2B**	**Group 3**
Age	1932-1938	1945-1966	1974-1990	1994-2013
Location of vent	NNE, E, W	EEN-ES	SW	Summit
Altitude of cinder cones, m	200~1000	800~2000	3400~4400	~4650
Geochemistry	Highest Mg, Ca. Lowest Sr, Ba, Rb, Y, K_2O, TiO_2,Na_2O. Lowest Ta-Nb min on the spiderdiagrams, lowest contents of HREES.	Highest Zr, Cs, Rb, Ba. Higher contents Ta-Nb on spiderdiagrams, Higher contents of HREES.		Highest MnO, Fe_2O_3, Y. Intermediate positions between 2B and 1 groups on Zr, K_2O, MgO, Na_2O.
		The highest Sr, P_2O_5, Al_2O_3, the highest K_2O.	Intermediate positions between 2A and 3 groups on Sr, P_2O_5, TiO_2.	
Petrography	Porphyric structure, huge mineral assemblage of Opx, Ol and Cpx. Microstructure of glass are crystallised by microcrystals of Pl.	The largest amount of Pl (40-60 %), all glass are crystallised by Pl. The biggest sizes of Cpx, Ol and Opx. However, amount of mafic minerals decreased.	The largest amount of Ol (12-15 %) and Opx (8-10 %). Length of Opx, Cpx and Pl are decreasing.	Amount of Pl is large (45%), decreased amount of Cpx (3-5%).

Fig. 1-36. Specific features and groups of historical eruptions.

Chapter 7. Discussion

7.1. Magma types

7.1.1. Classification of magma types

Fig. 1-37 shows a Zr-K_2O variation diagram for eruption products of the Klyuchevskoy volcano. In the figure, the data are scattered along the downward-sloping direction, as well as a upward-sloping direction. The Klyuchevskoy magmas are basalt and andesite in composition, and it is likely that zircon and alkali feldspar were not crystallized in the magmas. Therefore, the upward-sloping trend of the data can be explained primarily by magmatic differentiation. On the other hand, the variations in the downward-sloping direction cannot be explained by processes such as crystal fractionation in a crustal magma chamber and partial melting of the source mantle; rather, the variations are considered to reflect the heterogeneity in the source mantle. On this basis, the samples are divided into a low-K group (K/Zr <92) and a high-K group (K/Zr > 92). The K/Zr ratio of 92 is adopted so that the samples with more primitive features (relatively lower Zr contents) can be clearly divided into the two groups, although this is somewhat arbitrary. We note that the category of the “low-K” and “high-K” groups are not related to the traditional classification of low-K, medium-K, and high-K series of Peccerillo and Taylor (1976). The products of the Klyuchevskoy volcano have been commonly divided into “high-MgO basalts” and “high-Al_2O_3 basalts” (e.g., Kersting and Arculus, 1995) using a Al_2O_3-MgO diagram. The relatively MgO-poor samples of both the low-K and high-K groups of our classification belong to the “high Al_2O_3 basalts”, and the relatively MgO-rich samples of both the low-K and high-K groups belong to the “high MgO basalts”. On the basis of this classification, almost all of the pre-historical samples, including the older samples (>3500 BP) of Auer et al. (2009), belong to the low-K group, and the 1932

AD products and some other historical samples constitute the high-K group.

According to this classification, the data are plotted on MgO variation diagrams in Fig. 1-38. The low- and high-K samples appear to exhibit compositional trends with distinct features, and the low-K samples are characterized by relatively low SiO_2 and Ba, and high Al_2O_3 contents compared with the high-K samples.

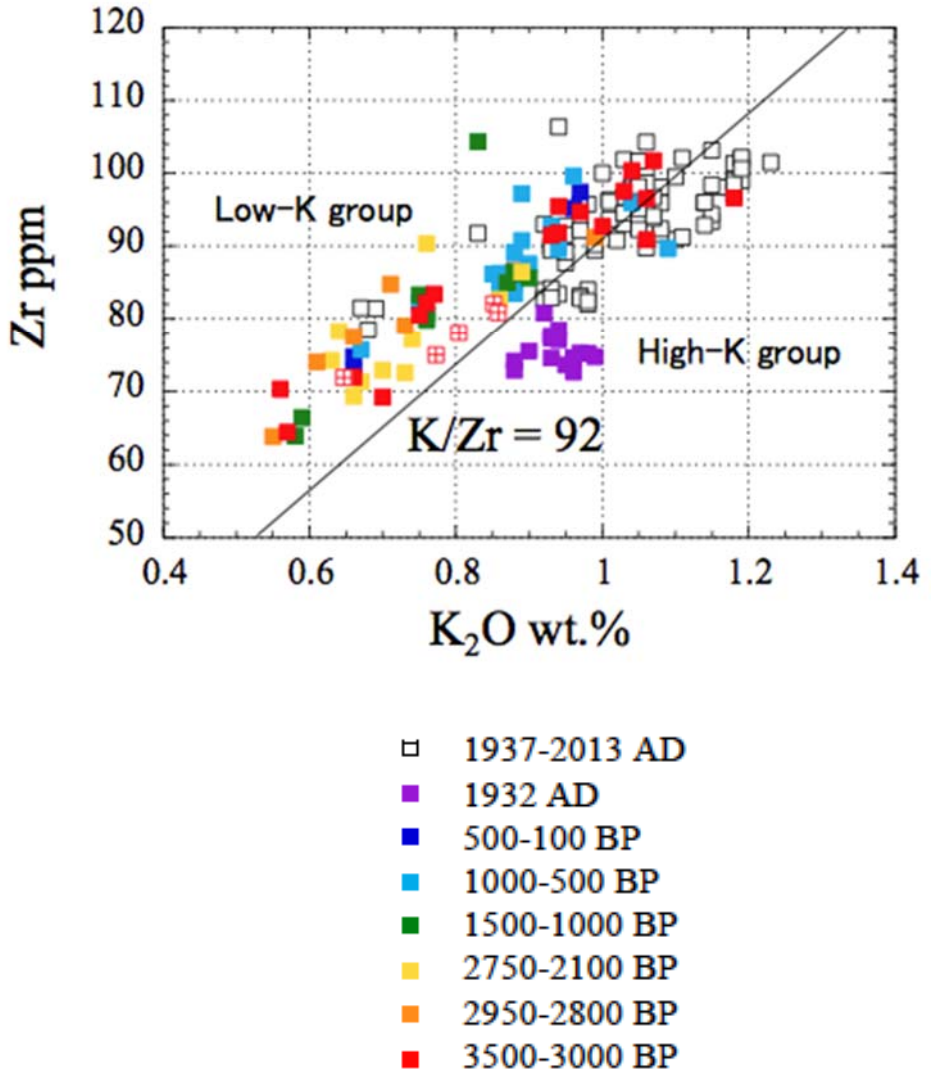

Fig. 1-37. The Zr-K_2O diagram for the Klyuchevskoy samples, showing the division of the samples into low-K and high-K groups on the basis of the K/Zr ratio of 92. The data for >3500 BP are taken from Auer et al. (2009).

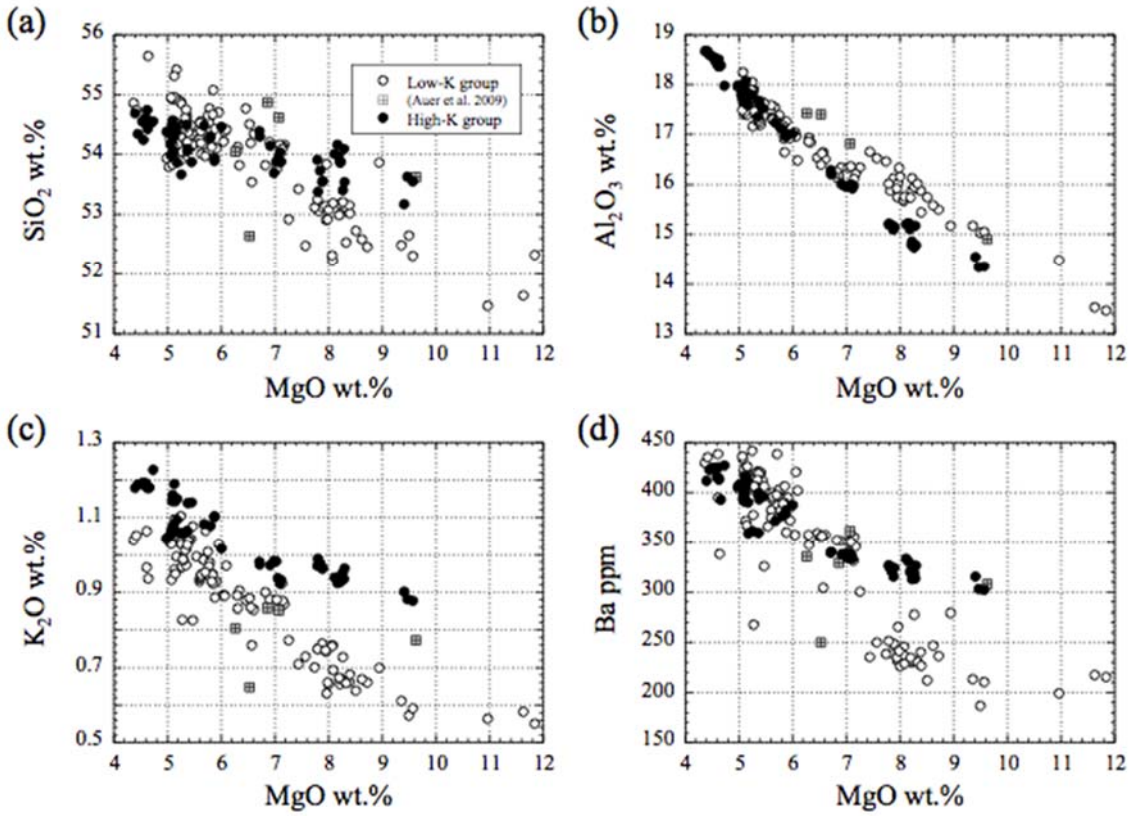

Fig. 1-38. The MgO variation diagram for SiO_2, Al_2O_3, K_2O, and Ba of samples from the Klyuchevskoy volcano. The data for >3500 BP are taken from Auer et al. (2009).

7.1.2. Genetic relationships of two primary magmas

It is notable that there exist two kinds of MgO-rich magmas (>9 wt.% MgO) with distinct K_2O content (Fig. 1-39); those with low K_2O content (~0.6 wt.%) and those with relatively high K_2O content (~0.9 wt.%). The Mg#'s of olivine in equilibrium with melts with the same compositions as the most magnesian low-K and high-K samples (KLC-026 and KLC-089) are calculated. Because the sub-arc upper mantle is considered to be slightly oxidized, the oxygen fugacity of NNO+1 (e.g., Righter et al. 2008) is assumed. In this case, the alphaMELTS model in MELTS mode (Ghiorso and Sack 1995; Asimow and Ghiorso 1998; Smith and Asimow 2005) shows that the $Fe^{3+}/(Fe^{2+}+Fe^{3+})$ ratios of the two melts are ~0.25. Then, the equilibrium Mg#'s of olivine are calculated to be 91.8 for low-K magma and 90.2 for high-K magma, using an equilibrium $(Fe^{2+}/Mg)^{olivine/melt}$ distribution coefficient of 0.3 (Roeder and Emslie 1970). Therefore, both the MgO-rich low-K and high-K samples represent primary magmas or near primary magmas. According to the fractionation calculations, high-K primary magma cannot be produced by simple fractional crystallization of low-K one (Fig. 1-39).

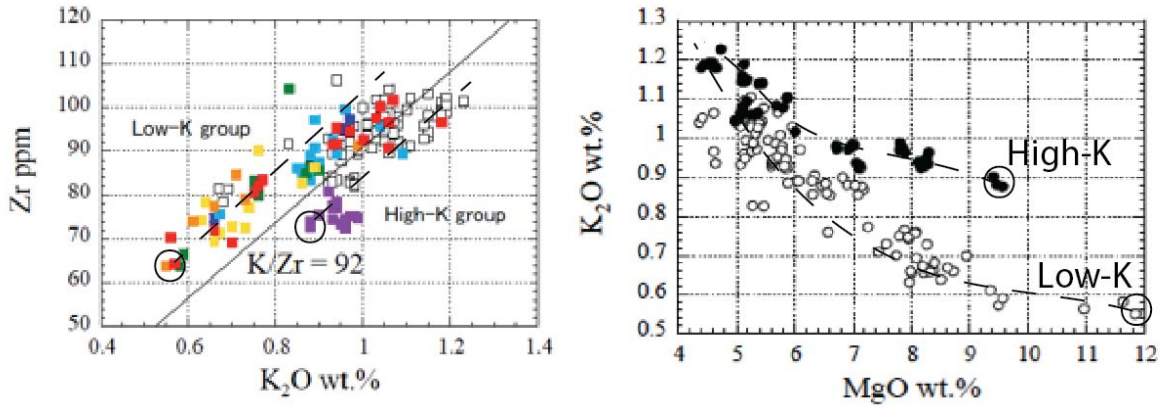

Fig. 1-39. Calculated fractionation paths from two primary magmas.

7.2. Origin of low-K and high-K primary magmas

7.2.1. Factors controlling primary magma compositions

As discussed above, the difference in the low and high-K primary magmas are suggested to have originated from the mantle processes. Auer et al. (2009) showed that "high-MgO basalts" essentially originated through melting of the source mantle through influx of slab-derived materials, and the "high-Al_2O_3 basalts" were produced by interaction of the "high-MgO basalt" magmas with the subcontinental lithospheric mantle with high $\delta^{18}O$, on the basis of water content and oxygen isotope data of the products. The primitive low-K basalts of our classification coincide with "high-MgO basalts" of Auer et al. (2009), but the primitive high-K basalts may not have been recognized by previous workers including Auer et al. (2009).

There is now a consensus that subduction-zone magmas are generated through melting of the upper mantle by influx of water-rich materials released from the subducting slab (e.g., Ringwood 1974; Sakuyama and Nesbitt 1986; Tatsumi 1986). The source mantle for the subduction-zone magmas is also widely believed to depleted MORB source mantle (DMM) (White and Dupré 1986; Ellam and Hawkesworth 1988; Ishikawa and Nakamura 1994; Elliott 2003, and references therein). Therefore, the compositions of the primary magmas are mainly controlled by parameters including the degree of melting of the source mantle, the compositions of the slab-derived materials, and the mixing ratios between the slab-derived materials and the source mantle. In these factors, the difference in the low- and high-K primary magmas cannot be explained solely by the difference in the degree of melting, because the isotopic ratios of the two primary magmas are different.

7.2.2. Difference of source compositions

Fig. 1-40 shows a Th/Yb-Ba/La diagram in which the compositions of the low- and high-K primary magmas, as well as that of the DMM (Salter and Stracke, 2004), are plotted. Trace element ratios such as Th/Yb and Ba/La have been widely used to identify the nature of slab-derived materials (e.g., Hawkesworth et al., 1991; Pearce and Peate, 1995). Because Ba is soluble in slab-derived aqueous fluids and La, Yb, and Th are immobile in the aqueous fluids, the addition of the fluids to the mantle results in high Ba/La and low Th/Yb ratios of the partial melts. On the other hand, because sediments have high Th/Yb and low Ba/La ratios, the partial melt is characterized by high Th/Yb and low Ba/La ratios by addition of the melt component to the mantle.

In the figure, partial melts of the DMM have similar Th/Yb and Ba/La ratios to those of the DMM, because Th, Yb, Ba, and La are all incompatible elements. The Th/Yb and Ba/La ratios of both the low-K and high-K primary magmas are different from those of the DMM, suggesting that these magmas were produced by mixing of the DMM component and slab-derived materials with distinct Th/Yb and Ba/La ratios. In addition, the low-K magma and high-K magma do not lie on the same line from the DMM. This observation suggests that the compositions of the slab-derived materials for the low-K primary magma were different from those for the high-K primary magma. Both the low-K and high-K primary magmas have relatively higher Th/Yb and Ba/La ratios. Therefore, the slab-derived materials are suggested to have been supercritical liquids, in which both Ba and Th are soluble (Kessel et al., 2005). The involvement of supercritical liquids in the source mantle beneath Klyuchevskoy was also suggested by Portnyagin et al. (2007). The melt-like component in supercritical liquids tends to increase with the slab depth from which the liquids are derived (Kessel et al., 2005). Therefore,

the slab-derived materials for the high-K primary magma may have been derived from deeper levels than those for the low-K primary magma. Comparing isotopic compositions of primary magmas with altered oceanic crust and sediment, slab-derived materials for low-K magma have been different from those for high-K magma (Fig. 1-41). This also indicates that slab-derived materials for high-K magma was more enriched in the sediment component.

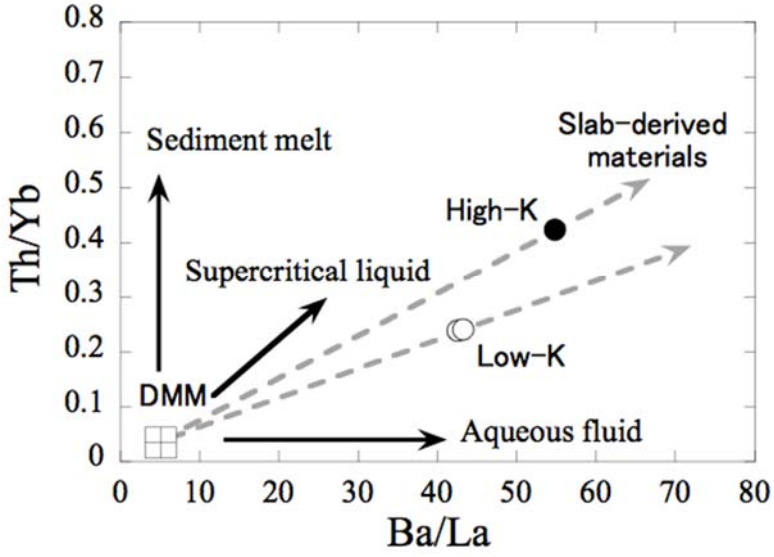

Fig. 1-40. The Th/Yb and Ba/La diagram, showing the compositions of the primary low-K and high-K magmas, as well as those of DMM. The compositions of DMM are from Salter and Stracke (2004).

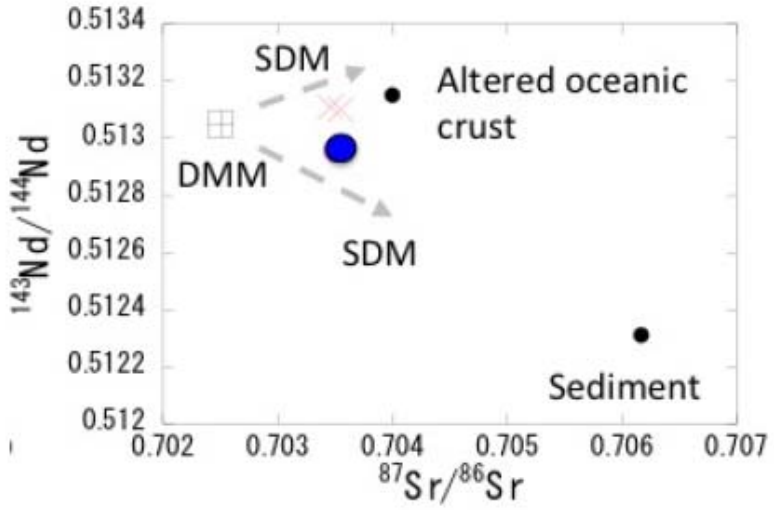

Fig. 1-41. Sr and Nd isotopic variations. Composition of Altered oceanic crust and sediment from Kimura et al., 2014.

7.2.3. Degrees of melting

The degrees of melting are estimated for both low-K and high-K primary magmas according to the distribution of Ti between the source mantle and melt using the method of Kelley et al. (2006). Using the bulk distribution coefficient for Ti of 0.04 and the TiO_2 content of DMM of 0.133 wt.% (Salters and Stracke 2004), as well as the TiO_2 concentrations of KLC-026 and KLC-089 of 0.78 wt.% and 0.87 wt.%, degrees of melting of 13.6% and 11.8% are obtained for the low-K and high-K primary magmas, respectively (Fig. 1-42).

$$F = \frac{(C^0_{TiO2} / C^L_{TiO2}) - D_{TiO2}}{1 - D_{TiO2}}$$

C^0_{TiO2}: Concentration of Ti in DMM
C^L_{TiO2}: Concentration of Ti in partial melt
D_{TiO2}: Mantle-melt bulk distribution coefficient

(Kelley et al., 2006)

Low-K primary magma: F = 13.6 wt.%
High-K primary magma: F = 11.8 wt.%

C^0_{TiO2}: 0.133 wt.% (Salters and Stracke, 2004)
C^L_{TiO2}: Low-K: 0.78 wt.%; High-K: 0.87 wt.%
D_{TiO2}: 0.04

Fig. 1-42. Cacluclations of degree of melting.

7.2.4. Generation conditions

For Mg-rich basalts, corresponding to the primitive basalts of the low-K group of this study, water contents have been determined by Auer et al. (2009). They obtained 3.92 wt.% H_2O for glass inclusions in a primitive basalt sample (KLV 5/8; 11.3 wt.% MgO), whose whole-rock major element compositions are essentially similar to those of KLC-026 of this study. Given that H_2O/K_2O ratios did not change significantly during magmatic differentiation, the H_2O content of the magma is obtained as 5.1 wt.% using the K_2O content of the sample of 0.55 wt.% and the H_2O/K_2O ratio of the glass inclusion of 9.3. In this case, using the estimated degree of melting of 13.6 %, the water content of the source mantle is calculated to be 0.75 wt.%, according to Eq. 10 of Kelley et al. (2006).

The temperature and pressure conditions of magma generation are estimated using the two constraint: (1) the primary magma was generated by 13.6% melting of the DMM, and (2) the primary magma was in equilibrium with olivine in the source mantle, according to the method of Kuritani et al. (2014). First, the pressure and temperature conditions required to generate a 13.6% partial melt of DMM are calculated for a source water content of 0.75 wt.% using the alphaMELTS model in pMELTS mode (Ghiorso et al. 2002; Smith and Asimow 2005), and the result is shown in Fig. 1-43. Then, the olivine-melt equilibria are examined for the calculated primary melt with a water content of 5.1 wt.% using the alphaMELTS model in pMELTS mode, and the calculated liquidus temperature in a temperature-pressure space is shown in Fig. 1-43. The temperature and pressure conditions for the Klyuchevskoy magma, which satisfy the 13.6% degree of melting of DMM and the equilibration of the melt with olivine in the source mantle, are constrained to ~1265°C and ~1.6 GPa, respectively.

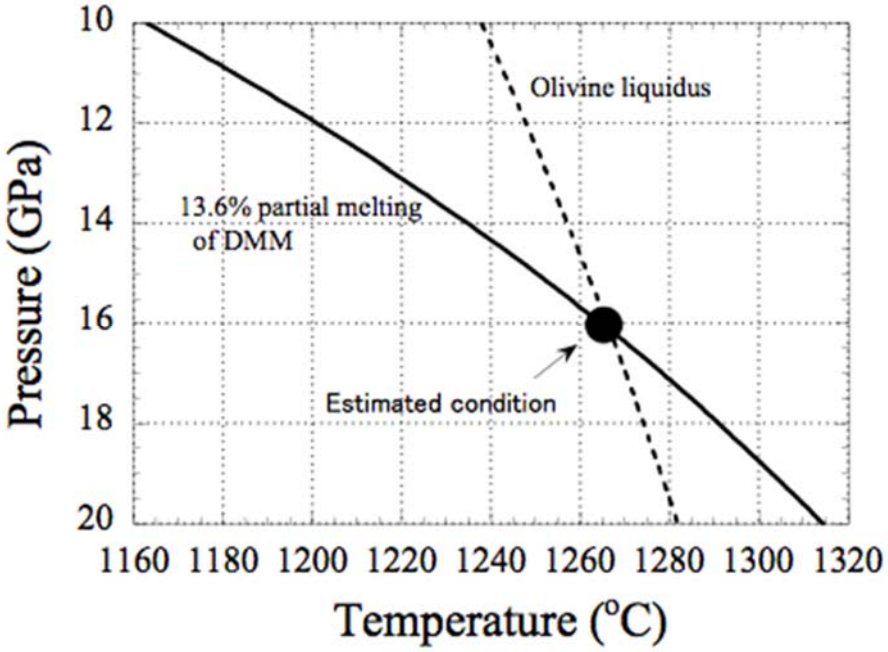

Fig. 1-43. Estimated generation conditions for the Klychevskoy magma. The P-T conditions of the source mantle required to generate 13.6% partial melt with source water contents of 0.7 wt.% (continuous lines) and the liquidus temperatures of olivine for primary magma with water contents of 5.1 wt.% (dashed lines), calculated using the alphaMELTS model (Asimow and Ghiorso 1998; Smith and Asimow 2005), are shown.

7.3. Origin of evolved magmas

As suggested above, the relatively Mg-poor low-K and high-K magmas were derived from the low-K and high-K primary magmas, respectively. As is shown in the $^{206}Pb/^{204}Pb$-MgO variation diagram, the low-K and high-K magmas appear to show different trajectories, suggesting that these magmas experienced different evolutionary processes (Fig. 1-44). For the high-K samples, the $^{207}Pb/^{204}Pb$ ratios are essentially constant with decreasing MgO content from 9.5 wt.% to 5.5 wt.%, but they seem to decrease from ~18.3 to ~18.29 with decreasing MgO content from ~5.5 wt.% to ~4.5 wt.%. Kayzar et al. (2014) shows that middle and lower crustal xenoliths from Bezymianny volcano, which is located only 9 km from the Klyuchevskoy volcano, have less radiogenic Pb isotopic compositions ($^{206}Pb/^{204}Pb$ = 18.18-18.23) than the products of the Klyuchevskoy volcano. Therefore, the compositional trends of the high-K magmas may have been produced through assimilation and fractional crystallization in the middle ~ lower crust. On the other hand, the $^{206}Pb/^{204}Pb$ ratios of the Mg-poor low-K samples (<6 wt.% MgO) are higher than those of the relatively Mg-rich low-K samples (>8 wt.% MgO), while these samples do not form a clear compositional trend in the $^{206}Pb/^{204}Pb$-MgO diagram. It is not likely that upper crustal materials beneath the Klyuchevskoy volcano have significantly radiogenic Pb isotopic composition, because they are considered to be composed of Cenozoic volcanic deposits (Fedotov and Masurenkov, 1991). Auer et al. (2009) suggested that the "high-Al_2O_3 basalt" magmas were produced through interaction of primitive magma with subcontinental lithospheric mantle, on the basis of the oxygen isotopic data. If this was the case, the high $^{206}Pb/^{204}Pb$ features of the relatively MgO-poor low-K basalts may have been inherited from the subcontinental lithospheric mantle, considering that these samples essentially belong to

the "high-Al_2O_3 basalt" of Auer et al. (2009). The upper limit of the $^{206}Pb/^{204}Pb$ ratios appears to decrease with decreasing MgO content from ~6 wt.% to ~4.5 wt.%; these may suggest that the low-K magmas also evolved in the middle ~ lower crust with low $^{206}Pb/^{204}Pb$ ratios.

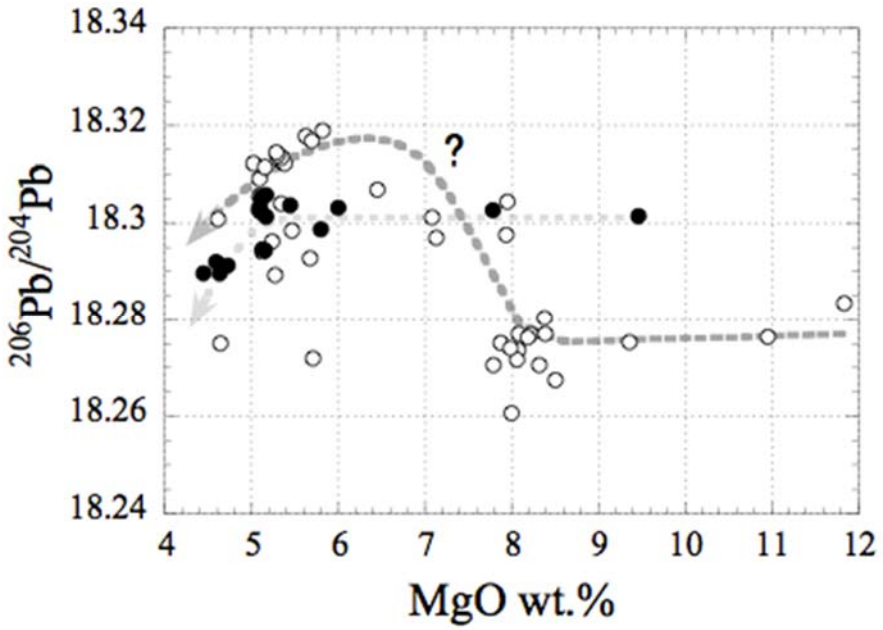

Fig. 1-44. The MgO variation diagram for $^{206}Pb/^{204}Pb$ of samples from the Klyuchevskoy volcano. Inferred evolution paths are shown with broken lines for each type.

7.4. Temporal variations of Klyuchevskoy magmas

Fig. 1-45 shows the temporal variation in the K/Zr ratios of the eruption products. During most of the evolution of the volcano, the low-K magmas have been dominated (Fig. 1-45a). The occurrence of the high-K magmas was almost limited to 1932 AD–1966 AD (Fig. 1-45b). Interestingly, the K_2O content of the high-K magmas tends to increase with age; from 0.9-1.0 wt.% at 1932 AD to ~1.2 wt.% at 1966 AD (Fig. 1-45c). This observation may suggest that the time scale of magmatic evolution for the magma with 0.9–1.0wt.% K_2O to evolve to ~1.2 wt.% K_2O in a lower crustal magma chamber was ~30 years. It is also notable that both low-K and high-K magmas were erupted in the 1937-1938 AD eruptions.

As we notice the historical activity of Klyuchevskoy volcano, summit eruptions are dominant since 1697 AD. However, flank eruptions started to form new cinder cones on the lower slopes of volcano in 1932 AD (Fig. 1-46). Futhermore, the volcano repeated voluminous eruptions during 1932-1945 AD (Fig. 1-47). These evidences suggest that eruption style and volume would be changed by injection of high-K magmas.

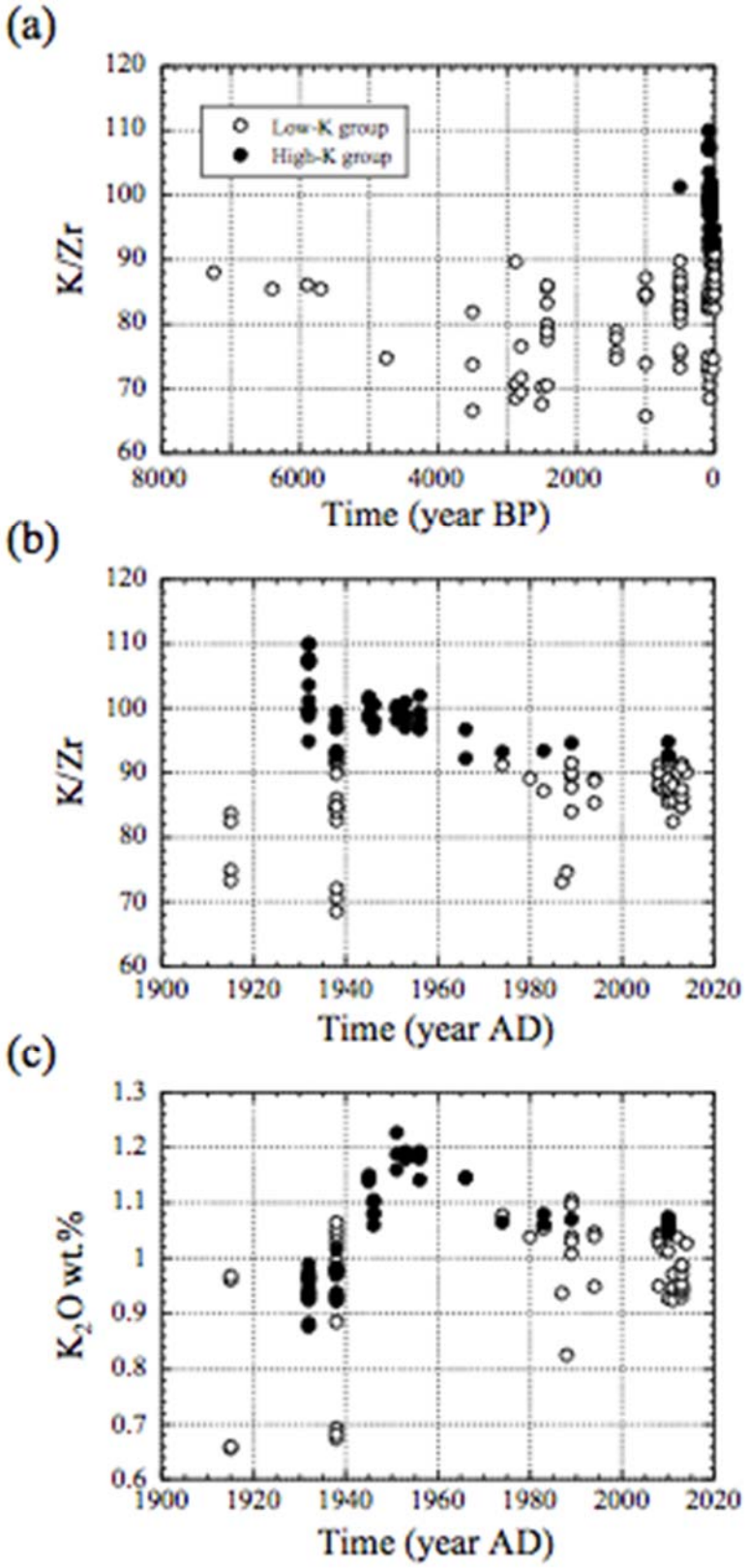

Fig. 1-45. Temporal variation of the K/Zr of the Klyuchevskoy samples (a) for ~7000 BP – present and for (b) 1900 AD – present, and (c) temporal variation of K_2O content of the samples for 1900 AD – present. The data for >3500 BP are taken from Auer et al. (2009).

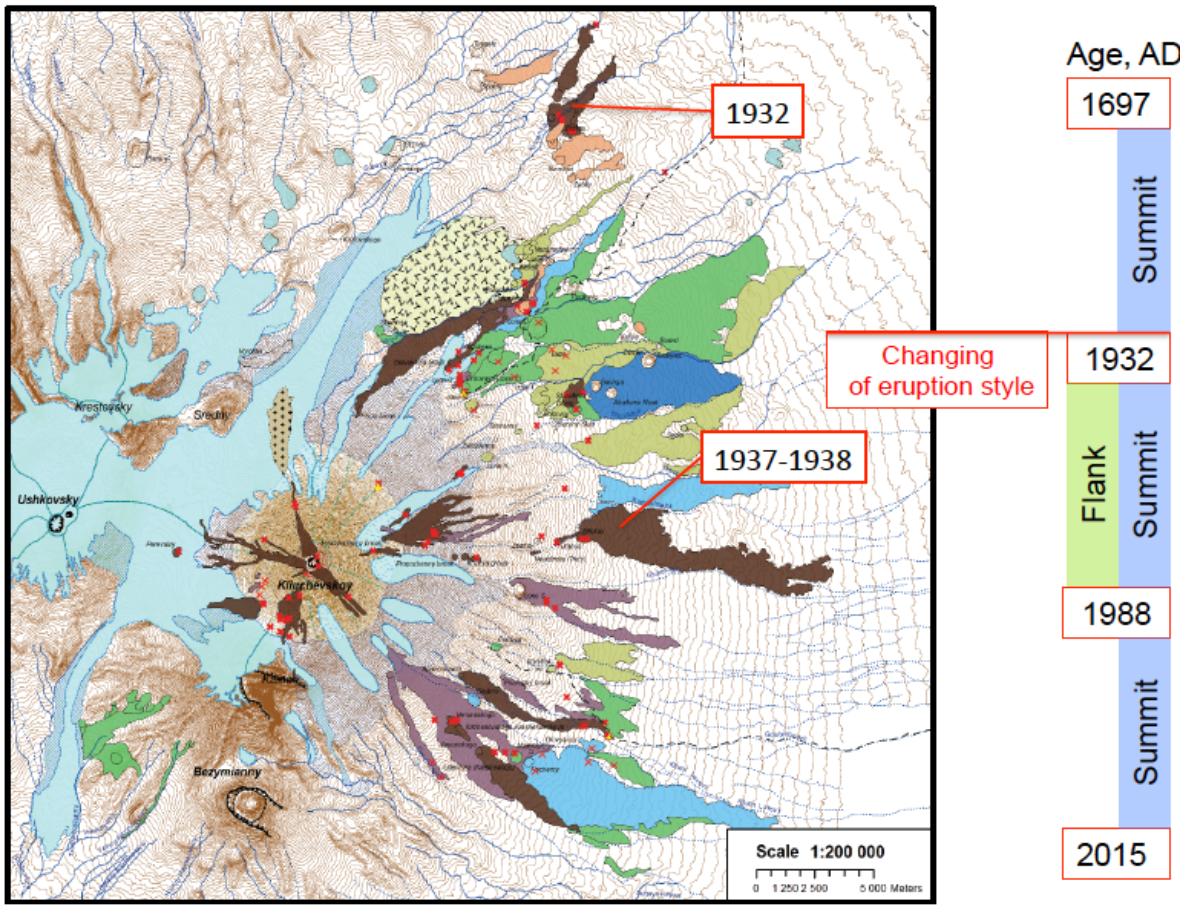

Fig. 1-46. Schematical map illustrated abnormaly, volumneous eruptions with high-K.

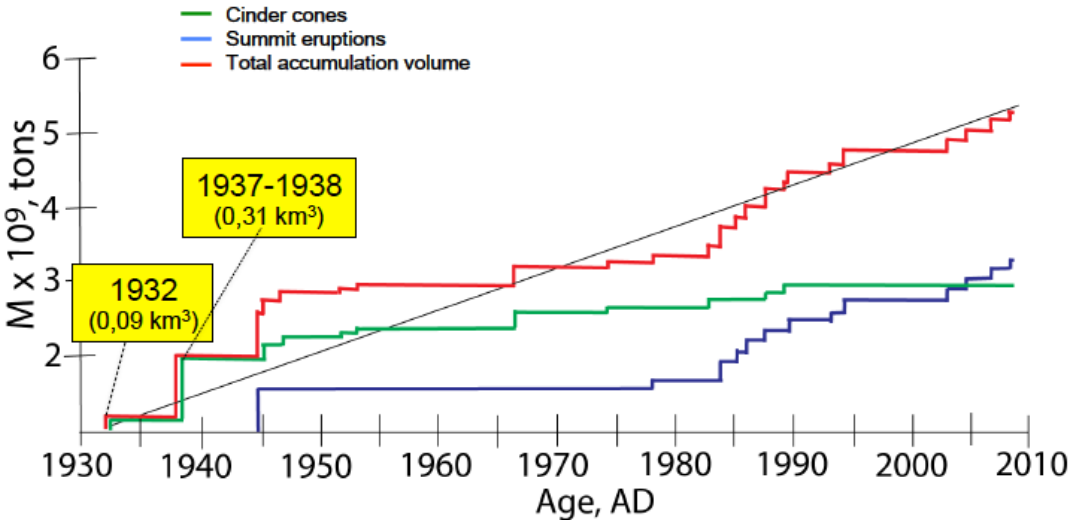

Fig. 1-47. Step diagram with high-K magmas in recently historical activities.

7.5. Schematic model of magma genesis and evolution of Klyuchevskoy volcano during last 4000 years

The slab-derived materials for the high-K primary magma were different from those of the low-K primary magmas. Therefore, the appearance of the high-K type at ~1932 AD may reflect that this magmatism was caused by a new influx of slab-derived materials, which were released from the subducting slab at deeper levels than those for the low-K magmas, into the melting region.

According to the detailed geochemical and isotopic study of Klyuchevskoy volcano, we suggest model of magmatic system of Klyuchevkskoy volcano (Fig. 1-48). The low-K magma has been dominated during last 4000 yrs. However, the new magma (high-K magma) became active since 1932 AD. The 1932 and following 1937-38 eruptions produced large volume of lava flows from the lower flank of volcano. After that, activity of high-K magma almost stopped since 1974 AD and low-K magma had been dominant in recent 40yrs.

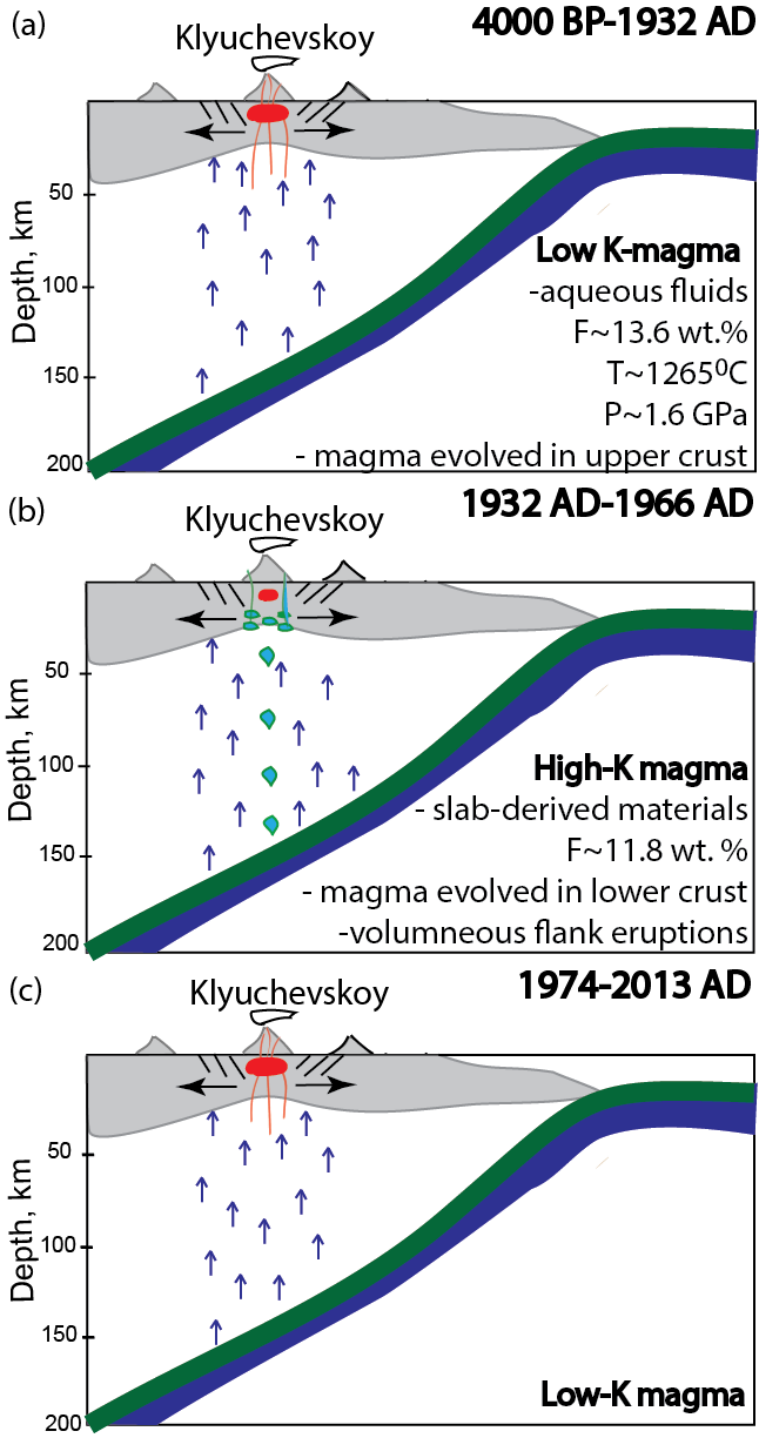

Fig. 1-48. Schematic model showing the relationship between the factors that influence on the observed geochemical features. (a) long time (~7000 BP – 1932 AD) magma formation by dehydration fluids from slab, (b) short time (1932 AD – 1966 AD) impact of enriched slab-derived materials, (c) renewal (1974 AD – 2013 AD) of low-K magma generation with dehydration fluids.

Chapter 8. Conclusions

To understand the origin of the temporal evolution of the Klyuchevskoy magmas, we carried out a petrological and geochemical study of basalts and andesites from the volcano, and reached the following conclusions:

(1) The eruptive products can be divided into low-K and high-K groups on the basis of the K/Zr ratios. The low-K group has been dominated throughout the evolution of the volcano, whereas the activity of the high-K group was mostly limited to 1932 AD–1966 AD.

(2) There must have been at least two different kinds of primary magmas with distinct K_2O contents. The low-K and high-K primary magmas are suggested to have been generated though ~13.6% and ~11.8% melting of the DMM, respectively, by influx of different slab-derived materials (supercritical liquids) into the melting region. The slab-derived materials for the high-K magmas are suggested to have contained higher sediment component than those for the low-K magmas.

(3) The low-K primary magma is estimated to have been generated through melting of the source mantle with 0.7 wt.% H_2O at 1265°C and at ~1.6 GPa.

(4) The high-K magmas became active since ~1932 AD, which may reflect that the magmatism was caused by a new influx of slab-derived materials into the melting region.

(5) The low- and high-K magmas are suggested to have evolved through assimilation and fractional crystallization in the middle ~ lower crust.

Part II

Origin of spatial compositional variations of volcanic rocks from the Northern Kurile Islands, Russia: Geochemical studies of active volcanoes on the Paramushir, Atlasov, Antsiferov islands and adjacent submarine volcanoes

Abstract

Although the Pacific plate has subducted beneath Kuril arc to cause intensive arc-type volcanism, the structure of the arc largely change from south to north. The central part of the arc has the oceanic crust with a back-arc basin, whereas continental crust dominates from the northern part of Kuril islands, continuing to Kamchatka peninsula. In order to clarify the structural and tectonic controls on magma genesis, new geochemical data from 10 volcanoes including submarine ones at the northern part of Kuril islands are presented, such as major and trace elements by XRF, REE and trace elements by ICP-MS, Sr-Nd isotopes by TIMS. Based on these data, geochemical variations are spatially investigated.

Rocks of these volcanoes are a typical arc type one with high LIL/HFS ratios, and also show across-arc compositional change, such as increasing of LIL elements and L-REE toward the back arc zone. However, the rocks of Alaid volcano have exceptionally high Nb content (2 – 8 ppm in basaltic rocks). According to the variation, these volcanoes can be divided into three zones (frontal, transitional and rear ones) and Alaid volcano. Although rocks from the volcanoes in three zones, such as frontal (Chikurachki, Tatarinov, Lomonosov and sub-marine volcano 1.3), transitional (Ebeko volcano) and rear (Fussa and Shirinki volcanoes) zones, range from SiO_2=49 to 63 wt.% and are mainly andesite, basaltic rocks (SiO_2=48 – 53 wt.%) are dominant in the Alaid volcano. The rocks from the frontal zone are characterized by lower contents of LIL elements (e.g. Rb, Ba, K), L-REE (e.g. Nd, Ce) and higher $^{87}Sr/^{86}Sr$ ratio (0.7031-0.7034). Toward the back-arc side, contents of LIL elements and L-REE increase toward the rear zone, whereas $^{87}Sr/^{86}Sr$ (0.7029-0.7031) ratios decrease. In addition to Nb contents, the basaltic rocks of the Alaid volcano are also characterized by highest contents of incompatible elements, such as Zr, Rb, Ba, Na and K. Sr isotope ratios of the rocks from each

volcano gradually increase with increasing of SiO_2 contents, suggesting that evolved rocks must be affected by crustal components. Moreover, variations of incompatible elements, such as Zr – Rb diagram, indicate that evolved rocks cannot be produced by simple fractional crystallization. Thus, basaltic rocks with SiO_2<55 wt.% are focused in this study to investigate the origin of primary magmas.

Nb/Zr ratios (0.019 – 0.032) of the basaltic rocks from the frontal and rear zones are low and similar to depleted MORB source (DMM). Basaltic magmas from these two zones are produced by partial melting of DMM which are assimilated with subduction components. Considering the relationship of fluid mobile and immobile incompatible elements in identification diagrams, such as a Th/Yb – Ba/Th one, assimilated materials are distinct between frontal and rear zones; aqueous fluids at frontal zone and sedimentary melts at rear zone. On the other hand, the basaltic rocks of Alaid are characterized by obviously high Nb/Zr ratios (0.047 – 0.071), indicating that the source mantle of the volcano is slightly fertile, affected with OIB component. Nb/Zr ratios of the basaltic rocks from Ebeko volcano, which is defined as the transitional type, show slightly high value (0.022 – 0.042). The source mantle of the volcano might be also affected with OIB component. Considering higher LIL/HFS ratios of these basaltic rocks from Alaid and Ebeko volcanoes, fertile wedge mantle beneath these volcanoes Alaid volcano should be assimilated by subduction components. However, highest contents of incompatible elements of the basaltic rocks of Alaid could be explained not only by subduction components but also OIB component in the wedge mantle.

Although all of the rocks from the studied area are arc type, the wedge mantle beneath the area is heterogeneous. According to spatial variations of Nb/Zr ratios of basaltic rocks from volcanoes in Kuril islands and southern Kamchatka peninsula, the wedge mantle of these area is essentially DMM type. However, the mantle beneath Alaid volcano and adjacent volcanoes,

such as Ebeko volcano, is obviously enriched with OIB component. The upwelling of OIB component at the rear zone might be controlled by tectonic setting at the traditional area between Kuril islands and Kamchatka. In order to reveal the structure of wedge mantle and tectonic setting of the area, additional geochemical study for volcanoes especially from southern Kamchatka peninsula must be essential.

Chapter 1. Introduction

Across and along arc variations in the composition of primary magmas were studied for many subduction zones, and can be related to many factors. Generation of magma are mainly controlled by following factors: (1) type of the convergent margin, such as: oceanic-continental or oceanic-oceanic with back arc basin (e.g. Sun & McDonough, 1989; Sajona et al., 1996; Stern, 2002); (2) geometry of the slab, for example: depth, dip, existence of large fracture zones or junction of plates (e.g. Bolge et al., 2009; Schuth et al., 2009; Ma et al., 2011; Haraguchi et al., 2012; Nakamura & Iwamori, 2013); (3) heterogeneous of the mantle wedge (e.g. Churikova et al., 2001; Genske et al., 2012; Shuto et al., 2013); (3) process on the subducting slab, namely: dehydration and involving sediment melts or slab melting (e.g. Pearce et al., 2005; Marske et al., 2011; Hanyu et al., 2012; Jacques et al., 2014); (4) partial melting of the mantle wedge (e.g. Pearce & Parkinson, 1993; Portnyagin et al., 2007; Straub et al., 2013) and (5) finally, there can be differences in the thickness of the crust and can affected on the process of fractionation or assimilation (e.g. Nakagawa, 1999; Kimura & Yoshida, 2006; Tamura et al., 2009). All above factors differ along and across the Kurile margin. With purpose to investigate processes which is really important for magma genesis and evolution, we focus on the Northern Kurile Islands, where is the boundary between continental southern Kamchatka-Kurile arc.

1.1. Overview of previous works for Kurile Arc and for Southern Kamchatka

There are many geochemical studies about Kurile Arc and southern Kamchatka. Avdeiko et al. (1991, 1992) discussed about spatial, geochemical and structural patterns of Quaternary subaerial and submarine volcanoes of the Kurile Island arc. Authors firstly defined two volcanic zones (front and rear) parallel to the trench are due to two levels of volatile separation from the subducting slab and hence two zones of melting. Volcanoes from volcanic front (VF) and rear zone (RZ) are characterized by specific geochemical, isotope and mineralogical peculiarity. Along-arc variations with increasing of K and incompatible elements from south to north, in addition to maximum concentrations on the Paramushir and Atlasov islands (i.e. Northern end of Kurile arc), were described.

Ryan et al. (1995) argued that geochemical variations of Kurile volcanoes were related to the changes in the compositions of fluids derived from slab. Researches show that enrichments of Na, Ba, ^{10}Be and LILE remained constant. These species may move in silica-rich fluids liberated from the slab at greater depths.

Distributions of the fluids in the Kurile mantle wedge are researched by Ishikawa and Tera (1997). B/Nb and B isotope of Kurile lavas shows clear across-arc variations in which both are the highest at the trench side and continuosly decrease as the slab depth increasing. B isotope values are different among Northern, Central, and Southern Kurile Islands. Authors interpreted that fluid compositions were consistent with a source constituted by mainly altered oceanic crust and sediment, with the slight differences between NKI and Central Kuriles resulting from the different lithologies of subducting sediments.

Bindeman and Bailey (1999) analyzed anorthite megacrysts from volcanic centers of the Kurile Island Arc. They proposed that anorthites were formed by low pressure and hydrous

magmas, not more than 10-15% fractionation. Crystallization can produced in the rather shallow magma chamber (3-8 km). The results of this study reveal linear increase or decrease of trace element concentrations across the arc, which can be explained by involving fluids and sediment melt in magma genesis. Authors suggested that various degree of partial melting had controlled on the magma variations across the arc.

Dreyer et al. (2010) studied B-Be-Nd geochemical characteristic for Kurile volcanic rocks. Authors reported that subducted sediments were recycled across the entire arc and the cross-arc geochemical behavior was linked to a transition from fluid-dominated transfer in shallow regions to supercritical or melt-like transfer beneath the rear-arc.

Martynov et al. (2007, 2009, 2010) argued that Sr and Nd isotopic ratio and trace element composition of Kurile volcanic rocks (Fig.2-1). They testify about anomalous characteristics on the Paramushir (in the north of the Kurile arc), Kunashir and Iturup (in the south) islands, which are the largest three islands of the Kurile island arc. The high K and LREE concentrations in the volcanic products in Paramushir Island was explained by the southward expansion of the mantle thermal anomaly of the Kamchatka Peninsula and the involvement of melts related to the melting of oceanic sediments in magma generation.

Volynets (1994) firstly used isotope and incompatible element ratios demonstrated along arc variations of Kurile-Kamchatka Island Arc. Based on the geochemical data and spatial characteristics of volcanoes researcher defined boundary between continental Kamchatka arc and Kurile island arc.

Avdeiko et al. (2006) demonstrated that present structure of the Kurile–Kamchatka island-arc system was controlled by volcanic belts of various ages, which developed above subduction zones. Authors proposed that Southern Kamchatka and Kurile were formed in the same time and conditions. They were generated in the mantle wedge, where water-saturated

peridotite melting was induced in the high-temperature zone by fluids released from the subducted slab. The existence of FV and RZ is related to two levels of water release from different hydrous minerals. Most hydrous minerals dehydrate beneath the frontal zone. The source of water beneath the rear zone is the dehydration of serpentine and talc.

Duggen et al. (2007) based on the geochemistry of lavas of Mutnovsky and Gorely volcanoes, southern Kamchatka, suggests that degree of partial melting decreases from RZ to VF (Fig. 2-2). The VF slab component is inferred to be primarily a hydrous fluid eventually containing minor amounts of silicate melt, where the RZ slab component involves a hydrous silicate melts. Pb isotope and trace element data provide geochemical evidence for the pollution of VF magmas with RZ melt components, most likely resulting from trench-ward mantle wedge corner flow.

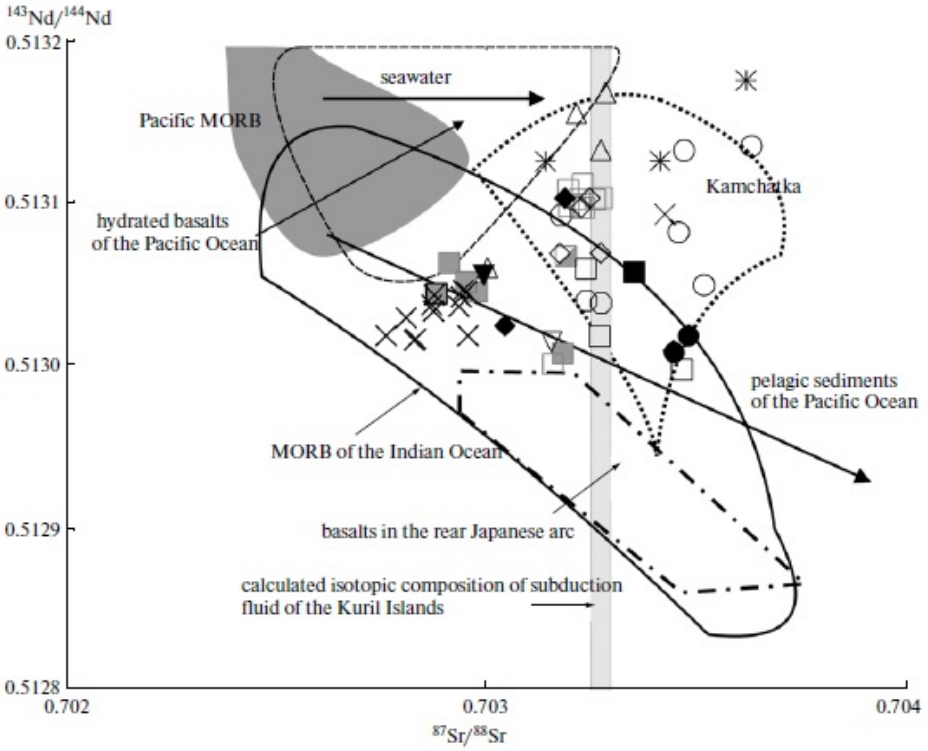

Fig. 2-1. Sr and Nd isotopic ratios of Quternary lavas from Kurile islands (Martynov et al., 2010).

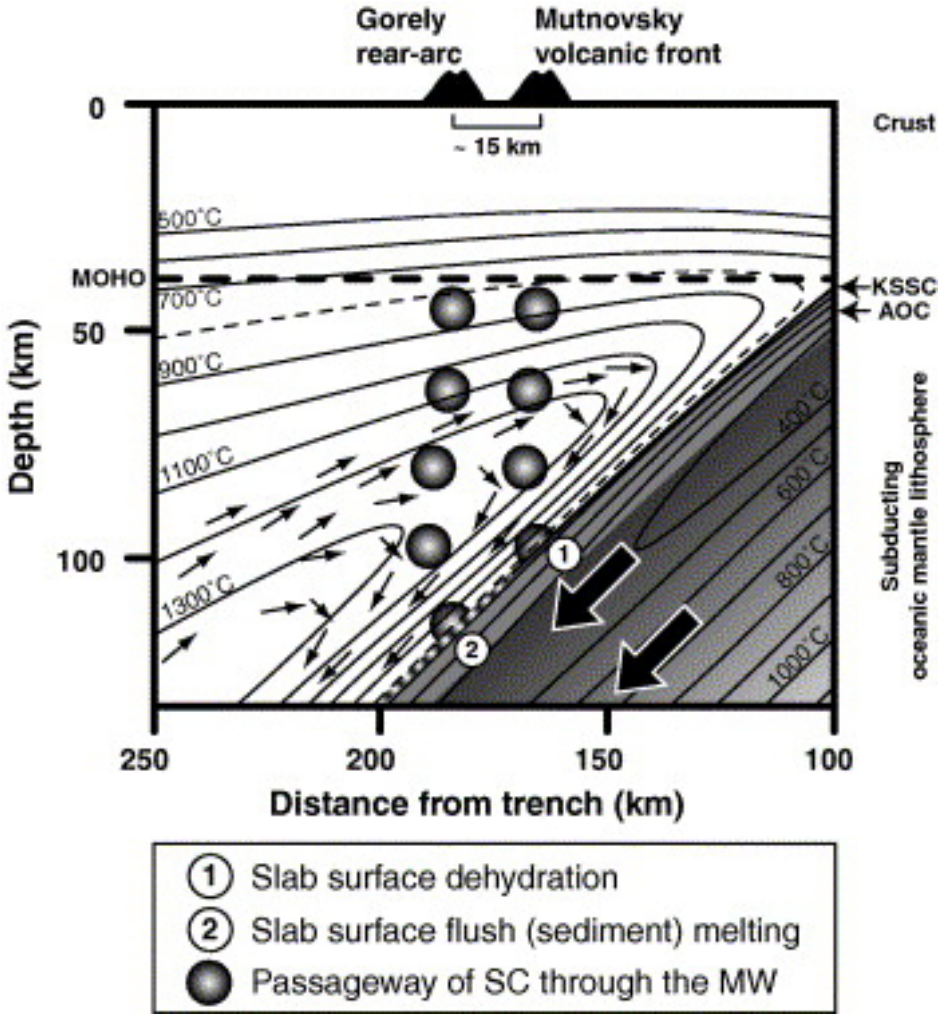

Fig. 2-2. Geodynamic model of magma genesis on Southern Kamchatka (Duggen et al., 2007).

1.2. Purpose of study

Despite on the numerous publications, there are the problems of magma genesis of NKI. The high-precision geochemical data of NKI are still absent. Union model which can explains transition from continental to oceanic crust is non-existent. Most important questions are (1) how mantle components (composition of the mantle, degree of partial melting, depleted factor) change and (2) which subduction components (dehydration of the fluid or sedimentary melting) vary across and along the arc. One of the largest island (Paramushir) of Kurile Arc is located in the investigated area. Also, one of the biggest rear volcanoes (Alaid) are situated. These characteristics of this studies area indicate on the abnormal high-frequency volcanism in comparison with Southern Kamchatka and all others Kurile Islands. Determination of the causes for voluminous volcanoes which belong to nonstandard subduction conditions seem be interesting.

Consequently, in this study, we will newly distinguish geochemical variations across and along the NKI for major, trace elements and isotope ratios. We note that this study is the first to present high-precision data of this region. We will focus on the processes at the mantle wedge and slab. Types of slab components are investigated. Using isotope and trace element variations, we will determinate source of the mantle and their difference across and along the arc. In order to clear the geochemical features of the NKI, the spatial variations of Quaternary volcanoes compared with the surrounding area are displayed. This result will reveal that the NKI is the geoshemically peculiar area.

Chapter 2. Tectonic setting and general geology of Kurile Island Arc

2.1. Tectonic setting of Kurile islands

The Kurile volcanic archipelago stretches for 1150 km a width from 100 to 200 km from Kamchatka (Russia) to Hokkaido (Japan). The system develops at the convergent plate boundary between the overriding Okhotsk lithospheric block and the subducting northwestward Pacific plate. The Kurile island arc is a classical Mariana type subduction system (Stern, 2002), which consists the Kurile–Kamchatka trench, the Greater Kurile volcanic islands, and the Kurile Basin. The Greater Kurile island arc and Southern Kamchatka started to develop in the Early Miocene or Oligocene (Avdeiko et al., 2006, 2007) (Fig. 2-3). Accoring to Baranov et al. (2002), back-arc spreading of Kurile Basin was predominant in the Miocene. However, since Late Miocene compression of the basin started and continues until now. Kimura (1986) divided the Kurile arc into northeastern and southwestern parts on the basis of the trough "Boussol Strait" (Fig. 2-4). In the northeastern part, there exist two areas: Central Kurile and North Kurile by "Kruzenshtern Strait" (Fig. 2-5). Northern Kurile Islands locates between Southern Kamchatka and Kurile Arc.

Using Rayleigh wave tomography Bourova et al. (2010) suggested that upper mantle of NE Eurasia was heterogeneous and composed of several anomalies. The mantle wedge above Pacific Plate is associated with low velocity anomalies on the depth from 80 to 160 km. This indicates on the active process of partial melting. On the NW of Okhotsk sea, Gorbatov et al. (2000) and Bourova et al. (2010) have determined high velocity anomaly subparallel to the present subduction zone. Obtained anomaly may be interpreted as a relict of the Okhotsk plate

subducted in the past. Manea et al. (2005) have described thermal models for Southern Kamchatka. Authors believed that the low velocity zone was obtained beneath the volcanic belt and a high velocity anomaly reflected on the cold subducted lithosphere.

On the basis of constant convergence velocity of incoming Pacific Plate (approximately 8.6 cm/year), the age of the oceanic crust near the Kuril–Kamchatka trench becomes older southward, varying from 90 to 118 Ma. The surface of the down going Pacific plate is located beneath the volcanic front at a depth of 94.2 km (Southern Kurile Islands) to 92 km (NKI) (Syracuse and Abers, 2006). The forearc basin of NKI is located in submarine ridge Vityaz. Among submarine mountains, the sedimentary deposits accumulates. The incoming sediment pile have lithology, and their chemical composition and thickness are typical for NW Pacific sediments (Dreyer et al., 2010).

According to Zlobin et al. (1987), the crustal thickness varies insignificantly from 28 to 33 km in the southern zone of Kurile Islands, from 25 to 30 km in the central zone, and from 32 to 36 km in the NKI. Data of Dreuer et al. (2010) are agreed with previous and confirmed more thinker crustal thickness in the central Kuriles (10-15 km) and increasing to the north and south (~25 km).

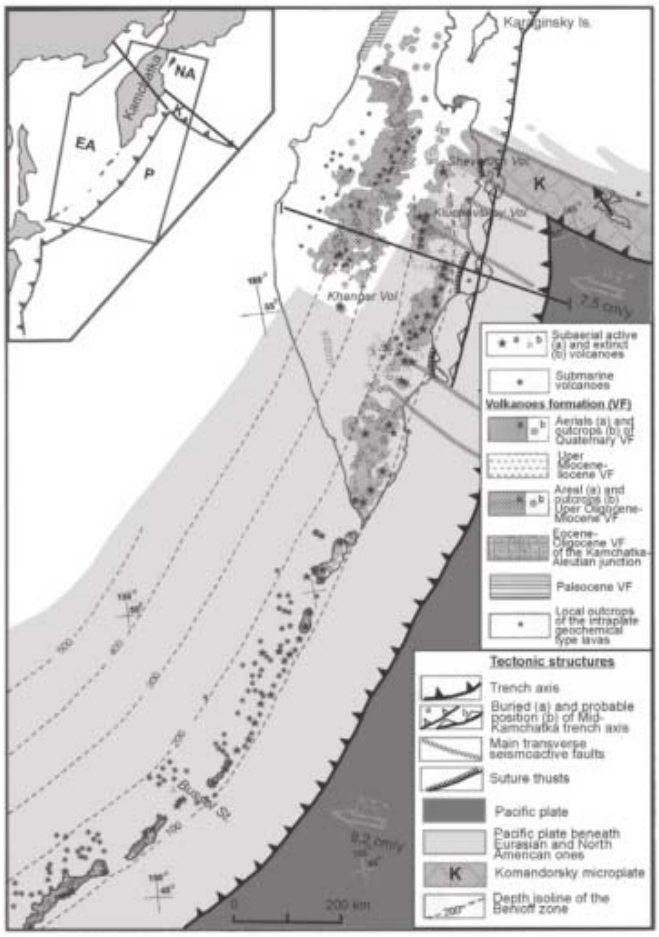

Fig. 2-3. Spatial distribution of Cenozoic subduction-related volcanic formations in the Kurie-Kamchatka island-arc system (Avdeiko et al., 2007).

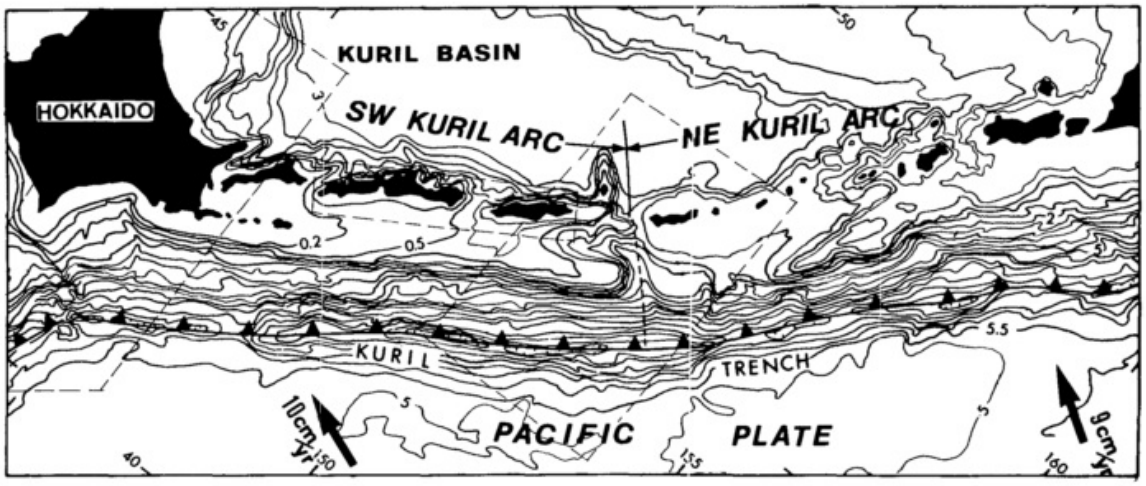

Fig. 2-4. Submarine topography of Kurile Arc (Kimura, 1986).

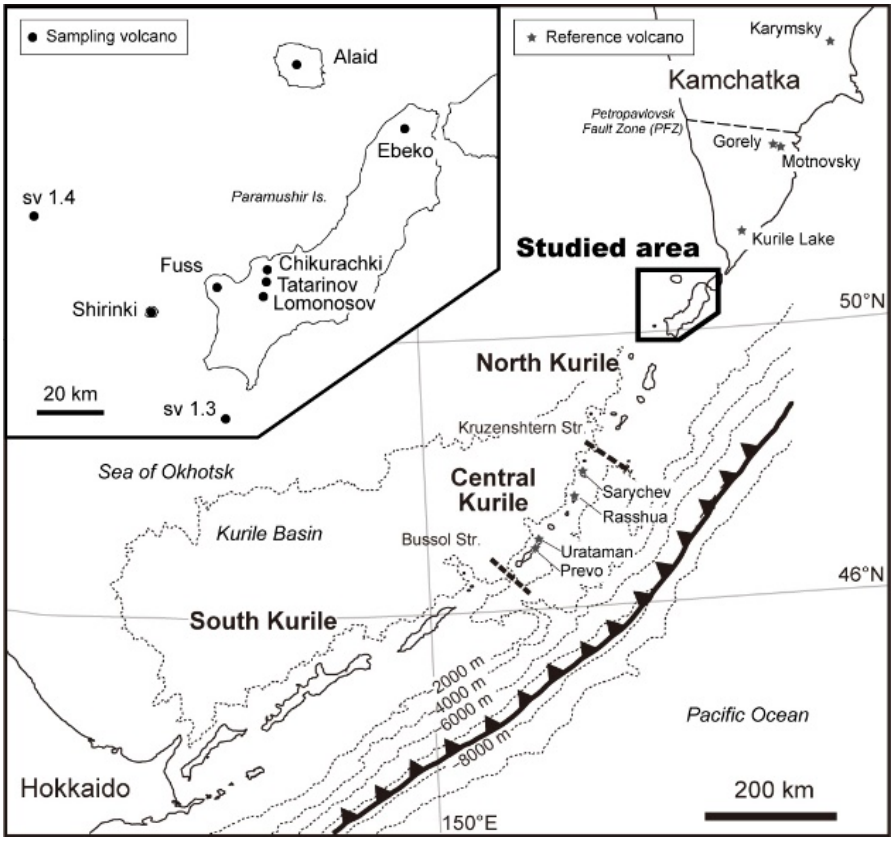

Fig.2-5. Outline of Kurile Islands and index map of Northern Kurile Islands. Kurile Islands divide into three regions: South, Central and North Kurile by Bussol and Kruzenshtern Straits.

2.2. General geology of the Northern Kurile Islands

The foundation of the Paramushir, one of the largest Kuril islands, composed of Miocene - Pliocene pyroclastic deposits Okruglovskoy Formation and overlying rocks of the Pliocene - Nizhnepleystotsenovogo Levashovsky complex. Levashovsky complex is represented by lava flows and dikes of andesite basalt (Kurile Islands (nature 2004) (Fig. 2-6).

In the Pleistocene and Holocene, blanket formed andesitic lava flows Vernadsky Ridge to the south-west of the Paramushir (Volcanic Group Chikurachiki, Tatarinov, University, Fuss Peak) and a group of volcanic islands in the north Ebeko (Fedorchenko V.I. 1989).

According to Gorshkov (1967), glaciations during the Quaternary occured twice: first, in the Pleistocene, the second in the Holocene. From these data it was found that the majority of the volcanic structures of the northern segment of the Northern Kurile Island Arc (NKIA) were formed in the Pliocene-Quaternary time.

It is also important to note that many researchers have emphasized the association of the volcanic centers to the regional faults, differently oriented with respect to deep-sea trench (Gorshkov 1967: Avdeiko, 1991). Certain patterns are observed in the spatial distribution of volcanoes along the arc. In accordance with the hypothesis of "hot fingers" (Tamura et al. 2002) in the mantle wedge, there are 10 fingers on the Kuril-Kamchatka subduction system, and two of them are located within the Northern Kuriles (Dobretsov 2010). One is confined to the transverse area: Ebeko - Alaid, and the other is corresponding to the volcanoes of the southern part of Paramushir Is. and Sirinki volcano.

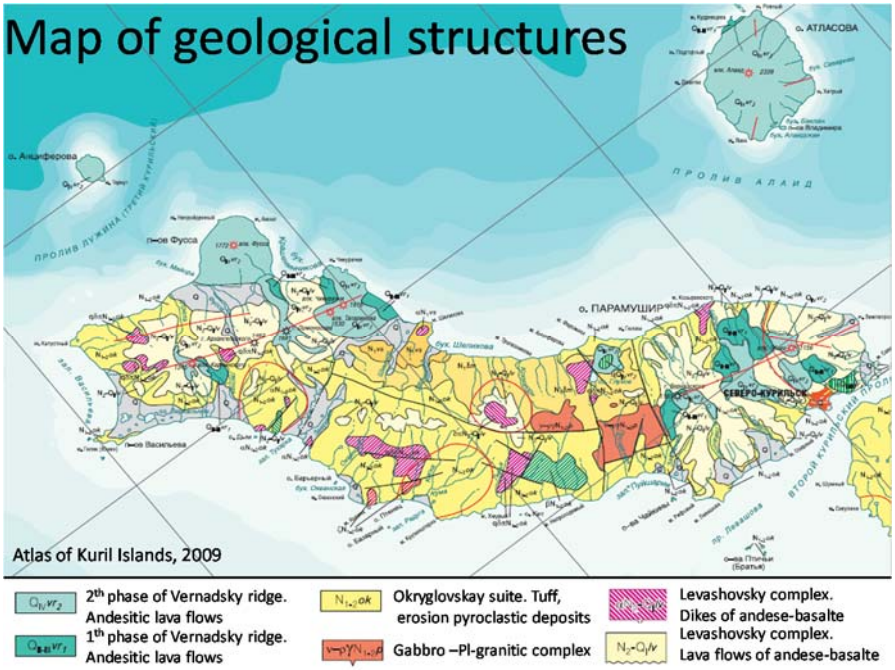

Fig. 2-6. Schematic map of geological structure for Northern Kurile Island Arc (Kurile Islands (Nature 2004).

2.3. Quaternary volcanoes in the studied area

2.3.1. Paramushir island

a) Chikurachki. Tatarinova, Lomonosova volcanoes

Volcanoes Karpinsky Ridge (Chikurachki, Tatarinova, Lomonosova volcanic group one of the structures of the Karpinsky Ridge volcanoes) is located on the southern island of Paramushir (Fig. 2-7) and have a "line-nested structure" that may indicate the association of a single fault (Gorshkov 1967).

Chikurachki volcano - a typical stratovolcano, composed primarily of pyroclastic deposits. It is based on ancient lava (Gorshkov 1967). Group volcanic Tatarinov, closely adjacent to the south of Chikurachki has a rather complicated structure and consists of at least six eruptive centers. Today's centers are located on the remains of the old, but fairly high (up to 1400 m) volcanic edifice, destroyed much of glacial activity. In the external appearance of this group of glacial landforms play an important role, and only on the eastern slopes are covered with modern forms lavas (Gorshkov 1967).

Group volcanic Lomonosov adjacent to the south of the volcano to an array Tatarinova, consists of five eruptive centers. The first of these centers is located on the border between the two arrays and is purely explosive no lava flows. The second cone - Mount Borisyak - is at the top of the crater, from which in an easterly direction for 3.5 miles down the lava flows Krupnoglybovye. From the south adjacent to the crater Borisyak two large cone. The first of these has a small crater, from which descends to the east a long lava flow (56% SiO_2). At 5.5 km from the crater, in the valley. Tuharki, he reaches the foot of the massif. Another cone - actually University (1681 m) - is an extrusive dome. From under the agglomerate mantle dome,

apparently from an old crater, now a sealed dome to the west of the lava flow down the length of more than 7 km. It extends almost to the shores of the Okhotsk Sea (Gorshkov 1967).

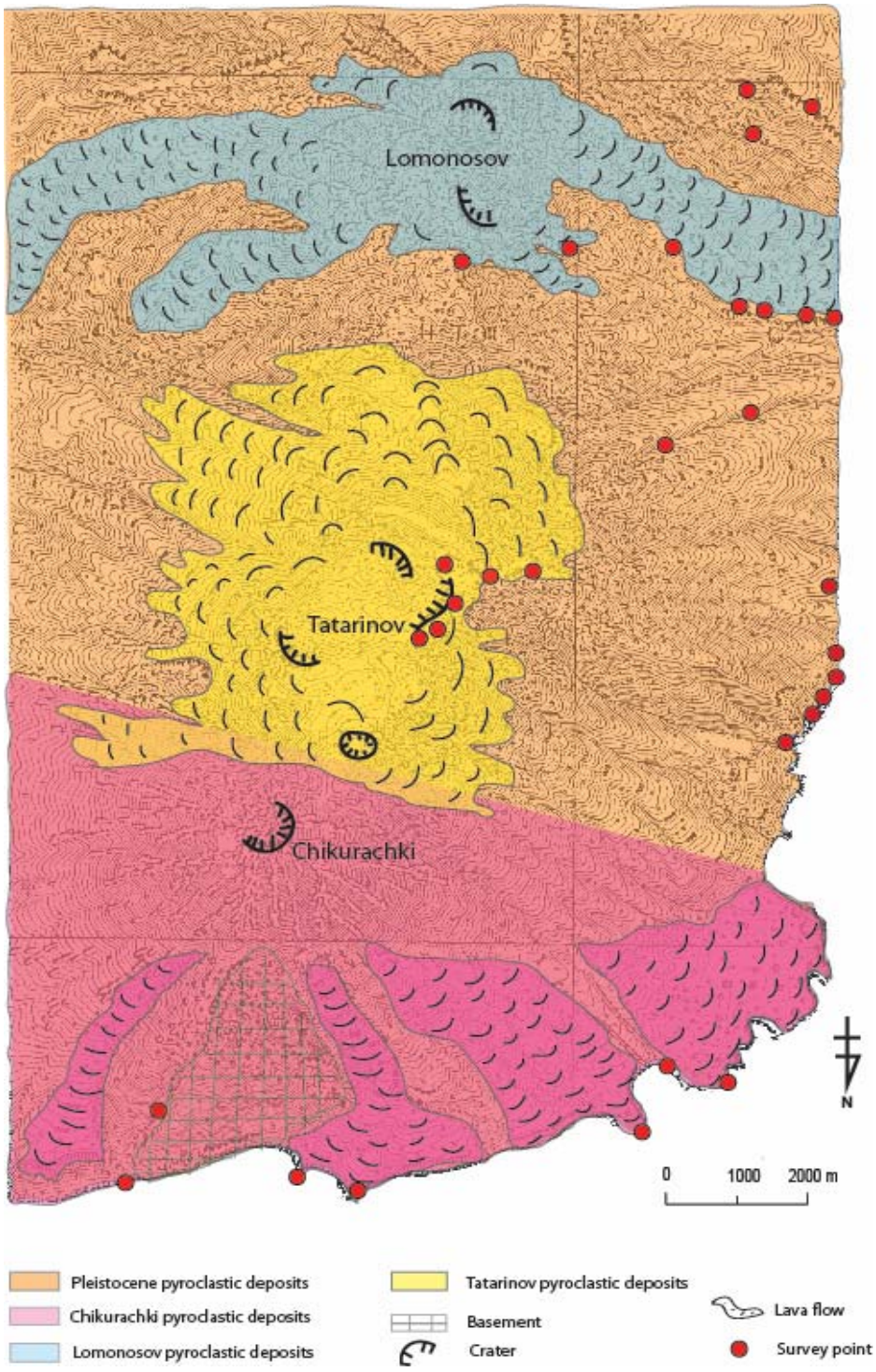

Fig. 2-7. Geological map of Chikurachki, Tatarinova, Lomonosova volcanic group (Gorshkov 1967).

b) Fuss volcano

Fuss Peak volcano is only single stratovolcano on Paramushir. The volcano forms a separate peninsula at the south-west coast of the island in a semicircle with a diameter of about 9 km and is connected to the foothills of the low-lying isthmus Karpinsky Ridge. Fuss Peak forms a regular, beautiful, highly truncated cone. At the top is a crater, which is very steep crater with a diameter of 700 m and a depth of 300 m (Gorshkov 1967) (Fig. 2-8).

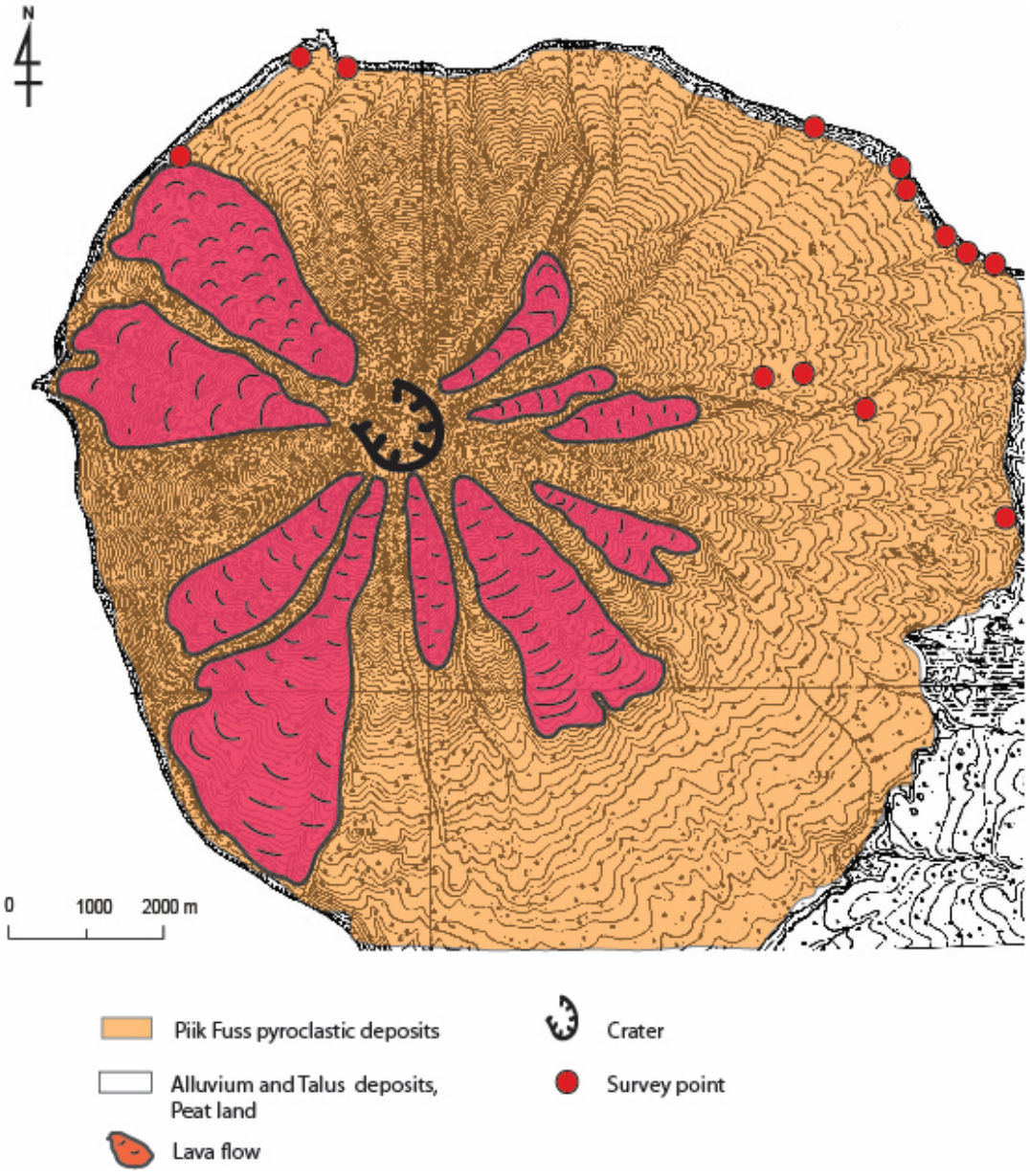

Fig. 2-8. Geological map of Fuss volcano (Gorshkov 1967).

c) Ebeko volcanic group

Ebeko volcanic group consists of Volcanoes Ebeko, Vetrovoy and Vlodavets part of Vernadsky Ridge. They have a "line-nested structure" (Gorshkov 1967). The volcano is a cone Ebeko relative height of 200-220 m (1037 m absolutly altitude), highly elongated in the meridional direction with three adjoining craters on top of that chain stretched from north to south. The dimensions of the three craters of about the same: the diameter of the ridge - about 300-350 m, bottom diameter - about 200 m total size of the summit crater - 350 × 800 m on the eastern and western slopes (Fig. 2-9) are two outdoor amphitheater, representing apparently, the lateral explosive craters, strongly enhanced the subsequent erosion, the crater of a smaller size with a small lake on the northern slope (Gorshkov 1967).

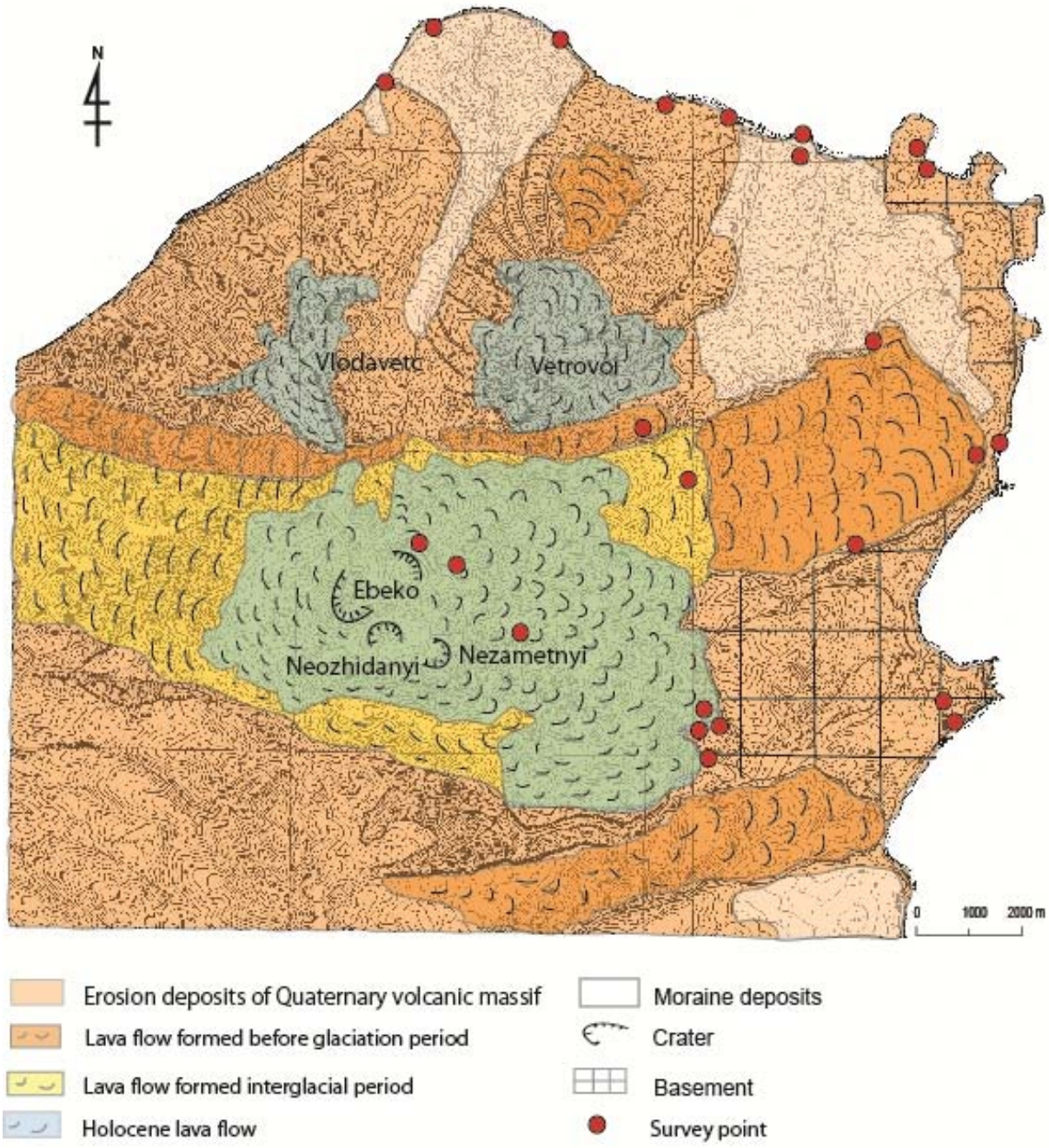

Fig. 2-9. Geological map of Ebeko volcanic group.

2.3.2. Atlasova island

a) Alaid volcano

Alaid is the northernmost and highest island of the Kuril Islands. It is an island-volcano, which forms an isolated island, which rises from the basement of the Okhotsk Sea, 20 km north-west of the coast of Paramushir and has an oval shape in plan, ancient summit crater with a diameter of about 1.5 miles and destroyed much wide open on the south ridge of its well-preserved in the form of half-rings in the northern half (Gorshkov 1967). The highest point of the volcano, the so-called main peak - 2339 m above sea level. m - is located in the northeastern part of the ridge. At the base of the cone and the bottom of its slopes are rather numerous small side craters (about 32) with scoria cones (Fig. 2-10). According to (Baranov et al. 2002) orientation of cinder cones is not random, it reflects the regional tectonic stress in the region may depend on actions of the Kurile back-arc basin. In historic times the volcano has repeatedly been active. Thus, in 1933-1934, there were lateral eruption, later known as' Taketomi, "which began as an underwater eruption, and then formed a small island, which eventually joined the land of the volcano Alaid. In 1972 there was another side eruption, which was named "Breakthrough of the Olympic." From 1981-1982, on the volcano there was a strong explosive eruption from the summit crater. Subsequently, there have been several publications describing the eruption of the volcano Alaid in 1981-1982.

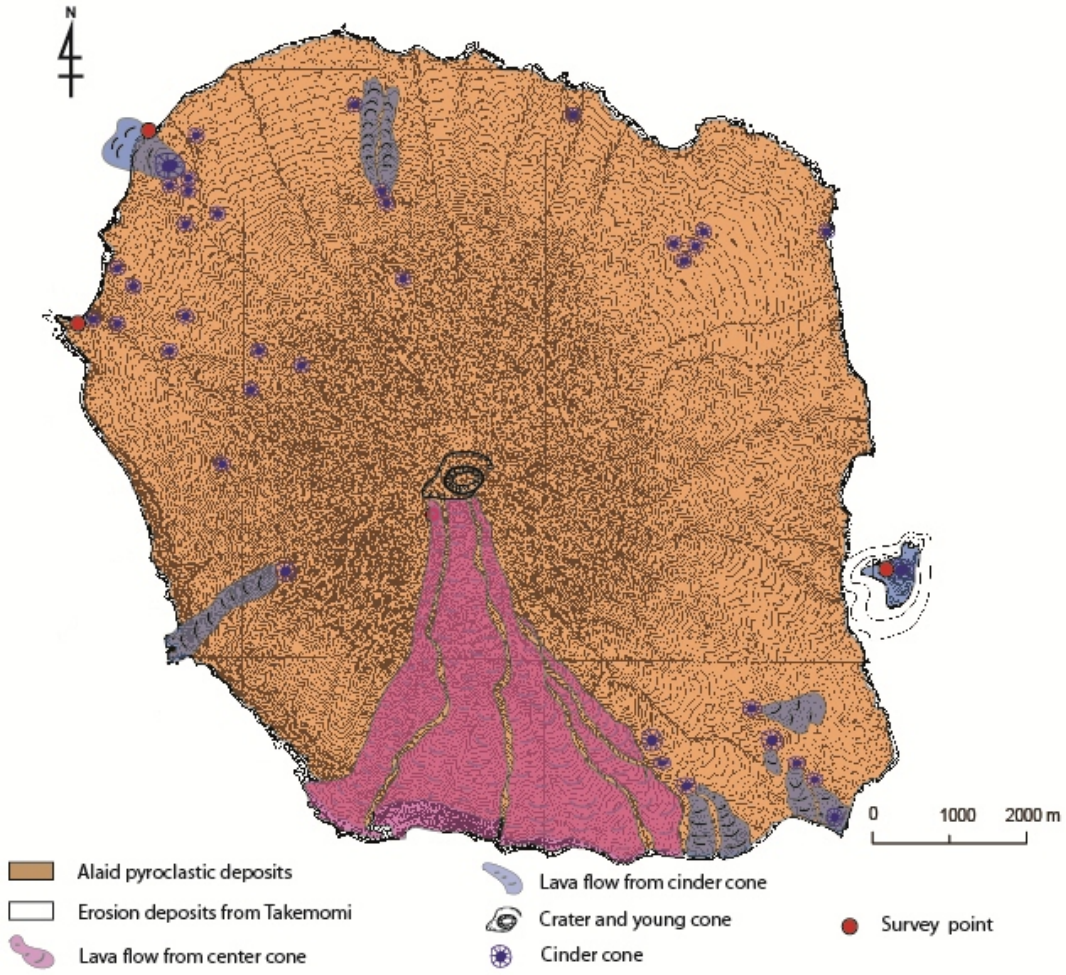

Fig. 2-10. Geological map of Alaid volcano (Gorshkov 1967).

2.3.3. Antsiferov island

a) Shirinki volcano

Shirinki volcano (or Antsiferova Island) forms an isolated island, rising from the waters of the Okhotsk Sea, 15 km west of the Peak Fuss. It has a shape almost perfect circle with a diameter of 3 km. The truncated cone of the volcano rises to 761 m above sea level. The summit crater about 750 meters is opened to the south. In several places on the slopes of the cone of the crater down lava flows that reach the sea. In the eastern part of the island (Fig. 2-11) exposed the remains of an older building with a monoclinal falling rocks to the east (Gorshkov 1967).

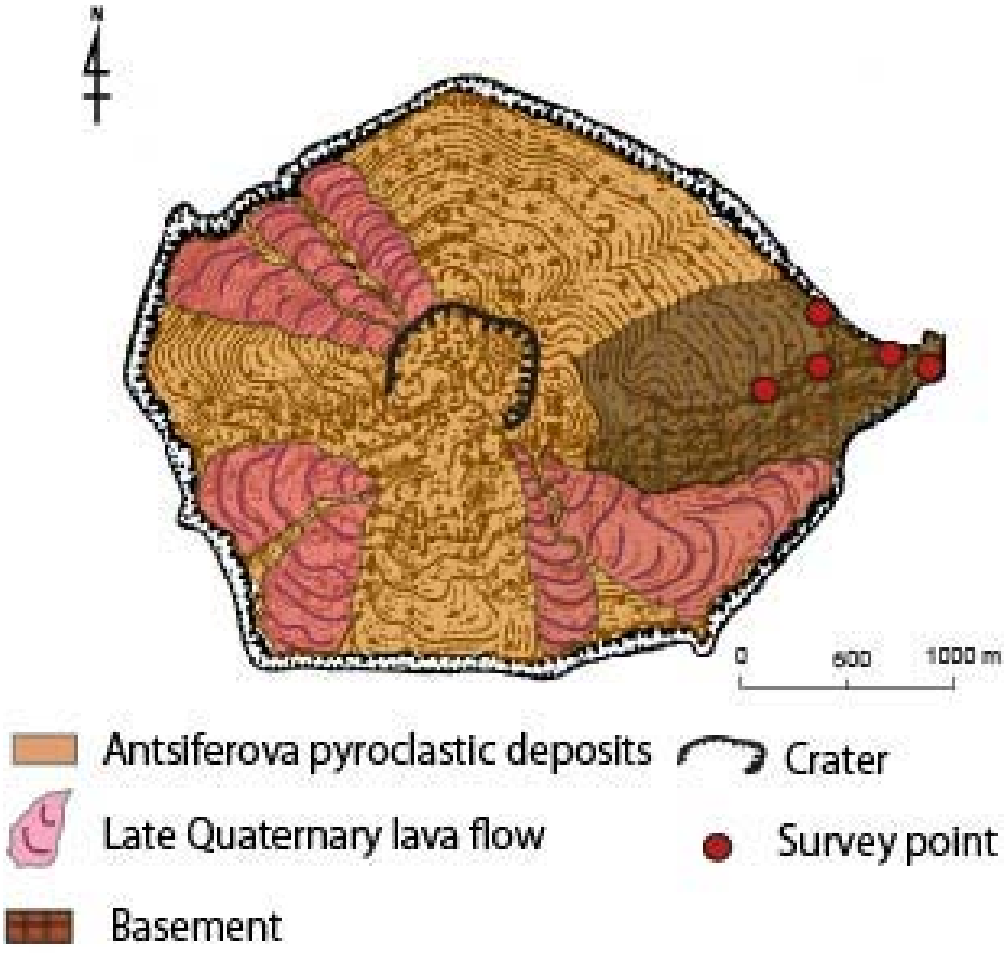

Fig. 2-11. Geological map of Sirinki volcano (Gorshkov 1967).

2.3.4. Submarine volcanoes

a) Grigoreva volcano

Volcano Grigorieva, or submarine volcano 1.1. (Avdeiko, 1992) rises from the depths of 800-850 m, and its base is merged with the base of the volcano Alaid (Bloch, 2006) (Fig. 2-12). The dimensions of the base of the volcano up 12.5 × 15 km and 500 m isobath to - 8.5 × 11.5 km. The top of the submarine volcano Grigorieva cut abrasion and leveled to the level of 120-140 m, which almost corresponds to the position of sea level during the Late Pleistocene. In the western and southwestern parts of the peaks marked by rocky ledges, rising to depths of 50-55 m may be they are the prepared necks, and can be formed after forming the top and represent a Holocene lava extrusion or small buildings (www.kscnet.ru).

b) Submarine volcano 1.4

Located at the intersection of the deflection Atlasov island the continuation of the transverse structure of the 4th Kuril basin, 80 km west of. Paramushir (Fig. 2-12). It is located far in the rear of the Kurile island arc at a distance of 280 km from the axis of the Kuril-Kamchatka Trench, towering above the surrounding bottom of the Sea of Okhotsk in the 650-700 m base his slightly elongated in a north-westerly direction and has a size of ~ 6.5 × 7 km. The top of the mountain is complicated by a number of peaks (Fig. 2-12). The negative form of relief is almost closed ring encircling the base of the volcano (www.kscnet.ru).

c) Submarine volcano 1.3

Located on the crest of the submarine ridge vent on the north of the north-eastern tip of Simushir in the 20 km from the coast. It takes an extreme position corresponding to the volcanic front, lying on his sharp bend. At the southern tip of the underwater ridge vent on

Simushir Island, at a depth of 500 m, there is a flat area, marking, apparently, the center of the volcanic massif. The western, southern and eastern slopes of the array of abrupt slope (20-25 °), uneven. Judging by the nature of the wave pattern on the seismograms NSP, they are composed of dense volcanic rocks. Low power (up to 250-300 m) Case of precipitation appears only at the base of the array (Avdeiko, 1992).

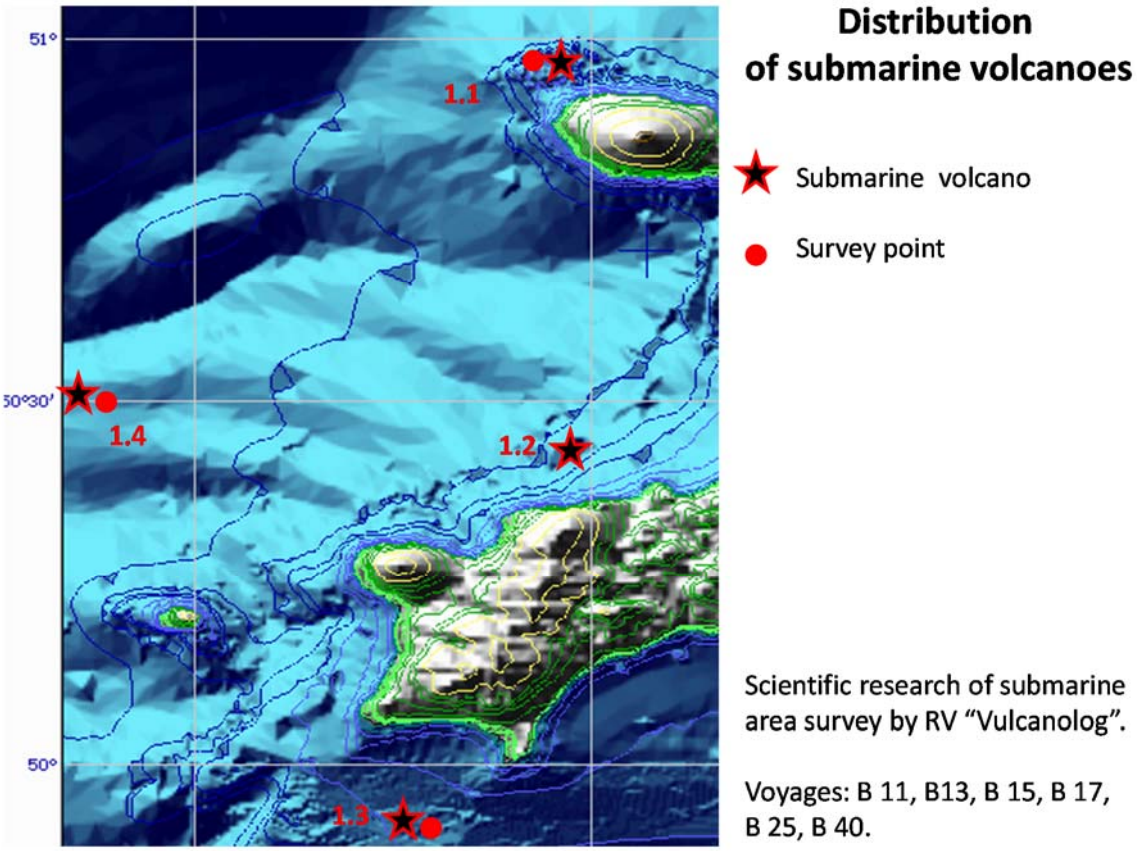

Fig. 2-12. Distribution map of submarine volcanoes.

Chapter 3. Sampling and analytical procedures

The rock samples from seven subaerial (Chikurachki, Tatarinova, Lomonosova, Peak Fussa, Shirinki, Ebeko, Alaid) and three submarine volcanoes (1.3, 1.4, 1.1 or Grigoreva) was treated. Submarine volcanoes and Sirinki, Alaid volcanoes had been investigated by RV "Vulcanolog" in the 1980-1990 years. Dragging samples from Research Cruise numbers 11, 24, 25, 34, 40 were analyzed. Volcanoes on the Paramushir Island were studied at the Kurile Biocomplexity project in 2007-2008. Part of the samples from historical eruptions of the Alaid volcano, kindly provided by V.A. Rashidov. Additionally XRF data of the volcanoes from southern part of Paramushir are used from Hasegawa et al. (2011). Hereinafter, submarine volcano 1.1 and Grigoreva are considered as “Alaid volcano” because of their similar features in addition to their close locations.

Sample preparation and analyses were carried out at Hokkaido University. Major elements and some trace elements were determined on 220 samples by X-ray fluorescene (XRF) analysis, using Spectris MagiX PRO system with Rh tube. All analyses were recalculated water-free and with total iron as FeO. Relative standart deviations are varied since 0.01 to 0.2 % for major elements. Additional trace elements were analysed by inductively coupled plasma mass spectrometry Thermo electron X-series (ICP-MS) on 46 samples. Experimental procedure used by the method of Miyashita et al. (2007). The Sr and Nd isotopic ration of 33 samples were determined by thermal ionization mass spectrometry using a Finnigan MAT 262 following analytical procedures of Orihashi et al. (1998). The analytical accuracy and reproducibility in this study were monitored by NIST-SRM987 for Sr and GSJ-JNdI-1for Nd. The results were $^{87}Sr/^{86}Sr = 0.71020788 \pm 0.000032$ (n=3) and $^{143}Nd/^{144}Nd = 0.512108857 \pm 0.000000971$ (n=3), respectively. Typical internal 2 SE for analazed samples are varied since 0.0000076468 to

0.0000121070 for Sr and since 0.000007593 to 0.000009193 for Nd. Representative geochemical and isotopic compositions were listed in Appendix II.

Chapter 4. Petrography

The volcanic rocks in this region is dominated basaltic andesite and andesite. They are different in the ratios of olivine, orthopyroxene, hornblende and clinopyroxene (Tables 2-1 and 2-2, Appendix II). The Chikurachki, Tatarinov, Lomonosov volcanoes is characterized by olivine-clinopyroxene-bearing orthopyroxene basaltic andesite, but for some volcanic rocks from Lomonosov volcano include quartz and olivine, which indicates the non-equilibrium solidification of magma. Ebeko volcano is more basic, and their rocks are often olivine-clinopyroxene-bearing orthopyroxene basaltic andesite. Fuss and Shirinki volcanoes are characterized by hornblende-bearing olivine and pyroxene-andesite. Those are only subaerial volcanoes of the NKI, which contain phenocrysts of hornblende. The rocks of Alaid volcano are typical pyroxene basaltic andesite. In the bulk rocks are characterized by olivine-bearing pyroxene-basaltic andesite (eruptions in 1933-1934). However, for eruptions in 1972, the eruptive materials often include the acid xenoliths (~ 63-72% SiO_2) (Avdeiko et al., 1977).

Except for Alaid volcano, the mineral assemblage of volcanic rocks of the NKI allowed us to assume the across-arc variation from the front to the rear of the island arc: Tatarinov and Lomonosov volcanoes are dominated by horblende-absent rocks. In contrast, Fuss and Sirinki volcanoes are characterized by hornblende-bearing rocks. Chikurachki and Ebeko volcanoes exhibit both types of rocks. The submarine volcano 1.3 and 1.4 also have two types of rocks.

Table 2-1. Summary of descriptions of the representative volcanic rocks from Northern Kurile Islands.

Sample No.	Source	Rock type	Occurrence	Groundmass (vol.%)	Crystal Content (vol.%)	Plg	Olv	Opx	Cpx	Hbl	Qtz	Fe-Ti oxide
A 14 – 03	**Tatarinov**	Cpx-Ol-bearing OPx basaltic andesite	scoria	78.6	21.4	16.8	0.7	2.5	0.5	-	-	0.9
A 14 – 8		Ol-Cpx-bearing Opx andesite	pumice	79.9	20.1	16.5	0.2	2.3	0.6	-	-	0.6
A 11		Ol-Cpx-bearing Opx basaltic andesite	lava	83.6	16.4	13.3	0.3	1.4	0.2	-	-	1.4
A 1	**Lomonosov**	Qtz-Ol-bearing Cpx-Opx andesite	lava	65.2	34.9	22.6	0.8	8.8	0.9	-	0.1	0.9
C 02 -01		Ol-bearing Cpx-Opx andesite	scoria	65.7	34.3	27.4	0.4	4.4	0.9	-	-	1.2
A 08 -08	**Chikurachiki**	Ol-Cpx-bearing Opx basaltic andesite	scoria	80.1	19.9	13.0	0.6	5.4	0.7	-	-	0.3
A 25 -02		Hbl-Cpx-bearing Opx basaltic andesite	lava	42.0	58.0	48.6	-	7.4	1.0	0.3	-	0.8
B 13 -02 B	**Fuss**	Hbl-Cpx-Ol-bearing Opx basaltic andesite	lava	64. 7	35.3	29.9	0.97	3.67	0.6	trace	-	0.1
B 15 - 03 C		Ol-Cpx bearing Opx-Hbl-andesite	pumice	87.7	12.4	7.0	trace	2.5	0.9	1.7	-	0.4
08 PR 11	**Ebeko**	Ol-bearing Cpx-Opx basaltic andesite	lava	53.7	45.4	39.5	0.5	3.6	1.6	-	-	0.2
08 PR 26 - 1		Ol-Cpx-bearing Opx basaltic andesite	scoria	59.1	40.9	35.9	trace	4.8	0.1	-	-	0.4
08 PR 16		Ol-Hbl-Cpx-bearing Opx andesite	pumice	53.2	46.8	40.3	0.2	4.6	0.8	trace	-	0.4

-: absent

Table 2-2. Summary of descriptions of the volcanic rocks from Northern Kurile Islands, taken from Avdeiko et al. (1992).

Volcano	Rock type	Occurrence	Mineral Assemblage
Shirinki	Hbl-bearing Px-Ol basaltic andesite	lava	Px>Pl>Hbl
Alaid	Ol-bearing Px basalt~basaltic andesite	lava	Pl>Px>>>Ol (,Mt)
1.3	Hbl andesite	lava	Pl>>Hbl>>Mt
	Px basaltic andesite	lava	Pl>>Opx>>Cpx, Mt
1.4	Cpx-bearing basaltic andesite	lava	Pl>>Hbl>Cpx>Mt
	Px-bearing Hbl andesite	lava	Pl>>Hbl>>Cpx>Mt

Chapter 5. Zonation of the volcanoes

On whole-rock chemistry, the silica contents of the rocks in the NKI range from 45 to 65 wt.% (Fig. 2-13). The most of the rocks have the range about 15 wt.% in SiO_2 in each volcano, except for Alaid. Alaid volcano are basalt and basaltic andesite. On K_2O contents, they show a wide variation: from 0.5 wt.% of sv. 1.3 to 3.0 wt.% of Alaid at SiO_2 = 55. On SiO_2 vs. K_2O plot, they draw linear trends in each volcano, except for sv. 1.4. The sv. 1.4 exhibit low-K in basaltic andesite and mid-K in silicic andesite. In contrast, on SiO_2 vs. Nb plot, Alaid volcano show higher than the others extremely.

According to the variations of petrography and whoe-rock chemistry as well as the location of the volcanoes, I can divide the Northern Kurile Islands into four areas: front, rear, Ebeko, and Alaid zones (Fig. 2-14). The frontal zone ("Front") includes Chikurachiki, Tatarinov, Lomonosov and submarine volcano 1.3 (120-140 km from subducting slab). Fuss and Shirinki volcanoes belong to rear zone ("Rear") (130-150 km from the subducting slab). Alaid volcano (160-180 km from the subducting slab) is the isolated group showing high-K and high-Nb features. Ebeko volcano (120-140 km from the subducting slab) should be separated from the previous two groups described below. Although submarine volcano 1.4 is located on the deep rear zone, more that 220 km from slab, chemical variations of the rocks show complicated: low-K and mid-K trends. Because of the complicated features, this volcano is not treated hereinafter.

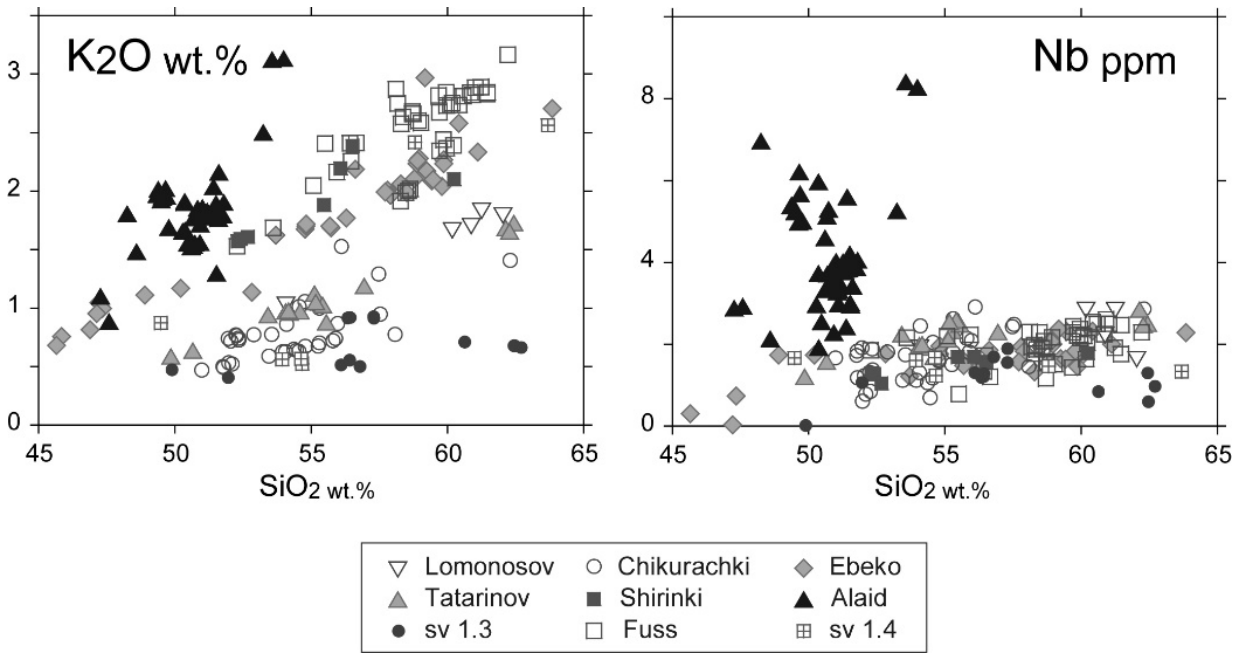

Fig. 2-13. Harker diagrams of the rocks from volcanoes in the Northern Kurile Islands.

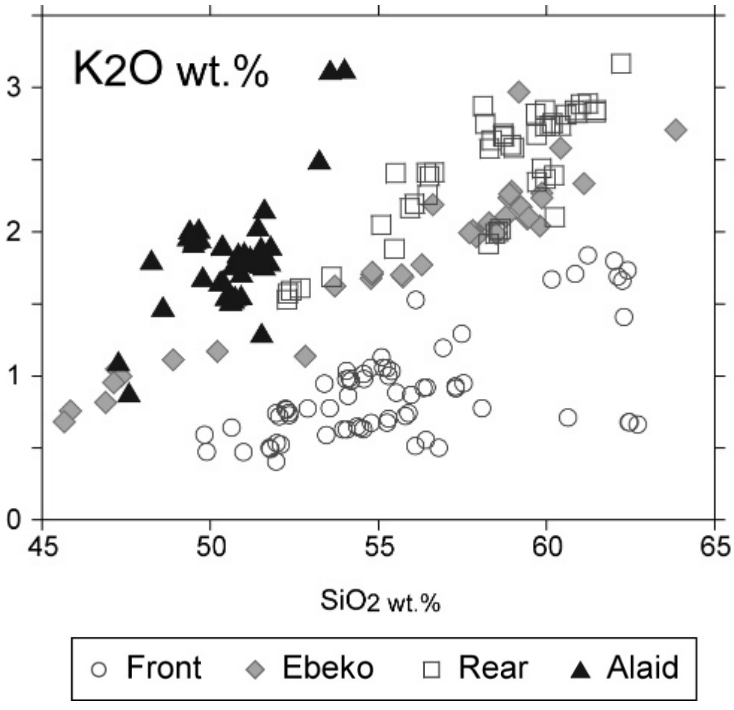

Fig. 2-14. SiO_2 vs. K_2O plot of the rocks from four groups in the Northern Kurile Islands. We can identify the four groups clearly.

Chapter 6. Geochemistry

6.1. Major and trace elements chemistry

On tha basis of the division of area described above, there are the distinct variations among four area groups (Figs. 2-15~2-16).

The rocks of frontal and rear zones exhibit the similar silica contents (50-65 wt.%, Fig 2-15). Frontal zone is characterized by lowest contents of incompatible elements (e.g. K_2O, Rb, Zr, Ba) at a given SiO_2. Nb contents seem to be the lowest. Some rocks show constant low contents of Zr with increasing silica, although another rocks typically increase Zr with SiO_2. In contrast, rear zone is characterized by high incompatible elements (e.g. K_2O, Rb, Ba). Andesitic rocks (53-64% wt. SiO_2) of the volcanoes are characterized by highest contents of Rb and K_2O. Some of andesitic rocks exhibit high-Ni content (Fig. 2-16).

Ebeko volcano includes varies types of rocks, from basalt to andesite (45~64 wt.% in SiO_2, Fig. 2-15). On andesitic rocks (SiO_2 >55 wt.%), some incompatible elements of Ebeko volcano are similar contents to those of rear zone (e.g., K_2O, Zr, Fig. 2-16). However, in Rb and Ba, the rocks of Ebeko volcano have the intermediate features between frontal and rear zones. The basaltic rocks (SiO_2 <55 wt.%) seem to be similar to those of basic parts of Alaid volcano (e.g., FeO*, CaO, Ba), whereas Ti and Ni contents are much lower.

The rocks of Alaid volcano are narrow in SiO_2, comprising basalt and basaltic andesite (Fig. 2-15). They show the highest contents of incompatible elements (K_2O, Rb, Zr, Ba). Interestingly, Nb contents exhibit much higher (exceeded 8 ppm, Fig. 2-16). They also draw the distinct linear trends from the others in CaO, converging at basic side of Ebeko volcano.

Considering the N-MORB normalized plots of the mafic rocks (SiO_2 <55 wt.%), all the

rocks in the Northern Kurile Islands are arc-type features (Fig. 2-17). Similar to the variations incompatible elements in Harger diagrams, frontal zone exhibits lower LIL elements (Rb, Ba) and L-REE (La, Ce) than rear zone. Ebeko volcano seems to have the intermediate contents between frontal and rear zones. Alaid volcano show higher Nb and Ta in addition to LILelements and L-REE.

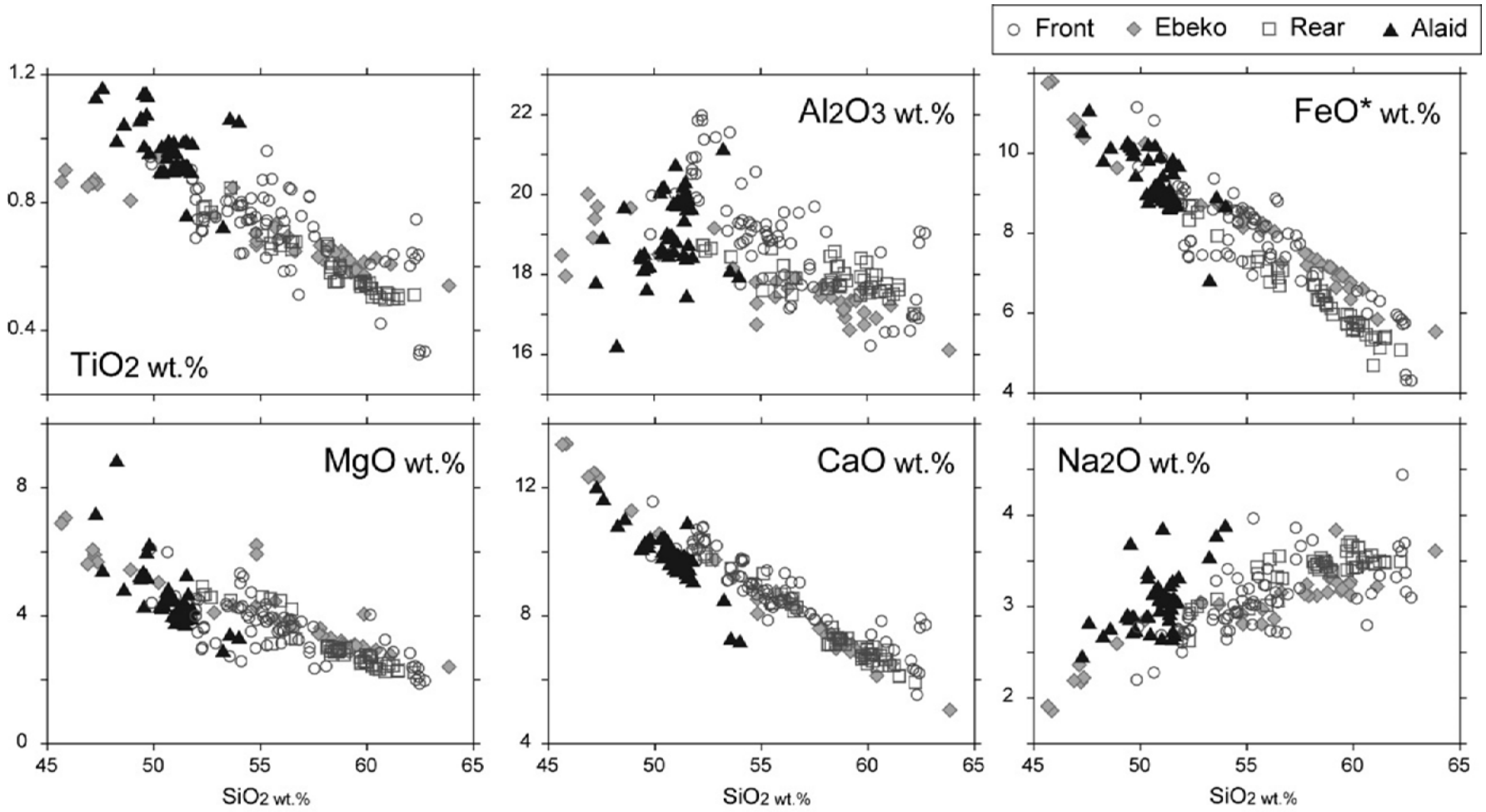

Fig. 2-15. Harker diagrams of major elements for whole-rock chemistry of the volcanic rocks from Nothern Kurile Islands in this study.

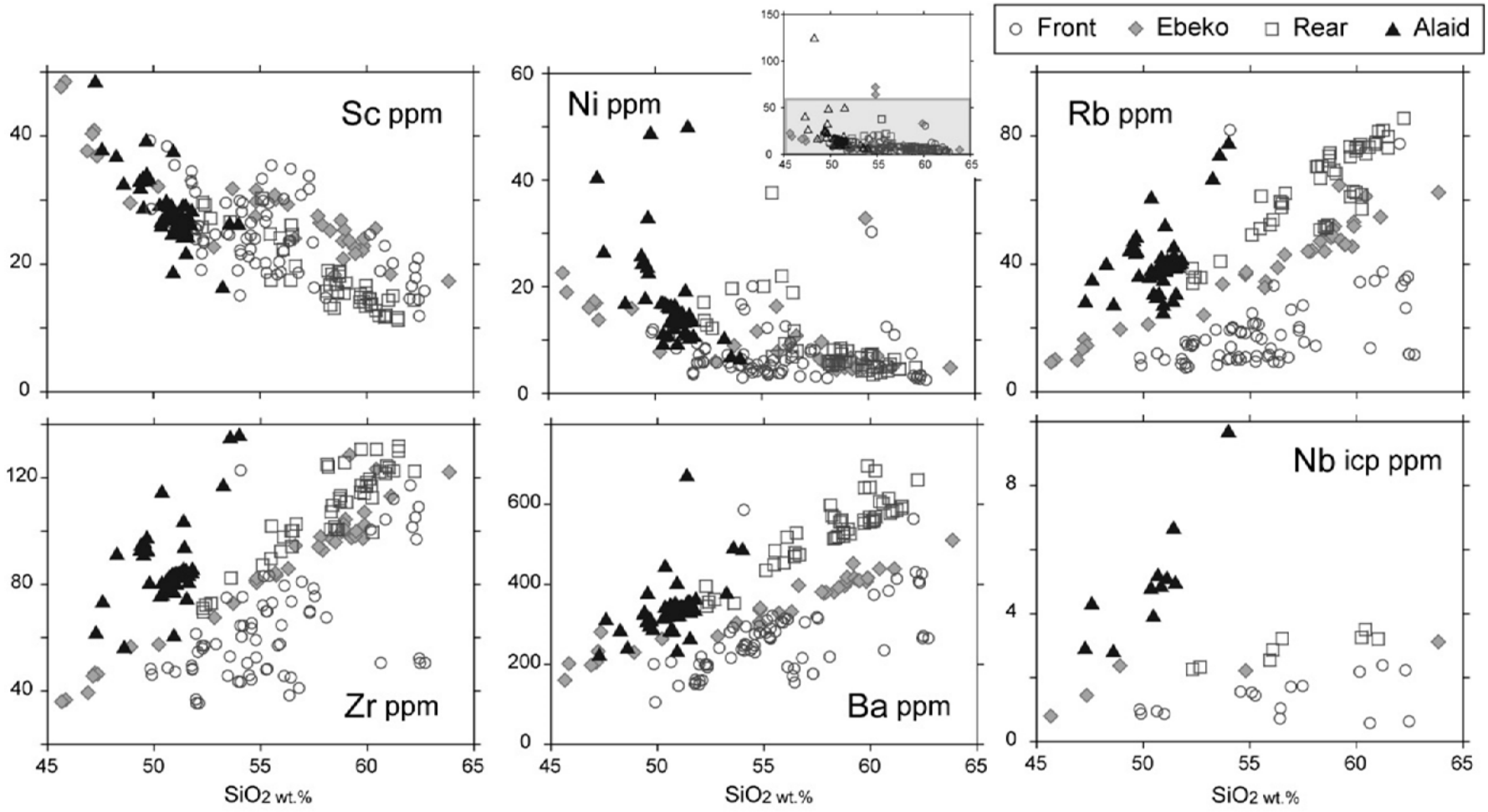

Fig. 2-16. Harker diagrams of trace elements for whole-rock chemistry of the volcanic rocks from Nothern Kurile Islands in this study.

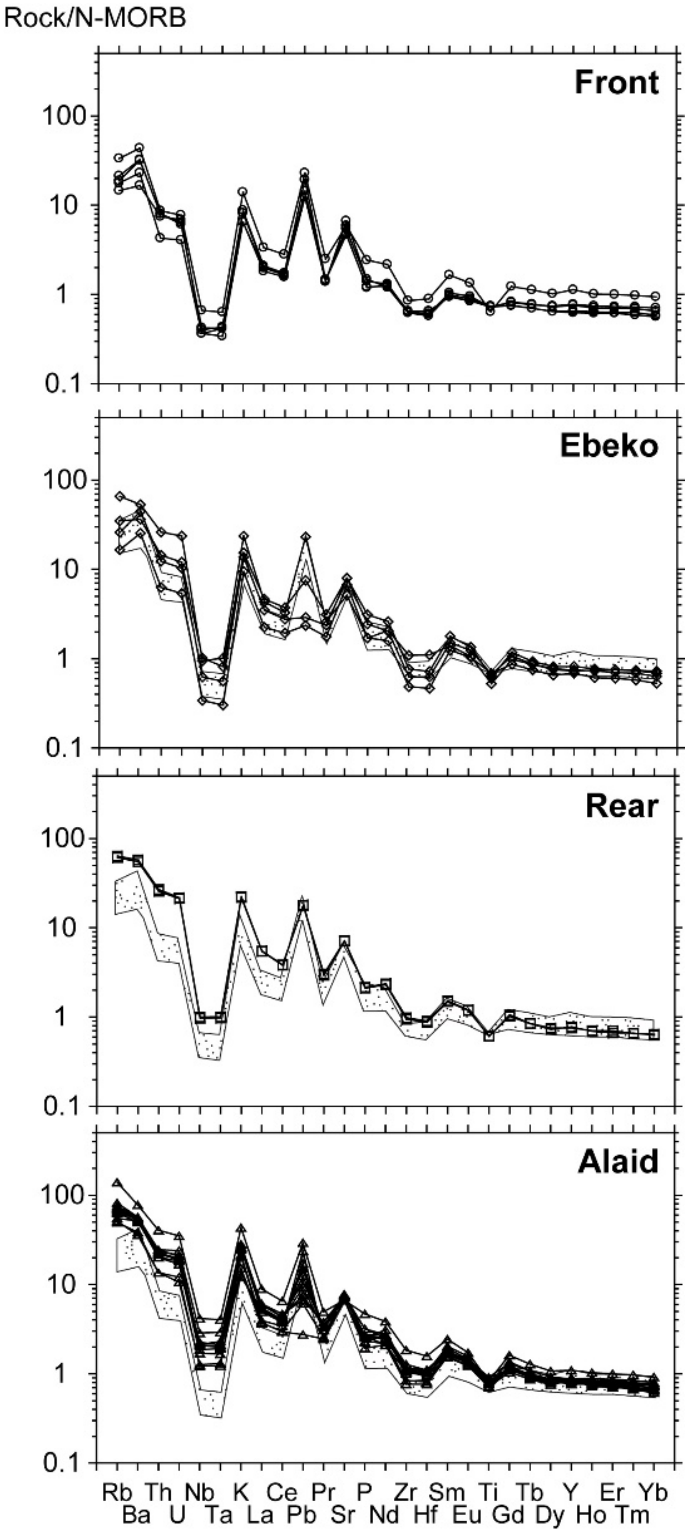

Fig. 2-17. N-MORB-normalized trace element patterns for the mafic rocks (SiO_2<55 wt. %) from Northern Kurile Islands. Dot area shows the range of the rocks from frontal zone. Data of N-MORB is taken from Sun and McDnough (1989).

6.2. Radiogenic isotopes

The volcanic rocks of Northern Kurile Islands show 0.7028-0.7034 in $^{87}Sr/^{86}Sr$ (Fig. 2-18a). They tent to increase in Sr isotopic ratio with increasing silica content, especially more than 55 wt.% SiO_2. The compositional range of the studied samples vary and determined across arc zones have specific isotopic features. Isotopic variations of the frontal zone has the highest value of $^{143}Nd/^{144}Nd$ and $^{87}Sr/^{86}Sr$ as 0.7031-0.7034 (Fig. 2-18b). In the opposite, rear zone and Alaid volcano show lower contents of $^{143}Nd/^{144}Nd$ and $^{87}Sr/^{86}Sr$ as 0.7029-0.7031. Although Alaid volcano is characterized by narrow range of $^{87}Sr/^{86}Sr$ variations (0.702964477-0.703062388), they show wider range of $^{143}Nd/^{144}Nd$ (0.51299-0.51305). Rear zone has a variated range in Sr isotope ratios (0.7288-0.7031), but near the same Nd isotope ratios (0.51302-0.51306). Range of isotopic variations of rear zones and Ebeko, Alaid volcanoes can be characterized as enriched mantle source. Comparing with the surrounding area, the rocks of Northern Kurile Islands exhibit the distinct isotopic ratios from the surrounding area: lower Sr and Nd isotope ratios (Fig. 2-18b).

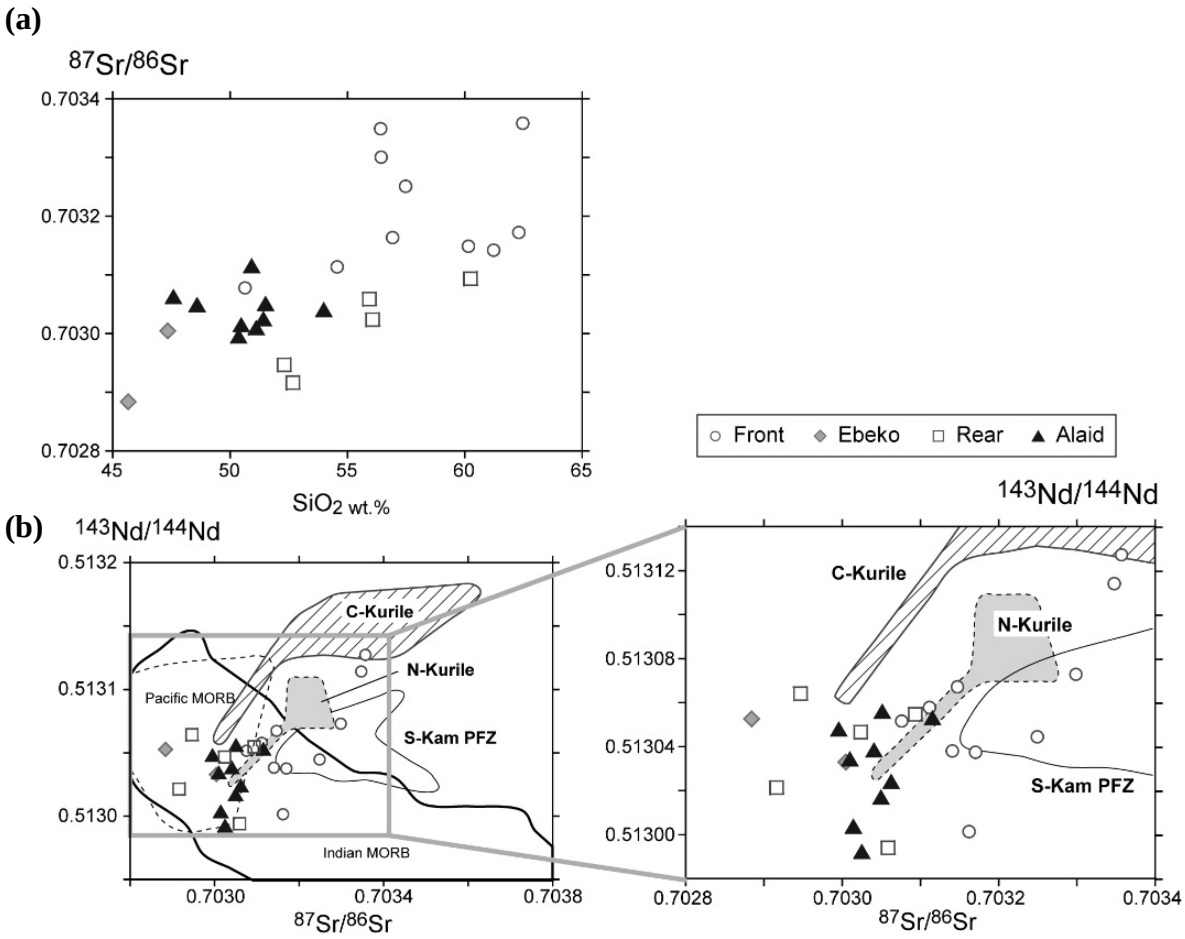

Fig. 2-18. Isotopic compositions of the volcanic rocks from Northern Kurile Islands. (a) $^{87}Sr/^{86}Sr$ vs. SiO_2 plot, (b) $^{87}Sr/^{86}Sr$ versus $^{143}Nd/^{144}Nd$. C-Kurile: Central Kurile, N-Kurile: Northern Kurile, S-Kam: southern part of Kamchatka. PFZ includes Gorely and Motnovsky volcanoes, and others include Karymsky and Kurile Lake caldera. These data of the rocks from the surrounding area are taken from Izbekov et al. (2004), Ponomareva et al. (2004), Duggen et al. (2007), Martynov et al. (2010) and Selegman et al. (2014). Data of MORB are from Stracke et al. (2003).

Chapter 7. Discussion

7.1. Comparison with the southern Kamchatka and central Kurile islands

Comparing to the surrounding area, there exists the remarkable feature of Northern Kurile Islands. At the mafic side in addition to the silicic side, the rock from Northern Kurile Islands (Rear aone, Ebeko and Alaid) show higher contents in incompatible elements than the southern Kamchatka as well as Central Kurile Islands (Fig. 2-19). Also, Alaid volcano exhibit much higher Nb content. Such incompatible-rich features of not only Alaid volcano, but also rear zone and Ebeko volcano, have not been reported. This is because that this study treated a large amount of samples with many kinds of data. Although previous study reported the data of Norther Kurile Islands, these wide variations cound not be found.

Similarly, isotopic compositions of Northern Kurile Islands are also unique: low Sr and Nd isotopic ratios (Fig. 2-18). The variations of isotope in the Kurile arc was also investigated by Martynov et al. (2010). Using these new data, we should reexamined the along arc variations in the future.

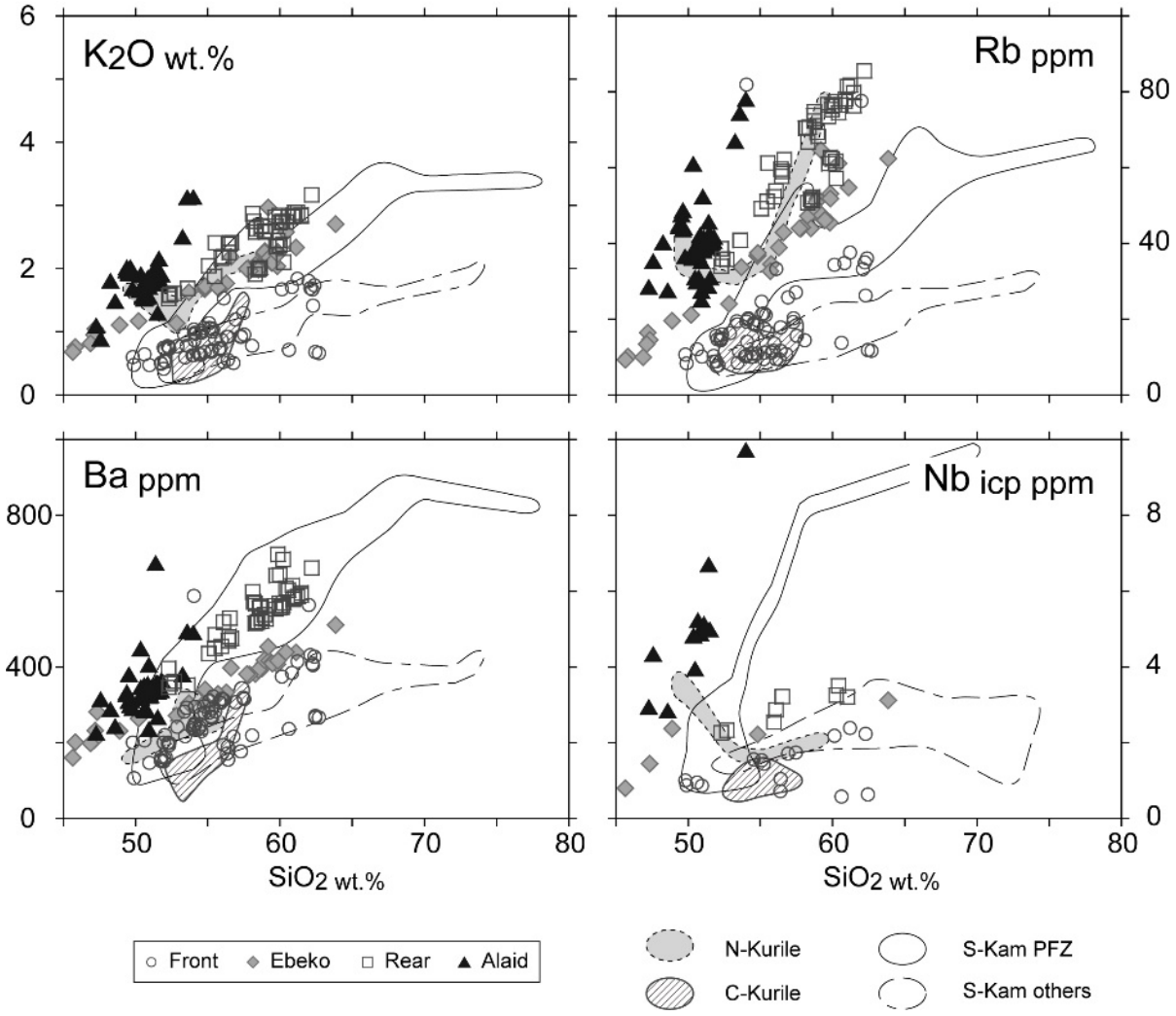

Fig. 2-19. Harker diagrams form NKI and surrounding areas of Kamchatka and Kurile Arc. C-Kurile: Central Kurile, N-Kurile: Northern Kurile, S-Kam: southern part of Kamchatka. PFZ includes Gorely and Motnovsky volcanoes, and others include Karymsky and Kurile Lake caldera. These data of the rocks from the surrounding area are taken from Izbekov et al. (2004), Ponomareva et al. (2004), Duggen et al. (2007), Martynov et al. (2010) and Selegman et al. (2014).

7.2. Possibility of fractional crystallization and assimilation

The volcanic rocks of Northern Kurile Islands show wide variation: from basaltic to silicic andesitic. This suggests that the magma evolution have been progressed by various situation: in sutu the magma source, generation in deeper level, and evolution in shallower level, i.e., in the crust. In order to reveal the relationships between geochemical fetures and tectonic setting, it should be important to eliminate the effect of the evolution process of shallower level.

In the crust, assimilation of the crustal components is one of the popular processes of the magma evolution in the arc magma system. Simple diagrams of the isotope compositions vs. SiO_2 (Figs. 2-18) help to investigate what kind process prefer in magma evolution. For example, if isotopic composition not change with increasing SiO_2 this suggest about fractional crystallization as main process for magma evolution. At the case of two distinct isotopic ratios at a given SiO_2, this mean different in source components. If increase contents of the isotopes with increasing SiO_2, this mean that process of assimilation and fractional crystallization (AFC) play important role in the magma evolution.

In a plot of Zr against Rb, most of the rocks in each groups (except for frontal zone) don't draw linear trends converging zero, suggesting that these variations cannot be explained by simple fractional crystallization (Fig. 2-20). On Sr isotopic compositions (Fig. 2-21), the rocks of Northern Kurile Islands show the tendency that increase $^{87}Sr/^{86}Sr$ with increasing SiO_2, as described above. Focusing on frontal and rear zones, more silicic samples (SiO_2 >55 wt.%) exhibit higher Sr isotopic ratios. This indicates the possibility that andesitic rocks have undergone the crustal assimilation. In contrast, on Alaid and Ebeko volcanoes as well as frontal

and rear zones, the mafic samples (SiO_2 <55 wt.%) have the lower, relatively constant in $^{87}Sr/^{86}Sr$ within each group. This feature suggests that mafic samples are non (or less) affected by crustal materials. Hereinafter, only the mafic rocks, less than 55 wt.% in SiO_2, are treated.

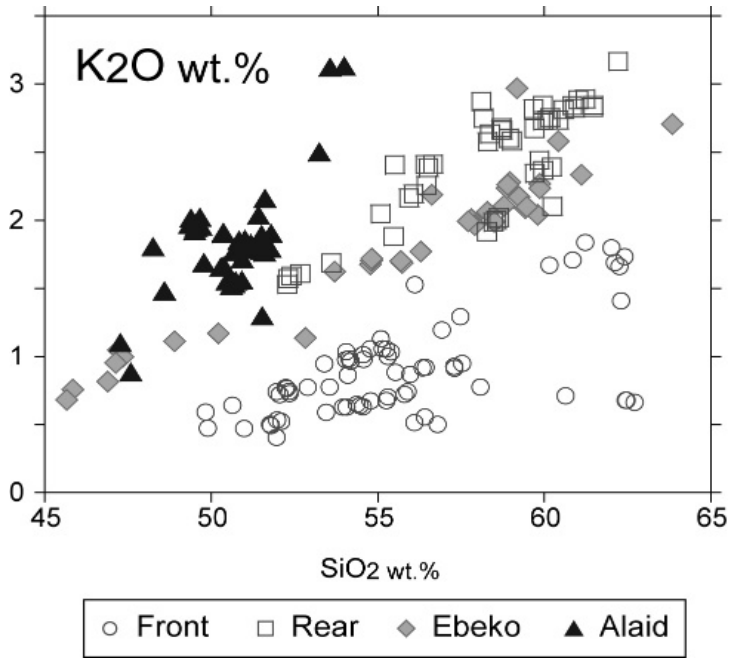

Fig. 2-20. Zr vs. Rb plot of the rocks from Northern Kurile Islands. Their variations in each group as well as among the groups cannot be explained by simple fractional crystallization.

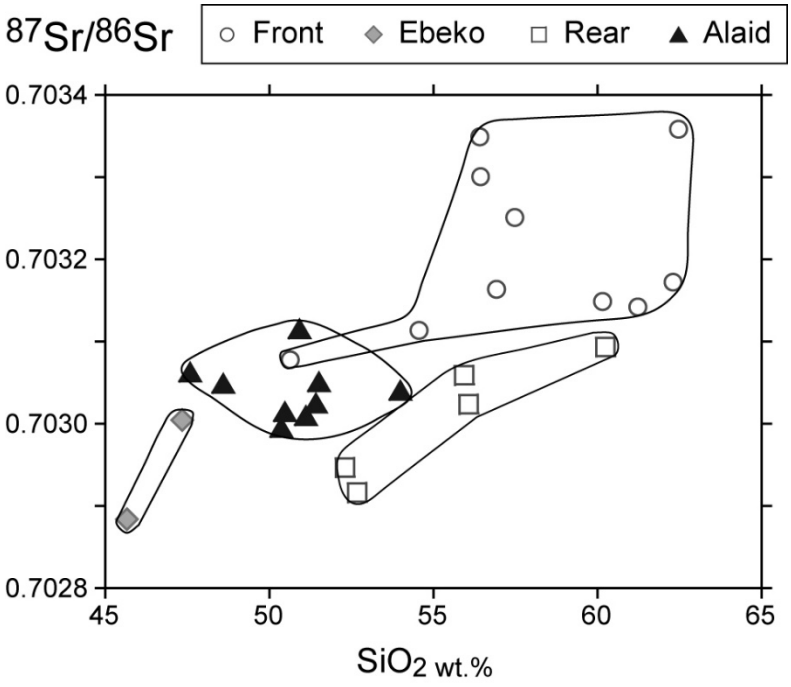

Fig. 2-21. $^{87}Sr/^{86}Sr$ against SiO_2 plot of the rocks from Northern Kurile Islands. On the mafic rocks (SiO_2 <55 wt.%), Sr isotopic ratios are distinguishable among the gourps, suggesting difference in source materials.

7.3. Variation of wedge mantle

Unmodified mantle represent by primary mantle before addition of the subduction components or processes in the crust. In determining the composition of the mantle source, we based on the assumption that transport of HFSE and HREE in the slab fluid are limited (Pearce J.A., 1983). Fluid immobile elements (e.g. Nb, Zr, Hf, Y,Yb) testify about mantle unmodified mantle composition (Kelley et al., 2006 ; Portnyagin et al., 2007).

Ratios of the fluid-immobile elements and isotope ratios clear illustrate several different groups with various concentrations. Frontal zone has lowest contents of Nb/Yb, Zr/Y, Nb/Y ratios (Fig.2-22a,b). In opposite, rear zone and Ebeko volcano show relatively higher Nb/Yb, Zr/Y, Nb/Y than frontal zone. Alaid volcanoes are characterized by highest concentrations of the fluid-immobile ratios, relatively close to OIB source. In Ta/Yb vs. Th/Yb plot, we can identify the relative difference of source materials (Fig. 2-22c). In frontal zone, mantle source is depleated, similar to that of Central Kurile Islands. For Ebeko volcano and rear zone, mantle source is slightly enrichment, similar to that of the southern part of Kamchatka. In contrast, the mantle source of the rocks from Alaid volcano shows the most enrichment in the southern Kamchatka and Kurile Islands. Interestingly, some rocks of Ebeko volcano exhibit similar variation to Alaid volcano, seeming to be plotted on the extended trend of Alaid volcano. Ebeko volcano is located the northeastern part in the studies area, near Alaid volcano. Therefore, this feature might suggest the petrogenetic relationship between Ebeko and Alaid volcanoes, for example, mantle source beneath the northeastern end of Kurile arc is affected by OIB component. Incidentally, comparing to the surrounding area, the Northern Kurile Islands have higher effect of subduction component (see below).

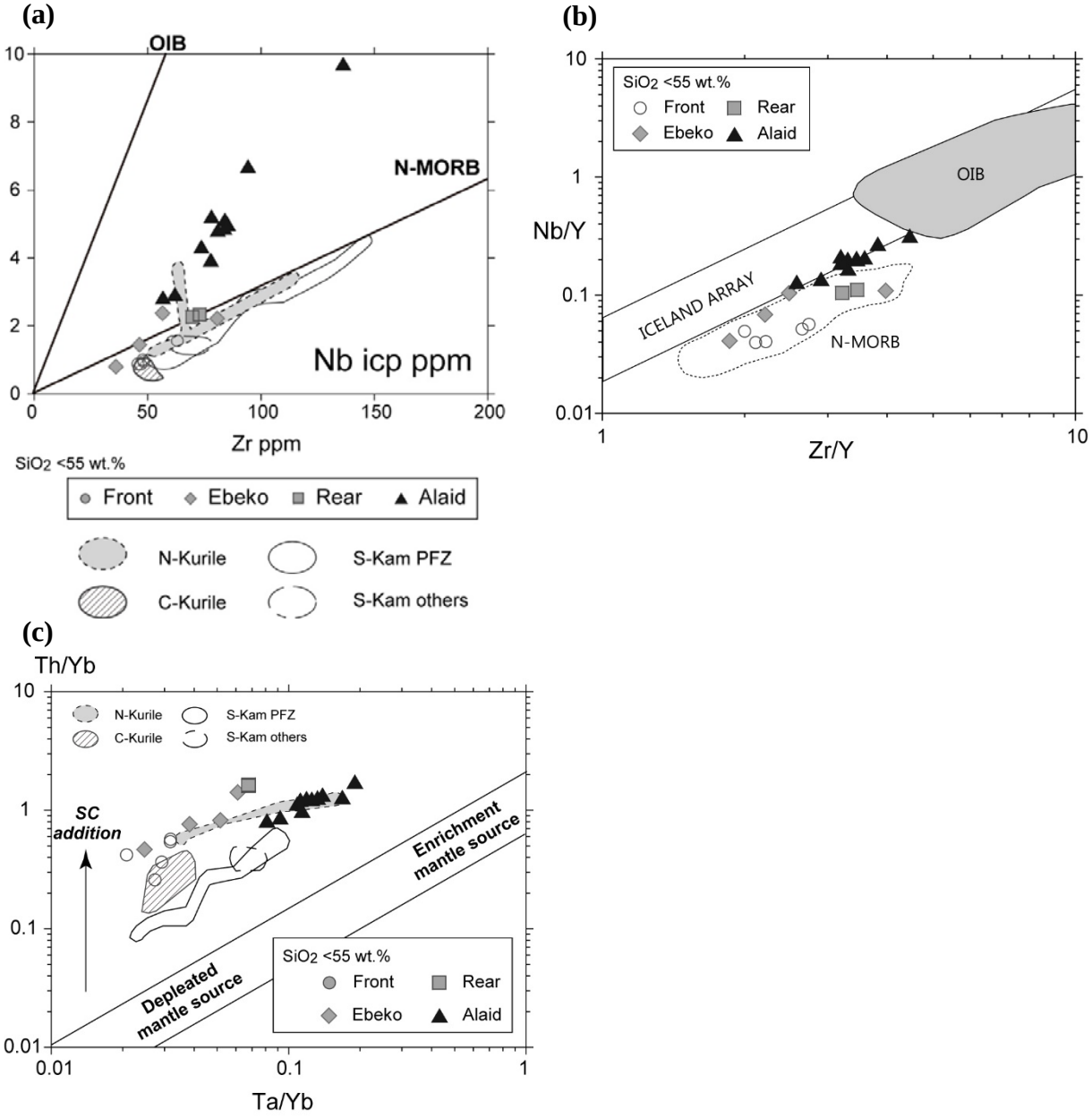

Fig. 2-22. Ratios of fluid immobile elements for the mafic rocks (SiO_2<55 wt. %). (a) Nb against Zr plot. Data of OIB and N-MORB are taken from Sun and McDnough (1989), (b) Zr/Y vs. Nb/Y plot (Fitton et al., 1997, 2003), and (c) Ta/Yb vs. Th/Yb plot (Pearce, 1983). SC: subduction component.

C-Kurile: Central Kurile, N-Kurile: Northern Kurile, S-Kam: southern part of Kamchatka. PFZ includes Gorely and Motnovsky volcanoes, and others include Karymsky and Kurile Lake caldera. These data of the rocks from the surrounding area are taken from Izbekov et al. (2004), Ponomareva et al. (2004), Duggen et al. (2007), Martynov et al. (2010) and Selegman et al. (2014)

7.4. Variations of subduction component

One of the important processes for magma genesis and variations in the arc systems is subduction component. As a rule, subdiction component include dehydration of the fluid from Altered Oceanic Crust (AOC) and/or “shallow”-subdiction component, and sediment melt fluid or “deep”- subduction component (Pearce et al., 2005).

Investigation of the different types of the fluids are based on the specific features of trace elements. The fluid-mobile elements (e.g. Cs, Ba, U, Th, Sr) are easily transported in dehydration fluid. Immobile elements (e.g. Nd, Nb, Zr, Hf) come in the fluid from sediment melting.

7.4.1. Front, Ebeko, Rear zones

At first, I examine the variations of the rocks from frontal and rear zone, and Ebeko volcano, because the source mantle in these areas are relatively similar, probably depleated MORB mantle source.

Ratios of the fluid-mobile/fluid immobile show that magmas in the frontal zone are characterized by largest concentration fluid mobile element (Fig. 2-23). This means that the magma was formed by a large amount of the dehydration fluids from AOC. Trend of frontal magma has a tendency to aqueous fluid deribed from slab fluids. In the opposite, magma from rear zone have largest concentration in fluid-immobile elements and trends of the variations near the same with sediment compositions from Kurile and Kamchatka.

In contrast, Ebeko volcano has two kinds of features in subduction component. Some samples have trend like aqueous fluid dehydration from AOC, similar to frontal zone. Only one

sample is characterized by high concentrations Th/Yb ratio, suggesting the effect of sediment melts, similar to rear zone.

Despite on fact that all volcanoes are located in one tectonic zone, subduction component for south and north is different. Distance from slab to the volcanoes are various (130 and 140-150 km consequently). Corresponding to differences in distance to slab, the wide geochemical diapason of intermediate zone magmas have a normal across arc zonation. The volcanoes which located near the trench are formed by dehydration fluids, and volcanoes which located on farther distance relatively to trench are formed by sediment melt.

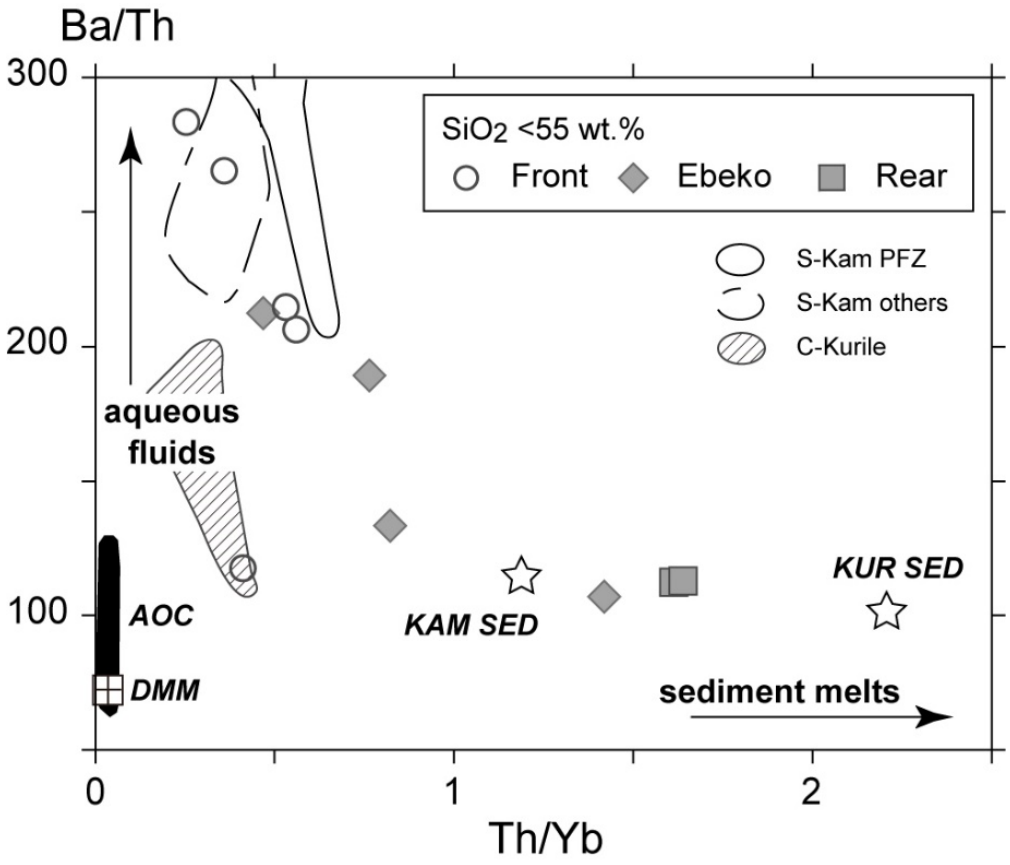

Fig. 2-23. Ba/Th vs. Th/Yb for mafic rocks from front, rear zones and Ebeko volcano. KAM SED: Kamchatka sediments, KUR SED: Kurile sediments, AOC: altered oceanic crust, data

from Plank and Luimir (1998). DMM: depleted MORB mantle source, data from Workman and Hart (2005).

7.4.2. Alaid volcano

The mafic rokcs from Alaid volcanoes also show high concentration in fluid-immobile elements and trends of the variations near the same with sediment compositions from Kurile and Kamchatka (Fig. 2-24). However, as discussed above, the source materials of Alaid volcano are affected by OIB source (Fig. 2-22). OIB source also show high-Th/Yb value. On whole-rock chemistry, the basic rocks from Ebeko volcano show similar trend to those of Alaid volcano in many kinds of Harker diagrams. In the ratio plots of fluid-inmobile elements, we can similar features. In Th/Yb vs. Ba/Th plot, Alaid volcano seems to draw the trend between DMM-OIB mixed source and Basic rocks of Ebeko volcano. Summarizing these features, it is probable that Ebeko and Alaid volcanoes have the petrogenetic relationships. Of course, previous works of studied influence of subduction components on the magma genesis on the Southern Kamchatka and Kurile Islands indicated that magma in the rear zones and Alaid volcanoes was formed by sediment melts (Dreyer et al., 2010; Duggen et al., 2007; Martynov et al., 2010). I don't discuss in detail here, but the identification of magma source of Alaid volcano is my future issue.

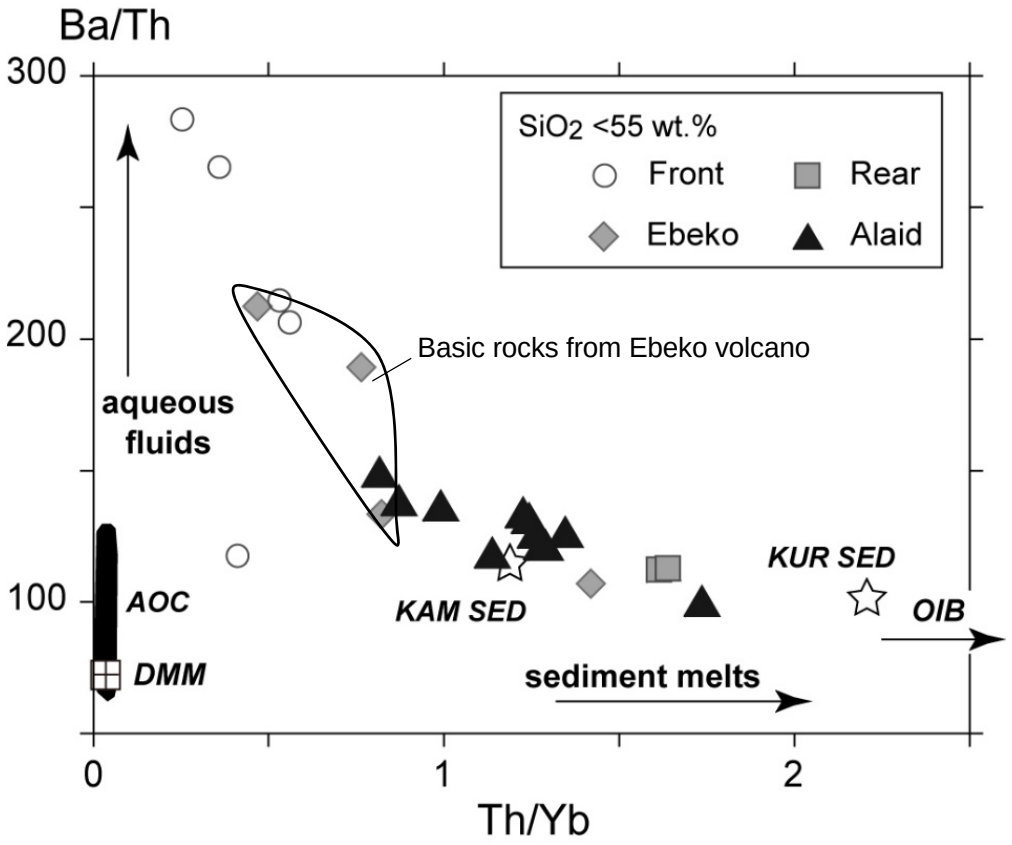

Fig. 2-24. Ba/Th vs. Th/Yb for mafic rocks from Alaid volcano. The data from the other groups are also shown. Data of OIB is taken from Sun and McDnough (1989).

7.5. Anomalous features of Alaid volcano

As discussed above, the rocks from Northern Kurile Islands show unique geoshemical features. These variations include many effects from mantle source as well as subduction component. Here, comparing to the surrounding area, spatial change of types of mantle wedge is exmanied.

The variation of Th/Yb vs. Ta/Yb was used for distinguishing between primitive island-arc rocks from depleted and enriched sources (Pearce J.A., 1983: Fig. 2-22c). The higher concentration in Th over in Yb can be explain by strong process of subduction input (from sediment melt) (Pearce et al., 2005). The highest contents of Ta/Yb ratio testify about more enriched mantle source. However, reference data are still not enough in Ta. Therefore, the ratio of Nb against Zr is used for the index of mantle source: MORB and OIB sources show low- and high-Nb/Zr (Fig. 2-22a).

The geochemical map shows in Fig. 2-25. According to this result, the following features are recognized. In Central Kurile Islands, mantle source is more depleted (less than 0.020). Compared with Central Kurile Islands, Northern Kurile Islands, except for Alaid, become higher Nb/Zr (0.019-0.032), that is, mantle source changes to be enrichment. In contrast, at the far northern area, i.e., the shouthern Kamchatka, the Nb/Zr values are not so high (0.019-0.029), similar to those of the Northern Kurile Islands. Only Alaid volcano exhibit abnormal features, reaching 0.071. Some of rocks from Ebeko volcano also show the relatively high Nb/Zr (0.042), comparable to the lowest value of Alaid volcano.

These features propose two conclusions. At first, the mantle wedge beneath Northern Kurile Islands is similar to that of the southern part of Kamchatka. Next, the mantle wedge beneath Alaid (and Ebeko) volcanoes is extremely abnormal, i.e., enrichment of OIB

component. The upwelling of OIB component at the rear zone might be controlled by tectonic setting at the traditional area between Kuril islands and Kamchatka. In order to reveal the structure of wedge mantle and tectonic setting of the area, additional geochemical study for volcanoes especially from southern Kamchatka peninsula must be essential.

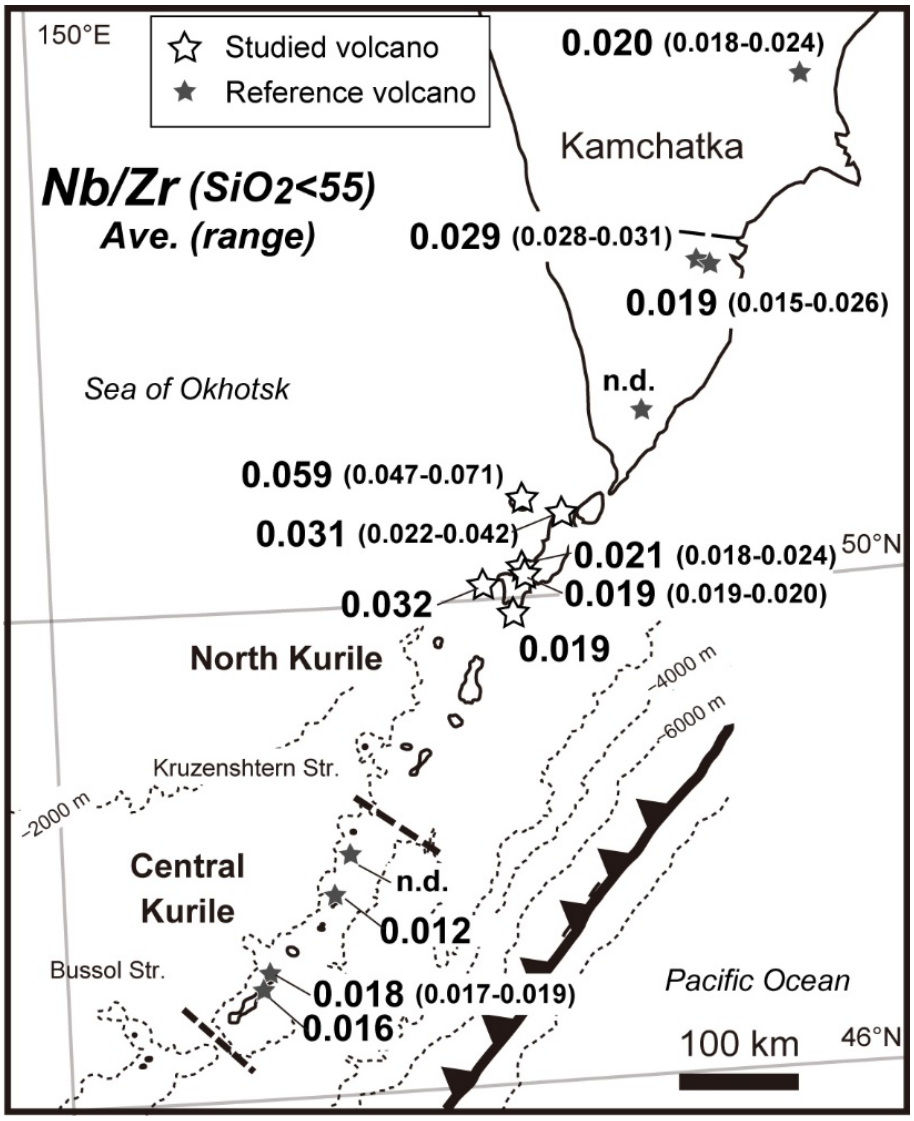

Fig. 2-25. Map illusttrted Nb/Zr values of the volcanic rocks in Northern Kurile Islands with those of the volcanoes in the surrounding area. Comparing with the surrounding area, Alaid volcano exhibits high-Nb/Zr significantly.

Chapter 8. Conclusions

Quaternary volcanism of the NKI was investigated in the represented work. New high-precision results of major and trace elements, and Nd-Sr isotopic compositions were determined and combined with pre-existing data. Peculiarities of whole-rock, trace elements chemistry, and petrography enable us to divide of all volcanoes into three main tectonic zones: frontal, intermediate and rear.

Fluid-immobile elements and isotope variations suggest about heterogeneity unmodified mantle along and across the NKI. Unmodified mantle continuously enriched toward to southern rear zone, consequently more depleted magma form frontal volcanoes, but more enriched mantle typical fore rear volcanoes. In comparing with southern area, the mantle source of Ebeko volcano is more enriched. Especially, involving more enriched mantle component like OIB may be explained peculiarities of Alaid volcanos.

Different types of fluids are exist. Dehydration fluid dominate in the frontal zone. Large amount of the sediment melting fluid are important for magma genesis in the rear zones. Various types of subduction components of rear zone in southern and northern area of NKI zone can be explained by differences in distance to slab and corresponding processes. Ebeko volcano exibits dehydration fluid as well as sediment melts.

The geochemical variations across and along the NKI mainly results from (1) heterogeneous mantle, (2) different types of subduction components, (3) anomaly of mantle source beneath Alaid volcano. The small enrichment of mantle source is also found in Ebeko volcano. The effect of OIB component in the mantle wedge exists in the northeastern end of Kurile arc.

References

Almeev, R. R., Kimura, J. I., Ariskin, A. A., & Ozerov, A. Y. (2013). Decoding crystal fractionation in calc-alkaline magmas from the Bezymianny Volcano (Kamchatka, Russia) using mineral and bulk rock compositions. Journal of Volcanology and Geothermal Research, 263, 141-171.

Antonov AV (2006). The Matter zoning of Kurile Island Arc volcanism and new Petrogenetic consequences. Litosphere, 1: 22-44 (in Russian)

Ariskin, A. A., Frenkel, M. Y., Barmina, G. S., & Nielsen, R. L. (1993). COMAGMAT: a Fortran program to model magma differentiation processes. Computers & Geosciences, 19(8), 1155-1170.

Ariskin, A. A. (1999). Phase equilibria modeling in igneous petrology: use of COMAGMAT model for simulating fractionation of ferro-basaltic magmas and the genesis of high-alumina basalt. Journal of Volcanology and Geothermal Research, 90(1), 115-162.

Auer, S., Bindeman, I., Wallace, P., Ponomareva, V., & Portnyagin, M. (2009). The origin of hydrous, high-δ18O voluminous volcanism: diverse oxygen isotope values and high magmatic water contents within the volcanic record of Klyuchevskoy volcano, Kamchatka, Russia. Contributions to mineralogy and petrology, 157(2), 209-230.

Avdeiko GP, Tokarev PI, Menyaylov IA (1977) Flank eruption Olimpiysky on the Alaid volcano in 1972. In: Volcanism in Islan Arcs. Moscow.Nauka, pp 55-64 (in Russian)

Avdeiko GP, Volynets ON, Antonov AY, Tsvetkov AA (1991) Kurile Island-Arc Volcanism - Structural and Petrological Aspects. Tectonophysics, 199(2-4): 271-287

Avdeiko G.P., Volynets O.N. 1992. Submarine volcanism and zoning of the Kurile Island Arc.

Avdeiko G.P, Palueva A.A. 2002. Tectonic evolution and volcanic, tectonic zoning of the Kurile-Kamchatka Island Arc.Tectonics **4**: 64-80.

Avdeiko, G. P., A. A. Palueva, et al. (2006). "Geodynamic conditions of volcanism and magma formation in the Kurile-Kamchatka island-arc system." Petrology **14**(3): 230-246.

Avdeiko, G. P., Palueva, A.A., Kuvikas, O.V. (2012). Type of volcanism in the modern subduction zone: geodynamic conditions, geochemical characteristics. Saint Petersburg, Saint Petersburg State University.

Avdeiko, G. P., D. P. Savelyev, A. A. Palueva, S. V. Popruzhenko (2007). Evolution of the Kurile Kamchatka volcanic arc and dynamics of the Kamchatka-Aleutian junction. In J. Eichelberger, E. Gordeev, P. Izbekov, M. Kasahara, and J. Lees eds. Volcanism and Subduction: the Kamchatka Region, 37-55.

Avdeiko, G. P., O. N. Volynets, et al. (1991). "Kurile Island-Arc Volcanism - Structural and Petrological Aspects." Tectonophysics 199(2-4): 271-287.

Avdeiko G.P., Bergal-Kuvikas O.V. Geodynamic conditions of genesis adakites and Nb enriched basalts on Kamchatka. Journal of Volcanology and Seismology. 2015. V. 9 (5). Accepted, in press.

Balesta S. (1981). Crustal and magmatic chambers in the areas of modern volcanism. Moscow. Nauka. 132. (in Russian).

Baranov, B. V., R. Werner, et al. (2002). "Evidence for compressionally induced high subsidence rates in the Kurile Basin (Okhotsk Sea)." Tectonophysics **350**: 63– 97.

Belousov, A. B., Belousova M.G., Grishin S.Y., Krestov P.V. (2003). "Historical eruptions of Chikurachki volcano (Paramushhir island, Kurile Islands)." Volcanology and seismology **3**: 15-34.

Bergal-Kuvikas OV (2012) Pecularities of the spatial variations from Paramushir volcanic group, Kurile Island Arc. Bulletin of Kamchatka regional association "Educational-scientific center". Earth Science, 20: 14 (in Russian)

Bergal-Kuvikas O., Malik N., Serovetnikov S., Klimenko E. (2012). First results of the Russian-Japanese project “The Complex geological and geophysical investigations of the northern volcanic group on Kamchatka, dynamic and forecast of eruptions for ensure safety of population”. Conference: Kamchatka regional conference for young scientists 28-20 November 2012. 69-84.

Bergal-Kuvikas O.V., Nakagawa M., Muravyev Y., Malik N., Ovsyannikov A., Ishizuka Y., Hasegawa T., Uesawa S. (2014). Japanese-Russian project of study Klyuchevskoy volcano (Kamchatka, Russia): First results of the geological and petrological investigations. JKASP. Sapporo. 23-26 September 2014. http://hkdrcep.sci.hokudai.ac.jp/map/jkasp2014/pdf/R10-1.pdf

Best, G. (2003). Igneous and Metamorphic Petrology.

Bindeman, I. N. and J. C. Bailey (1999). "Trace elements in anorthite megacrysts from the Kurile Island Arc: a window to across-arc geochemical variations in magma compositions." Earth and Planetary Science Letters **169**: 209–226.

Bloch Y.I., B. V. I., Rashidov V.A., Trysov A.A. (2006). "Submarine volcano Grigoreva (Kurile Island Arc)." Volcanology and seismology **5**: 1-10.

Bourova E, Yoshizawa K, Yomogida K (2010) Upper mantle structure of marginal seas and subduction zones in northeastern Eurasia from Rayleigh wave tomography. Phys Earth Planet In, 183(1-2): 20-32

Braitseva, O.A., Melekestsev, I.V., Bogoyavlenskaya, G.E., Maksimov, A.P., 1991. Bezymyannyi: eruptive history and dynamics. Volcanology and Seismology, 12, 165–194.

Braitseva, O.A., Melekestsev, I.V., Ponomareva, V.V., Sulerzhitsky, L.D., 1995. The ages of calderas, large explosive craters and active volcanoes in the Kuril-Kamchatka region, Russia, Bull. of Volcanology, 57(6), 383–402.

Braitseva, O. A., Ponomareva, V. V., Sulerzhitsky, L. D., Melekestsev, I. V., & Bailey, J. (1997). Holocene key-marker tephra layers in Kamchatka, Russia. Quaternary research, 47(2), 125-139.

Brenan JM, Shaw HF, Ryerson FJ, Phinney DL (1995) Mineral-Aqueous Fluid Partitioning of Trace-Elements at 900-Degrees-C and 2.0 Gpa - Constraints on the Trace-Element Chemistry of Mantle and Deep-Crustal Fluids. Geochim Cosmochim Ac, 59(16): 3331-3350.

Castillio PR (2008) Origin of the adakite-high-Nb basalt association and its implications for postsubduction magmatism in Baja, California, Mexico. Geol. Soc. Am. Bull., 120

Churikova,T., F. Dorendorf, et al. (2001). Sources and Fluids in the Mantle Wedge below Kamchatka, Evidence from Across-arc Geochemical Variation. Journal of Petrology **42**(8): 1567-1593.

Churikova, T. G., Gordeychik, B. N., Ivanov, B. V., & Wörner, G. (2013). Relationship between Kamen Volcano and the Klyuchevskaya group of volcanoes (Kamchatka). Journal of Volcanology and Geothermal Research, 263, 3-21.

Churikova, T., Gordeychik, B., Iwamori, H., Nakamura, H., Nishizawa, T., Haraguchi, S., Yasukawa, K., Ishizuka, O., 2014. Petrology and geochemistry of the Tolbachik stratovolcano. 8nd International Seismic-Volcanic Workshop on North-Japanese,

Kurile-Kamchatkan, and Aleutian-Alaskan Subduction Processes, Hokkaido, Japan, http://hkdrcep.sci.hokudai.ac.jp/map/jkasp2014/pdf/R50.pdf.

Churikova T., Gordeychik B., Edwards B., Ponomareva V., Zelenin E. (201X). The Tolbachik volcanic massif: a review of the petrology, volcanology and eruption history prior to the 2012-2013 eruption. Submitted to Journal of volcanology and Geotjermal Research.

Danyushevsky, L. V., & Plechov, P. (2011). Petrolog3: Integrated software for modeling crystallization processes. Geochemistry, Geophysics, Geosystems, 12(7).

Davaille, A., & Lees, J. M. (2004). Thermal modeling of subducted plates: tear and hotspot at the Kamchatka corner. Earth and Planetary Science Letters, 226(3), 293-304.

Defant, M. J. and M. S. Drummond (1990). "Derivation of some modern arc magmas by melting of young subducted lithosphere." Nature **347**(6294): 662-665.

Dobretsov, N. L. (2010). "Distinctive petrological, geochemical, and geodynamic features of subduction-related magmatism." Petrology **18**(1): 84-106.

Dreyer BM, Morris JD, Gill JB (2010) Incorporation of Subducted Slab-derived Sediment and Fluid in Arc Magmas: B-Be-Be-10-epsilon Nd Systematics of the Kurile Convergent Margin, Russia. J Petrol, 51(8): 1761-1782.

Duggen S, Portnyagin M, Baker J, Ulfbeck D, Hoernle K, Garbe-Schonberg D, Grassineau N (2007) Drastic shift in lava geochemistry in the volcanic-front to rear-arc region of the Southern Kamchatkan subduction zone: Evidence for the transition from slab surface dehydration to sediment melting. Geochim Cosmochim Ac, 71(2): 452-480

Faccenna C, Becker TW, Lallemand S, Lagabrielle Y, Funiciello F, Piromallo C (2010) Subduction-triggered magmatic pulses: A new class of plumes? Earth Planet Sc Lett, 299(1-2): 54-68

Fedotov, S. A., Gorelchik, V. I., & Zharinov, N. A. (1992). Deformation, Earthquakes and Mechanism of Activity of Klyuchevskoy Volcano. In Volcanic Seismology (pp. 20-44). Springer Berlin Heidelberg.

Fedotov, S. A., & Zharinov, N. A. (2007). On the eruptions, deformation, and seismicity of Klyuchevskoy volcano, Kamchatka in 1986–2005 and the mechanisms of its activity. Journal of Volcanology and Seismology, 1(2), 71-97.

Fedorchenko VI, Rodionova RI (1975) Xenolits inl avas of Kurile Islands (compositions, genesis, geological meaning). Novosibirsk. Nauka. 139 p (in Russian).

Fedorchenko V.I., A. A. I., Rodionova R.I. (1989). "Volcanism of Kurile Island Arc: geology and penrogenesis." Nauka: 237.

Geist, E. L. and D. W. Scholl .1994.Large-Scale Deformation Related to the Collision of the Aleutian Arc with Kamchatka. Tectonics **13**(3): 538-560.

Genske FS, Beier C, Haase KM, Turner SP, Krumm S, Brandl PA (2013) Oxygen isotopes in the Azores islands: Crustal assimilation recorded in olivine. Geology, 41(4), 491-494

Gerya, T. V., & Yuen, D. A. (2003). Rayleigh–Taylor instabilities from hydration and melting propel 'cold plumes' at subduction zones. Earth and Planetary Science Letters, 212(1), 47-62.

Girina O., Manevich A., Melnikov D., Nuzdaev A., Demyunchuk A. (2014) Eruption of Klyuchevkoy volcanp in 2012-2013. Materials of annually conference to Volcanologist day. 46-52.

Gorbatov, A., Dominguez, J., Suarez, G., Kostoglodov, V., Zhao, D., & Gordeev, E. (1999). Tomographic imaging of the P-wave velocity structure beneath the Kamchatka peninsula. Geophysical Journal International, 137(2), 269-279.

Gorbatov A, Widiyantoro S, Fukao Y, Gordeev E (2000) Signature of remnant slabs in the North Pacific from P-wave tomography. Geophysical Journal International, 142(1), 27-36.

Gorshkov, A. 1967. Volcanism of Kurile Island Arc. Nauka: 288.

Hanyu T, Gill J, Tatsumi Y, Kimura J, Sato K, Chang Q, Zulkarnain (2012) Across-and along-arc geochemical variations of lava chemistry in the Sangihe arc: Various fluid and melt slab fluxes in response to slab temperature, Geochem. Geophys. Geosyst., doi: 10.1029/2012GC004346, in press.

Haraguchi S, Ishii T, Kimura JI, Kato Y (2012). The early Miocene (~ 25 Ma) volcanism in the northern Kyushu-Palau Ridge, enriched mantle source injection during rifting prior to the Shikoku backarc basin opening. Contributions to Mineralogy and Petrology, 163(3), 483-504

Hasegawa T, Nakagawa M, Yoshimoto M, Ishizuka Y, Hirose W, Seki S, Ponomareva, Alexander R (2011) Tephrostratigraphy and petrological study of Chikurachki and Fuss volcanoes, western Paramushir Island, northern Kurile Islands: Evaluation of Holocene eruptive activity and temporal change of magma system. Quatern Int, 246: 278-297.

Hastie AR, Mitchell SF, Kerr AC, Minifie MJ, Millar IL (2011) Geochemistry of rare high-Nb basalt lavas: Are they derived from a mantle wedge metasomatised by slab melts? Geochim Cosmochim Ac, 75(17): 5049-5072.

Ishikawa, T. and F. Tera .1997. Source, composition and distribution of the fluid in the Kurile mantle wedge: Constraints from across-arc variations of B/Nb and B isotopes. Earth and Planetary Science Letters **152**: 123–138.

Ivanov V. (2009) Currently circle of Klyuchevskoy volcano 1995-2008, sesmic, foto, video data. Materials of annually conference to Volcanologist day. 27-29.

Izbekov, P., Eichelberger, J.C., Ivanov, B.V. (2004) The 1996 eruption of Karymsky volcano, Kamchatka: Historical record of basaltic Replenishment of an andesite reservoir. Journal of Petrology 45, 2325-2345.

Jacques G, Hoernle K, Gill J, Hauff F, Wehrmann H, Garbe-Schönberg D, Lara LE (2013) Across-arc geochemical variations in the Southern Volcanic Zone, Chile (34.5–38.0 S): constraints on mantle wedge and slab input compositions. Geochimica et Cosmochimica Acta, 123, 218-243

Kelley KA, Plank T, Grove TL, Stolper EM, Newman S, Hauri E (2006) Mantle melting as a function of water content beneath back-arc basins. J Geophys Res-Sol Ea, 111(B9).

Kepezhinskas P, Defant M, Drummond MS (1996). Progressive enrichment of island arc mantle by melt-peridotite interaction inferred from Kamchatka xenoliths. Geochim Cosmochim Ac, 60(7): 1217-1229.

Kennet J. (1987). Marine Geology. 2 Volums. Mir. 273.

Kersting, A. B., and Arculus, R. J. (1994). Klyuchevskoy volcano, Kamchatka, Russia: the role of high-flux recharged, tapped, and fractionated magma chamber (s) in the genesis of high-Al2O3 from high-MgO basalt. Journal of Petrology, 35(1), 1-41.

Kimura G. (1986) Oblique subduction and collision: forearc tectonics of the Kuril arc. Geology 14, 404-407.

Kimura, J. I. and T. Yoshida. 2006. Contributions of slab fluid, mantle wedge and crust to the origin of quaternary lavas in the NE Japan arc. Journal of Petrology **47**(11): 2185-2232.

Kimura, J. I., & Ariskin, A. A. (2014). Calculation of water‐bearing primary basalt and estimation of source mantle conditions beneath arcs: PRIMACALC2 model for WINDOWS. *Geochemistry, Geophysics, Geosystems*, *15*(4), 1494-1514.

Kulakov V. (1934). Parasitic craters which were formed on the slopes of Klyuchevskoy volcano in 1932 on Kamchatka. Notes of Leningrad mining ingenering. Volume 8: 17-30.

Kuno H (1935) Petrology of Alaid volcano, North Kurile. Japanese Journal of Geology and Geography, XII: 9.

Kurile Islands (nature, geology, earthquakes, volcanoes, history, economics). Yuzno-Sakhalinsk Publishing House (2004) 227.

Khabynaya S., Gontovaya L., Moskoleva S., Sobolev A., Batanova V., Kuzmin D., Kuzmina O. (2012). Olivens and pyrozens of magnesium and high Al basalts and andesibasalts from Klyuchevkoy volcano as a indicator of process of fractional crystallization in shallow magmatic chamber. Materials of Volcaniligical days 30th March 2012. 82-91 (in Russian).

Khabynaya S., Bogoyavlensky S., Novgorodtseva T., Okrugina A. (1993). Mineralogical features of magmesian basalts as a indicator of process of magmatic chamber of Klyuchevskoy volcano. Journal of Volcanology and Sesmology. 3: 46-68 (in Russian).

Khrenov, A. P., Dvigalo, V. N., Kirsanov, I. T., Fedotov, S. A., Gorel'chik, V. I., & Zharinov, N. A. (1991). Klyuchevskoy volcano. Active volcanoes of Kamchatka, 1, 146-163.

Krasheninnikov, S., & Portnyagin, M. V. (2011). Parental melts of Avachinsky Volcano (Kamchatka) inferred from data on melt inclusions.

Le Maitre RW (1989) A Classification of igneous rocks and glossary of terms. Blackwell Scientific, Oxford, xi, 193.

Ma GS, Malpas J, Xenophontos C, Chan GHN (2011) Petrogenesis of latest Miocene–Quaternary continental intraplate volcanism along the northern Dead Sea Fault System

(Al Ghab–Homs Volcanic Field), western Syria: evidence for lithosphere–asthenosphere interaction. Journal of Petrology,085.

Manea V C, Manea M, Kostoglodov V, Sewell G (2005) Thermal models, magma transport, and velocity anomaly estimation beneath southern Kamchatka. Geological Society of America Special Papers, 388, 517-536.

Martynov YA, Kimura JI, Khanchuk AI, Rybin AV, Chashchin AA, Martynov AY. (2007). Magmatic sources of quaternary lavas in the Kuril island arc: New data on Sr and Nd isotopy. In Doklady Earth Sciences (Vol. 417, No. 1, pp. 1206-1211). MAIK Nauka/Interperiodica.

Martynov YA, Rybin AV, Dril SI, Martynov AY (2009). Zone of anomaly volcanism in the Kurile Islands, Paramushir isl. Vestnik DVO RAN (in Russian).

Martynov, Y., A. Khanchuk, et al. (2010). "Geochemistry and petrogenesis of volcanic rocks in the Kuril island arc." Petrology **18**(5): 489-513.

Marske J P, Pietruszka AJ, Trusdell FA, Garcia MO (2011) Geochemistry of southern Pagan Island lavas, Mariana arc: the role of subduction zone processes. Contributions to Mineralogy and Petrology, 162(2), 231-252.

Melekestsev IV, Ponomareva VV (2005) Modern (N22-Q4) surface and submarine volcanism of the Kuril Island Arc. Modern and Holocene volcanism in Russia: 102 (in Russian).

Mironov, N., Portnyagin, M. V., & Pletchov, P. Y. (2003). The origin and composition of primitive melts of Klyuchevskoy volcano, Kamchatka-insight from melt inclusions study. In Geophysical Research Abstracts (Vol. 5, No. 01966).

Mironov N. (2009). Genesis and evolution magma of Klyuchevskoy volcano on the base of melt inclusion in olivine. PhD dissertation. GEOHi. 31 (in Russian).

Mironov, N. L., & Portnyagin, M. V. (2011). H 2 O and CO 2 in parental magmas of Kliuchevskoi volcano inferred from study of melt and fluid inclusions in olivine. Russian Geology and Geophysics, 52(11), 1353-1367.

Miashita M, Tanaka S, Nakagawa M, Kimura J (2007) Genesis of the Poroshiri ophiolite, Hokkaido, Japan; inference from geochemical evidence. Geological Society of Japan, 113(5): 9

Miyashir A (1974) Volcanic Rock Series in Island Arcs and Active Continental Margins. Am J Sci, 274(4): 321-355

Nakagawa M (1999) Origin of Spatial Compositional Variations in Differentiated Arc Volcanics at Arc-Arc Junctions: A Case study of Major and Trace Element Variations in Quaternary Volcanics from Hokkaido, Japan. Resource Geology Special Issue, 20: 15.

Nakamura H, Iwamori H (2013) Generation of adakites in a cold subduction zone due to double subducting plates. Contributions to Mineralogy and Petrology 165.6: 1107-1134

Nikulin, A., Levin, V., Carr, M., Herzberg, C., & West, M. (2012). Evidence for two upper mantle sources driving volcanism in Central Kamchatka. Earth and Planetary Science Letters, 321, 14-19.

Le Bas, M. J., Le Maitre, R. W., Streckeisen, A., & Zanettin, B. (1986). A chemical classification of volcanic rocks based on the total alkali-silica diagram. Journal of petrology, 27(3), 745-750.

Le Maitre, R. W., Bateman, P., Dudek, A., & Keller, J. Lameyre Le Bas MJ, Sabine PA, Schmid R, Sorensen H, Streckeisen A, Woolley AR, Zanettin B (1989) A classification of igneous rocks and glossary of terms.

Levin, V., Shapiro, N., Park, J., & Ritzwoller, M. (2002). Seismic evidence for catastrophic slab loss beneath Kamchatka. Nature, 418(6899), 763-767.

Nakamura, H. and H. Iwamori (2009). "Contribution of slab-fluid in arc magmas beneath the Japan arcs." Gondwana Research **16**(3-4): 431-445.

Nakagawa M (1999) Origin of Spatial Compositional Variations in Differentiated Arc Volcanics at Arc-Arc Junctions: A Case study of Major and Trace Element Variations in Quaternary Volcanics from Hokkaido, Japan. Resource Geology Special Issue, 20: 15

Orihashi, Y., J. Maeda, et al. (1998). "Sr and Nd isotopic data for the seven GSJ rock reference samples; JA-1, JB-1a, JB-2, JB-3, JG-1a, JGb-1 and JR-1." Geochemical Journal **32**(3): 205-211.

Ozerov A. (2000). The evolution of high-alumina basalts of the Klyuchevskoy volcano, Kamchatka, Russia, based on microprobe analyses of mineral inclusions. Journal of Volcanology and Geothermal Research. 2000. V. 95. No 1-4. P. 65-79.

Ponomareva, V., Portnyagin, M., Pevzner, M., Blaauw, M., Kyle, P., & Derkachev, A. (2015). Tephra from andesitic Shiveluch volcano, Kamchatka, NW Pacific: chronology of explosive eruptions and geochemical fingerprinting of volcanic glass. International Journal of Earth Sciences, 1-24.

Pearce J.A., (1983). Role of the sub-continental lithosphere in magma genesis at active continental margins. Shiva Publ., Nantwich, 19 pp.

Pearce J.A., P.I.J., (1993). Trace element model for mantle melting; application to volcanic arc petrogenesis. Geol Soc London Spec Publ, 30 pp.

Pearce, J.A., Stern, R.J., Bloomer, S.H. and Fryer, P., (2005). Geochemical mapping of the Mariana arc-basin system: Implications for the nature and distribution of subduction components. Geochem Geophy Geosy, 6.

Piskunov, V.I., Abdurahmoniv, A.I., Kim Chun Yun, (1979). Relation of composition - depth and petrological importance (In Russian). Volcanology and Seismology, 4: 57-67.

Plank, T. and Langmuir, C.H., (1998). The chemical composition of subducting sediment and its consequences for the crust and mantle. Chem Geol, 145(3-4): 325-394.

Portnyagin, M., Bindeman, I., Hoernle, K., & Hauff, F. (2007a). Geochemistry of primitive lavas of the Central Kamchatka Depression: Magma generation at the edge of the Pacific Plate. Volcanism and subduction: The Kamchatka region, 199-239.

Portnyagin, M., Hoernle, K., Plechov, P., Mironov, N., & Khubunaya, S. (2007b). Constraints on mantle melting and composition and nature of slab components in volcanic arcs from volatiles (H 2 O, S, Cl, F) and trace elements in melt inclusions from the Kamchatka Arc. Earth and Planetary Science Letters, 255(1), 53-69.

Portnyagin, M., Almeev, R., Matveev, S., & Holtz, F. (2008). Experimental evidence for rapid water exchange between melt inclusions in olivine and host magma. Earth and Planetary Science Letters, 272(3), 541-552

Portnyagin M., Ponomareva V., Bindeman I., van den Bogaard C., Kuvikas O., Krasheninnikov S., Mironov N., Plechova A., Hoernle K. (2009) Millennial Variations of Major and Trace Element and Isotope Compositions of Klyuchevskoy Magmas, Kamchatka // KALMAR-First Bilateral Workshop on Russian-German Cooperation on Kurile-Kamchatka and the Aleutean Marginal Sea-Island Arc Systems. Terra Nostra, v. 2009/1, p. 64-65.

Portnyagin, M., & Ponomareva, V. (2012). Kliuchevskoi volcano diary. International Journal of Earth Sciences, 101(1), 195-195.

Portnyagin M., Duggen S., Hauff F., Mironov N., Bindeman I., Thirlwall M., Hoernle K (201X). Geochemistry of the Late Holocene rocks from the Tolbachik volcanic field, Kamchatka:towards quantitative modeling of subduction-related open magmatic system (submitted to the Journal of Volcanology and Geothermal Research).

Rashidov A.A., M.N.A., Firstov P.P., Anikin L.P., Dubrovskaya I.K., Melnikov D.V., Pilopenko O.V., Sokorenko S.A., chirkov A.A., Shakirova S.S., Yaschuk P.V., 2012. New activity at Alaid volcano, the Kurile Island, in 2012 (In Russian). Bulletin of Kamchatka regional association "Educational-scientific center". Earth Science, 20: 6.

Reagan, M.K. and Gill, J.B., 1989. Coexisting Calcalkaline and High-Niobium Basalts from Turrialba Volcano, Costa-Rica - Implications for Residual Titanates in Arc Magma Sources. J Geophys Res-Solid, 94(B4): 4619-4633.

Ruprecht, P., & Plank, T. (2013). Feeding andesitic eruptions with a high-speed connection from the mantle. Nature, 500(7460), 68-72.

Saginor I, Gazel E, Condie C, Carr MJ (2013) Evolution of geochemical variations along the Central American volcanic front. Geochemistry, Geophysics, Geosystems, 14(10), 4504-4522.

Sajona FG, Maury RC, Bellon H, Cotton J, Defant M (1996) High Field Strength Element Enrichment of Pliocene—Pleistocene Island Arc Basalts, Zamboanga Peninsula, Western Mindanao (Philippines). Journal of Petrology, 37(3), 693-726.

Shinjo R, Woodhead JD, Hergt JM (2000) Geochemical variation within the northern Ryukyu Arc: magma source compositions and geodynamic implications. Contrib Mineral Petr, 140(3): 263-282

Sun SS, McDonough W (1989) Chemical and isotopic systematics of oceanic basalts: implications for mantle composition and processes. Geological Society, London, Special Publications, 42(1), 313-345

Shuto K, Ishimoto H, Hirahara Y, Sato M, Matsui K, Fujibayashi N, Rezanov AI (2006) Geochemical secular variation of magma source during Early to Middle Miocene time in the Niigata area, NE Japan: Asthenospheric mantle upwelling during back-arc basin opening. Lithos, 86(1), 1-33

Stern R (2002) Subduction zones. Reviews of geophysics 40.4: 3-1.

Stracke, A., Bizimis, M. and Salters V. J. M. (2003) Recycling oceanic crust: Quantitative constraints. Geochemistry Geophysics Geosystems, 4(3).

Straub SM, Gómez-Tuena A, Zellmer GF, Espinasa-Perena R, Stuart FM, Cai Y, Mesko GT(2013) The processes of melt differentiation in arc volcanic rocks: Insights from OIB-type arc magmas in the central Mexican volcanic belt. Journal of Petrology, 54(4), 665-701.

Syracuse, E. M. and G. A. Abers (2006). "Global compilation of variations in slab depth beneath arc volcanoes and implications." Geochemistry Geophysics Geosystems **7**(5): 1-18.

Takada, A. (1997). Cyclic flank-vent and central-vent eruption patterns. Bulletin of volcanology, 58(7), 539-556.

Takeshita A, Shinjo K, Higuchi M, Miyawaki S, Takemoto Y, Kishimoto Y, Saito K, Takuchi H, Kuriyama K, Kimura Y, Asou N, Takahashi M, Hotta T, Kanamaru A, Ueda R, Ohno R, Grp (2000). Quantitative expression of erythropoietin receptor (EPO-R) on acute leukaemia cells: relationships between the amount of EPO-R and CD phenotypes,

in vitro proliferative response, the amount of other cytokine receptors and clinical prognosis. British Journal of Haematology, 108(1): 55-63.

Tamura, Y., Y. Tatsumi, et al. (2002). "Hot fingers in the mantle wedge: new insights into magma genesis in subduction zones." Earth and Planetary Science Letters **197**(1-2): 105-116.

Tamura Y, Gill JB, Tollstrup D, Kawabata H, Shukuno H, Chang Q, Tatsumi Y (2009) Silicic Magmas in the Izu–Bonin oceanic arc and implications for crustal evolution. Journal of Petrology, egp017

Tararin I., Badredinov Z., Dril S. (2007). Geochemistry and age of metamorphic rocks of Havuveskaya upland of Eastern Kamchatka. Geochemistry. 9: 962-980.

Tokarev P. (1990). Dynamic and large deformation of volcanoes. Volcanology and Seismology (2): 53-65.

Volynets ON (1994). Geochemical types, petrology, and genesis of Late Cenozoic volcanic rocks from the Kurile-Kamchatka island-arc system. International Geology Review, 36(4), 373-405.

Volynets, A. O., T. G. Churikova, et al. (2010). "Mafic Late Miocene-Quaternary volcanic rocks in the Kamchatka back arc region: implications for subduction geometry and slab history at the Pacific-Aleutian junction." Contributions to Mineralogy and Petrology **159**(5): 659-687.

Vlodavets V., Piip B. (1957). Katalog of active volcanoes of Kamchatka.Bulleten of volcanic station. 25: 5-95.

Workman RK, Hart SR (2005) Major and trace element composition of the depleted MORB mantle (DMM). Earth Planet Sc Lett, 231(1-2): 53-72

Yogodzinski, G. M., J. M. Lees, et al. (2001). "Geochemical evidence for the melting of subducting oceanic lithosphere at plate edges." Nature **409**(6819): 500-504.

Zavaritsky A. (1935). Northern group of Kamchatka volcanoes. Works of volcanological laboratory. 1:55.

Zlobin TK, Puskunov VN, Frolova TI (1987). New Data on the Earth`s Crust Structure in the Central part of the Kurile Island Arc. Dokl. Akad. Nauk SSSR, 293: 2 (in Russian).

www.kscnet.ru.

www.wiki.com.

www.volcano.si.edu.

Appendix I

Table 1. Historical activity of Klyuchevskoy volcano by data http://www.kscnet.ru/ivs/kvert/index_eng.php; Active volcanoes of Kamchatka, Klyuchevskoy volcano, 1991; Tokarev (1989); Fedotov et al (1987); Fedotov et al., (2007); Ivanov (2008).

Years of activity	Type of eruptions			Flank eruptions				Volume of lava from summit eruptions (km^3)	duration of the eruptions
	summit, exposive	summit, effusive	flank (explosive and effusive)	Name of flank eruptions	altitude of cinder cones, m	distance from summit to cinder cones (km)	Volume of lava from flank eruptions (km^3)		
1697-1698									
1720-1721									
1727-1731									
1737									
1762									
1767									
1770									
1772									
1785									
1788-1791									
1807									
1812-1813									
1821									
1829									
1840									
1848									
1852-1854									
1865									
1877-1879									
1882-1883									
1890									
1896-1898									
1904									
1907									
1909-1911									
1913									
1915									
1922-1923									
1925-1926									
1929									
1931									

Years of activity	Type of eruptions			Flank eruptions				Volume of lava from summit eruptions (km^3)	duration of the eruptions
	summit, exposive	summit, effusive	flank (explosive and effusive)	Name of flank eruptions	altitude of cinder cones, m	distance from summit to cinder cones (km)	Volume of lava from flank eruptions (km^3)		
1932			Kirgurich - 23.01.1932 : Tuila - 01.06.1932 : Biokos' - 10.1932	Tuila	450-500	20	0,09		~1 year
1935-1936	31.10.1936								
1937-1938		6.06.1937	26.07.1937 - Radist, Kamuli, 2.10.1937 - Perevalny	Radist, Kamuli,Pereval'ny	2500	5,7	0,0002		
1938-1939			07.02.1938	Bilyukai	1000-1900	11,4	0,31		13 months
1944-1945		01.01.1945	19.06.1945	Yubileiny	1100-1400	10,2	0,06	0,1	19 days flank eruptions, ~1 month summit, effusive eruption
1946			23.10.1946	Apakhonchich	1500	6,8	0,04		29 days
1949									
1951			20.11.1951	A. Bylinkinoy	950	13	0,015		10 days
1953			07.06.1953	D. Belyankin	1300-1400	10,6	0,01		11 days
1954									
1956			27.07.1956	V. Vernadsky, Kryzhanovsky	1360-1380	8,4	0,08		5 days
1958-1959									
1960-1963									
1963-1964									
1966-1967			06.10.1966	B. Piip	1900-2100	8	0,09		3 months
1968									
1969-1970									
1971									
1974			23.08.1974	IV National Volcanological Conference	3340-3600	2,4	0,02	0,018	3 months
1978		06.1978						0,021	3 months
1980			06.03.1980	8 March	1600-1800	6,9	0,0003		7 days
1981 - 1982									

Years of activity	Type of eruptions			Flank eruptions				Volume of lava from summit eruptions (km^3)	duration of the eruptions
	summit, exposive	summit, effusive	flank (explosive and effusive)	Name of flank eruptions	altitude of cinder cones, m	distance from summit to cinder cones (km)	Volume of lava from flank eruptions (km^3)		
1983			08.03.1983	Predskazanny	2300-2900	3,3	0,07		~4 months
1984 - 1985		06.04.1984						0,026	18 months
1985 - 1986								0,01	5 months
1987			24.02.1987	Predvidenny	2300-2900	2,8	0,0002	0,01	10 days
1988			29.01.1988	XXV Years Institute Volcanology	4000	2,5	0,034	0,012	230 days of flank eruptions
			23.02.1988	23 February 1988	4200-4400		0,0015		25 days
			14.02.1988	14 December 1988	3900-4250		0,005		6 days
1989 - 1990			26.08.1989	Yu. Skuridin	4100-4400	2	0.026		198 days, flank eruption - 6 months
1991									
1993		19.07.1993							4 months
1994		12.09.1994						0,066	1 month
1995									
1996									
1997									
1998									
1999									
2000									
2002									
2003	January-June								
2004	15.01.								7 months
2005	16.01.-15.04.								3 months
2007	15.02.-26.07.	18.03.2007							> 1 year
2008	October-December	10.2008							3 monts
2009-2010	16.09.2009 - 12.08.2010	08.2009							<1 year
2011	29.05.2011								
2012-2013	14.10.2012 - 01.10.2013								1 year
2013	15.08.-15.12.								3 months
2015	01.01.-24.03.								

Table 2. Petrographical descriptions of historical lavas from Klyuchevskoy volcano.

Sample number	Name of cinder cones	Age, AD	Length, µm				Contents of mineral and glass, %						Name of the rocks	Remarks
			Pl	Ol	Cpx	Opx	Pl	Ol	Cpx	Opx	Glass	Fe-Ti oxides		
12KY-9-1	Biokos	1932	63	343	827	271	28	10	12	8	40	2	Opx bearing Ol,Cpx basaltic andesite	all glass crystalazated in diraction with moving magma, alone debris of Pl cryst, honey comb
12KY-9-2	Biokos	1932	85	76	291	475	38	5	12	13	30	2	Ol bearing Cpx, Opx basaltic andesite	mineral assembladge of Opx, Cps, glass crystallizated by Pl
12KY-9-3	Biokos	1932	77	91	309	309	28	10	12	18	30	2	Ol bearing Cpx, Opx basaltic andesite	mineral assembadge Opx, Cpx, Ol, all glass crystal, few crystalls of large Pl
12KY-10-1	Biokos	1932	81	179	649	315	45	13	25	8	7	2	Opx bearing Cpx, Olbasaltic andesite	all glass crystallated, honey bomb of Pl
12KY-10-2	Biokos	1932	84	123	422	303	50	8	20	7	13	2	Opx, Ol bearing Cpx basaltic andesite	glass crystallated, euhedral crystal of Pl
12KY-11-2	Kirgurich	1932	90	73	386	329	47	10	15	13	10	5	Ol bearing Opx, Cpx basaltic andesite	glass crystallated, euhedral crystal, honeu comb
12KY-12-1	Kirgurich	1932	269	768	1190	593	55	10	17	10	5	3	Ol, Opx bearing Cpx basaltic andesite	honey comb, euhendral crystal, glass crystallis, dusty zone of Pl
12KY-13-1	Kirgurich	1932	102	593	326	639	60	8	10	10	10	2	Ol bearing Cpx, Opx basaltic andesite	
12KY-13-2	Kirgurich	1932	83	710	520	269	50	10	5	25	8	2	Cpx, Ol bearingOpx basaltic andesite	all glass crystallizated, honey comb, 2 different size of Opx
10KY-18	Tuila	1932	126	190	619	718	45	7	10	23	10	5	Ol, Cpx bearing Opx basaltic andesite	good forming Pl, 2 different size of Opx
10KY-17	Tuila	1932	131	228	832	221	42	15	15	15	8	5	Ol,Cpx,Opx basaltic andesite	good forming Pl, 2 different size of Opx
10Ky-20	Tuila	1932	93	235	197	303	55	5	15	20	5		Ol bearing Cxp, Opx basaltic andesite	many bubbles, good shape of crystalls, 2 different size of Opx
11KY-104-1	Perevalny	1937	714	1156	839	3240	48	5	3	16	27	1	Opx, Cpx bearing Opx basaltic andesite	hige inclusion of Opx
11KY-104-2	Perevalny	1937	1011	6090	5587	2720	32	10	8	15	30	5	Cxp, Ol bearing Opx basaltic andesite	inside of Ol exist Opx, secondary changing in glass
11KY-104-3	Perevalny	1937	359	101	762	6589	41	3	6	17	25	8	Ol, Cpx bearing Opx basaltic andesite	varies size of Pl, honey comb of Pl, huge Opx, all glass crystallised by Opx and Pl microcrystalls

Sample number	Name of cinder cones	Age, AD	Length, μm				Contents of mineral and glass, %						Name of the rocks	Remarks
			Pl	Ol	Cpx	Opx	Pl	Ol	Cpx	Opx	Glass	Fe-Ti oxides		
11KY-102-1	Bilyukai	1938	350	265	885	908	40	8	5	32	15		Cpx, Ol bearing Opx basaltic andesite	honey comb of Pl, good fortming Pl, mineral assembledge
11KY-102-3	Bilyukai	1938	306	339	912	887	62	8	8	12	8	2	Ol, Cpx bearing Opx basaltic andesite	zoning Pl, honey comb of Pl, good-forming crystalls of Pl and Opx.
11KY-102-4	Bilyukai	1938	541	293	1002	832	53	12	15	5	15		Opx bearing Ol,Cpx basaltic andesite	honey comb on the Pl and Cpx crystals, good formig Pl
11KY-102-5	Bilyukai	1938	394	101	897	525	53	15	15	3	12	2	Opx bearing Cpx, Ol basaltic andesite	twing of Pl crystalls, good forming crystalls
11KY-108-1	Tiranus	1938	347	218	1389	461	56	16	8	5	15		Opx, Cpx bearing Ol basaltic andesite	twing of Pl, good forming shape of Ol, Pl zonation, honey comb of Pl
11KY-108-2	Tiranus	1938	396	449	1091	459	54	16	7	3	20		Opx, Cpx bearing Ol basaltic andesite	Ol margin of crystalls is melt, evedence of magma mixing?
11KY-108-3	Tiranus	1938	257	807	450	810	46	21	12	1	18	2	Opx bearing Cpx, Ol basaltic andesite	Pl twining, zonation, honey comb of Pl
11KY-108-4	Tiranus	1938	536	189	753	289	59	16	15	2	8		Opx bearing Cpx, Ol basaltic andesite	dusty zone of Pl, honey bomb of Pl, goof gorming Pl, thiming and zonations
11KY-108-5	Tiranus	1938	439	278	846	467	51	19	18	2	10		Opx bearing Cpx, Ol basaltic andesite	eihundral Of Cpx, durty of Pl crystallls
11KY-109-1	Nezametny	1938	3588	583	1862	1922	55	17	5	8	10	5	Cpx, Opx bearing Ol basaltic andesite	durty zone and eihidral crystal of Pl, zoning crystalls of Pl
11KY-109-2	Nezametny	1938	3489	2913	1696	2462	57	18	6	5	12	2	Opx, Cpx bearing Ol basaltic andsite	all glass crystallized by small crystalls of Opx, pl, durty crtystalls of Pl, Ol, Cpx
11KY-110-1	Kolizey	1938	1768	91	591	4233	54	19	3	8	16		Cpx, Opx bearing Ol basaltic andesite	Pl zonallity, durty zone of Pl, good forming shape of Ol
11KY-110-2	Kolizey	1938	1241	868	1501	1389	62	15	2	9	12		Cpx, Opx bearing Ol basaltic andesite	Pl zonnality, duty zone of Pl
11KY-110-3	Kolizey	1938	2109	808	2214	1265	57	8	12	3	20		Opx bearing Ol,Cpx basaltic andesite	Pl zonallity, almost in all Pl durty or honey comb of Pl

Sample number	Name of cinder cones	Age, AD	Length, µm				Contents of mineral and glass, %						Name of the rocks	Remarks
			Pl	Ol	Cpx	Opx	Pl	Ol	Cpx	Opx	Glass	Fe-Ti oxides		
11KY-110-5	Kolizey	1938	3740	825	3147	3391	42	8	10	5	35		Opx, Ol bearing Cpx basaltic andesite	porfiric structure of the rock, good-forming shape of Ol, Cpx crystalls, durty zone of Pl
11KY-110-6	Kolizey	1938	2127	1159	0	2765	39	10	3	8	40		Cxp, Opx bearing Ol basaltic andesite	honey comb of Pl, Pl twininng, glass crystallizated by Pl microcrystalls
11KY-8-1	Yubileiny	1945	1836	676	2999	2270	55	12	5	8	15	5	Cpx, Opx bearing Ol basaltic andesite	big crystal of Opx, thininng Pl crystal, in glass microcrystal of Ol
11KY-8-2	Yubileiny	1945	1844	706	1894	128	49	12	5	19	10	5	Cpx bearing Ol, Opx basaltic andesite	microcrystals of Ol, opx, thininng Pl, honey comb of Pl
11KY-8-3	Yubileiny	1945	1934	768	2775	1839	49	10	3	8	30		Cpx, Opx bearing Ol basaltic andesite	secondaary changing in glass, glass not crystallited, Pl zonallity
11KY-8-4	Yubileiny	1945	1937	950	7176	4930	40	12	5	8	30	5	Cpx, Opx bearing Ol basaltic andesite	huge crystalls of Cpx, honey comb and durty zone of Pl, secondary changing of glass
10Ky-1	Apakhonchich	1946	2791	3143	2308	2155	50	8	3	15	12	12	Cpx, Ol bearing Opx basaltic andesite	uige crystals of Ol, Cpx ,honey and durty comb of Pl, secondary changing of glass
10Ky-2	Apakhonchich	1946	2794	1316	6090	3987	44	5	3	8	30	10	Cpx, Ol, Opx bearing basaltic andesite	honey comb of Pl, huge inclusion of Opx and Cpx
10Ky-4	Apakhonchich	1946	1108	1886	1781	1606	40	10	7	8	35		Cpx, Opx bearing Ol basaltic andesite	huge crystalls of Ol, honey comb Pl, goog shape of crystalls
10Ky-5	Apakhonchich	1946	2960	656	2515	6555	54	8	5	10	15	8	Cpx, Ol bearing Opx basaltic andesite	honey comb of Pl, huge crystalls of Ol, Opx, Pl twining
11Ky-100-1	Bylinkinoy	1951	1929	534	4427	2801	56	8	5	3	25	3	Opx, Cpx, ol basaltic andesite	honey comb of Pl, twining of Pl, all glass crystalleted by micro Pl crystalls, huge crystlalls of Cpx
11KY-100-2	Bylinkinoy	1951	1531	1377	2653	1442	39	12	2	2	35	10	Opx, Cpx bearing Ol basaltic andsite	secondary changing in glass, microcrystalls of Pl, crystalline glass, mineral assembladge of Ol in Pl

Sample number	Name of cinder cones	Age, AD	Length, µm				Contents of mineral and glass, %						Name of the rocks	Remarks
			Pl	Ol	Cpx	Opx	Pl	Ol	Cpx	Opx	Glass	Fe-Ti oxides		
11Ky-100-3	Bylinkinoy	1951	2032	762	1004	1256	55	10	6	4	25		Opx, Cpx bearing Ol basaltic andesite	Pl zonality, dursty and honey comb of Pl, secondary change in glass, many bubles
11KY-100-4	Bylinkinoy	1951	3377	542	2113	1690	43	8	5	6	30	8	Cpx, Opx, Ol bearing basaltic andesite	all glass crystallised by microcrystal Pl, twininng of Pl
11KY-6-1	Belyankina	1953	1605	527	731	1117	46	8	3	6	34	3	Cpx, Opx, ol bearing basaltic andesite	secondary changing in glass
11KY-6-2	Belyankina	1953	2771	1277	675	640	43	12	5	3	35	2	Opx, Cpx bearing Ol basaltic andesite	honey comb, durty zone of Pl, Pl zonality, in Pl rim microcrystalls of Cpx
11KY-6-3	Belyankina	1953	1101	1102	954	750	40	13	6	4	35	2	Opx, Cpx bearing Ol basaltic andesite	good forming shape of Pl
10KY-15	Belyankina	1953	2660	748	965	1600	50	15	3	5	20	7	Cpx, Opx, Ol bearing basaltic andesite	all glass crystallized by microcrystalls of Pl, secondary changing in glass, durty zone of Pl
10KY-16	Belyankina	1953	1310	1094	1334	722	51	10	6	3	25	5	Opx, Cpx bearing Ol basaltic andesite	all glass crystallised by microcrystal Pl, twininng of Pl, secondary change in glass, Ol in Opx
11KY-16-1	Krzanovskogo	1956	1814	1110	1409	1200	40	5	4	5	40	6	Cpx, Opx, Ol bearing basaltic andesite	secondary changing in glass
11KY-16-2	Krzanovskogo	1956	1021	696	5910	2577	35	10	5	5	40	5	Opx, Cpx bearing Ol basaltic andsite	secondary changing in glass, twininng of Pl, in the rim of Opx are crystallised small microcrystalls of Ol and Cpx, inclusiions of Cpx
11KY-16-3	Krzanovskogo	1956	1825	1442	496	855	38	12	8	4	35	3	Opx, Cpx bearing Ol basaltic andesite	secondary changing in glass, twining of Pl, inclusion of Ol and Cpx
11KY-16-4	Krzanovskogo	1956	2422	1494	997	1368	39	17	2	2	35	5	Opx, Cpx bearing Ol basaltic andesite	secondary changing in glass, honey comb and durty zone of Pl, zoning of Pl
11KY-16-5	Krzanovskogo	1956	1063	1292	2802	1946	30	14	6	8	34	8	Opx, Cpx bearing Ol basaltic andesite	secondary changing in glass, Pl twining and zoning
11KY-2-1	Piipa	1966	1445	770	2607	3061	34	10	8	6	36	6	Opx, Cpx bearing Opx basaltic andesite	secondary changing in glass, mineral assembedge of Cpx, Ol and Pl, Pl zoning
11KY-2-2	Piipa	1966	3454	1000	1432	1976	32	15	4	3	38	8	Opx, Cpx bearing Ol basaltic andesite	secondary changing in glass, Pl twining and zoning

Sample number	Name of cinder cones	Age, AD	Length, μm				Contents of mineral and glass, %						Name of the rocks	Remarks
			Pl	Ol	Cpx	Opx	Pl	Ol	Cpx	Opx	Glass	Fe-Ti oxides		
11KY-2-3	Piipa	1966	2456	734	1692	3553	34	12	5	4	38	7	Opx, Cpx bearing Opx basaltic andesite	secondary changing in glass, Pl twining
12KY-5-1-	Piipa	1966	2331	1464	1223	1123	36	10	6	8	34	6	Opx, Cpx bearing Opx basaltic andesite	secondary changing in glass
12KY-110-1	4 USSR	1974	2785	769	2189	1964	35	13	8	8	30	6	Opx, Cpx bearing Opx basaltic andesite	secondary changing in glass, honey comb and durty zone of Pl
12KY-110-2	4 USSR	1974	1879	600	745	1530	42	12	3	5	32	6	Cpx, Opx bearing Ol basaltic andesite	secondary chnaging in glass, honey and durty zone of Pl
12KY-110-4	4 USSR	1974	1704	675	3256	3384	35	15	3	7	30	10	Cpx, Opx bearing Ol basaltic andesite	secondary changing in glass, twining of Pl
12KY-110-5	4 USSR	1974	1210	1017	1244	2364	33	16	5	12	30	4	Cpx bearing Ol, Opx basaltic andesite	secondary changing in glass, mineral assembladge of Cpx, Ol
11KY-103-2	8th March	1980	1640	499	982	887	30	15	6	10	35	4	Cpx bearing Ol, Opx basaltic andesite	all glass crystallized by microcrystalls of Pl, evidence for magma mixing
11KY-103-3	8th March	1980	1102	844	999	1984	45	15	1	1	30	8	Opx, Cpx bearing Ol basaltic andesite	secondary changing in glass, honey comb of Pl
11KY-103-4	8th March	1980	1736	1043	832	1113	49	16	1	6	20	8	Opx, Cpx bearing Ol basaltic andesite	secondary changign in glass, honey comb of Pl, durty zone of Pl
11KY-11-1	Predskazanny	1983	1373	548	1150	1661	38	15	2	5	30	10	Opx, Cpx bearing Ol basaltic andesite	secondary changing in glass
11KY-11-2	Predskazanny	1983	1713	1072	1285	603	39	17	1	3	30	10	Opx, Cpx bearing Ol basaltic andesite	secondary changign in glass, Pl twining
11KY-11-4	Predskazanny	1983	1487	808	732	1003	49	15	2	6	20	8	Opx, Cpx bearing Ol basaltic andesite	secondary changing in glass, all glass crystallised by microcrystalss of Pl, Pl twining
1987E	Predvideny	1987	1916	993	991	1256	36	15	3	8	30	8	Opx, Cpx bearing Ol basaltic andesite	mineral assembladge of Opx, ol, Cps, secondary changing in glass, twining of Pl
12KY-108-1	Predvideny	1987	2515	1450	1198	2833	40	10	2	10	28	10	Cpx bearing Ol, Opx basaltic andesite	secondary changing in glass, honey comb of Pl
12KY-108-2	Predvideny	1987	1769	1973	1451	1094	23	10	3	4	50	10	Cpx, Opx bearing Ol basaltic andesite	secondary changing, Pl twining, honey comb of Pl

Sample number	Name of cinder cones	Age, AD	Length, µm				Contents of mineral and glass, %						Name of the rocks	Remarks
			Pl	Ol	Cpx	Opx	Pl	Ol	Cpx	Opx	Glass	Fe-Ti oxides		
12KY-105-1	25 Yrs IVS	1988	1559	1258	2658	1552	31	8	3	8	45	5	Cpx bearing Ol, Opx basaltic andesite	in Ol small crystalls of Pl and Cpx, honey comb of Pl, seconddary changing in glass
12KY-105-2	25 Yrs IVS	1988	2335	1791	2210	2428	31	10	2	7	45	5	Cpx bearing Ol, Opx basaltic andesite	in the rim of Opx are crystallized small crystalls of Cpx and Ol
12KY-106-1	25 Yrs IVS	1988	1663	1471	1148	1859	27	8	4	8	45	8	Cpx, Opx, Ol bearing basaltic andesite	evidence for magma mixing, differenct textures of rocks, all rocks crystallezed by Pl and Opx microcrystalls
12KY-106-2	25 Yrs IVS	1988	2808	495	3601	2799	36	6	8	10	35	5	Ol, Cpx, Opx bearing basaltic andesite	secondary changing in glass
12KY-107-1	25 Yrs IVS	1988	1663	1754	998	1785	38	6	4	10	34	8	Ol, Cpx, Opx bearing basaltic andesite	secondary changing in glass, glass crystallized by microcrystalls of Pl, Opx
12KY-107-3	25 Yrs IVS	1988	1878	1395	1056	1040	43	5	6	8	30	8	Ol, Cpx, Opx bearing basaltic andesite	secondary changing in glass, Pl twining, mineral assembladge of Opx and Cpx
12KY-103-1	Top eruptions	1994	1776	537	727	1189	43	12	2	8	27	8	Cpx, opx bearing Ol basaltic andesite	evidence for magma mixing, different texture of the rocks, secondary changing in the glass
12KY-103-3	Top eruptions	1994	2393	492	1317	1040	27	4	6	3	45	15	Opx, Ol, Cpx bearing basaltic andesite	secondary changing in glass, Pl twining, Fe-Ti rim on the Cpx crystalls
12KY-104-3	Top eruptions	1994	2443	347	866	558	46	10	2	4	30	8	Cpx, Opx bearing Ol basaltic andesite	all glass crystallised, Pl twining, glass crystallazed by microcrystalls of Pl, Ol crystalls
12KY-104-4	Top eruptions	1994	3140	879	2681	1627	37	6	5	10	30	12	Cpx, Ol, Opx bearing basaltic andesite	secondary changing in glass, all rock crystallisd dy microcrystalls of Pl, Opx, ehindral type of the rocks

Table 3. Selected samples of major and trace element geochemistry of Klyuchevkoy rocks (XRF data).

Sample	SiO_2	TiO_2	Al_2O_3	FeO*	MnO	MgO	CaO	Na_2O	K_2O	P_2O_5	Sum	Sc	V	Cr	Co	Ni	Cu	Rb	Z	Sr	Y	Zr	Nb	Ba	Pb	Th	Ga	La	Ce
Kly10-9	53,84	0,94	17,07	8,92	0,17	5,66	8,52	3,63	1,06	0,20	100,00	26,95	238,55	79,43	32,09	42,23	74,81	19,92	90,93	370,82	25,24	101,74	3,24	438,37	4,85	1,32	19,97	7,94	16,77
13KY-1	50,95	0,87	14,34	10,00	0,17	10,85	9,43	2,69	0,56	0,14	100,00	36,72	245,50	522,22	40,28	161,17	80,01	11,63	77,64	264,22	21,20	70,32	2,52	199,43	2,73	0,19	14,70	7,40	10,42
13KY-2	51,99	0,92	15,04	9,47	0,16	9,27	9,43	2,95	0,61	0,16	100,00	36,01	259,84	424,63	37,58	116,62	84,88	11,62	76,10	274,38	21,32	74,05	2,87	213,45	1,89	0,19	14,48	2,13	11,42
13KY-4	53,68	1,01	17,39	9,13	0,16	5,62	8,32	3,52	0,98	0,19	100,00	32,29	260,38	70,11	32,26	38,34	89,77	18,83	85,51	337,22	24,80	91,26	2,90	377,61	3,18	0,38	17,46	3,60	21,85
13KY101-2	52,66	0,91	15,73	9,35	0,16	8,31	9,14	2,93	0,66	0,16	100,00	33,65	249,72	298,22	37,93	90,36	91,96	11,91	79,92	291,76	21,90	77,54	2,41	240,38	7,29	0,08	17,05	5,55	13,08
13KY101-4	52,29	0,94	15,50	9,40	0,17	8,37	9,69	2,88	0,60	0,17	100,00	33,78	249,06	313,84	35,45	85,27	42,35	12,91	78,19	294,09	21,68	78,85	2,83	236,13	2,16	1,09	16,41	5,66	14,58
11KY-101	52,24	0,91	15,60	9,18	0,16	8,43	9,83	2,87	0,63	0,15	100,00	33,05	248,48	323,15	36,21	87,92	84,98	11,14	72,51	289,23	20,84	78,34	2,83	212,34	2,67	1,90	13,84	6,28	9,47
11KY-10	52,63	0,95	15,98	9,21	0,16	7,81	9,28	3,03	0,76	0,19	100,00	32,12	244,42	267,57	35,19	85,27	107,66	13,13	78,45	305,22	21,41	90,34	3,49	249,23	3,87	1,50	14,34	4,18	15,38
13KY102-1	53,73	0,95	16,90	9,11	0,16	5,99	8,65	3,44	0,88	0,18	100,00	32,11	250,59	118,79	30,62	41,28	66,21	17,44	85,32	336,35	24,69	86,47	2,51	357,74	3,53	0,29	17,10	8,68	16,95
13KY102-2	53,63	0,95	16,78	9,16	0,16	6,25	8,58	3,46	0,85	0,18	100,00	34,05	257,25	114,09	33,94	43,13	57,59	15,55	82,05	321,83	22,83	82,72	2,25	347,83	2,94	0,07	16,24	5,26	14,68
13KY103-2	53,34	0,88	15,88	9,21	0,15	7,89	8,97	2,88	0,63	0,16	100,00	31,20	240,28	268,65	36,34	93,27	32,17	12,49	75,68	311,74	19,22	74,20	2,58	265,84	2,36	0,55	14,42	3,16	11,35
13KY-110	52,40	0,96	15,60	9,54	0,17	7,88	9,43	3,12	0,74	0,18	100,00	36,67	255,76	269,36	35,21	69,99	72,54	14,22	76,50	307,99	21,50	77,16	2,57	231,92	2,97	0,10	15,06	7,02	12,06
13KY-3	52,53	0,85	15,98	9,15	0,16	8,15	9,39	2,98	0,66	0,15	100,00	35,19	238,69	278,43	36,55	87,60	81,81	12,86	77,73	315,74	20,74	71,39	2,32	232,15	3,32	0,39	16,35	4,40	9,73
13KY-5	52,03	0,86	15,87	9,43	0,16	8,25	9,61	3,00	0,65	0,15	100,00	35,62	241,84	278,67	35,26	85,09	67,10	12,55	74,70	308,81	19,89	69,33	2,45	230,94	2,96	1,23	17,57	6,40	14,38
13KY-105-1	51,71	0,96	15,52	10,01	0,17	8,00	9,58	3,11	0,75	0,18	100,00	35,54	262,65	260,39	34,74	74,84	89,73	13,62	79,86	325,51	23,41	79,87	2,64	245,88	3,44	0,23	16,24	7,16	10,98
13KY-105-2	52,37	0,97	15,88	9,58	0,16	7,72	9,20	3,18	0,76	0,19	100,00	35,54	262,65	260,39	34,74	74,84	89,73	13,62	79,86	325,51	23,41	79,87	2,64	245,88	3,44	0,23	16,24	7,16	10,98
13KY-106-1	51,80	0,98	15,54	9,84	0,17	7,99	9,67	3,09	0,75	0,18	100,00	35,94	261,60	268,91	35,07	78,24	94,42	15,18	83,69	334,10	23,96	83,34	1,90	251,69	3,12	2,16	16,91	7,75	19,35
13KY-106-2	52,76	0,96	15,87	9,31	0,16	7,72	9,20	3,09	0,74	0,18	100,00	33,25	255,29	263,93	33,60	74,14	90,31	15,46	80,48	328,07	23,66	80,77	2,32	237,51	3,70	0,13	14,09	6,05	11,08
13KY-108	52,89	0,96	16,00	9,21	0,16	7,71	9,02	3,12	0,75	0,19	100,00	33,25	255,29	263,93	33,60	74,14	90,31	15,46	80,48	328,07	23,66	80,77	2,32	237,51	3,70	0,13	14,09	6,05	11,08
11KY-111-2	54,28	0,94	16,39	9,00	0,16	6,40	8,55	3,24	0,87	0,17	100,00	27,25	248,44	156,28	33,87	53,14	73,39	17,31	89,63	332,98	23,34	89,20	3,25	359,30	5,61	3,50	17,51	5,36	18,18
11KY-111-4	53,36	1,10	17,66	9,46	0,17	5,12	8,47	3,38	1,08	0,20	100,00	30,27	279,50	27,48	32,07	25,14	114,22	20,23	86,43	352,27	23,55	89,66	3,22	359,53	4,84	2,76	17,81	8,46	14,27

Sample	SiO_2	TiO_2	Al_2O_3	FeO*	MnO	MgO	CaO	Na_2O	K_2O	P_2O_5	Sum	Sc	V	Cr	Co	Ni	Cu	Rb	Z	Sr	Y	Zr	Nb	Ba	Pb	Th	Ga	La	Ce
11KY-17-1	54,04	0,97	17,29	9,08	0,16	5,55	8,34	3,47	0,92	0,19	100,00	24,25	247,47	92,95	33,71	33,59	68,24	16,77	85,53	333,97	24,35	92,76	3,34	382,94	4,97	4,06	16,27	9,14	14,93
13KY-107-1	52,65	0,96	15,77	9,38	0,16	7,86	9,24	3,05	0,74	0,18	100,00	35,32	258,77	258,75	36,45	72,72	81,80	15,04	74,27	319,31	23,67	82,29	2,78	234,95	2,25	1,59	14,61	8,86	10,66
13KY-107-2	52,65	0,96	15,77	9,38	0,16	7,86	9,24	3,05	0,74	0,18	100,00	35,32	258,77	258,75	36,45	72,72	81,80	15,04	74,27	319,31	23,67	82,29	2,78	234,95	2,25	1,59	14,61	8,86	10,66
13KY-13	53,25	0,95	16,19	9,35	0,16	6,97	8,79	3,29	0,87	0,18	100,00	33,37	249,82	199,44	34,07	66,62	82,76	17,75	89,63	328,79	25,07	85,09	2,36	350,65	3,77	0,91	17,20	8,59	14,07
11KY-5-1	53,87	0,96	16,81	9,19	0,16	6,01	8,52	3,40	0,88	0,18	99,99	24,67	253,83	39,22	33,01	26,02	101,18	19,03	86,05	361,96	24,67	97,25	3,34	420,78	5,39	1,16	16,23	5,50	21,94
11KY-5-3	53,56	0,95	16,71	9,16	0,17	6,24	8,74	3,41	0,88	0,18	100,00	29,95	251,28	124,75	32,83	45,17	87,89	16,63	89,83	336,04	24,00	90,81	3,20	357,82	4,59	1,04	17,70	6,14	13,64
Kly10-13	52,58	0,89	16,01	9,37	0,16	7,93	9,36	2,90	0,65	0,15	100,00	31,25	245,47	247,82	35,31	79,84	61,93	11,77	74,73	303,07	20,54	72,74	2,73	226,11	3,69	1,47	14,41	5,92	10,19
Kly10-14	52,42	0,87	16,18	9,43	0,16	7,91	9,24	2,98	0,65	0,15	100,00	32,75	258,73	232,04	37,13	88,20	93,84	12,50	80,80	326,26	21,36	74,79	3,47	241,42	4,29	1,10	16,38	2,92	11,76
Kly10-12	53,56	1,08	17,73	9,10	0,16	5,22	8,25	3,74	0,96	0,20	100,00	26,47	263,40	32,09	31,17	26,23	79,57	16,25	86,26	364,09	23,97	97,42	2,72	377,81	4,83	1,15	16,94	2,07	18,16
12KY-9-1	53,07	0,87	15,02	9,14	0,17	7,82	9,94	2,84	0,95	0,18	100,00	35,57	259,71	221,53	34,18	59,52	99,26	15,97	76,14	353,10	20,19	74,53	2,43	324,08	4,79	1,04	15,00	6,42	11,45
12KY-10-2	53,42	0,87	15,09	8,96	0,16	7,72	9,80	2,82	0,96	0,18	100,00	34,33	260,22	211,35	33,97	58,30	97,62	16,46	75,05	353,13	19,40	75,28	2,87	326,97	4,86	2,43	14,39	4,99	13,76
12KY-13-1	53,15	0,86	14,21	9,03	0,16	9,38	9,44	2,72	0,87	0,16	100,00	34,85	243,67	523,19	36,98	129,37	85,62	15,71	72,61	306,50	20,23	74,13	3,08	303,06	4,14	2,19	14,33	3,30	15,73
Kly10-17	53,39	0,87	14,73	9,02	0,16	8,15	9,80	2,79	0,92	0,17	100,00	32,96	249,77	301,58	34,33	74,05	84,63	16,89	74,80	350,84	20,59	77,32	3,08	313,02	4,24	1,24	16,58	7,58	14,36
11KY-104-1	52,70	0,96	15,61	9,28	0,16	8,01	9,34	3,08	0,69	0,17	100,00	33,12	244,63	284,36	34,65	75,81	52,54	10,95	73,97	283,97	20,98	81,46	3,68	228,88	3,43	6,41	13,94	4,71	12,85
11KY-104-2	52,48	0,94	15,59	9,48	0,16	8,12	9,45	2,95	0,67	0,17	100,00	32,69	251,31	300,64	36,56	80,96	83,64	11,84	79,17	298,37	20,43	81,56	3,51	234,80	3,85	1,45	15,49	8,43	10,82
11KY-104-3	52,51	0,94	15,30	9,51	0,16	8,31	9,50	2,91	0,68	0,17	100,00	32,83	247,32	327,95	36,66	81,38	42,74	11,76	75,27	282,41	20,65	78,51	3,34	226,84	3,61	1,22	13,23	5,84	12,52
11KY-104-4	53,94	0,97	17,11	8,96	0,16	5,83	8,55	3,41	0,88	0,18	100,00	29,67	252,83	82,71	33,04	37,53	81,77	15,76	79,51	322,02	22,14	86,66	2,66	360,50	4,54	2,96	14,75	6,51	18,63
11KY-102-3	53,39	0,97	15,83	9,19	0,17	6,96	9,21	3,13	0,97	0,19	100,00	33,93	252,83	195,45	31,99	53,52	78,74	15,83	79,02	336,04	20,68	82,05	3,38	334,00	3,81	1,22	15,24	2,80	13,97
11KY-108-1	53,59	0,92	15,83	9,35	0,17	7,07	8,93	3,05	0,91	0,18	100,00	33,30	262,51	186,86	34,62	55,38	73,73	15,88	78,97	332,26	22,62	83,98	3,09	331,48	5,24	1,37	15,10	1,96	14,23
11KY-108-4	53,49	0,92	15,86	9,39	0,17	7,03	8,97	3,04	0,92	0,18	100,00	33,37	266,10	177,49	35,65	57,99	82,20	16,72	86,77	349,93	23,22	84,21	3,32	335,89	4,48	1,14	16,52	8,38	15,98
11KY-	53,96	0,97	16,86	9,04	0,16	5,95	8,54	3,33	1,01	0,19	100,00	27,13	247,56	92,51	33,04	38,71	76,95	17,92	85,84	355,84	21,94	90,77	2,67	387,47	4,59	1,31	17,00	8,59	17,05

Sample	SiO_2	TiO_2	Al_2O_3	FeO*	MnO	MgO	CaO	Na_2O	K_2O	P_2O_5	Sum	Sc	V	Cr	Co	Ni	Cu	Rb	Z	Sr	Y	Zr	Nb	Ba	Pb	Th	Ga	La	Ce
109-2																													
11 KY-110-1	54,26	1,01	17,80	8,83	0,16	5,05	8,06	3,66	0,98	0,19	100,00	25,80	251,79	40,01	30,32	26,51	56,82	17,43	83,81	356,67	23,85	95,02	2,99	407,34	4,15	1,91	17,84	8,24	20,09
11 KY-110-6	54,02	1,00	18,25	8,79	0,16	4,57	8,08	3,87	1,06	0,20	100,00	23,43	250,46	28,24	31,10	23,58	79,86	19,01	94,03	391,74	25,52	104,24	3,41	438,33	5,27	2,53	19,96	7,97	19,53
11KY-8-2	54,02	1,04	17,70	9,04	0,16	5,04	8,17	3,46	1,13	0,22	100,00	28,20	271,16	36,50	32,36	27,87	112,25	18,27	86,15	397,91	23,71	95,90	3,13	397,26	4,83	1,83	16,70	7,42	17,36
11KY-8-3	53,96	1,05	17,58	9,06	0,16	5,13	8,19	3,52	1,14	0,22	100,00	28,52	266,85	37,41	31,07	27,37	104,36	18,03	83,18	387,46	23,96	94,34	3,08	390,54	4,78	3,24	15,83	7,44	17,52
Kly10-5	53,79	1,05	16,96	9,13	0,16	5,75	8,55	3,32	1,07	0,21	100,00	30,02	268,35	84,20	31,74	34,01	104,88	18,97	85,62	379,51	24,71	92,36	3,32	376,55	4,84	1,87	16,00	7,90	17,40
11KY-100-2	53,81	1,09	17,91	8,87	0,15	5,08	8,07	3,61	1,18	0,23	100,00	24,40	259,75	50,97	32,79	34,87	105,11	18,48	83,91	389,33	23,78	98,97	3,12	413,41	4,58	1,21	15,86	7,73	22,27
11KY-100-3	54,06	1,11	17,82	9,05	0,15	4,68	8,00	3,67	1,22	0,24	100,00	25,72	270,08	46,42	30,79	29,88	97,36	19,80	81,68	388,43	24,18	101,48	3,12	427,37	5,75	1,53	17,11	8,81	22,31
11KY-6-2	54,13	1,11	18,27	8,89	0,15	4,55	7,83	3,65	1,18	0,23	100,00	26,21	268,51	23,98	32,17	25,55	133,27	17,17	87,18	396,98	25,09	100,79	3,50	416,14	4,90	10,57	17,38	8,69	18,42
Kly10-15	53,94	1,12	18,20	9,08	0,15	4,59	7,89	3,63	1,17	0,22	100,00	22,51	267,92	25,37	30,26	25,30	94,41	17,66	81,55	383,83	23,54	97,27	2,88	413,04	6,01	1,79	16,56	6,06	21,41
11KY-2-3	53,90	1,08	17,44	9,20	0,16	5,11	8,21	3,53	1,13	0,22	100,00	26,85	265,23	56,82	31,78	28,46	108,28	19,46	84,62	363,58	25,49	98,33	3,00	412,96	5,26	0,71	15,90	5,61	16,87
12KY-110-2	53,99	1,07	17,21	9,26	0,17	5,31	8,37	3,36	1,05	0,21	100,00	30,86	263,98	52,46	33,52	29,44	85,29	17,56	85,54	349,85	24,23	94,75	3,38	399,21	4,94	2,84	16,00	3,08	19,62
12KY-110-5	53,65	1,07	17,22	9,31	0,17	5,42	8,48	3,41	1,07	0,21	100,00	30,64	269,40	52,24	33,78	30,44	99,64	18,15	86,57	358,85	25,66	95,79	2,99	407,70	5,01	1,18	16,94	3,28	17,09
11KY-103-3	52,43	1,13	17,12	9,98	0,18	5,49	8,86	3,52	1,08	0,21	100,00	29,05	276,61	31,98	35,66	27,52	95,53	17,48	86,15	339,36	24,89	89,82	3,36	364,46	5,19	2,45	18,52	5,16	10,93
11KY-103-4	53,70	1,12	17,46	9,32	0,16	5,29	8,34	3,38	1,03	0,21	100,00	27,44	265,64	47,21	33,56	31,06	96,94	18,59	87,52	366,31	23,83	96,75	3,27	398,86	4,39	1,25	17,73	6,79	14,30
11KY-11-1	53,63	1,11	17,63	9,59	0,17	5,05	8,12	3,45	1,05	0,21	100,00	27,16	277,36	40,00	34,08	26,78	100,00	18,09	92,09	369,51	26,58	100,78	3,36	410,79	5,18	6,65	18,64	3,47	19,91
11KY-11-3	53,58	1,10	17,55	9,51	0,17	5,14	8,26	3,44	1,04	0,21	100,00	27,16	266,01	39,40	31,43	26,37	104,08	15,36	84,73	344,70	24,53	94,35	3,24	398,33	4,64	12,88	18,27	8,31	20,07
12KY-108-1	55,19	0,96	18,26	8,20	0,14	4,61	7,70	3,81	0,93	0,20	100,00	20,52	217,90	30,86	30,38	26,26	67,72	17,66	91,04	399,72	23,79	106,36	3,29	338,32	6,21	2,86	19,35	8,41	18,25
12KY-108-2	53,67	1,01	17,46	9,27	0,16	5,42	8,34	3,66	0,82	0,19	100,00	26,99	262,75	71,74	32,33	30,75	81,74	15,16	84,33	329,39	22,44	91,80	3,27	325,79	4,53	1,75	18,96	6,80	14,52
12KY-107-1	53,80	1,10	17,62	9,40	0,16	5,05	8,24	3,41	1,03	0,20	100,00	27,45	274,44	35,70	33,06	26,99	84,46	18,06	87,65	366,74	25,83	98,28	3,50	407,86	4,38	4,21	18,07	10,08	23,67
12KY-107-3	53,50	1,09	17,53	9,53	0,17	5,06	8,37	3,48	1,06	0,20	100,00	25,48	265,22	34,60	32,01	25,89	55,60	17,41	84,85	356,10	24,43	93,87	3,20	391,32	4,17	0,84	17,97	4,62	16,94

Sample	SiO_2	TiO_2	Al_2O_3	FeO*	MnO	MgO	CaO	Na_2O	K_2O	P_2O_5	Sum	Sc	V	Cr	Co	Ni	Cu	Rb	Z	Sr	Y	Zr	Nb	Ba	Pb	Th	Ga	La	Ce
12KY-107-3	53,86	1,12	17,85	9,35	0,16	4,83	8,10	3,47	1,04	0,20	100,00	30,87	270,96	32,82	31,54	24,67	104,82	18,07	85,50	361,65	24,21	95,82	4,03	417,12	5,28	1,83	16,49	10,47	20,29
12KY-103-1	53,28	1,15	17,81	9,54	0,17	4,97	8,33	3,51	1,04	0,20	100,00	24,89	264,85	22,19	33,09	27,08	88,60	18,24	94,67	376,50	25,85	97,53	3,28	408,80	5,62	2,17	19,30	7,66	16,35
12KY-103-2	53,86	1,12	17,85	9,35	0,16	4,83	8,10	3,47	1,04	0,20	100,00	27,25	268,46	25,19	31,66	23,86	85,66	17,84	86,36	361,88	24,53	97,17	3,31	418,02	4,08	2,28	18,41	7,57	24,54
11KY-105-1	54,12	1,08	17,04	9,39	0,17	5,31	8,26	3,39	1,03	0,20	100,00	26,13	263,47	63,81	32,99	28,26	79,78	17,83	88,22	336,85	25,83	97,92	3,81	420,89	5,75	2,88	16,89	6,10	17,62
11KY-106-3	53,86	1,07	17,09	9,43	0,17	5,34	8,42	3,40	1,03	0,20	100,00	29,22	263,76	62,42	32,56	27,46	78,17	18,28	84,54	330,59	24,38	95,78	3,44	417,98	4,98	1,05	17,18	8,51	19,02
11KY-107-2	54,42	1,06	17,23	9,12	0,17	5,11	8,22	3,42	1,04	0,21	100,00	26,98	248,20	54,49	30,89	25,38	44,64	17,71	81,81	329,69	23,08	95,12	3,73	425,95	5,02	1,48	15,61	8,33	16,98
13KY-8	54,60	1,08	17,31	9,63	0,18	5,82	8,75	3,40	0,94	0,19	101,88	30,22	273,22	80,57	33,39	33,83	81,12	17,35	92,98	343,31	25,91	92,40	3,32	397,55	4,80	0,62	17,95	3,90	19,83
13KY-9	54,44	1,05	17,28	9,46	0,17	5,85	8,75	3,38	0,93	0,19	100,00	32,86	266,27	77,89	32,89	33,13	89,84	16,82	86,43	328,52	25,90	89,47	3,04	389,09	3,27	0,15	16,54	7,39	15,04
013KY-11	54,38	1,06	17,42	9,72	0,17	5,67	8,65	3,44	0,95	0,19	100,00	30,60	266,91	70,38	32,53	32,46	87,43	17,98	90,15	340,55	25,30	92,78	3,48	396,51	4,02	1,02	20,14	9,57	14,77
13KY-12	54,16	1,05	17,33	9,53	0,18	5,72	8,73	3,44	0,96	0,19	100,00	33,55	269,29	74,71	32,26	32,52	99,56	17,42	88,17	336,03	25,02	91,64	2,82	398,14	3,99	0,39	17,56	7,29	21,27
2013.1	55,96	1,09	18,00	9,17	0,18	5,47	8,59	3,49	0,99	0,21	100,00	29,63	263,73	64,28	32,35	28,45	67,04	16,73	86,49	333,66	25,30	92,21	3,20	413,25	4,32	3,06	18,07	6,28	15,41
2013.2	53,81	1,07	17,28	9,34	0,17	5,24	8,38	3,35	0,97	0,20	100,00	28,86	258,23	61,72	31,76	28,44	73,12	17,25	87,63	329,31	25,16	89,45	2,47	406,57	4,41	2,90	16,38	5,19	15,60
2013.3	54,60	1,08	17,52	9,52	0,17	5,31	8,44	3,39	0,99	0,20	100,00	29,04	262,22	62,26	32,66	29,18	81,53	17,78	90,02	335,56	25,38	90,17	2,51	406,49	4,43	2,09	15,70	9,59	13,64

Table 4. Trace element geochemistry of Klyuchevkoy volcano (ICP-MS data).

Sample	Li	Sc	V	Co	Z	Ga	Rb	Sr	Y	Zr	Nb	In	Cs	Ba	La	Ce	Pr	Nd	Sm	Eu	Gd	Tb	Dy	Ho	Er	Tm	Yb	Lu	Hf	Ta	W	Re	Pb	Bi	Th	U
Kly10-9	14,02	27,26	267,40	29,40	10,30	18,21	16,69	340,30	23,90	100,90	1,99	0,92	0,63	440,60	7,18	17,52	2,73	12,72	3,42	1,08	3,81	0,62	3,84	0,82	2,35	0,35	2,23	0,34	2,59	0,13	0,05	0,91	0,16	0,79	0,92	0,54
13KY-1	19,03	44,84	303,70	58,98	115,60	16,01	8,03	239,50	21,83	69,29	0,90	0,98	0,25	180,90	4,25	11,19	1,78	8,83	2,57	0,87	3,11	0,51	3,14	0,67	1,96	0,28	1,85	0,28	1,41	0,04	0,10	0,99	2,97	0,98	0,44	0,28
13KY-2	10,83	37,71	273,90	44,14	97,09	16,47	9,35	254,50	22,82	78,47	1,37	0,93	0,33	216,00	4,99	12,93	2,06	10,28	3,01	0,96	3,49	0,58	3,55	0,76	2,17	0,32	2,03	0,31	1,83	0,09	0,06	0,94	5,01	0,92	0,49	0,31
13KY-4	18,18	37,01	331,00	34,89	77,77	19,32	17,14	313,60	26,23	100,40	1,55	0,95	0,57	393,50	6,81	16,87	2,63	12,69	3,54	1,10	4,01	0,66	4,06	0,85	2,51	0,36	2,31	0,36	2,32	0,11	0,15	0,96	4,57	0,97	0,74	0,46
13KY101-2	7,61	30,96	209,70	36,55	117,60	15,72	9,92	275,00	21,44	77,67	1,36	0,94	0,52	238,90	5,36	13,68	2,21	10,71	3,04	0,98	3,42	0,58	3,54	0,76	2,20	0,33	2,05	0,31	2,03	0,10	0,08	0,96	7,61	0,95	0,54	0,35
13KY101-4	7,57	49,68	228,80	42,35	125,60	13,30	7,61	201,40	17,96	53,47	0,39	1,01	0,27	202,10	3,93	10,48	1,68	8,14	2,34	0,79	2,69	0,47	2,89	0,61	1,79	0,26	1,67	0,26	1,26	0,02	0,14	0,99	2,36	1,03	0,36	0,23
11KY-101	7,17	34,98	172,70	36,90	70,40	15,87	9,77	290,40	21,05	80,46	1,69	0,97	0,35	214,00	5,33	13,88	2,17	10,43	2,96	0,98	3,33	0,57	3,37	0,73	2,08	0,31	1,97	0,30	2,01	0,11	0,05	0,96	1,98	0,86	0,52	0,33
11KY-10	10,16	46,86	216,60	32,73	30,14	15,53	10,51	280,20	20,67	83,63	0,73	1,02	0,36	228,30	5,88	14,64	2,31	10,86	2,98	0,97	3,21	0,55	3,33	0,71	2,04	0,30	1,93	0,30	1,91	0,04	0,06	1,00	2,05	1,05	0,52	0,34
13KY102-1	13,64	31,09	274,50	30,01	38,21	17,68	13,97	318,20	23,25	91,72	1,80	0,99	0,49	362,50	6,30	15,59	2,45	11,60	3,18	1,06	3,52	0,61	3,64	0,79	2,24	0,34	2,15	0,33	2,27	0,12	0,06	0,99	1,77	0,91	0,72	0,45
13KY102-2	10,87	48,33	146,60	27,85	44,23	15,39	12,44	296,60	21,34	77,95	0,65	1,03	0,40	338,20	5,79	14,47	2,28	10,90	2,98	0,98	3,34	0,58	3,45	0,74	2,11	0,31	2,02	0,31	1,91	0,05	0,06	1,01	1,60	1,07	0,56	0,36
13KY103-2	10,30	33,40	171,10	36,53	4,81	16,08	10,51	296,90	20,90	79,06	1,48	0,97	0,41	282,50	5,22	13,32	2,10	10,10	2,82	0,95	3,15	0,54	3,27	0,72	2,01	0,30	1,92	0,29	1,98	0,09	0,07	0,97	1,72	0,82	0,60	0,41
13KY-110	14,20	36,80	278,50	42,34	194,50	17,73	11,96	306,80	24,63	85,19	1,12	0,93	0,37	241,00	5,97	15,06	2,39	11,49	3,27	1,07	3,73	0,62	3,76	0,80	2,33	0,34	2,16	0,33	1,90	0,06	0,16	0,93	3,77	0,91	0,59	0,36
13KY-3	10,76	32,65	305,90	36,49	240,80	16,42	10,76	287,20	20,79	75,97	1,49	1,00	0,40	238,20	5,15	13,04	2,06	9,94	2,80	0,95	3,17	0,54	3,26	0,70	2,04	0,30	1,88	0,29	1,92	0,09	0,05	0,98	2,29	0,83	0,55	0,34
13KY-5	9,36	55,17	187,60	33,36	40,70	15,17	9,39	286,00	19,26	64,01	0,56	1,01	0,34	217,60	4,71	11,85	1,92	9,37	2,63	0,89	2,95	0,51	3,05	0,66	1,91	0,28	1,81	0,28	1,55	0,03	0,05	0,99	2,19	1,02	0,43	0,28
13KY-105-1	10,43	32,70	416,30	39,04	281,00	16,96	11,90	303,60	23,98	90,96	1,92	0,96	0,41	248,30	6,10	15,29	2,40	11,50	3,23	1,06	3,58	0,61	3,65	0,80	2,25	0,33	2,07	0,31	2,14	0,12	0,08	0,87	1,19	0,81	0,52	0,32
13KY-105-2	9,43	33,42	233,80	35,60	1557,00	16,19	16,28	311,50	22,88	86,97	1,78	1,06	0,44	244,80	5,98	15,51	2,38	11,42	3,22	1,04	3,64	0,61	3,72	0,80	2,30	0,34	2,14	0,32	2,23	0,12	0,07	1,03	6,19	0,92	0,60	0,38
13KY-	10,84	34,52	324,90	41,91	94,50	18,79	12,91	336,70	26,05	84,07	1,2	0,9	0,3	264,20	6,4	16,22	2,5	12,53	3,5	1,1	3,9	0,6	4,0	0,8	2,5	0,3	2,3	0,3	1,9	0,0	0,2	0,9	3,50	0,9	0,6	0,3

Sample	Li	Sc	V	Co	Z	Ga	Rb	Sr	Y	Zr	Nb	In	Cs	Ba	La	Ce	Pr	Nd	Sm	Eu	Gd	Tb	Dy	Ho	Er	Tm	Yb	Lu	Hf	Ta	W	Re	Pb	Bi	Th	U
106-1											0	1	9		1		9		4	4	5	7	2	7	1	6	1	4	4	8	0	3		2	2	7
13KY-106-2	7,71	21,74	183,20	31,22	152,70	15,79	11,02	271,90	22,39	78,61	1,11	0,98	0,35	240,00	5,88	14,92	2,37	11,54	3,27	1,03	3,56	0,61	3,69	0,79	2,28	0,33	2,12	0,32	1,97	0,07	0,15	0,96	3,53	0,97	0,56	0,33
13KY-108	10,95	31,53	409,30	37,68	94,24	17,24	12,55	319,90	23,96	93,25	1,94	1,01	0,42	258,60	6,25	15,76	2,45	11,63	3,22	1,05	3,67	0,61	3,68	0,80	2,29	0,34	2,09	0,32	2,24	0,12	0,06	0,93	2,15	0,79	0,62	0,38
11KY-111-2	11,19	29,93	221,40	33,41	244,60	17,80	16,41	291,10	24,38	85,82	1,54	0,91	0,63	385,00	6,67	16,68	2,59	12,16	3,39	1,06	3,71	0,64	3,84	0,82	2,35	0,35	2,16	0,33	2,04	0,09	0,26	0,93	6,94	0,91	0,83	0,48
11KY-111-4	15,89	26,88	342,00	31,40	67,87	19,16	17,30	365,60	26,72	99,39	1,84	0,96	0,66	383,50	6,83	16,96	2,69	12,89	3,56	1,16	4,10	0,67	4,08	0,89	2,51	0,38	2,36	0,35	2,40	0,11	0,04	0,86	2,77	0,72	0,73	0,45
11KY-17-1	15,19	29,85	373,60	31,82	127,20	18,93	16,41	340,40	25,18	100,60	1,96	0,97	0,66	406,30	7,04	17,39	2,69	12,62	3,49	1,10	3,88	0,64	3,86	0,83	2,36	0,36	2,23	0,33	2,38	0,12	0,06	0,88	2,23	0,73	0,80	0,47
13KY-107-1	20,08	45,93	303,40	48,07	353,30	17,49	11,68	296,10	22,52	78,67	1,07	1,01	0,38	235,70	5,32	13,69	2,08	10,21	2,81	0,96	3,33	0,55	3,29	0,70	2,06	0,29	1,92	0,29	1,63	0,04	0,11	1,01	5,68	0,97	0,58	0,39
13KY-107-2	13,07	27,14	232,30	26,88	43,90	17,63	15,91	321,90	24,81	99,02	1,99	1,01	0,52	426,30	7,09	17,55	2,74	12,84	3,49	1,11	3,83	0,65	3,96	0,86	2,46	0,36	2,33	0,35	2,49	0,13	0,05	0,98	1,56	0,94	0,77	0,48
13KY-13	12,96	32,37	252,30	34,00	30,41	17,11	14,35	296,40	23,08	88,86	1,74	0,99	0,49	359,00	6,15	15,32	2,41	11,51	3,21	1,02	3,68	0,60	3,76	0,80	2,27	0,34	2,13	0,33	2,25	0,12	0,09	0,99	1,44	0,89	0,71	0,44
11KY-5-1	14,21	31,99	287,10	33,02	107,10	19,00	15,22	336,00	25,32	96,79	1,74	0,95	0,50	401,10	6,88	17,17	2,68	12,79	3,54	1,15	3,96	0,67	4,06	0,87	2,48	0,37	2,31	0,35	2,45	0,11	0,03	0,94	0,44	0,73	0,94	0,58
11KY-5-3	15,46	28,53	347,10	33,90	100,50	18,36	15,90	322,70	25,07	97,17	1,81	0,95	0,62	389,10	6,73	16,68	2,61	12,18	3,41	1,08	3,87	0,63	3,80	0,82	2,36	0,35	2,20	0,33	2,29	0,16	0,04	0,85	2,38	0,72	0,75	0,45
Kly10-13	18,10	44,60	333,80	46,70	174,00	18,36	11,27	314,10	23,17	72,10	1,00	0,93	0,39	233,90	5,15	12,92	2,05	9,96	2,83	0,96	3,40	0,56	3,38	0,71	2,10	0,31	1,98	0,30	1,51	0,04	0,17	0,94	5,68	0,92	0,55	0,36
Kly10-14	10,12	33,63	196,10	37,75	12,36	16,76	10,46	321,70	21,63	77,16	1,50	0,96	0,37	243,60	5,19	13,16	2,11	10,22	2,86	0,97	3,23	0,56	3,39	0,73	2,11	0,31	1,97	0,30	1,97	0,09	0,06	0,96	1,90	0,86	0,54	0,36
Kly10-12	14,51	28,79	196,90	30,30	10,92	19,31	15,09	358,70	24,69	101,50	1,97	0,97	0,47	392,30	7,07	17,79	2,79	13,16	3,65	1,15	4,05	0,65	3,93	0,83	2,42	0,35	2,25	0,35	2,53	0,12	0,04	0,97	1,19	0,85	0,72	0,48
12KY-9-1	12,47	37,65	280,30	35,35	287,80	16,22	14,55	356,80	20,75	76,61	1,54	0,97	0,48	338,30	6,38	15,71	2,41	11,46	3,08	0,99	3,38	0,56	3,37	0,73	2,09	0,30	1,96	0,29	2,00	0,10	0,09	0,94	1,47	0,84	0,80	0,46
12KY-10-2	11,85	36,18	222,70	34,14	331,50	15,76	14,53	348,50	20,40	75,19	1,50	1,02	0,44	333,10	6,18	15,05	2,34	11,03	2,96	0,96	3,27	0,54	3,29	0,71	2,02	0,30	1,90	0,28	1,95	0,09	0,05	1,00	0,66	0,85	0,83	0,47
12KY-13-1	11,50	35,80	231,40	38,47	61,42	15,30	13,73	309,50	20,63	75,88	1,46	0,98	0,44	319,40	5,82	14,47	2,24	10,65	2,95	0,93	3,29	0,54	3,30	0,71	2,04	0,30	1,93	0,28	1,95	0,09	0,08	0,97	1,27	0,80	0,81	0,47
Kly10-17	13,51	35,21	392,90	37,19	400,40	16,30	15,62	353,50	21,02	79,04	1,6	0,9	0,6	341,40	6,4	15,60	2,3	11,16	2,9	0,9	3,3	0,5	3,2	0,6	2,0	0,3	1,8	0,2	1,8	0,1	0,0	0,8	2,30	0,7	0,7	0,4

Sample	Li	Sc	V	Co	Z	Ga	Rb	Sr	Y	Zr	Nb	In	Cs	Ba	La	Ce	Pr	Nd	Sm	Eu	Gd	Tb	Dy	Ho	Er	Tm	Yb	Lu	Hf	Ta	W	Re	Pb	Bi	Th	U
											9	4	3		4		7		8	7	0	4	7	9	2	0	5	8	9	1	5	4		2	2	1
11KY-104-1	11,89	32,26	341,80	38,55	114,60	16,56	10,67	270,10	22,70	88,82	1,92	0,86	0,40	242,70	5,60	14,30	2,23	10,76	3,06	1,00	3,44	0,57	3,50	0,75	2,15	0,32	2,03	0,30	2,10	0,12	0,07	0,78	1,25	0,64	0,52	0,36
11KY-104-2	20,50	46,52	309,10	46,52	168,30	17,68	10,28	287,70	23,47	84,56	1,16	1,01	0,35	221,80	5,25	13,32	2,10	10,24	2,90	0,96	3,45	0,55	3,43	0,73	2,16	0,31	2,03	0,31	1,76	0,06	0,14	1,00	3,69	0,97	0,56	0,36
11KY-104-3	10,57	34,18	181,80	36,56	120,80	16,03	10,55	284,40	21,97	82,97	1,67	0,99	0,39	236,70	5,38	14,61	2,18	10,58	3,01	0,99	3,40	0,57	3,57	0,76	2,15	0,32	2,05	0,31	2,07	0,11	0,03	0,98	1,62	0,82	0,59	0,39
11KY-104-4	16,65	26,55	347,00	34,18	2747,00	18,42	15,36	317,00	24,08	95,26	1,83	0,88	0,61	377,60	6,56	16,77	2,55	11,91	3,30	1,06	3,71	0,62	3,67	0,81	2,31	0,34	2,14	0,32	2,28	0,12	0,05	0,79	3,92	0,62	0,74	0,44
11KY-102-3	14,33	35,54	259,30	34,74	50,80	17,88	15,57	357,60	23,82	90,74	1,85	0,96	0,50	374,70	6,71	16,52	2,60	12,33	3,37	1,11	3,77	0,62	3,83	0,81	2,35	0,35	2,23	0,33	2,27	0,13	0,07	0,94	0,93	0,84	0,79	0,49
11KY-108-1	12,34	34,93	187,90	33,94	51,44	16,86	15,40	330,70	23,05	86,33	1,71	0,97	0,50	346,70	6,35	15,60	2,44	11,69	3,21	1,02	3,60	0,61	3,67	0,81	2,26	0,33	2,19	0,33	2,21	0,11	0,06	0,96	1,39	0,87	0,72	0,45
11KY-108-4	14,30	31,65	372,10	35,52	122,10	17,47	15,85	348,70	23,84	89,39	1,86	0,99	0,60	353,70	6,58	16,11	2,50	11,90	3,24	1,04	3,59	0,60	3,61	0,79	2,26	0,34	2,10	0,31	2,14	0,11	0,05	0,89	1,69	0,82	0,66	0,38
11KY-109-2	16,90	28,96	292,00	33,52	98,96	18,50	17,32	358,30	24,55	99,61	2,06	0,93	0,64	416,30	7,22	17,40	2,68	12,57	3,34	1,09	3,73	0,63	3,82	0,80	2,34	0,35	2,14	0,33	2,38	0,12	0,05	0,83	2,43	0,69	0,82	0,48
11KY-110-1	14,69	26,74	336,90	30,47	209,20	19,59	16,52	368,90	25,26	106,60	2,09	0,98	0,44	434,00	7,37	18,13	2,78	13,06	3,56	1,13	3,93	0,65	3,88	0,83	2,38	0,35	2,19	0,33	2,49	0,15	0,04	0,88	2,53	0,73	0,77	0,47
11KY-110-6	15,77	22,47	309,20	28,23	159,00	19,56	17,08	367,50	25,28	106,60	1,95	1,00	0,56	451,90	7,52	18,45	2,82	13,33	3,60	1,13	3,93	0,65	3,91	0,84	2,40	0,36	2,27	0,34	2,58	0,12	0,04	0,95	3,33	0,68	1,00	0,61
11KY-8-2	16,07	29,52	274,90	30,78	246,70	19,77	19,00	411,80	25,84	101,70	1,78	0,92	0,56	423,30	7,82	20,11	3,03	14,32	3,88	1,19	4,15	0,68	4,07	0,87	2,54	0,37	2,33	0,36	2,40	0,11	0,12	0,93	5,82	0,91	0,81	0,51
11KY-8-3	18,53	25,70	324,60	31,39	97,41	19,31	18,59	408,20	25,47	104,40	2,17	0,91	0,73	419,00	7,80	19,02	2,93	13,68	3,65	1,17	4,01	0,66	3,93	0,84	2,40	0,36	2,21	0,33	2,45	0,13	0,07	0,82	2,39	0,70	0,76	0,48
Kly10-5	17,59	29,90	367,50	32,17	346,40	18,94	17,22	387,50	25,47	101,00	2,07	0,88	0,63	400,10	7,41	18,22	2,82	13,32	3,57	1,13	4,03	0,66	3,87	0,83	2,44	0,36	2,19	0,34	2,36	0,12	0,05	0,80	1,81	0,67	0,74	0,47
11KY-100-2	16,68	26,62	276,40	30,06	53,34	19,65	18,47	403,50	25,60	107,30	2,09	0,96	0,61	445,10	7,98	19,65	3,05	14,42	3,94	1,20	4,10	0,68	4,14	0,88	2,51	0,36	2,31	0,35	2,66	0,13	0,04	0,96	0,54	0,78	0,96	0,60
11KY-100-3	16,36	26,15	260,00	27,57	124,00	19,56	18,52	393,70	25,27	107,40	2,08	0,99	0,59	439,90	7,83	19,20	3,02	14,20	3,79	1,19	4,08	0,66	4,04	0,86	2,47	0,36	2,31	0,35	2,61	0,13	0,05	0,99	0,58	0,85	0,91	0,58
11KY-6-2	9,39	19,93	233,00	25,72	111,80	18,42	17,15	382,60	24,67	99,14	1,81	0,90	0,68	445,80	8,07	19,67	3,12	14,87	3,97	1,23	4,24	0,71	4,32	0,93	2,61	0,39	2,46	0,37	2,70	0,11	0,23	0,92	4,86	0,96	0,80	0,49

Sample	Li	Sc	V	Co	Z	Ga	Rb	Sr	Y	Zr	Nb	In	Cs	Ba	La	Ce	Pr	Nd	Sm	Eu	Gd	Tb	Dy	Ho	Er	Tm	Yb	Lu	Hf	Ta	W	Re	Pb	Bi	Th	U
Kly10-15	16,89	26,04	314,40	28,93	10,58	19,92	17,45	403,40	25,65	106,00	2,12	0,94	0,48	436,80	7,73	19,08	3,01	14,08	3,80	1,20	4,14	0,67	4,12	0,87	2,49	0,37	2,37	0,36	2,66	0,14	0,06	0,92	0,28	0,82	0,88	0,56
11KY-2-3	16,88	28,77	297,10	29,24	23,92	19,15	17,60	369,30	26,18	104,20	2,05	0,94	0,80	428,00	7,61	19,34	2,95	13,93	3,79	1,19	4,17	0,68	4,21	0,89	2,59	0,37	2,41	0,37	2,62	0,13	0,05	0,94	0,57	0,84	0,88	0,53
12KY-110-2	16,87	27,57	345,10	31,59	534,10	18,64	17,52	360,40	25,97	103,80	2,15	0,95	0,68	418,10	7,42	17,99	2,78	13,18	3,64	1,13	3,99	0,66	4,01	0,85	2,45	0,37	2,27	0,34	2,42	0,13	0,07	0,85	8,86	0,75	0,73	0,45
12KY-110-5	23,17	44,02	349,60	38,30	100,50	20,57	17,82	370,40	28,36	105,90	1,75	0,96	0,56	419,50	7,35	17,99	2,80	13,35	3,70	1,16	4,26	0,68	4,18	0,88	2,58	0,38	2,41	0,36	2,27	0,10	0,19	0,98	4,85	0,98	0,79	0,50
11KY-103-3	15,49	30,29	231,70	31,38	215,30	18,76	15,99	360,30	26,36	100,40	1,98	0,98	0,48	422,80	7,23	18,11	2,83	13,44	3,78	1,17	4,15	0,69	4,21	0,91	2,61	0,38	2,46	0,37	2,59	0,13	0,07	0,96	0,66	0,81	0,90	0,54
11KY-103-4	14,91	29,53	309,50	30,75	17,52	18,60	15,97	355,20	26,13	99,29	2,07	1,02	0,54	419,10	7,19	18,63	2,82	13,41	3,74	1,16	4,18	0,69	4,22	0,90	2,62	0,38	2,41	0,36	2,53	0,14	0,10	1,01	0,64	0,95	0,78	0,47
11KY-11-1	13,47	24,38	286,80	30,28	91,34	18,89	16,78	356,60	26,53	98,86	1,56	0,99	0,70	430,90	7,44	18,36	2,90	13,90	3,90	1,18	4,29	0,71	4,34	0,92	2,66	0,40	2,50	0,37	2,45	0,10	0,38	0,98	4,59	1,01	0,79	0,47
11KY-11-3	16,80	26,84	311,30	34,16	54,66	20,96	17,19	387,50	29,35	106,20	1,47	0,90	0,49	440,80	7,73	19,20	3,05	14,64	3,99	1,25	4,45	0,75	4,50	0,98	2,81	0,41	2,61	0,39	2,43	0,09	0,19	0,92	4,90	0,93	0,85	0,49
12KY-108-1	14,23	20,49	304,80	26,39	189,50	18,88	14,90	373,30	23,17	109,90	2,07	1,02	0,47	338,10	6,97	17,11	2,64	12,25	3,24	1,08	3,55	0,59	3,54	0,77	2,21	0,33	2,10	0,31	2,59	0,13	0,03	0,97	24,19	0,74	0,78	0,54
12KY-108-2	12,94	29,25	174,70	30,07	84,91	19,01	12,85	341,70	25,00	100,20	1,75	0,94	0,44	338,90	6,65	17,23	2,71	12,88	3,52	1,16	3,93	0,66	3,98	0,83	2,39	0,36	2,27	0,36	2,46	0,11	0,15	0,94	1,20	0,79	0,69	0,46
12KY-107-1	9,72	20,51	258,50	27,13	20,80	17,93	15,49	345,20	25,17	92,00	1,20	0,94	0,55	429,50	7,31	17,84	2,86	13,87	3,78	1,17	4,16	0,71	4,25	0,93	2,64	0,39	2,46	0,37	2,45	0,10	0,11	0,94	5,14	0,98	0,76	0,45
12KY-107-3	15,88	26,69	416,90	31,92	77,52	19,72	17,43	372,80	26,94	105,60	2,22	0,98	0,18	436,50	7,49	18,39	2,84	13,40	3,65	1,18	4,17	0,69	4,12	0,88	2,51	0,37	2,34	0,35	2,51	0,14	0,07	0,91	2,78	0,84	0,73	0,44
12KY-107-3	15,88	26,69	416,90	31,92	77,52	19,72	17,43	372,80	26,94	105,60	2,22	0,98	0,18	436,50	7,49	18,39	2,84	13,40	3,65	1,18	4,17	0,69	4,12	0,88	2,51	0,37	2,34	0,35	2,51	0,14	0,07	0,91	2,78	0,84	0,73	0,44
12KY-103-1	14,91	27,47	318,00	31,15	262,30	19,46	16,82	365,40	26,63	98,34	1,49	0,96	0,51	428,30	7,17	17,70	2,79	13,51	3,76	1,21	4,23	0,70	4,20	0,93	2,64	0,39	2,41	0,37	2,37	0,11	0,10	0,96	4,99	0,96	0,77	0,46
12KY-103-2	17,11	25,45	356,30	31,38	127,80	19,78	18,40	376,50	27,51	108,90	2,19	0,96	0,72	450,30	7,64	18,64	2,90	13,74	3,74	1,21	4,21	0,71	4,19	0,92	2,59	0,39	2,44	0,36	2,57	0,14	0,08	0,86	2,33	0,75	0,78	0,47
11KY-105-1	15,76	27,92	407,90	31,50	74,38	19,16	17,59	339,80	27,04	105,70	2,16	1,01	0,63	443,30	7,38	18,20	2,83	13,35	3,67	1,16	4,03	0,68	4,15	0,89	2,55	0,38	2,35	0,36	2,53	0,13	0,04	0,94	3,08	0,75	0,87	0,52
11KY-106-3	11,34	23,92	249,70	29,10	50,10	18,24	16,18	330,40	26,03	99,19	1,51	1,00	0,59	444,20	7,34	18,09	2,88	13,70	3,82	1,17	4,19	0,72	4,34	0,94	2,71	0,40	2,50	0,38	2,53	0,10	0,22	0,99	4,61	1,01	0,81	0,47

Sample	Li	Sc	V	Co	Z	Ga	Rb	Sr	Y	Zr	Nb	In	Cs	Ba	La	Ce	Pr	Nd	Sm	Eu	Gd	Tb	Dy	Ho	Er	Tm	Yb	Lu	Hf	Ta	W	Re	Pb	Bi	Th	U
11KY-107-2	15,85	25,53	444,80	30,98	1645,00	19,51	18,13	354,40	26,93	109,20	2,20	0,98	0,70	453,20	7,66	19,29	2,88	13,57	3,60	1,17	4,06	0,69	4,08	0,89	2,54	0,38	2,38	0,36	2,60	0,13	0,09	0,92	3,63	0,83	0,78	0,48
13KY-8	14,17	32,82	192,30	31,82	52,24	18,25	15,42	325,60	26,14	97,30	1,92	0,97	0,50	414,90	6,68	16,78	2,65	12,71	3,54	1,13	3,99	0,68	4,08	0,89	2,55	0,38	2,38	0,37	2,41	0,12	0,10	0,96	1,13	0,85	0,76	0,46
13KY-9	14,66	32,60	267,50	32,36	104,40	18,78	15,70	331,90	26,41	99,70	1,95	0,98	0,52	423,20	6,85	17,32	2,70	12,92	3,61	1,16	4,07	0,69	4,21	0,91	2,62	0,38	2,44	0,37	2,52	0,12	0,07	0,97	1,19	0,88	0,77	0,46
013KY-11	13,27	28,81	273,30	29,52	143,00	17,99	15,77	291,90	25,52	91,37	1,86	0,96	0,54	399,40	6,56	16,24	2,57	12,29	3,46	1,09	3,88	0,66	4,00	0,88	2,49	0,36	2,34	0,35	2,18	0,11	0,19	0,97	4,12	0,98	0,70	0,41
13KY-12	17,25	30,16	324,10	34,51	532,10	18,99	16,78	307,70	27,14	102,80	2,18	0,90	0,64	426,60	6,94	17,36	2,71	12,76	3,49	1,14	4,03	0,69	4,09	0,88	2,56	0,39	2,35	0,36	2,44	0,13	0,08	0,81	2,16	0,72	0,68	0,41
2013.1	14,59	27,57	287,30	29,39	170,60	18,39	16,30	330,50	26,24	100,80	2,13	1,02	0,51	426,70	6,99	17,29	2,72	13,05	3,64	1,10	3,89	0,03	5,12	1,28	3,45	1,08	2,02	0,27	2,04	0,09	0,08	1,05	2,14	1,00	0,76	0,44
2013.2	14,87	28,25	295,10	30,41	61,78	18,64	16,51	332,30	26,64	102,20	2,11	1,01	0,51	432,80	7,06	17,47	2,74	13,18	3,73	1,09	4,01	0,03	5,18	1,31	3,49	1,10	2,06	0,27	2,04	0,14	0,12	1,03	2,13	0,99	0,75	0,46
2013.3	14,03	27,95	297,90	30,29	59,54	18,74	16,68	331,50	26,83	102,70	2,12	0,99	0,51	434,50	7,10	17,63	2,76	13,33	3,72	1,10	3,96	0,03	5,23	1,30	3,47	1,10	2,06	0,28	2,08	0,10	0,07	1,02	a	0,98	0,77	0,45

Table 5. Sr-Nd-Pb isotope data of Klyuchevskoy rocks.

Sample	Age	87Sr/86Sr	2 SE	146Nd/144Nd	2SE	206Pb/204Pb	2 SE	207Pb/204Pb	2 SE	208Pb/204Pb	2 SE
13KY-1	2800 BP	0,703483546	0,0000086174	0,512895797	0,000009846	18,2763	0,0008	15,4857	0,0007	37,9072	0,0019
13KY-2	2800 BP	0,703457508	0,0000082965	0,513109907	0,000009864	18,2752	0,0010	15,4840	0,0009	37,9031	0,0026
13KY-3	2800 BP	0,703520769	0,0000077901	0,513080574	0,000008891	18,2769	0,0011	15,4843	0,0010	37,9086	0,0030
13KY-4	2800 BP	0,703585158	0,0000109518	0,512964072	0,000000600	18,2927	0,0007	15,4907	0,0007	37,9418	0,0017
13KY-101-2	2800 BP	0,703571100	0,0000712663	0,513106753	0,000008963	18,2803	0,0006	15,4876	0,0005	37,9180	0,0014
12KY-2-2	2800 BP	0,703548588	0,0000082345	0,513102288	0,0000046	18,2834	0,0009	15,4893	0,0008	37,9448	0,0020
11KY-101	2500 BP	0,703486338	0,0000099628	0,513008946	0,0000039	18,2674	0,0013	15,4848	0,0010	37,9200	0,0029
11KY-10	2500 BP	0,703494461	0,0000084935	0,513094777	0,0000055	18,2751	0,0007	15,4854	0,0006	37,9116	0,0019
13KY-102-2	2500 BP	0,703608242	0,0000080717	0,513071353	0,000008829	18,3492	0,0005	15,5288	0,0006	38,2542	0,0016
13KY-110	2500 BP	0,703503486	0,0000084692	0,513134187	0,0000052	18,3044	0,0006	15,4945	0,0006	37,9654	0,0017
13KY-5	2500 BP	0,703474290	0,0000080105	0,513101064	0,0000037	18,2706	0,0007	15,4846	0,0004	37,8957	0,0011
13KY-105-2	1500 BP	0,703426347	0,0000094436	0,513093694	0,0000050	18,2736	0,0007	15,4880	0,0007	37,9121	0,0018
13KY-106-1	1500 BP	0,703485090	0,0000082655	0,513085756	0,000009472	18,2717	0,0007	15,4825	0,0007	37,8917	0,0020
13KY-106-2	1500 BP	0,703480783	0,0000082187	0,513064844	0,000009114	18,2705	0,0007	15,4820	0,0007	37,8891	0,0018
10KY-9	500 BP	0,703645253	0,0000086874	0,512952143	0,000009964	18,2719	0,0008	15,4829	0,0006	37,8920	0,0019
11KY-111-2	500 BP	0,703665823	0,0000085388	0,513063568	0,000009098	18,3069	0,0011	15,4964	0,0010	37,9730	0,0028
11KY-111-4	500 BP	0,703467924	0,0000079744	0,513100914	0,0000064	18,3058	0,0007	15,4950	0,0008	37,9694	0,0020
11KY-5-3	500 BP	0,703669143	0,0000088942	0,513094383	0,0000057	18,2970	0,0008	15,4911	0,0007	37,9412	0,0017
13KY-13	500 BP	0,703604823	0,0000095213	0,513047323	0,000008952	18,3011	0,0006	15,4943	0,0008	37,9617	0,0019
13KY-107-1	500 BP	0,703536019	0,0000089689	0,513077323	0,000009339	18,2976	0,0009	15,4928	0,0009	37,9513	0,0024

10KY-13	100 BP	0,703483793	0,0000083314	0,513045992	0,0000050	18,2606	0,0007	15,4891	0,0006	37,9063	0,0018
10KY-14	100 BP	0,703484926	0,0000090657	0,513045992	0,0000050	18,2740	0,0007	15,4852	0,0006	37,9077	0,0017
10KY-12	100 BP	0,703577168	0,0000090533	0,512696089	0,000010580	18,2893	0,0007	15,4873	0,0007	37,9190	0,0020
12KY-10-2	1932	0,703475396	0,0000100632	0,512958236	0,000008854	18,3027	0,0007	15,4917	0,0005	37,9490	0,0013
12KY-13-1	1932	0,703515042	0,0000085029	0,512958236	0,000008854	18,3015	0,0007	15,4930	0,0007	37,9524	0,0020
11KY-104-1	1937	0,703495343	0,0000091268	0,513067643	0,000098903	18,2769	0,0007	15,4855	0,0006	37,9069	0,0016
11KY-104-2	1937	0,703507534	0,0000096855	0,513067643	0,000098903	18,2763	0,0008	15,4851	0,0007	37,9053	0,0019
11KY-104-3	1937	0,703478652	0,0000075782	0,513045862	0,0000062	18,2770	0,0009	15,4853	0,0007	37,9074	0,0020
11KY-108-1	1938	0,703498758	0,0000082543	0,513101544	0,0000058	18,2969	0,0011	15,4915	0,0009	37,9424	0,0028
11KY-109-2 (3)	1938	0,703589403	0,0000085302	0,513084232	0,000009384	18,3032	0,0006	15,4947	0,0005	37,9641	0,0015
11KY-110-6	1938	0,703660822	0,0000091801	0,513091333	0,0000073	18,3008	0,0006	15,4923	0,0005	37,9511	0,0018
11KY-8-2	1945	0,703547019	0,0000097477	0,513109644	0,000008237	18,3028	0,0007	15,4924	0,0007	37,9432	0,0017
11KY-8-3	1945	0,703559642	0,0000083028	0,513099614	0,0000054	18,3013	0,0006	15,4907	0,0007	37,9380	0,0018
10KY-5	1946	0,703595171	0,0000092325	0,51311275	0,0000056	18,2987	0,0008	15,4916	0,0008	37,9384	0,0021
11KY-100-2	1951	0,703597779	0,0001002592	0,513090481	0,000009706	18,2945	0,0006	15,4911	0,0005	37,9369	0,0014
11KY-100-3	1951	0,703596158	0,0000947042	0,512972703	0,000009955	18,2913	0,0008	15,4920	0,0007	37,9372	0,0019
11KY-6-2	1953	0,703583549	0,0000087829	0,513053636	0,000007741	18,2920	0,0008	15,4913	0,0007	37,9356	0,0019
10KY-15	1953	0,703601954	0,0000084197	0,513054321	0,000008149	18,2896	0,0009	15,4889	0,0007	37,9284	0,0019
11KY-16-2	1956	0,703617490	0,0000079826	0,513097382	0,000009326	18,2896	0,0007	15,4886	0,0006	37,9289	0,0018
11KY-16-4	1956	0,703588297	0,0000885840	0,513103376	0,0000043	18,3037	0,0008	15,4935	0,0007	37,9483	0,0021
11KY-2-3	1966	0,703623805	0,0000087872	0,513066273	0,000010339	18,2943	0,0011	15,4904	0,0009	37,9378	0,0021
12KY-110-5	1974	0,703600129	0,0000099301	0,513075783	0,000009246	18,2984	0,0007	15,4919	0,0006	37,9506	0,0017
11KY-103-3	1980	0,703607821	0,0000104909	0,513069138	0,000009625	18,3015	0,0008	15,4935	0,0007	37,9552	0,0017
11KY-103-4	1980	0,703593906	0,0000087914	0,513099614	0,0000054	18,3040	0,0005	15,4944	0,0005	37,9580	0,0014
11KY-11-1	1983	0,703604144	0,0000076843	0,513097059	0,0000031	18,3056	0,0007	15,4953	0,0006	37,9609	0,0018

11KY-11-3	1983	0,703620266	0,0000080800	0,513058546	0,000009371	18,3052	0,0006	15,4951	0,0006	37,9609	0,0016
12KY-108-1	1987	0,703555965	0,0000082457	0,513112297	0,0000052	18,2750	0,0009	15,4832	0,0009	37,8880	0,0029
12KY-106-1	1988	0,703648379	0,0000100000	0,513094121	0,000009004	18,2940	0,0006	15,4930	0,0006	37,9553	0,0018
12KY-107-1	1988	0,703607654	0,0000087175	0,513084996	0,000009482	18,3036	0,0005	15,4942	0,0004	37,9582	0,0013
12KY-107-3	1988	0,703635518	0,0000068000	0,513090916	0,000010342	18,3022	0,0005	15,4967	0,0005	37,9632	0,0013
12KY-103-1	1994	0,703621962	0,0000080846	0,513071229	0,000008961	18,3122	0,0009	15,4956	0,0009	37,9685	0,0022
12KY-103-3	1994	0,703625936	0,0000065000	0,513097668	0,000008789	18,2962	0,0005	15,4917	0,0005	37,9430	0,0014
11KY-106-1	1994	0,703621925	0,0000082	0,513085921	0,000009502	18,3125	0,0006	15,4964	0,0006	37,9716	0,0017
11KY-106-3	2009	0,703593026	0,0000076425	0,513085921	0,000009502	18,3122	0,0007	15,4953	0,0007	37,9693	0,0018
11KY-107-1	2010	0,703628240	0,0000094000	0,513075972	0,000010484	18,3090	0,0007	15,4950	0,0006	37,9674	0,0017
11KY-107-2	2010	0,703569206	0,0000088245	0,513098811	0,0000043	18,3115	0,0006	15,4980	0,0005	37,9739	0,0014
13KY-9	2013	0,703633160	0,0000091598	0,513093694	0,0000039	18,3188	0,0005	15,4992	0,0006	37,9841	0,0017
13KY-11	2013	0,703605522	0,0000091558	0,513106753	0,000008963	18,3178	0,0005	15,4986	0,0005	37,9833	0,0014
13KY-12	2013	0,703627602	0,0000077412	0,513114745	0,0000074	18,3168	0,0007	15,4981	0,0008	37,9818	0,0019
2013.1	2013	0,703633462	0,0000061000	0,513095616	0,000009452	18,3134	0,0007	15,4961	0,0007	37,9761	0,0018
2013.2	2013	0,703626621	0,0000090000	0,513088310	0,000008705	18,3138	0,0008	15,4960	0,0007	37,9759	0,0019
2013.3	2013	0,703627568	0,0000084000	0,513105934	0,000007566	18,3145	0,0007	15,4976	0,0008	37,9798	0,0021

Years activity	Alaid	Ebeko	Chikurachki	Karpinskogo	Pik Fussa
1793					
1853					
1854					
1855					
1856					
1857					
1858					
1859					
1860					
1869					
1878					
1881					
1882					
1894					
1933					
1934					
1935					
1946					
1947					
1948					
1949					
1950					
1951					
1952					
1953					
1954					
1955					
1956					
1957					
1958					
1959					
1961					
1964					
1967					
1969					
1972					
1973					
1975					
1981					
1983					
1987					
1989					
1991					
1998					
2002					
2003					
2004					
2005					
2006					
2007					
2008					
2009					
Volume of eruptive material	114	13	47	5	33

Note:

	1		2		3

Table 1. Activity of volcanoes from NKI. Note: 1- explosive eruption, 2 – phreato-magmatic eruption, 3 – fumaroles activity (www.kscnet.ru).

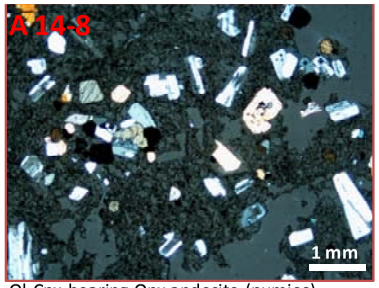

Ol-Cpx-bearing Opx andesite (pumice)

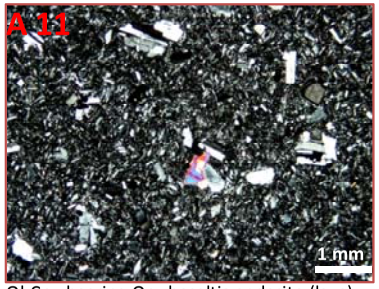

Ol-Cpx-bearing Opx basaltic andesite (lava)

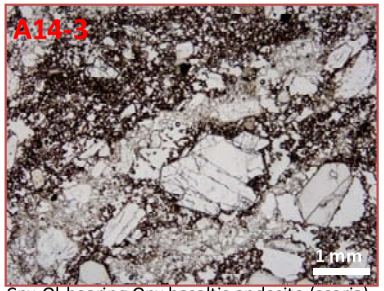

Cpx-Ol-bearing Opx basaltic andesite (scoria)

Main petrological types from Tatarinov volcano

Main petrological types from Lomonosov volcano

Ol-bearing Cpx-Opx andesite

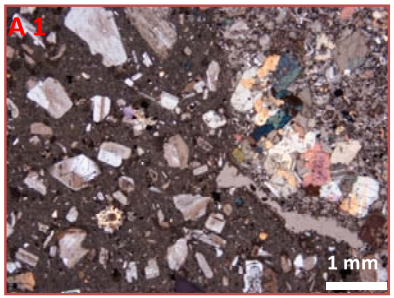

Qtz-Ol-bearing Cpx-Opx andesite

Fig. 1. Main petrological type of the rocks from frontal zone.

Main petrological types from Fuss volcano

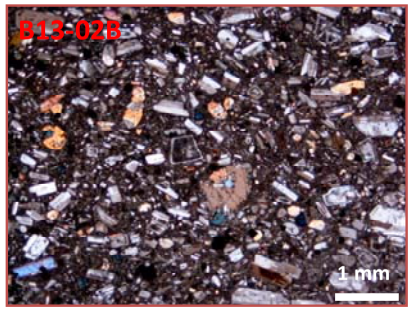

Hbl-Cpx-Ol-bearing Opx basaltic andesite (lava)

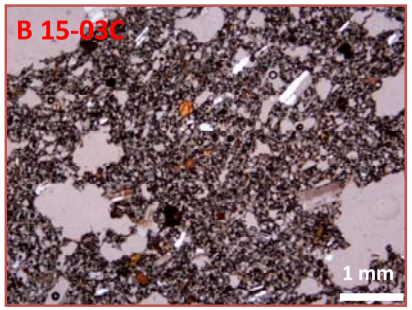

Ol-Cpx bearing Opx-Hbl andesite (pumice)

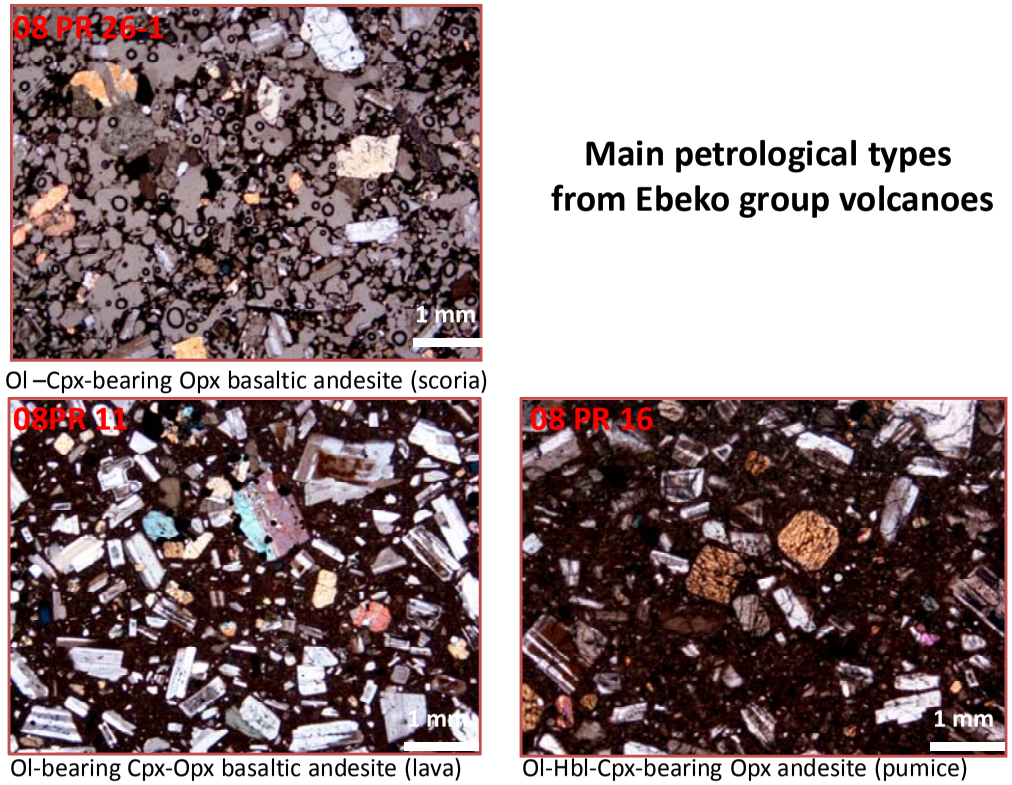

Fig. 2. Main petrological types of Intrermediate zone.

Table 2. Description of the thin sections.

Sample No.	Source	Inferred Age	Type	SiO2	Th/CaA	K-type	Formula	Phenocrysts%	Matrix texture	**Ol** (%)	**Opx** (%)	**Cpx** (%)	**Pl** (%)	**Hbl** (%)	**Bt** (%)	**Qtz** (%)	G.m. assemblage	**Rock name**
A11	Tatarinov	Plestocene	Lava				Pl>>>Opx>>Mt>Ol~Cpx	20-25	pilotaxitic	~1	5	1	15				Pl, Opx	Cpx, Opx basaltic-andesite
A12	Tatarinov	Plestocene	Lava				Pl>>>Opx>>Mt>Cpx	20-30	pilotaxitic		5,-7,	3	18-20					Cpx-bearing Opx basaltic andesite
A14-01	Tatarinov crater rim	early Holocene	pumice	62.43	CaA	MK	Pl>>Ol>~Cpx~>Opx		pumice									Opx-Cpx-Ol andesite
A14-01	Tatarinov crater rim	early Holocene	pumice	62.43	CaA	MK	Pl>>Opx>Mt											Opx-bearing basaltic andesite
A 14-02	Tatarinov crater rim	early Holocene	banded pumice				Pl>>>Opx>Cpx~Mt>Ol	20-25	banded pumice	1	5	3	15				Pl, Ol, Opx	Ol-Cpx-bearing Opx basaltic basaltic andesite
							Pl>Opx>Cpx	15-20			5	3	10					Cpx-bearing Opx andesite
A14-02AR2	Tatarinov crater rim	early Holocene	banded pumice	62.14	CaA	MK												
A14-02B	Tatarinov crater rim	early Holocene		55.28	CaA	MK												
A14-03	Tatarinov crater rim	early Holocene	scoria				Pl>>Ol~Opx>>Mt		scoria									Opx-Ol basaltic andesite
A14-03	Tatarinov crater rim	early Holocene	scoria				Pl>>Ol>~Opx		scoria									Opx-Ol basaltic andesite
A14-04	Tatarinov crater rim	early Holocene	agglutinate	55.12	CaA	MK	Pl>Opx>Cpx		agglutinate									Cpx-bearing Opx basaltic andesite
A14-04	Tatarinov crater rim	early Holocene	agglutinate	55.12	CaA	MK	Pl>>Opx>>Cpx~Ol		agglutinate									Cpx-bearing Opx basaltic andesite
A 14-05	Tatarinov crater rim	early Holocene	pumice ?	56.95	CaA	MK	Pl>>Opx>>Ol>>Hbl		pumice									Ol-Opx bearing basaltic andesite
A14-05	Tatarinov crater rim	early Holocene	pumice ?	56.95	CaA	MK	Pl>>Cpx~Opx>>Ol~Mt		pumice									Ol-bearing-Opx-Cpx andesite
A14-06	Tatarinov crater rim	early Holocene	pumice ?	55.56	CaA	MK	Pl>>Cpx>Opx		pumice									Opx-bearing Cpx basaltic andesite
A14-07	Tatarinov crater rim	early Holocene	pumice ?				Pl>>Opx>>Mt		pumice									Opx basaltic andesite
A14-08	Tatarinov crater rim	early Holocene	pumice ?	62.29	CaA	MK	Pl>>Ol>Opx		pumice									Opx-bearing Ol andesite
A14-08	Tatarinov crater rim	early Holocene	pumice ?	62.29	CaA	MK	Pl>>Cpx>>Opx>Ol~Hbl		pumice									Hbl-Ol-Opx-bearing Cpx andesite
A15	Tatarinov crater rim	early Holocene	essential block	54.60	CaA	MK												
A15A	Tatarinov	early Holocene	essential block	54.60	CaA	MK	Pl>>Opx~>Ol>Mt	30-40	pilotaxitic	3,-5,	3,-5,		25-30					Ol-Opx-bearing basaltic andesite
							Pl>>Opx~>Ol>>Mt		crystals									Ol-Opx basalt?
A15B	Tatarinov	early Holocene	essential block				Pl>>Ol>Mt>Opx	40-50	pilotaxitic	0,5,	3,-5,		30-35					Opx-Ol basaltic andesite
A16	Tatarinov	Plestocene	Lava				Pl>>>Opx>>Cpx~Mt	30-40	intersental?		5-10,	3-5,	25-30					Cpx-bearing Opx basaltic andesite
A17	Tatarinov	Plestocene	lava				Pl>>>Ol>Opx	20-35	intersertal-pilotaxitic	5	3		15-20					Ol-Opx-bearing basaltic andesite
B15-49A	Tatarinov			50.66	Th	MK												
B15-49B	Tatarinov			49.85	Th	MK												
C01-04A	Tatarinov		pfa	53.41	Th	MK												
C01-04B	Tatarinov		pfa	55.42	Th	MK												
C01-05A	Tatarinov		pfa	55.16	Th	MK												
C01-05B	Tatarinov		pfa	55.16	Th	MK												
A 01	Lomonosov	early Holocene	lava	60.17	CaA	MK	Pl>>>Cpx>>Opx>Mt>Ol>Qt	35.00	pilotaxitic	1	2	7	23	trace		trace	PL, Px, Mt, Ol,Qtz, glass	Qt, Ol-bearing Opx-Cpx andesite
							Cpx>Pl>>Opx>Mt>Ol	38-40	intersertal	1	3	18	15				Pl, Px,Ol,Mt, glass	Ol, Opx-bearing Cpx basalt?

Sample No.	Source	Inferred Age	Type	SiO2	Th/CaA	K-type	Formula	Phenocrysts%	Matrix texture	**Ol** (%)	**Opx** (%)	**Cpx** (%)	**Pl** (%)	**Hbl** (%)	**Bt** (%)	**Qtz** (%)	G.m. assemblage	**Rock name**
A03	Lomonosov	early Holocene	lava	60.87	CaA	MK	Pl>>Cpx>>Opx	15-20	pilotaxitic	trace?	3	5	10				Pl,Mt	Opx-bearing Cpx andesite
C02-01Ra2	Lomonosov	Pleistocene	lava, rolling stone	65.27	CaA	MK												
A -08 A							Pl>>Ol>Opx>Cpx											Cpx-bearing Opx-Ol basaltic andesite
A -08 C							Pl>>Ol>>Cpx>~Opx											Opx-Cpx-bearing Ol basaltic andesite
A 02 -13																		
A 08 - 01	Chikurachki		sfa				Pl>>Cpx>Ol		scoria									Ol-Cpx bering basaltic andesite tephra
A 08 - 02			afa				Pl>>Cpx>>Opx		ash									Opx-Cpx bearing basaltic andesite
A 08 - 03			pfa				Pl>Opx>>>Hbl~CPx		ash									Cpx-Hbl - bearing Opx basaltic andesite
A 08 - 03			pfa				Pl>Opx>>>Hbl~>CPx		ash									Cpx-Hbl - bearing Opx basaltic andesite
A 08 - 04			pfa				Pl>Opx>>Hbl>~Ol~>CPx		ash									Ol-Cpx-Hbl -bering Opx basaltic andesite
A 08 - 04			pfa				Pl>Opx>>Hbl>~Ol		ash									Ol-Cpx-Hbl -bering Opx basaltic andesite
A 08 - 05			pfa				Pl>>Opx>>Cpx~Ol											Cpx-Ol-bearing Opx basaltic andesite
A 08 - 05			pfa				Pl~>Opx>>>Hbl		ash									Hbl-bearing Opx basaltic andesite
A 08 - 06			afa				Pl>>Ol~Cpx		ash									Ol-Cpx bering basaltic andesite
A 08 - 07			sfa				Pl>>Op>>Ol		scoria									Ol-bearing Opx basalte
A 08 -08	Chikurachki		sfa				Pl>>Opx>>Cpx~Ol											Ol-Cpx-bearing Opx basaltic andesite
A 08 - 08	Chikurachki		sfa				Pl>>Ol>>Opx											Qtz-Opx-bearing Ol basaltic andesite
A 08 - 09			sfa															
A 08 - 09			sfa				Pl>>>Opx>~Ol		scoria									Ol-Opx-bearing basaltic andesite
A 08 - 10			afa				Pl>>>Ol>Cpx>Opx>Qtz		ash									Qtz-Opx-Cpx bearing Ol basaltic andesite
A 08 - 11			sfa				Pl>>Ol>Opx~Mt>Qtz		scoria									Qtz-Opx-bearing Ol basalte
A 08 -12			afa				Pl>>Mt>>Cpx>>Ol>>Hbl>>Qrz		ash									Qtz-Hbl-Ol-bearing Cpx basaltic andesite
A 08-13			sfa				Pl>>>Opx>>Ol~Mt>>Qtz		scoria									Qtz-Ol-bearing Opx basalte
A 08-14			pfa				Pl>>Cpx>~Opx>Ol		ash									Ol-bearing Opx-Cpx basaltic andesite
A 08 -14			pfa				Pl>>Cpx>~Opx>Ol		ash									Ol-bearing Opx-Cpx basaltic andesite
A 08 - 15 A			re-pfa				Pl>>Opx>Mt		ash									Opx basaltic andesite
A 08 - 15 B			re-pfa				Pl>>Opx~Mt>Cpx>Ol~Hbl		ash									Hbl-Ol-bearing Cpx-Opx basaltic andesite
A 08 -15 C			re-pfa				Pl>Hbl~Opx>>Ol>Cppx		ash									Cpx-Opx-bearing Opx-Hbl-basaltic andesite
A 08 - 16			pfa				Pl>>Opx>>Ol>Cpx>Hbl		ash									Hbl-Cpx-Ol-bearing opx basaltic andesite
A 08 - 16			pfa				Pl>>Opx>>Hbl		ash									Hbl-bearing Opx basaltic andesite
A 08 - 17			afa				Pl>>Opx>Cpx>>Ol~>Qtz		ash									Qtz-Ol-Cpx-bearing Opx basaltic andesite
A 08 -18			pfa				Pl>>Opx>Hbl>Cpx>Qtz~Ol		ash									Ol-Qtz-Cpx bearing Hbl-Opx basaltic andesite
A 08 -18			pfa				Pl>>Opx>>Hbl		ash									Hbl-bearing opx basaltic andesite
A 08 - 19			pfa				Pl>>Hbl>Opx>>Cpx>Qtz		ash									Qtz-Cpx-bearing Opx-Hbl-basaltic andesite
A 08 - 19			pfa				Pl>>Opx>Cpx~Hbl		ash									Hbl-Cpx-bearing Opx basaltic andesite
A 08 - 20			pfa				Pl>>Opx>>Ol>>Qtz		ash									Qtz-Ol-bearing Opx basaltic andesite
A 08 - 20			pfa				Pl>>Opx>>Hbl>~Mt>Cpx		ash									Hbl-bearing Opx basaltic andesite
A 08 - 21			pfa				Pl>>Opx>>Hbl>>Ol~Cpx		ash									Ol-Cpx-Hbl-bering Opx basaltic andesite
A 08 - 21			pfa				Pl>>Opx>>Hbl>~Mt		ash									Hbl-bearing Opx basaltic andesite
A 08 - 22			afa				Pl>>Opx>>Mt~Ol~Cpx		ash									Ol-Cpx-bearing Opx basalte, Basaltic-andesite?
A 08 - 23			sfa				?Qtz>Pl>Ol>Opx		scoria									Opx-bearing Ol-Qtz? basaltic andesite
A 08 - 23			sfa				Pl>Ol>Cpx>~Opx		scoria									Opx-Cpx-bearing Ol basaltic andesite
A 08 - 23			sfa				Pl~?Qtz>Ol>Cpx~Opx		scoria									Opx-Cpx-bearing Ol-Qrt basaltic andesite

Sample No.	Source	Inferred Age	Type	SiO2	Th/CaA	K-type	Formula	Phenocrysts%	Matrix texture	**Ol** (%)	**Opx** (%)	**Cpx** (%)	**Pl** (%)	**Hbl** (%)	**Bt** (%)	**Qtz** (%)	G.m. assemblage	**Rock name**
C 01 - 01			pfa				Pl>>Cpx>Mt>Opx	6.00	scoria		1	1	3				Pl, Cpx	Opx-bearing Cpx andesite
C 01 - 01			pfa				Pl>>Cpx>Mt>Ol											Ol-bearing Cpx basaltic andesite
C 01 - 01 A			pfa				Pl>Opx>Cpx>Mt>Ol	10-15,	pumice	1	2-3,	1-3,	7-9,				Pl	Ol-bearing Cpx-Opx basaltic andesite
C 01 -02 A			lapili				Pl>Opx>>Mt>Cpx	15-20,	scoria		5-8,	1-2,	7-10,				Pl	Cpx-bearing Opx basalte
C 01 - 03			soil				Pl>Cpx~Opx>Mt>Ol	42,278.00	pumice	1	3-4,	3-5,	5-7,					Ol-bearing Opx-Cpx basaltic andesite
C 01 - 04			pfa				Pl>>>Opx~Cpx~Ol	20-25	pumice	1	2	2	15				Pl, Cpx, Opx, Ol	Ol-bearing Opx-Cpx basaltic andesite
C 01 - 04			pfa				Pl>Opx>~Ol>Mt	15-20	pumice	3-5,	5-7,		7-10,				Pl	Ol-Opx basaltic andesite
C 01 - 05			pfa				Pl>>Opx~Cpx	15-18	scoria		3	2	13					Opx-Cpx bearing basaltic andesite
C 02 - 01	Lomonosov	Pleistocene	scoria-pumice (rolling stone)				Pl>Opx>Cpx>Mt>~Ol	20-30	intersertal	1	3-5,	1-3,	15-17,				Pl, Mt	Ol-Cpx bearing Opx basaltic-andesite
C 02 - 02 A	Lomonosov	Pleistocene	scoria-pumice (rolling stone)				Opx>~Pl>>Hbl	15-18	scoria		8		6	2				Hbl-bearing Opx basaltic andesite
C 02 - 02 B	Lomonosov	Pleistocene	scoria-pumice (rolling stone)				Pl~Opx>>>Ol	20-25	scoria	2	7	6	7					Ol-bearing , Opx basaltic andesite
C 02-02 C	Lomonosov	Pleistocene	scoria-pumice (rolling stone)				Pl>>>Ol>~Opx~cpx	13-15	scoria	1	1	1	10					Ol - bearing Cpx, Opx basaltic andesite?
C 02 - 02 C	Lomonosov	Pleistocene	scoria-pumice (rolling stone)				Pl>>Opx>Cpx	10.00	scoria		3	1	6					Cpx-bearing Opx basaltic andesite?
C 02 - 02 D	Lomonosov	Pleistocene	scoria-pumice (rolling stone)				Pl>>Opx>>Ol~Mt	15-17,	scoria	<1	2-3,		8-10,				Pl	Ol-bearing Opx basaltic andesite
C 02 - 02 D2	Lomonosov		scoria-pumice (rolling stone)				Pl>>Opx>Cpx>>Ol	20-25	scoria	1	3	2	15					Ol, Opx, Cpx bearing andesite?
C 03	Lomonosov	Pleistocene	agglutinate	65.87	CaA	MK	Pl>>>Opx>Cpx>Mgt>Ol	25.00	pilotaxitic	1	5	3	17			trace	Pl, Cpx, Opx	Ol-bearing Opx-Cpx andesite
				59.10	CaA	MK	Pl>>>Cpx>Opx>Mgt	40-50	intergranular		5	8	30				Pl, Cpx, Opx	Opx-Cpx andese-basalt?
C 04A-01			scoria				Pl>>Opx>Ol~Mt											Ol-bearing Opx basaltic andesite
C 04A-02			scoria				Pl~Opx>Ol										Pl	Ol-bearing Opx basaltic andesite
C 04A-03			scoria				Pl>Ol>Opx>Cpx>Mt		scoria									Cpx-bearing Opx-Ol basaltic andesite
C 04A-04			scoria				Pl>Ol~Opx>Cpx>Mt		scoria									Cpx-bearing Opx-Ol basaltic andesite
C 04 -01			sfa				Pl>Ol~Opx		scoria									Ol-Opx basalte
C 04 -02			sfa				Pl>>Opx>>Mt		scoria		1-3,		5-7,				Pl, Mt	opx basaltic andesite
C 04 -03			ash				Pl>Opx>Cpx>Ol>Mt		scoria									Ol-bearing Cpx-Opx basaltic andesite
C 04 -04			sfa				Pl>Ol>Opx		scoria									Opx-ol basalte
C 04B-08			ash				Pl~Opx>>Ol~Mt>Qtz											?Qtz-bearing Ol-Opx basaltic andesite ash
C 04B-07			ash				Pl>>Mt>>Opx>Cpx>~Ol											?Ol-cpx-bearing Opx basaltic andesire ash
C 04B-09			ash				Pl>>Mt>Opx											Opx basaltic andesite
C 04B-6			ash				Pl>>Cpx>Opx>~Ol~Mt											Ol-Opx-bearing Cpx basaltic andesite

Sample No.	Source	Inferred Age	Type	SiO2	Th/CaA	K-type	Formula	Phenocrysts%	Matrix texture	**Ol** (%)	**Opx** (%)	**Cpx** (%)	**Pl** (%)	**Hbl** (%)	**Bt** (%)	**Qtz** (%)	G.m. assemblage	**Rock name**
																		ash
C 04 - 08 A			afa				Pl>>Opx>>Cpx>~Ol>>Mt											Ol-Cpx bearing Opx basaltic andesite ash
C 04 - 08 A			afa				Pl>>Cpx~Opx>Mt>Ol											Ol-bearing Opx-Cpx basaltic andesite
A20-01	Old Chikurachki	Pleistocene	lava	54.793	Th	MK	Pl>>Opx>Cpx~-Mt	30-40	intersertal	1-3,	5-7,	3-5,	25				Pl, Cpx, Ol	Ol-Cpx-bearing Opx basaltic-andesite
A20-02	Old Chikurachki	Pleistocene	lava	55.328	Th	MK	Pl>>Cpx>~Opx>Mt	40.00	hyaloophitic		5-7,	10	20-30				Pl, Mt, Qtz	Opx-Cpx basaltic andesite
A20-03	Old Chikurachki	Pleistocene	lava	53.574	Th	MK	Pl>>Cpx>Opx>>Ol>Mt	30.00	pilotaxitic	3	3-5,	5-7,	15			1	Pl, Ol, Cpx	Ol-bearing Opx-Cpx basaltic andesite
A21	Old Chikurachki	Pleistocene	lava	53.574	Th	MK	Pl>>Ol~>Opx>Mgt	25-30	intersertal	5	3		18				Ol, Pl, Mt	Opx-Ol bearing basaltic andesite
A22-01	Old Chikurachki	Pleistocene	lava	54.122	Th	MK	Pl>>Ol>>Mt	30-40	intergranular	15-17			20				Ol, Pl, Mt	Ol basaltic andesite
A22-02	Old Chikurachki	Pleistocene	lava	54.585	Th	MK	Pl>>Opx~>Ol	30-40	intersertal	3-5,	5		28-30				Ol, Pl	Ol-Opx basaltic andesite
A23-01	Old Chikurachki	Pleistocene	lava	54.574	Th	MK	Pl>>Opx>Ol>~Mt	30-40	intersertal	3-5,	5-10,		20-25				Pl	Ol-bearing Opx basaltic andesite
A23-02	Old Chikurachki	Pleistocene	lava	55.822	Th	MK	Pl>>Opx>>Cpx>Mt	40-50	integranular		7-10,	1-3,	30-35				Pl	Cpx-bearing Opx basaltic andesite
A24	Old Chikurachki	Pleistocene	lava	54.481	Th	MK	Pl>>Ol~Cpx>Opx	30-35	integranular	5-7,	5	5-7	20				Pl	Cpx-Ol-Opx basaltic andesite
A25-01	Old Chikurachki	Pleistocene	lava	54.809	Th	MK	Pl>>Opx>>Ol>>Mt	30-35	intersertal	3-5,	7-10,		20				Pl, Ol	Ol-bearing Opx basaltic andesite
A25-02	Old Chikurachki	Pleistocene	lava	55.918	Th	MK	Pl>>Opx>>Ol>Cpx>Mt	30-40	pilotaxitic	3-5,	8-10,	1-3,	25-30				Pl, Mt	Cpx-Ol bearing Opx basaltic andesite
A26	Old Chikurachki	Pleistocene	lava	55.999	Th	MK	Pl>>Opx>Cpx>~Ol>Mt	40-50	intergranular, pilotaxitix	3-5,	7-10,	5-7,	30-35				Ol, Opx, Pl	Ol-bearing Cpx-Opx basaltic andesite
B 02 - 01	Fuss ?		depris avalanche				Pl>Opx>Cpx>Ol>Mt	30-40	pilotaxitic, intrusive	1-3,	8-10,	3-5,	17-20,					Cpx-Ol-bearing basaltic andesite
B 02 - 02	Fuss ?		depris avalanche				Pl>Opx>Cpx>Ol>Mt	30-40	porphyritic, intrusive	3-5,	5-8,	1	15-20					Ol-Cpx bearing Opx basaltic andesite
B12	Fuss		lava	55.082	CaA	HK	Pl>>Opx>>Ol>Cpx>Mt	40-50	intersertal	5-8,	10-15,	3-5,	20-25,				Pl, Opx	Cpx-Ol- bearing opx basaltic andesite
B 13-01	Fuss		lava	55.947	CaA	HK	Pl>>Cpx>~Opx>~Ol>Mt	50-60	pilotaxitic	1-3,	5-8,	5-10,	35-40,				Pl	Ol-bearing Opx-Cpx basaltic andesite
B 13 - 02	Fuss		lava				Pl>>Opx>Ol>Cpx~Mt	25-35	intergranular	3-5,	5-8,	1	10-15,				Pl, Opx	Cpx-Ol-bearing Opx basaltic andesite
			lava				Pl>>Cpx>Mt	50-60	devitrify			5-10,	50-55,					Cpx andesite
B13-02host	Fuss		lava	56.464	CaA	HK	Pl>>>Opx>Ol>Cpx	50-60	devitrify	1-3,	8-10,	5-8,	40-35					Ol-bearing Cpx-Opx andesite
B13-02enclave	Fuss		lava	52.289	CaA	HK	Pl>>Opx>>Ol>Cpx>Mt	40-50	intersertal	5-8,	15-17,	3-5,	20-25,				Pl, Mt	Cpx-bearing Ol-Opx basaltic andesite
B14-01A	Fuss		pfa	61.023	CaA	HK	Pl>>Opx>Cpx>~Mt	12-17,	pumice		3-5,	1-2,	7-9,					Cpx-bearing Opx andesite
B14-01B	Fuss		pfa	59.954	CaA	HK	Pl>>Opx>Mt		pumice									Opx andesite
B14-01C	Fuss		pfa	59.968	CaA	HK	Pl>Opx>Hbl>Mt>~Cpx	7-13,	ash		1-3,	1	3-5,					Cpx-bearing Hbl-Opx andesite
B14-02			afa				Pl>>Cpx>Mt		ash									Cpx basaltic andesite
B14-03							Pl>>Ol>Opx		small pieces of scoria									Opx-bearing Ol basalte
B14-04	Fuss		pfa	57.273	CaA	HK	Pl>>Opx>Mt		small pieces of pumice									Opx andesite
B 14-06			sfa				Pl>Ol>Cpx		scoria									Cpx-bearing Ol basaltic andesite
B 14-06			sfa				Pl>~Ol>Opx>Mt		scoria									Opx-bearing Ol basaltic andesite
B 14-06			sfa				Pl>Cpx>Opx>Ol>Mt		scoria									Ol-bearing Opx-Cpx basaltic andesite
B 14-07			afa				Pl>>Cpx>Ol		ash									Ol-bearing Cpx basaltic andesite
B 14-08			afa				Pl>>Opx>Mt		ash									Opx basaltic andesite

Sample No.	Source	Inferred Age	Type	SiO2	Th/CaA	K-type	Formula	Phenocrysts%	Matrix texture	**Ol** (%)	**Opx** (%)	**Cpx** (%)	**Pl** (%)	**Hbl** (%)	**Bt** (%)	**Qtz** (%)	G.m. assemblage	**Rock name**
B 14-08			ash				Pl>>Cpx>Opx>Mt>Ol											Ol-bearing Opx-Cpx basaltic andesite
B 14-09			ash				Pl>>Cpx>Ol>Opx>>Mt		ash									Opx-bearing Ol-Cpx basaltic andesite
B14-10A	Fuss		pdc	61.463	CaA	HK	Pl>Hbl>~Opx>>Ol>Mt	10-20,	pumice	1-2,	3-4,		5-8,	3-5,				Ol-bearing Opx-Hbl dacitic andesite
B14-10B	Fuss		pdc	61.471	CaA	HK	Pl>>Opx>>Mt>Ol~> Hbl		???									Hbl-Ol bearing Opx andesite
B14-11			small pieces of scoria				Pl>>Opx>Mt		pumice									Opx basaltic andesite
B14-13			pumice				Pl>Opx>~Hbl>~Ol>Mt	10-20,	pumice	1-3,	3-5,		5-8,	3-4,				Ol-bearing Opx-Hbl andesite
B14-13A			pumice				Pl>Opx>Mt>Ol~Hbl		pumice									Ol-Hbl-bearing Opx basaltic andesite
B14-13B	Fuss		pfa	59.716	CaA	HK	Pl>Opx>>Cpx>~Ol~Mt		pumice									?Hbl-Cpx-Ol bearing Opx andesite
B14-13C	Fuss		pfa				Pl-Cpx bearing Opx basaltic andesite		pumice									Ol-Cpx bearing Opx basaltic andesite
B14-14			pfa				Pl>Cpx>Mt>Ol		ash									Ol-bearing Cpx basaltic andesite
B14-14			pfa				Pl>Opx>>Mt>Cpx>~Hbl		pumice									Hbl-Cpx-bearing Opx basaltic andesite
B14-15			pfa				Pl>>Opx>~ Hbl>Mt		pumice									Hbl-bearing Opx basaltic andesite
B14-15			pfa				Pl>Mt>Opx>Cpx		ash									Cpx-bearing Opx basaltic andesite
B14-16			ash				Pl>>Opx>Mt		ash									Opx basaltic andesite
B14-16			ash				Pl>>Cpx>Opx>Ol~Mt		ash									Ol-bearing Cpx-Opx basaltic andesite
B14-17			ash				Pl>>Mt>Ol		ash									Ol-bearing basaltic andesite
B14-19			ash				Pl>>Mt		ash									Pl basaltic andesite
B15-03A	Fuss		pfa	60.111	CaA	HK	Pl>>Opx>>Hbl>Mt~Cpx	25-30	pumice		5-7,	1	15-18	3-5,				Cpx-Hbl-bearing andesite
B15-03B	Fuss		pfa	59.716	CaA	HK	Pl>Opx>Hbl>Ol>Cpx	10-20,	pumice	1	3-5,	1	5-8,	3-4,				Cpx-Ol-bearing Hbl-Opx andesite
B15-03C	Fuss		pumice	59.711	CaA	HK	Pl>Opx>~Hbl>Cpx>~Ol>Mt	10-20,	pumice	1	3-5,	1	5-8,	3-2,				Cpx-Ol-bearing Opx-Hbl andesite
B15-03D	Fuss		pumice	59.444	CaA	HK	Pl>Opx>~Hbl>Cpx>Ol~Mt	44,105.00	pumice	1	3-5,	1-2,	5-8,	3-4,				Ol-Cpx bearing Opx-Hbl andesite
B15-10			pumice ash				Pl>Cpx>Mt>Ol-Opx		ash									Ol-Opx-bearing Cpx basaltic andesite
B15-10			scoria				Pl>Ol		scoria	3-5,			8-10,					Ol-basaltic andesite
B15-10B			scoria				Pl>Ol		scoria	3-5,			7-10,					Ol-basaltic andesite
B15-15-1			pumice				Pl>>Opx>~Hbl>>Mt>Cpx~Ol	15-25	pumice	1	3-5,	1-2,	5-8,	3-4,				Ol-Cpx-bearing Hbl-Opx basaltic andesite
B15-15-2			pumice				Pl>Opx>>Mt>Ol>~Hbl	20-30	pumice	1-3,	8-10,		13-15,	1-2,				Ol-Hbl-bearing Opx basaltic andesite
B15-15-3			pumice				Pl>Opx>>Ol>>Cpx>~Hbl		pumice									Hbl-Cpx-Ol-bearing Opx basaltic andesite
B15A-20			pumice				Cpx-basaltic andesite		pumice									Cpx-basaltic andesite
B15A-33			pumice				Pl>Opx>Hbl>~Cpx-Ol		pumice									Ol-Cpx-Hbl-bearing Opx basaltic andesite
B15A-35			pumice				Pl>Opx>Mt>Ol		pumice									Ol-bearing Opx basaltic andesite
B15A-40			pumice				Pl>Opx>>Cpx>Ol		pumice									Ol-Cpx-bearing Opx basaltic andesite
B15A-43			pumice				Pl>Opx>Ol~Cpx		pumice									Ol-Cpx? - bearing Opx basaltic andesite
B15A-48			small pieces of pumice				Pl>Opx>Mt		ash									Opx-basaltic andesite
B15C-16			ash				PL>>Mt>~Opx		ash									Opx-bearing andesite
B15C-19			ash				Pl>>Opx>Mt		ash									Opx basaltic andesite
B15C-21			ash				Pl>Cpx>~Opx>Mt		ash									Cpx-Opx basaltic andesite
B15C-26			ash				Pl>Opx~Ol>>Cpx>Mt		ash									Cpx-bearing Ol-opx basaltic andesite
B15C-37			ash				Pl>Opx>Ol		ash									Cpx-Opx basaltic andesite
B15-40 white pumice			pfa				Pl>Opx>~Hbl>>Mt>~Ol~Cpx	10-20,	pumice	1	3-4,	1	5-8,	2-3,				Ol-Cpx-bearing Hbl-Opx basaltic andesite
B15-40			pfa				Pl>Opx~Hbl>Ol>~Cpx>Mt	15-25	pumice	1-2,	3-5,	1-2,	5-8,	3-5,				Ol-Cpx-bearing Hbl-Opx basaltic andesite
B15-43			re-pfa				Pl>Opx>~Hbl>Mt>Cpx	10-15,	pumice		3-5,	1	5-8,	2-4,				Cpx-bearing Hbl-Opx basaltic andesite

Sample No.	Source	Inferred Age	Type	SiO2	Th/CaA	K-type	Formula	Phenocrysts%	Matrix texture	**Ol** (%)	**Opx** (%)	**Cpx** (%)	**Pl** (%)	**Hbl** (%)	**Bt** (%)	**Qtz** (%)	G.m. assemblage	**Rock name**
B15-43-1	Fuss		re-pfa				Pl>Opx>Hbl>Mt	10-15,	pumice		3-5,		5-8,	1-3,				Hbl-Opx basaltic andesite
B15-43-2			re-pfa				Pl>>Opx~Hbl>Mt~Cpx	15-20	pumice		3-5,	<1	8-10,	3-5,				Cpx-bearing Opx-Hbl basaltic andesite
B15-47			pumice				Pl>Ol>Mt		pumice									Ol basaltic andesite
B15-48			small pieces of pumice				Pl>>Opx>Hbl>Mt>Cpx>Ol											Ol-Cpx-bearing Hbl-Opx basaltic andesite
B15-48			small pieces of pumice				Pl>Opx>~Hbl		pumice									Ol-Hbl-basaltic andesite
B15-15			pumice				Pl>>Opx>Mt>Ol~Cpx	10-20,	pumice	1-2,	3-6,	1-2,	5-8,					Ol-Cpx-bearing Opx andesite
B15-20			pumice				Pl>Opx>~Hbl>Mt>Ol>~Cpx	15-25,	pumice	1	3-5,		8-10,	2-4,				Ol-Cpx bearing Hbl-Opx basaltic andesite
B15-20-1			pumice				Pl>>Cpx>~Opx>~Ol>Mt	15-20	pumice	1-2,	1-3,	3-5,	8-10,					Ol-bearing Opx-Cpx basaltic andesite
B15-29A			lava				Pl>Opx>~Hbl>~Cpx>Mt>~Ol		pilotaxitic									Ol-bearing Cpx-Hbl-Opx basaltic andesite
B15-33A			pumice				Pl>Hbl>~Opx>Mt>Ol>~Cpx	10-20,	pumice	<1	1-2,	<1	3-6,	1-3,				Cpx-Ol-bearing Opx-Hbl basaltic andesite
B15-35			pumice				Pl>Hbl>~Opx>~Cpx>Mt>Ol	20-25,	pumice	1	3-5,	2-4,	5-8,	3-5,				Ol-bearing Cpx-Opx-Hbl basaltic andesite
B15-49																		Ol basaltic andesite
B15-51			ash				Pl>>Opx>~Ol>~Cpx>Mt		ash									Cpx-Ol-Opx-bearing basaltic andesite
B15-52			ash				Pl>>Cpx>~Opx>~Ol>Mt		ash									Ol-bearing Opx-Cpx basaltic andesite
B15-61			ash				Pl>>Mt>Ol>Cpx>Opx		ash									Opx-Cpx-Ol-bearing basaltic andesite
B15-64			ash				Pl>>Opx>Mt>Ol		ash									Ol-bearing Opx basaltic andesite
B15-65			pumice				Pl>>Mt>Opx>~Cpx		pumice									Opx-Cpx-bearing basaltic andesite
A 30 - 01			lava?				Pl>Opx>Cpx>>Ol~Mt	30-40	intergranular crystal	3	8-10,	5-8,	15-20					Ol-bearing Cpx-Opx basaltic andesite
A 30 - 02			lava?				Pl>>Opx>>Cpx>Ol>Mt	30-40	intergranular crystal	3-5,	10-13,	5-8,	15-20					Ol-bearing Cpx-Opx basaltic andesite
A 32 - 01			lava?				Pl>>Opx>~Cpx>~Ol>Mt	20-30	intersertal	1-3,	8-10,	3-5,	15-18					Ol-bearing Cpx-Opx basaltic andesite
B16-01			lava?				Pl>Hbl>Opx>~Ol>~Cpx>Mt	20-30,	intergranular	1-3,	1-3,	1-3,	10-15,	3-5,			Pl	Ol-Cpx-Opx-bearing Hbl basaltic andesite
B16-02			lava?				Pl>>Opx>>Mt>Ol>~Cpx	20-30	pilotaxitic	1	3-5,	1	10-15,				Pl	Cpx-Ol-bearing Opx basaltic andesite
08 PR 1-1	Ebeko		Dome or intrusive	57.908	Tn	Hk	Pl>>Opx>~Cpx>Mt>Qtz?	50-60	crystallic		5-8,	5-7,	30-35,			2-4,		?Qtz-bearing Cpx-Opx basaltic andesite
08 PR 1-2	Ebeko		1 を貫く Dyke	63.874	CaA	Hk	Pl>>Opx>Mt>Cpx~Ol	50-60,	crystallic intrusive	1	10-15,	1-3,	30-35,					?Ol-Cpx bearing Opx dacitic andesite
8 PR 2	Ebeko		lava flow (upper)				Pl>Opx>Mt>Ol>~Cpx	20-30,	pilotaxitic	1-3,	5-8,	1-2,	10-13,					Cpx-Ol bearing Opx basaltic andesite
8 PR 3	Ebeko		Hyaroclastite				Pl>Opx>>Cpx>Ol	10-20,	hyloophitic	1	3-5,	1	8-10,					?Ol-Cpx bearing opx basaltic andesite
8 PR 6	Ebeko		lava				Pl>Opx>~Mt>Cpx>~Hbl	20-30,	undergranular		3-5,	1-2,	10-12,	1				?Hbl-Cpx bearing Opx basaltic andesite
8 PR 7	Ebeko		lava flow				Pl>Opx>Mt>~Cpx>~Ol	20-30	pilotaxitic	1	3-5,	1-3,	10-13,					Ol-Cpx bearing Opx basaltic andesite
8 PR 8	Ebeko		Pyroclastic bomb				Pl>Opx>Mt>~Hbl>~Ol~Cpx	20-30	pilotaxitic	1	3-5,	1-3,	8-10,	1-3,				Ol-Cpx-Hbl bearing Opx basaltic andesite
8 PR 9	Ebeko						Pl>Opx>Mt>~Hbl>~Cpx>Ol	20-30	pilotaxitic	1	3-5,	1-2,	10-15,	1-2,				Ol-Cpx-Hbl bearing Opx basaltic andesite
8 PR 10	Ebeko						Pl>Opx>Mt>~Ol>~Cpx	20-30,	pilotaxitic	1-3,	5-8,	1-2,	10-13,					Cpx-Ol bearing Opx basaltic andesite
8 PR 11	Ebeko		lava flow (upper)				Pl>Cpx>~Ol>Opx>~Mt	20-30,	intergranular	3-5,	1-3,	4-5,	10-15,				Pl	Opx-bearing Ol-Cpx basaltic andesite
8 PR 12	Ebeko		lava flow (lower)				Pl>Opx>Cpx>Mt	30-40	pilotaxitic	1-3,	5-8,	3-5,	18-20					Cpx-Ol bearing Opx basaltic andesite
8 PR 13	Ebeko			57.8	CaA	HK	Pl>Opx>~Cpx~Ol	30-40	pilotaxitic	<1	5-8,	1	20-				Pl	Ol-Cpx bearing Opx andesite

Sample No.	Source	Inferred Age	Type	SiO2	Th/CaA	K-type	Formula	Phenocrysts%	Matrix texture	**Ol** (%)	**Opx** (%)	**Cpx** (%)	**Pl** (%)	**Hbl** (%)	**Bt** (%)	**Qtz** (%)	G.m. assemblage	**Rock name**
													25					
8 PR 13-2	Ebeko			59.471	CaA	HK	Pl>Opx>Cpx>Ol>Ol	20-30,	intersertal	1-2,	5-7,	3-5,	10-13,				Pl, Opx	Ol-Cpx bearing Opx andesite
8 PR 14	Ebeko			59.42	CaA	HK	Pl>Cpx>~Ol>Mt>Opx	20-30,	intergranular-pilotaxitic	3-4,	1-3,	3-5,	10-15,				Pl	Opx-bearing Ol-Cpx andesite
8 PR 14-2	Ebeko						Pl>Cpx>~Ol>~Opx>Mt	30-40,	intergranular-pilotaxitic	3-4,	2-3,	3-5,	15-25,				Pl	Opx-Ol-Cpx andesite
8 PR 15	Ebeko			59.234	CaA	MK-Th	Pl>Cpx>~Opx>Mt>Ol	20-30,	pilotaxitic	1	1-3,	2-3,	10-15,				Pl	Ol-bearing Opx-Cpx andesite
8 PR 16	Ebeko			58.907	CaA	Th	Pl>Opx>Ol>~Cpx>Mt>	12-15,	pilotaxitic	2-5,	3-5,	1-2,	12-15,				Pl	Cpx-Ol-Opx andesite
8 PR 18	Ebeko			46.89	MK	Th	Pl>Cpx>~Ol>Mt>~Opx	20-30,	intersertal	3-4,	2-3,	3-5,	10-13,				Pl, Opx	Opx-bearing Ol-Cpx basalte
8 PR 19-1	Ebeko			45.66	MK	Th	Pl>Cpx>Opx>Ol>Mt	20-30,	porphyritic	1-3,	4-6,	5-8,	13-15,				Pl, Opx	Ol-bearing Opx-Cpx basalte
8 PR 19-2	Ebeko			45.845	MK	Th	Pl>Cpx>Opx>Ol~Mt	40-50,	intergranular-crystal	3-5,	5-8,	10-15,	20-25,				Opx, Pl, Ol	Ol-bearing Opx-Cpx basalte
8 PR 19-3	Ebeko			48.903	MK	Th	Pl>Cpx>Opx>Ol>~Mt	20-3,	intersertal	2-3,	3-4,	3-5,	10-15,				Pl, Opx	Ol-bearing Opx-Cpx basalte
8 PR 19-4	Ebeko			55.876	MK-HK	Th-CaA	Pl>Cpx>Opx>Mt	20-30,	intergranular	1	3-5,	5-8,	10-13,				Pl	Ol-bearing Opx-Cpx basaltic andesite
8 PR 20	Ebeko			47.133	MK	Th	Pl>Ol>~Cpx>~Opx~Mt	20-30,	intergranular	4-6,	3-5,	3-5,	10-12,				Opx, Pl	Opx-Cpx-Ol basaltic andesite
8 PR 21	Ebeko			52.824	HK	CaA	Pl>Cpx>Opx>Ol>Mt	20-30,	intersertal	1-3,	2-4,	3-5,	10-13,				Pl	Ol-bearing Opx-Cpx basaltic andesite
8 PR 22	Ebeko			56.621	HK	CaA	Pl>Cpx>Opx>Mt>Ol	20-30	intergranular	1	1-3,	3-5,	10-13,				Pl	Ol-bearing Opx-Cpx basaltic andesite
8 PR 23	Ebeko			47.231	MK	Th	Pl>Opx>Cpx>Mt>Ol	20-30,	intergranular-crystal	1	5-8,	3-5,	10-15,				Pl	Ol-bearinf Cpx-Opx basaltic andesite
8 PR 24	Ebeko			47.214	MK	Th	Pl>Cpx>~Opx>~Ol>~Mt	40-50,	intergranular-crystal	3-5,	4-7,	5-8,	20-25,				Opx, Pl	Ol-Opx-Cpx basalte
8 PR 26-1	Ebeko		Bomb Scoria	54.822	Hk	CaA	Pl>Opx>Cpx>Ol>Mt	10-20,	scoria	1	1-3,	1-2,	5-8,				Pl	Ol-Cpx-bearing Opx basaltic andesite
8 PR 26-2	Ebeko		Bomb Scoria banded	54.8	Hk	CaA	Pl>Cpx>Opx>Ol>Mt	10-20,	scoria	1-2,	1-3,	2-5,	5-8,					Ol-bearing Opx-Cpx basaltic andesite
8 PR 27	Ebeko			58.496	Hk	CaA	Pl>Opx>~Cpx>Ol>Mt	25-35,	intersertal	1-3,	3-5,	2-4,	15-17,				Pl	Ol-bearing Cpx-Opx andesite
8 PR 30-1	Ebeko			55.732	MK-HK	CaA	Pl>Cpx>Opx>Mt>Ol	20-30,	intersertal	1	3-5,	5-8,	10-13,				Pl	Ol-bearing Opx-Cpx andesite
8 PR 30-2	Ebeko			56.28	Mk-Hk	CaA	Pl>Cpx>Opx>Mt>Ol	20-30,	interseral	1	3-5,	5-8,	10-13,				Pl	Ol-bearing Opx-Cpx andesite
8 PR 31	Ebeko			53.704	Mk-Hk	CaA	Pl>Cpx>>Opx>~Mt>~Ol	30-40,	intersertal-intergranular	1-2,	3-5,	8-10,	15-18,				Pl	Ol-bearing Opx-Cpx basaltic andesite
8 PR 32	Ebeko			58.875	Hk	CaA	Pl>Cpx>Opx>Mt>Ol	20-30,	pilotaxitic	1	3-5,	5-8,	10-13,				Pl	Ol-bearing Opx-Cpx andesite
08 PR 33	Ebeko			58.292	HK	CaA	Pl>Cpx>Opx>Mt>Ol	20-30	intergranular	1	3-5,	5-8,	10-13,				Pl	Ol-bearing Opx-Cpx andesite
08 PR 34	Ebeko			58.781	Hk	CaA	Pl>Opx>Cpx>Mt>Hbl?	10-15,	pumice		1-3,	1-2,	5-8,	<1?			Pl	?Hbl-bearing Cpx-Ol-Opx andesite
8 PR 35	Ebeko			54.786	Hk	CaA	Pl>Ol>~Cpx>Mt>Ol	20-30,	intersertal	1	3-5,	3-5,	10-13,				Pl	Ol-bearing Cpx-Opx basaltic andesite
8 PR 36	Ebeko			58.958	Hk	CaA	Pl>Cpx>~Opx>Mt>Ol	30-40	pilotaxitic-indergranular	1	4-7,	5-8,	18-20,				Pl	Ol-bearing Cpx-Opx andesite
8 PR 37-1	Ebeko			61.107	Hk	CaA	Pl>Opx>~Cpx>Mt>Ol	20-30,	intersertal	1	3-5,	2-4,	10-12,				Pl	Ol-bearing Cpx-Opx dacitic andesite
8 PR 37-2	Ebeko			59.863	Hk	CaA	Pl>Cpx>~Opx>Mt>Ol	20-30,	indergranular, crystal	1	2-4,	3-5,	10-12,					Ol-bearing Opx-Cpx andesite

Table. 3. Major element compositions.

Volcano	Sample name	SiO_2	TiO_2	Al_2O_3	FeO*	MnO	MgO	CaO	Na_2O	K_2O	P_2O_5	Sum
Chikurachiki	07PAR-A27-02	53.48	0.77	19.08	9.36	0.21	4.28	9.10	2.91	0.58	0.22	100.00
Chikurachiki	07PAR-A27-01	54.39	0.74	18.87	8.99	0.22	4.00	8.87	3.01	0.64	0.25	100.00
Chikurachiki	A05	57.50	0.72	17.67	7.73	0.19	3.63	7.88	3.20	1.29	0.18	100.00
Chikurachiki	A07	56.14	0.74	17.98	7.47	0.17	3.93	8.77	3.06	1.52	0.22	100.00
Chikurachiki	A11	62.33	0.75	17.36	5.72	0.18	1.98	5.52	4.44	1.40	0.33	100.00
Chikurachiki	A17	52.92	0.75	21.42	7.45	0.16	3.13	10.17	3.03	0.77	0.20	100.00
Chikurachiki	A20-01	54.79	0.75	20.56	7.29	0.17	2.97	9.00	3.17	1.05	0.24	100.00
Chikurachiki	A20-02	55.33	0.74	18.94	8.34	0.21	3.81	8.67	3.05	0.70	0.21	100.00
Chikurachiki	A20-03	55.28	0.73	19.06	8.23	0.20	3.81	8.79	3.01	0.67	0.21	100.00
Chikurachiki	A21	53.57	0.80	21.55	7.43	0.17	2.71	9.48	3.28	0.77	0.23	100.00
Chikurachiki	A22-01	54.12	0.80	20.27	7.82	0.22	2.56	9.69	3.41	0.86	0.25	100.00
Chikurachiki	A22-02	54.58	0.81	19.23	8.31	0.20	3.50	8.77	3.31	1.01	0.28	100.00
Chikurachiki	A22-03	54.09	0.79	19.26	8.58	0.19	4.22	9.20	2.86	0.62	0.18	100.00
Chikurachiki	A22-03R2	53.97	0.79	19.28	8.64	0.19	4.23	9.23	2.86	0.62	0.18	100.00
Chikurachiki	A23-01	54.57	0.77	19.07	8.54	0.20	4.13	8.96	2.94	0.62	0.19	100.00
Chikurachiki	A23-02	55.82	0.68	18.95	8.16	0.21	3.49	8.44	3.23	0.72	0.30	100.00
Chikurachiki	A24	54.48	0.75	19.30	8.56	0.21	3.93	9.00	2.94	0.63	0.20	100.00
Chikurachiki	A25-01	54.81	0.70	19.19	8.61	0.21	3.84	8.65	3.06	0.67	0.26	100.00
Chikurachiki	A25-02	55.92	0.68	18.79	8.18	0.22	3.54	8.41	3.22	0.73	0.29	100.00
Chikurachiki	A26	56.00	0.77	19.22	7.64	0.20	3.13	8.50	3.41	0.86	0.28	100.00
Chikurachki	tephra 1	51.19	0.81	21.42	8.84	0.17	3.70	10.85	2.24	0.61	0.16	100.00
Chikurachki	tephra 2	52.17	0.77	21.63	8.04	0.17	3.18	10.85	2.37	0.66	0.16	100.00
Chikurachki	1853	54.99	0.81	19.81	7.95	0.19	2.83	9.47	2.84	0.90	0.21	100.00
Chikurachki	1986	53.27	0.83	19.81	8.73	0.19	3.35	10.31	2.60	0.70	0.19	100.00
Chikurachki?	A19-11A	51.82	0.87	20.91	8.84	0.20	3.76	10.22	2.72	0.49	0.17	100.00
Chikurachki?	A19-11B	51.81	0.87	20.61	8.92	0.20	3.88	10.30	2.74	0.49	0.17	100.00

Volcano	Sample name	SiO_2	TiO_2	Al_2O_3	FeO*	MnO	MgO	CaO	Na_2O	K_2O	P_2O_5	Sum
Chikurachki?	A19-11C	51.79	0.90	20.50	9.17	0.21	3.96	10.06	2.75	0.49	0.18	100.00
Chikurachki?	B15-10A	52.38	0.74	21.37	7.79	0.17	3.64	10.30	2.73	0.72	0.17	100.00
Chikurachki?	B15-10Br	52.36	0.75	21.36	7.80	0.16	3.59	10.33	2.74	0.74	0.17	100.00
Chikurachki?	B15-10CR2	52.07	0.75	21.84	7.68	0.16	3.46	10.43	2.72	0.71	0.17	100.00
Chikurachki?	A08-01A	51.99	0.81	20.92	8.73	0.17	4.17	9.71	2.60	0.73	0.18	100.00
Chikurachki?	A08-08A	51.01	0.91	20.01	9.87	0.21	4.60	10.08	2.68	0.47	0.17	100.00
Chikurachiki	B25-868S	57.56	0.69	19.69	6.80	0.19	2.33	7.85	3.66	0.94	0.30	100.00
Chikurachiki	B25-867	52.12	0.84	19.84	9.07	0.19	4.49	10.08	2.70	0.52	0.14	100.00
Chikurachiki	B25-866	52.01	0.84	19.91	9.14	0.19	4.52	10.08	2.64	0.53	0.14	100.00
Chikurachiki	B25-865	58.11	0.65	19.06	6.92	0.21	2.41	7.86	3.72	0.77	0.29	100.00
Chikurachiki	B25-864S	55.33	0.96	18.97	8.39	0.21	3.05	7.84	3.96	0.99	0.28	100.00
Chikurachiki	B25-863	52.25	0.71	21.97	7.42	0.15	2.94	10.74	2.87	0.76	0.17	100.00
Chikurachiki	B25-862	52.29	0.71	21.84	7.39	0.15	3.00	10.77	2.91	0.76	0.17	100.00
Ebeko	08PR-37-2	59.86	0.61	17.05	6.76	0.18	2.96	6.84	3.28	2.27	0.20	100.00
Ebeko	08PR-37-1	61.11	0.61	17.23	5.84	0.17	2.77	6.51	3.22	2.33	0.20	100.00
Ebeko	08PR-36	58.96	0.64	16.92	7.14	0.18	3.10	7.18	3.42	2.28	0.18	100.00
Ebeko	08PR-35	54.79	0.70	17.81	8.54	0.20	4.29	8.86	2.92	1.68	0.21	100.00
Ebeko	08PR-34	58.78	0.65	17.31	7.18	0.17	3.21	7.26	3.16	2.10	0.19	100.00
Ebeko	08PR-33	58.29	0.66	17.43	7.34	0.17	3.30	7.43	3.12	2.06	0.19	100.00
Ebeko	08PR-32	58.88	0.64	17.10	7.16	0.18	3.14	7.18	3.31	2.23	0.19	100.00
Ebeko	08PR-31	53.70	0.85	18.16	8.69	0.20	4.33	9.21	3.03	1.62	0.22	100.00
Ebeko	08PR-30-2	56.28	0.69	17.65	8.05	0.18	3.88	8.45	2.87	1.77	0.19	100.00
Ebeko	08PR-30-1	55.73	0.73	17.83	8.25	0.18	3.89	8.54	2.97	1.69	0.19	100.00
Ebeko	08PR-27	58.50	0.64	17.75	7.19	0.20	3.01	6.97	3.49	1.99	0.25	100.00
Ebeko	08PR-26-2	54.80	0.67	16.75	8.15	0.19	6.21	8.52	2.82	1.70	0.20	100.00
Ebeko	08PR-26-1	54.82	0.68	17.28	8.30	0.19	5.93	8.07	2.81	1.72	0.21	100.00
Ebeko	08PR-24	47.21	0.87	19.40	10.48	0.20	5.91	12.43	2.18	1.05	0.27	100.00

Volcano	Sample name	SiO_2	TiO_2	Al_2O_3	FeO*	MnO	MgO	CaO	Na_2O	K_2O	P_2O_5	Sum
Ebeko	08PR-23	47.34	0.86	19.70	10.39	0.21	5.68	12.33	2.22	1.00	0.28	100.00
Ebeko	08PR-22	56.62	0.65	17.91	7.27	0.17	3.69	8.19	3.16	2.19	0.17	100.00
Ebeko	08PR-21	52.82	0.76	19.16	8.70	0.22	4.10	9.75	3.05	1.13	0.31	100.00
Ebeko	08PR-20	47.13	0.86	18.92	10.71	0.21	6.07	12.46	2.36	0.96	0.32	100.00
Ebeko	08PR-19-3	48.90	0.81	19.66	9.64	0.20	5.43	11.29	2.60	1.11	0.36	100.00
Ebeko	08PR-19-2	45.85	0.90	17.96	11.80	0.21	7.07	13.37	1.86	0.76	0.22	100.00
Ebeko	08PR-19-1	45.66	0.87	18.48	11.76	0.20	6.89	13.36	1.91	0.68	0.20	100.00
Ebeko	08PR-18	46.89	0.85	20.01	10.85	0.20	5.62	12.35	2.19	0.82	0.24	100.00
Ebeko	08PR-16	58.91	0.61	17.12	7.15	0.18	3.06	7.17	3.34	2.26	0.20	100.00
Ebeko	08PR-15	59.23	0.58	17.34	6.89	0.18	3.03	7.11	3.26	2.17	0.20	100.00
Ebeko	08PR-14-3	59.80	0.57	17.64	6.63	0.17	3.04	6.69	3.24	2.04	0.19	100.00
Ebeko	08PR-14	59.42	0.59	17.37	6.99	0.17	3.09	6.90	3.17	2.09	0.20	100.00
Ebeko	08PR-13-2	59.47	0.59	17.35	6.94	0.17	3.07	6.91	3.19	2.10	0.20	100.00
Ebeko	08PR-13	57.80	0.67	17.44	7.21	0.17	3.61	7.66	3.24	2.01	0.21	100.00
Ebeko	08PR-12	63.84	0.54	16.11	5.54	0.16	2.40	5.05	3.61	2.71	0.05	100.00
Ebeko	08PR-11	57.91	0.62	17.72	7.44	0.17	3.38	7.49	3.12	1.96	0.18	100.00
Ebeko	08PR-10	55.69	0.72	17.44	8.07	0.18	4.45	8.75	2.81	1.70	0.19	100.00
Ebeko	08PR-9	59.86	0.57	16.74	6.35	0.16	4.06	6.74	3.13	2.23	0.16	100.00
Ebeko	08PR-8	57.71	0.63	17.62	7.51	0.18	3.44	7.60	3.14	1.99	0.18	100.00
Ebeko	08PR-7	59.18	0.62	16.61	6.64	0.17	2.86	6.89	3.84	2.97	0.22	100.00
Ebeko	08PR-6	60.42	0.63	16.91	6.60	0.16	2.92	6.12	3.45	2.58	0.20	100.00
Ebeko	08PR-3	50.21	0.94	18.50	10.24	0.21	5.04	10.57	2.85	1.17	0.26	100.00
Lomanosov	C03host	62.04	0.60	16.58	5.95	0.15	2.82	6.59	3.32	1.79	0.15	100.00
Lomanosov	C03enclave	54.08	0.74	17.75	8.66	0.19	5.01	9.77	2.64	1.03	0.14	100.00
Lomanosov	C02-01Ra2	61.25	0.64	16.56	6.29	0.16	2.86	6.91	3.34	1.83	0.16	100.00
Lomanosov	A01	60.17	0.61	16.20	6.55	0.16	4.01	7.40	3.08	1.66	0.14	100.00
Lomanosov	A03	60.87	0.61	16.54	6.42	0.17	3.23	7.16	3.14	1.70	0.15	100.00

Volcano	Sample name	SiO_2	TiO_2	Al_2O_3	FeO*	MnO	MgO	CaO	Na_2O	K_2O	P_2O_5	Sum
Tatarinov	A14-01	62.43	0.63	16.89	5.74	0.17	2.34	6.19	3.69	1.73	0.19	100.00
Tatarinov	A14-02AR2	62.14	0.64	16.94	5.89	0.17	2.37	6.32	3.65	1.68	0.19	100.00
Tatarinov	A14-02B	55.28	0.63	19.24	6.94	0.16	4.34	9.40	2.80	1.05	0.16	100.00
Tatarinov	A14-03A	54.20	0.64	18.80	7.41	0.17	5.21	9.73	2.73	0.96	0.16	100.00
Tatarinov	A14-03B	54.07	0.64	18.76	7.48	0.17	5.31	9.72	2.73	0.97	0.15	100.00
Tatarinov	A14-04	55.12	0.87	17.89	8.52	0.19	4.13	8.77	3.19	1.13	0.19	100.00
Tatarinov	A14-05	56.95	0.76	17.72	7.98	0.18	3.80	8.12	3.13	1.19	0.17	100.00
Tatarinov	A14-06	55.56	0.87	18.85	7.91	0.18	3.94	8.26	3.31	0.88	0.24	100.00
Tatarinov	A14-08	62.29	0.62	16.97	5.83	0.17	2.41	6.26	3.60	1.66	0.20	100.00
Tatarinov	A15	54.60	0.75	18.45	8.25	0.18	4.72	9.00	2.92	0.97	0.16	100.00
Tatarinov	B15-49A	50.66	0.92	18.49	10.81	0.20	5.97	9.90	2.27	0.64	0.14	100.00
Tatarinov	B15-49B	49.85	0.94	18.99	11.15	0.19	6.09	9.86	2.19	0.59	0.14	100.00
Tatarinov	C01-04A	54.17	0.79	19.34	8.39	0.18	4.28	8.77	2.90	0.98	0.20	100.00
Tatarinov	C01-04B	53.41	0.80	19.58	8.58	0.18	4.35	9.09	2.85	0.94	0.20	100.00
Tatarinov	C01-05A	55.42	0.81	18.82	8.33	0.19	3.89	8.33	3.01	1.03	0.19	100.00
Tatarinov	C01-05B	55.16	0.81	18.63	8.47	0.19	3.94	8.53	3.02	1.05	0.19	100.00
Piik Fussa	A08-15A	58.93	0.58	18.03	6.12	0.18	2.78	7.10	3.40	2.60	0.26	100.00
Piik Fussa	A08-15B	60.43	0.52	17.99	5.69	0.18	2.34	6.43	3.48	2.74	0.21	100.00
Piik Fussa	A08-15C	59.70	0.55	17.94	5.97	0.18	2.56	6.75	3.40	2.67	0.28	100.00
Piik Fussa	A19-08A	59.03	0.58	17.85	5.97	0.17	3.00	7.30	3.38	2.58	0.14	100.00
Piik Fussa	B12	55.08	0.70	17.60	7.27	0.17	4.59	9.32	2.98	2.05	0.25	100.00
Piik Fussa	B13-01	55.95	0.67	17.57	7.06	0.17	4.47	8.68	3.01	2.16	0.27	100.00
Piik Fussa	B13-02host	56.46	0.65	17.49	6.89	0.16	4.20	8.55	3.06	2.25	0.27	100.00
Piik Fussa	B13-02enclave	52.29	0.74	18.74	8.33	0.19	4.91	10.36	2.63	1.53	0.28	100.00
Piik Fussa	B14-01A	61.02	0.51	17.39	5.40	0.16	2.51	6.45	3.46	2.89	0.21	100.00
Piik Fussa	B14-01B	59.95	0.54	17.54	5.58	0.17	2.68	6.97	3.52	2.84	0.20	100.00
Piik Fussa	B14-01C	59.97	0.55	17.63	5.62	0.16	2.78	6.93	3.42	2.73	0.21	100.00

Volcano	Sample name	SiO_2	TiO_2	Al_2O_3	FeO*	MnO	MgO	CaO	Na_2O	K_2O	P_2O_5	Sum
Piik Fussa	B14-04A	58.27	0.58	18.46	7.00	0.21	2.89	7.09	3.46	1.92	0.12	100.00
Piik Fussa	B14-04B	58.47	0.55	18.57	6.56	0.21	2.87	7.13	3.53	1.98	0.13	100.00
Piik Fussa	B14-10A	61.46	0.51	17.74	5.37	0.17	2.26	6.10	3.49	2.83	0.07	100.00
Piik Fussa	B14-10B	61.47	0.50	17.62	5.42	0.17	2.30	6.12	3.48	2.85	0.07	100.00
Piik Fussa	B14-13A	59.97	0.55	18.30	5.77	0.19	2.54	6.50	3.67	2.37	0.13	100.00
Piik Fussa	B14-13B	59.72	0.54	18.41	5.72	0.19	2.51	6.65	3.67	2.35	0.24	100.00
Piik Fussa	B15-03A	60.11	0.55	17.54	5.79	0.17	2.75	6.77	3.43	2.74	0.15	100.00
Piik Fussa	B15-35	60.91	0.52	17.77	4.70	0.17	2.41	6.93	3.48	2.82	0.29	100.00
Piik Fussa	A30-01	60.58	0.50	17.57	5.47	0.17	2.32	6.75	3.54	2.81	0.28	100.00
Piik Fussa	A30-02	60.84	0.50	17.60	5.33	0.16	2.25	6.64	3.56	2.84	0.28	100.00
Piik Fussa	A32-01	58.30	0.60	17.86	6.35	0.18	2.78	7.63	3.46	2.58	0.28	100.00
Piik Fussa	B02-02	62.21	0.51	17.02	5.08	0.15	2.22	5.92	3.49	3.17	0.24	100.00
Piik Fussa	B15-15A	58.64	0.55	18.21	6.44	0.21	2.87	7.25	3.50	2.02	0.32	100.00
Piik Fussa	B15-15B	58.57	0.55	18.21	6.43	0.21	2.92	7.31	3.50	2.00	0.30	100.00
Piik Fussa	B15-20A	58.12	0.67	17.65	6.73	0.18	3.00	7.10	3.50	2.87	0.20	100.00
Piik Fussa	B15-20B	58.17	0.66	17.75	6.70	0.18	3.05	7.11	3.43	2.75	0.19	100.00
Piik Fussa	B15-43A	59.85	0.55	17.86	5.93	0.20	2.58	6.68	3.71	2.44	0.19	100.00
Piik Fussa	B15-43B	60.22	0.53	18.00	5.70	0.20	2.43	6.59	3.64	2.39	0.30	100.00
Fuss ?	C02-02A	60.17	0.53	17.68	5.56	0.16	2.68	6.81	3.43	2.75	0.21	100.00
Fuss ?	C02-02B	61.23	0.50	17.51	5.13	0.16	2.44	6.44	3.50	2.89	0.22	100.00
Piik Fussa	B25-861	56.43	0.68	17.92	7.13	0.18	3.30	8.36	3.32	2.41	0.26	100.00
Piik Fussa	B25-860	56.66	0.68	17.91	7.06	0.18	3.27	8.26	3.31	2.41	0.26	100.00
Piik Fussa	B25-856?	58.37	0.61	17.80	6.33	0.17	3.02	7.41	3.41	2.63	0.25	100.00
Piik Fussa	B25-856	58.72	0.60	17.69	6.24	0.17	2.93	7.25	3.48	2.68	0.25	100.00
Piik Fussa	B25-856	58.70	0.60	17.71	6.26	0.17	2.91	7.29	3.44	2.66	0.25	100.00
Piik Fussa	B25-854	59.68	0.55	17.48	5.74	0.17	2.70	7.03	3.61	2.82	0.24	100.00
Piik Fussa	B25-853arim	58.74	0.60	17.75	6.19	0.17	2.97	7.24	3.43	2.66	0.25	100.00

Volcano	Sample name	SiO_2	TiO_2	Al_2O_3	FeO*	MnO	MgO	CaO	Na_2O	K_2O	P_2O_5	Sum
Piik Fussa	B25-853a	53.61	0.85	18.45	7.94	0.20	4.48	9.49	3.08	1.69	0.23	100.00
Piik Fussa	B25-850S	55.51	0.66	18.65	7.41	0.17	3.13	8.40	3.36	2.41	0.31	100.00
Taketomi	BA-43	51.11	0.91	19.88	8.98	0.18	3.99	9.79	3.05	1.80	0.31	100.00
Taketomi	BA-42	51.50	0.91	20.06	8.95	0.17	3.89	9.78	2.65	1.78	0.31	100.00
Taketomi	BA-40	51.38	0.91	20.22	8.85	0.16	3.78	9.67	2.92	1.79	0.31	100.00
Taketomi	BA-39	51.76	0.90	19.66	8.70	0.18	3.93	9.73	3.05	1.79	0.30	100.00
Taketomi	BA-38s	51.12	0.92	19.74	9.07	0.18	3.97	9.81	3.07	1.81	0.31	100.00
Taketomi	BA-37	51.36	0.92	19.84	9.11	0.18	3.93	9.67	2.86	1.82	0.31	100.00
Taketomi	BA-36	50.88	0.91	19.76	9.10	0.18	4.00	9.96	3.08	1.82	0.31	100.00
Taketomi	BA-33	51.60	0.91	19.89	8.88	0.18	4.01	9.76	2.69	1.76	0.31	100.00
Taketomi	BA-31	51.01	0.90	20.75	8.85	0.17	3.79	9.69	2.65	1.86	0.31	100.00
Taketomi	BA-30	51.46	0.91	20.32	8.97	0.17	3.74	9.34	2.98	1.79	0.31	100.00
Taketomi	BA-28	49.39	1.07	18.42	10.29	0.20	5.19	10.10	2.91	2.01	0.42	100.00
Taketomi	BA-27	49.35	1.06	18.49	10.25	0.20	5.26	10.11	2.89	1.97	0.41	100.00
Taketomi	BA-26	49.65	1.08	17.64	9.98	0.19	6.00	10.32	2.72	2.02	0.40	100.00
Taketomi	BA-22	49.63	1.14	18.19	10.11	0.19	5.28	10.20	2.89	1.96	0.41	100.00
Taketomi	BA-20	50.48	0.90	20.20	8.91	0.18	4.34	10.44	2.70	1.55	0.31	100.00
Taketomi	BA-17	50.37	0.89	20.17	8.80	0.18	4.27	10.45	2.89	1.66	0.31	100.00
Taketomi	BA-16	51.18	0.91	19.79	8.80	0.18	4.02	9.85	3.12	1.83	0.31	100.00
Taketomi	BA-14	51.34	0.90	19.90	8.66	0.18	3.96	9.87	3.09	1.79	0.30	100.00
Taketomi	BA-13	51.54	0.92	19.64	8.81	0.18	3.96	9.74	3.09	1.80	0.31	100.00
Taketomi	BA-12	51.11	0.90	19.83	8.89	0.18	3.98	9.89	3.09	1.82	0.31	100.00
Taketomi	BA-11	50.29	0.90	20.07	8.99	0.18	4.30	10.42	2.89	1.66	0.31	100.00
Taketomi	BA-10	51.27	0.90	19.81	8.94	0.18	3.94	9.78	3.08	1.79	0.31	100.00
Taketomi	BA-6	51.38	0.92	19.90	8.64	0.19	3.98	9.88	2.99	1.82	0.31	100.00
Taketomi	BA-5s	49.51	1.14	18.12	10.21	0.19	5.37	10.27	2.87	1.92	0.40	100.00
Taketomi	BA-4	51.04	0.92	19.75	8.93	0.18	3.98	9.92	3.13	1.84	0.31	100.00

Volcano	Sample name	SiO_2	TiO_2	Al_2O_3	FeO*	MnO	MgO	CaO	Na_2O	K_2O	P_2O_5	Sum
Taketomi	BA-1	49.69	1.14	18.21	10.12	0.19	5.20	10.18	2.89	1.96	0.41	100.00
Alaid, 1972	6003/3	50.60	0.94	19.04	9.14	0.19	4.77	10.34	3.15	1.52	0.30	100.00
Alaid, 1972	6002	51.79	0.99	18.45	9.70	0.20	4.24	9.09	3.33	1.90	0.32	100.00
Alaid, 1972	6001/6	51.37	0.99	18.50	9.69	0.20	4.43	9.43	3.24	1.83	0.31	100.00
Alaid, 1972	B40-947	50.93	0.99	18.59	9.94	0.20	4.55	9.71	3.10	1.71	0.29	100.00
Alaid, 1972	5807-OB-72	50.68	0.99	18.48	10.20	0.20	4.57	9.63	3.18	1.77	0.30	100.00
Alaid, 1972	5800-OB-72incl	77.17	0.44	10.55	3.89	0.04	1.74	2.23	2.28	1.55	0.10	100.00
Alaid, 1972	5800-OB-72	50.92	0.90	19.79	9.26	0.20	4.48	9.49	2.96	1.56	0.44	100.00
Alaid, 1972	5791/7 OB-72	51.51	0.99	18.42	9.85	0.20	4.33	9.20	3.28	1.89	0.32	100.00
Alaid, 1972	5790/7 OB-72	50.73	0.96	18.98	9.20	0.20	4.72	10.16	3.18	1.55	0.32	100.00
Alaid, 1972	5790-08-72	50.67	0.96	18.92	9.20	0.19	4.84	10.21	3.15	1.54	0.31	100.00
Alaid, 1972	5790-3	50.60	0.94	19.04	9.14	0.19	4.77	10.34	3.15	1.52	0.30	100.00
Alaid, 1972	B40-952	47.58	1.16	18.92	11.09	0.20	5.43	11.65	2.83	0.88	0.26	100.00
Alaid, 1972	B40-951	50.93	0.99	18.59	9.94	0.20	4.55	9.71	3.10	1.71	0.29	100.00
Alaid, 1972	B40-947	58.87	0.59	18.01	5.91	0.16	2.98	7.21	3.71	2.33	0.22	100.00
Alaid, 1981	BA-5A-81	49.54	0.98	18.54	10.18	0.21	4.31	10.29	3.69	1.95	0.31	100.00
Alaid, 1981	BA-4-1A-81	51.61	0.91	18.75	8.79	0.18	4.68	9.47	3.08	2.16	0.36	100.00
Alaid, 1981	A-3(6)A-81	62.76	0.76	17.20	6.01	0.10	3.32	4.73	3.48	1.47	0.18	100.00
Alaid, 1981	A-2(7)A-81	50.37	0.98	18.54	10.22	0.21	4.25	9.84	3.37	1.91	0.31	100.00
Alaid, 1981	A-1(3)A-81	51.05	0.96	18.83	9.44	0.20	4.12	9.41	3.86	1.83	0.31	100.00
Alaid	B11-526S	48.26	1.00	16.22	9.83	0.19	8.87	10.83	2.68	1.81	0.33	100.00
Alaid	B11-524	51.53	0.76	17.46	9.52	0.22	5.28	10.91	2.73	1.30	0.28	100.00
Alaid	B11-516	47.26	1.13	17.81	10.55	0.18	7.20	12.03	2.46	1.10	0.27	100.00
Alaid	B11-515	53.25	0.72	21.15	6.83	0.15	2.92	8.50	3.54	2.50	0.42	100.00
Alaid	B11-403	51.10	0.92	19.81	8.95	0.18	3.98	9.85	3.09	1.82	0.31	100.00
Alaid	B11-401	49.78	0.96	18.21	9.46	0.18	6.23	10.44	2.74	1.69	0.30	100.00
Alaid	2006-14	50.36	0.97	18.67	9.86	0.21	4.38	10.03	3.32	1.90	0.31	100.00

Volcano	Sample name	SiO_2	TiO_2	Al_2O_3	FeO*	MnO	MgO	CaO	Na_2O	K_2O	P_2O_5	Sum
Antsiferova	B25-846	60.25	0.50	17.79	5.75	0.19	2.48	7.02	3.65	2.10	0.27	100.00
Antsiferova	B25-843	56.52	0.68	17.91	6.69	0.16	3.65	8.16	3.55	2.38	0.29	100.00
Antsiferova	B25-836	52.68	0.77	18.65	8.53	0.19	4.57	9.76	3.00	1.61	0.25	100.00
Antsiferova	B25-832	52.40	0.79	18.60	8.70	0.19	4.67	9.84	2.97	1.59	0.25	100.00
Antsiferova	B25-828	52.30	0.78	18.72	8.68	0.18	4.65	9.93	2.93	1.57	0.25	100.00
Antsiferova	B25-825	56.08	0.71	18.23	6.78	0.17	3.59	8.43	3.52	2.19	0.30	100.00
Antsiferova	B25-821S	55.48	0.67	17.90	7.30	0.17	4.53	8.39	3.43	1.88	0.24	100.00
sv1,4	B34-101	58.81	0.57	18.02	5.85	0.23	2.80	7.20	3.86	2.42	0.23	100.00
sv1,4	B40-32/10	53.94	0.90	19.17	9.66	0.21	2.97	9.12	3.33	0.56	0.13	100.00
sv1,4	B40-32/9	49.48	0.86	17.73	8.64	0.23	8.46	10.92	2.58	0.87	0.22	100.00
sv1,4	B40-32/6a	54.67	0.85	18.20	9.07	0.16	3.90	9.27	3.21	0.52	0.16	100.00
sv1,4	B40-32/6	54.64	0.86	18.56	8.74	0.17	3.53	9.49	3.18	0.57	0.26	100.00
sv1,4	B40-32/4	63.69	0.39	17.89	4.02	0.21	1.73	5.39	3.89	2.56	0.23	100.00
sv1,3	B24-35/9	56.46	0.84	17.20	8.79	0.18	3.87	8.56	3.04	0.91	0.14	100.00
sv1,3	B24-35/8	49.92	0.92	19.96	9.66	0.17	4.39	11.56	2.77	0.47	0.17	100.00
sv1,3	B24-35/6	51.99	0.69	20.51	8.99	0.17	3.98	10.68	2.50	0.40	0.10	100.00
sv1,3	B24-35/3	62.49	0.33	19.06	4.31	0.14	1.86	7.90	3.16	0.67	0.08	100.00
sv1,3	B24-35/1host	62.73	0.33	19.02	4.30	0.13	1.95	7.70	3.09	0.66	0.08	100.00
sv1,3	B24-35/1incl	56.82	0.51	19.53	7.40	0.19	3.22	9.03	2.71	0.50	0.10	100.00
sv1,3	B24-35/1S	62.47	0.32	18.78	4.46	0.15	2.07	7.62	3.37	0.67	0.09	100.00
sv1,3	B24-34/13	60.67	0.42	18.55	5.98	0.15	2.83	7.82	2.79	0.71	0.08	100.00
sv1,3	B24-35/9	56.36	0.84	17.15	8.86	0.18	3.86	8.55	3.15	0.91	0.14	100.00
sv1,3	B24-34/8	56.43	0.59	18.77	7.90	0.20	3.68	9.03	2.72	0.55	0.13	100.00
sv1,3	B24-34/4S	56.13	0.58	19.54	7.38	0.18	3.51	9.31	2.73	0.51	0.13	100.00
sv1,3	B24-34/3	57.32	0.82	18.23	7.68	0.15	2.84	8.03	3.86	0.92	0.15	100.00
sv1,3	B24-34/3	57.33	0.82	18.13	7.93	0.18	2.99	8.06	3.51	0.91	0.14	100.00
sv 1,1	B40-30 ? (B34-30?)	58.87	0.59	18.01	5.91	0.16	2.98	7.21	3.71	2.33	0.22	100.00

Volcano	Sample name	SiO_2	TiO_2	Al_2O_3	FeO*	MnO	MgO	CaO	Na_2O	K_2O	P_2O_5	Sum
sv 1,1	B11-67/5	50.84	0.97	18.99	8.97	0.18	4.62	10.00	3.22	1.85	0.37	100.00
sv 1,1	B11-67/1	51.42	0.91	19.36	8.67	0.17	4.43	9.55	3.08	2.04	0.37	100.00
sv 1,1	B11-52/8S	54.00	1.05	17.96	8.69	0.18	3.34	7.21	3.89	3.13	0.55	100.00
sv 1,1	B11-52/2	53.57	1.06	18.10	8.92	0.18	3.42	7.29	3.78	3.12	0.55	100.00
sv 1,1	B11-52/1	48.59	1.05	19.69	10.16	0.18	4.83	11.04	2.76	1.48	0.23	100.00

Table 4. Trace element compositions.

Volcano	sample #	Li	Sc	V	Co	Zn	Ga	Rb	Sr	Y	Zr	Nb	In	Cs	Ba	La	Ce	Pr	Nd	Sm	Eu	Gd	Tb	Dy
Lomonosov	C02-01R2	13.78	25.15	216.70	15.80	58.15	16.03	38.76	413.00	29.73	124.20	2.37	1.02	1.77	424.30	12.11	28.20	3.98	17.13	4.31	1.07	4.29	0.71	4.36
Lomonosov	A01	12.59	27.01	222.80	19.89	53.67	15.43	35.44	403.80	27.27	108.00	2.17	1.03	1.70	383.40	10.75	25.34	3.59	15.60	3.93	0.98	3.94	0.64	4.04
Chikurachki ?	PAR 07 A08-08A	5.05	32.84	299.60	26.36	119.60	16.91	5.81	554.70	20.97	44.00	0.85	1.00	0.32	142.70	4.95	12.33	1.93	9.55	2.74	0.98	3.05	0.53	3.30
Chikurachki	A11	13.14	21.14	108.90	9.08	21.63	15.28	20.45	536.60	38.88	97.90	2.22	0.98	0.38	392.40	13.67	31.43	4.69	21.57	5.57	1.56	5.87	0.93	5.84
Chikurachki	A05	10.01	24.08	225.60	18.84	25.42	15.99	24.17	525.30	26.85	79.72	1.72	1.00	0.67	317.70	9.01	21.56	3.23	14.89	3.93	1.13	4.07	0.65	4.10
Chikurachki	A22-02	7.75	19.88	277.50	20.02	68.19	17.18	15.62	498.00	31.39	58.69	1.55	0.98	0.79	260.80	8.39	21.03	3.29	15.87	4.35	1.37	4.52	0.75	4.64
Tatarinov	A14-5	9.67	28.48	288.10	21.39	67.44	16.60	22.30	426.40	25.26	75.30	1.70	0.98	1.06	314.20	9.43	22.48	3.18	14.11	3.64	1.07	3.75	0.62	3.90
Tatarinov	B15-49A	5.23	38.80	404.70	31.10	79.46	15.84	9.68	453.20	18.25	46.37	0.93	1.00	0.45	169.80	5.24	13.05	1.93	9.21	2.49	0.87	2.79	0.47	2.94
Tatarinov	B15-49B	4.79	38.12	378.60	31.21	146.30	16.17	8.79	426.50	17.57	47.45	0.99	1.00	0.42	158.70	5.18	12.93	1.91	9.14	2.47	0.86	2.76	0.47	2.93
Tatarinov	Par A14-02B	8.23	25.31	217.10	22.69	46.79	15.42	18.43	424.60	21.90	64.76	1.43	1.03	0.97	259.10	7.72	18.35	2.67	12.40	3.19	0.93	3.35	0.55	3.42
Tatarinov	A14-4	9.62	34.83	338.40	22.85	41.32	17.20	20.98	507.80	25.58	70.97	1.52	1.00	0.94	274.60	8.23	19.96	2.94	13.50	3.64	1.16	3.86	0.63	3.91
Piik Fussa	B13-01	7.57	26.64	258.00	20.96	23.06	16.93	54.65	585.00	20.05	92.94	2.55	0.99	1.06	467.10	14.19	29.70	3.90	16.38	3.78	1.11	3.54	0.53	3.12
Piik Fussa	PAR07 A08-15B	14.12	14.75	155.80	12.21	69.59	18.26	76.17	638.80	20.47	137.20	3.50	0.99	2.85	621.20	17.55	35.72	4.58	18.94	4.12	1.27	3.54	0.53	3.14
Piik Fussa	B14-01a	16.41	12.81	211.60	13.81	72.47	17.75	79.84	505.40	19.17	111.30	3.21	0.95	3.44	633.60	17.91	36.98	4.49	17.90	3.74	1.04	3.40	0.49	2.94
Antciferova	B25-836	8.80	33.55	290.90	26.41	39.41	17.32	36.49	723.00	21.39	72.73	2.33	0.97	1.23	377.40	13.77	28.93	4.02	17.21	4.00	1.23	3.90	0.57	3.42
Antciferova	B25-821	8.77	25.52	228.00	21.96	45.11	17.81	48.50	638.20	20.22	87.83	2.86	1.00	0.70	468.40	15.17	31.35	4.02	16.62	3.72	1.18	3.44	0.53	3.12
Antciferova	B25-843	8.19	24.77	182.00	17.61	32.07	18.17	63.30	691.70	21.93	107.20	3.22	1.01	1.04	585.00	18.07	36.16	4.70	19.07	4.22	1.28	3.95	0.57	3.41
Antciferova	B25-828	7.98	29.46	308.00	26.94	43.65	17.71	36.83	728.60	20.74	70.60	2.26	1.00	1.35	370.60	13.61	28.51	3.88	16.74	3.91	1.21	3.77	0.56	3.31
Antciferova	B25-846	12.55	16.54	113.30	12.93	82.81	18.31	61.15	660.90	22.02	105.20	3.26	1.03	2.49	608.00	19.66	39.18	4.99	19.89	4.31	1.24	3.84	0.56	3.30
1.3	B24-35/3	13.61	14.17	129.00	10.00	45.91	15.99	10.74	329.30	11.49	50.27	0.62	1.04	0.62	274.70	3.86	9.26	1.27	5.45	1.43	0.55	1.54	0.27	1.69
1.3	B24-34/13	9.71	17.92	200.00	12.47	80.91	15.08	11.24	260.20	13.68	49.08	0.57	0.99	1.24	228.80	3.22	7.92	1.10	5.16	1.46	0.55	1.73	0.31	2.05

Volcano	sample #	Li	Sc	V	Co	Zn	Ga	Rb	Sr	Y	Zr	Nb	In	Cs	Ba	La	Ce	Pr	Nd	Sm	Eu	Gd	Tb	Dy
1.3	B24-35/8	6.72	30.25	340.00	26.89	79.36	16.29	5.33	670.40	21.87	42.72	0.86	0.99	0.22	91.19	4.58	11.86	1.83	8.75	2.61	0.92	2.99	0.51	3.36
1.3	B24-34/8	8.00	21.50	217.20	20.48	50.50	15.49	9.71	409.00	21.76	41.22	0.70	0.95	0.74	193.80	3.58	9.08	1.44	7.24	2.27	0.81	2.77	0.49	3.21
1.3	B24-35/9	9.64	32.36	276.70	23.59	74.08	17.13	15.26	295.60	29.68	77.01	1.03	0.93	1.20	163.80	5.25	13.84	2.10	10.14	3.12	0.96	3.72	0.67	4.45
1.4	B40-32/9	7.39	35.29	299.50	35.56	42.40	16.53	15.17	500.60	21.50	62.99	2.09	0.94	0.63	247.80	9.52	21.25	3.02	13.82	3.47	1.11	3.55	0.55	3.33
1.4	B40-32/10	8.51	39.77	250.70	22.69	85.60	18.26	6.50	433.40	24.19	42.82	0.78	1.03	0.36	135.90	3.68	9.73	1.57	8.07	2.61	1.03	3.17	0.57	3.74
1.4	B34-101	11.39	10.26	210.20	14.64	61.88	17.70	66.34	560.20	16.97	94.64	3.58	0.93	2.17	780.60	13.43	32.17	3.63	14.67	3.26	0.99	2.92	0.44	2.61
1.4	B40-32/6a	15.01	36.09	322.60	27.55	1264.00	18.27	5.83	345.20	23.27	45.78	0.92	0.97	0.23	149.80	4.59	11.85	1.84	9.05	2.73	0.98	3.17	0.56	3.55
1.4	B40-32/4	15.24	7.76	85.10	9.16	37.10	18.81	78.97	783.30	18.33	95.66	4.98	1.01	3.08	1072.00	27.16	51.28	6.03	22.41	4.16	1.12	3.38	0.46	2.64
Ebeko	08PR 26-2	10.32	31.64	251.30	30.20	68.59	15.91	37.40	462.50	22.58	77.18	2.21	0.95	1.64	345.60	10.89	24.52	3.45	15.12	3.68	1.08	3.64	0.58	3.46
Ebeko	08PR23	4.84	39.21	404.80	36.93	85.37	19.46	15.96	772.60	21.03	43.49	1.44	1.03	0.52	303.30	8.76	20.81	3.14	14.82	3.96	1.26	3.92	0.59	3.51
Ebeko	08PR-19-3	6.07	33.20	355.00	33.51	96.21	20.40	19.95	770.40	22.90	54.74	2.37	1.02	0.17	254.70	11.62	28.07	4.15	19.04	4.71	1.38	4.33	0.63	3.71
Ebeko	08PR-12	16.33	12.24	135.30	13.68	167.60	14.84	65.71	303.40	15.18	126.20	3.12	0.99	2.75	502.50	6.24	17.34	1.82	7.54	1.93	0.64	1.91	0.33	2.15
Ebeko	08PR 19-1	4.20	51.30	420.50	44.18	161.90	19.11	8.09	630.80	17.84	30.87	0.80	1.03	0.09	154.60	5.61	14.57	2.32	11.62	3.29	1.05	3.20	0.50	2.98
1.1	B11-52/8	14.00	25.44	236.60	21.33	74.59	19.57	76.95	573.70	30.73	168.50	9.72	0.98	2.48	518.30	22.26	49.04	6.52	28.15	6.40	1.75	5.94	0.86	4.89
1.1	B11-67/5	9.06	23.30	317.10	27.65	65.25	19.85	44.54	620.40	24.33	80.08	4.89	0.98	1.38	382.90	12.29	28.42	4.08	18.37	4.61	1.39	4.36	0.65	3.84
1.1	B11-52/1	7.33	37.70	420.40	34.14	89.35	20.37	30.69	652.60	22.60	58.97	2.84	1.03	0.86	266.70	9.39	22.15	3.26	15.25	4.08	1.27	4.08	0.62	3.70
1.1	B11-67/1	8.63	24.59	283.30	24.78	59.93	18.64	46.84	643.60	23.19	88.56	6.70	0.95	1.11	370.30	14.71	32.76	4.51	19.87	4.70	1.41	4.49	0.66	3.87
Alaid	BA-43	7.67	26.35	420.60	25.71	55.78	19.40	45.14	677.30	22.41	80.66	5.13	0.94	1.46	356.90	13.71	30.18	4.13	18.33	4.39	1.33	4.13	0.61	3.57
Alaid	5800 OB-72	17.26	20.54	390.60	28.19	76.65	21.25	27.96	731.70	26.58	83.92	5.23	0.93	0.80	456.40	15.10	35.09	4.97	22.63	5.35	1.60	5.01	0.73	4.21
Alaid	BA-20	8.45	20.59	307.10	28.96	67.34	19.70	31.20	639.50	21.71	70.65	3.95	0.97	0.96	333.30	9.84	25.73	3.39	15.52	4.00	1.25	3.83	0.58	3.42
Alaid	A2-7 A81	11.84	30.38	349.80	29.91	61.85	20.14	40.71	707.70	23.80	74.52	4.83	0.97	1.27	359.80	13.10	29.02	4.04	17.86	4.46	1.37	4.24	0.64	3.73
Alaid	B40-952	7.26	44.04	354.70	33.39	53.52	19.42	39.12	648.10	25.20	72.16	4.34	0.95	0.61	357.30	13.21	30.69	4.39	20.12	5.11	1.48	4.83	0.72	4.24
Alaid	B11-516	3.98	44.7	395.1	34.4	83.04	16.5	22.3	548.7	20.8	56.97	2.9	0.9	0.9	223.40	9.17	22.7	3.4	16.3	4.4	1.3	4.1	0.6	3.7

Volcano	sample #	Li	Sc	V	Co	Zn	Ga	Rb	Sr	Y	Zr	Nb	In	Cs	Ba	La	Ce	Pr	Nd	Sm	Eu	Gd	Tb	Dy
			5	0	1		6	6	0	4		4	0	4			5	0	6	3	7	7	5	4
Alaid	5791/7 OB 72	7.85	25.79	366.80	25.61	124.20	18.89	42.72	650.70	23.85	84.21	4.99	0.97	1.54	381.40	14.66	32.33	4.49	19.79	4.72	1.43	4.27	0.67	3.99
Alaid	A-3 (6) A-81	10.41	29.86	454.10	29.79	91.22	19.98	44.05	700.20	24.05	82.76	4.91	0.92	1.48	372.90	13.55	30.05	4.24	18.76	4.56	1.40	4.51	0.66	3.90

Table 5. Sr-Nd isotopic composition.

	Name of samples	$^{87/86}$ SR	2 SE	$^{143/144}$ Nd	2 SE
1.4	B24-35/9	0.703593457	0.000008486	0.512866088	0.000010784
1.4	B40-32/6a	0.703295635	0.000007647	0.513044563	0.000009865
1.4	B34-101	0.703011329	0.000008054	0.513027527	0.000009308
1.4	B40-32/9	0.703123162	0.000008143	0.513043358	0.000009350
1.4	B40-32/10	0.703328286	0.000008064	0.513092842	0.000008135
Ebeko	08PR-19-1	0.702884152	0.000011435	0.513052666	0.000007593
Ebeko	08PR-23	0.703004692	0.000009910	0.513032936	0.000009326
Antsiferova	B25-846	0.703093501	0.000009388	0.513054720	0.000008326
Antsiferova	B25-828	0.702946653	0.000007792	0.513064168	0.000007261
Antsiferova	B25-836	0.702916074	0.000008488	0.513021417	0.000012739
Antsiferova	B25-821	0.703023637	0.000009702	0.513046597	0.000009183
Piik Fussa	B 13-01	0.702964477	0.000009833	0.513047398	0.000009314
Alaid	A3(6)-A-81	0.702964477	0.000009833	0.513047398	0.000009314
Alaid	5800 OB-72	0.703115239	0.000009461	0.513052996	0.000007635
Alaid	A 2 (7) A 81	0.702995386	0.000008268	0.513047953	0.000008068
Alaid	5791/7 OB-72	0.703050888	0.000007166	0.513055970	0.000009238

Name of samples	$^{87/86}$ SR	2 SE	$^{143/144}$ Nd	2 SE	0.000011545
Alaid	BA-20	0.703014281	0.000009189	0.513003674	0.000090711
1.3	B 24 -35/9	0.703299347	0.000008734	0.513072572	0.000012870
1.3	B24-35/3	0.703357701	0.000008484	0.513126960	0.000011537
1.3	B24-34/8	0.703348376	0.000008776	0.513113822	0.000008317
1.3	B24-35/8	0.704584971	0.000008781	0.513037210	0.000009212
Tatarinova	A14-5	0.703162780	0.000007993	0.513001140	0.000010403
Tatarinova	B15-49B	0.703076812	0.000010084	0.513051420	0.000009089
Chikurachki	A05	0.703250064	0.000011371	0.513044286	0.000010015
Chikurachki	07PAR A22-02	0.703112368	0.000009105	0.513057536	0.000007747
Chikurachki	A11	0.703171353	0.000008481	0.513037207	0.000009982
Lomonosova	C02-01R2	0.703141398	0.000008296	0.513037765	0.000008195
Lomonosova	A01	0.703147895	0.000008633	0.513066967	0.000009293
Grigoreva	B11-52/8	0.703040570	0.000009427	0.513038398	0.000009309
Grigoreva	BA-43	0.703009799	0.000008932	0.513034349	0.000009103
Grigoreva	B11-67/1	0.703024936	0.000012107	0.512992226	0.000008412
Grigoreva	B11-52/1	0.703049306	0.000008005	0.513016898	0.000010839